Technische Universität München
TUM School of Engineering and Design

On the edge of structural code development: Effects of hidden safeties, system behavior, and non-linear models on the structural reliability

Philip Maximilian Teichgräber

Vollständiger Abdruck der von der TUM School of Engineering and Design zur Erlangung eines Doktors der Ingenieurwissenschaften (Dr.-Ing.) genehmigten Dissertation.

Vorsitz:
Prof. Dr. Kai-Uwe Bletzinger

Prüfende der Dissertation:
1. Prof. Dr. Daniel Straub
2. Prof. Dr. Jochen Köhler
3. Prof. ir. Ton Vrouwenvelder

Die Dissertation wurde am 02.04.2024 bei der Technischen Universität München eingereicht und durch die TUM School of Engineering and Design am 17.06.2024 angenommen.

Abstract

This thesis is about advancements in the development of the partial safety factor concept which is the basis of most modern structural design codes. Three adaptation ideas are formalized, including the explicit inclusion of the effects of hidden safeties, the inclusion of system effects, and the consideration of non-linear effects. The first adaptation idea about hidden safeties becomes necessary if standard models get replaced by more advanced models. This can have two counteracting effects on structural reliability that need to be balanced out. The second adaptation idea regarding the inclusion of system effects aims at an extension of the partial safety factor concept to system-level. This is achieved by establishing a link between general structural systems and an extended version of the Daniels system. The third adaptation idea investigates non-linear structural response functions and questions the state-of-the-art approach of considering the maximum of the design action effect derived via the application of the partial safety factor directly to the action or to the action effect. For each of the three adaptation ideas, detailed investigations are conducted at a higher and abstract level in order to establish a generic basis. Moreover, concrete suggestions for adapting the partial safety factor concept are proposed and various application examples are presented. The common goal is the homogenization of the level of safety and a reduction of material consumption without decreasing overall reliability.

Acknowledgements

I would like to take this opportunity to express my sincere gratitude to all those who contributed to the completion of this dissertation.

First and foremost, my deepest appreciation goes to my doctoral advisor, Daniel Straub, whose guidance and support were well balanced between close mentorship and the freedom essential for creative thinking.

Secondly, I appreciate Jochen Köhler for his thoughtful input and warm hospitality during my research stays in Trondheim.

I would also like to thank my colleagues, friends and family who engaged in fruitful discussions, provided constructive feedback, and stood by me during challenging moments.

Your contributions have left a lasting impression and are documented in this dissertation. Thank you.

Contents

1. Introduction

The word "engineer" is derived from the Latin verb ingeniare (to create, to generate, to contrive) and the noun ingenium (cleverness) [1]. Hence, an engineer is someone who manipulates the world in a clever way. This thesis is restricted to the manipulation of engineering structures. The cleverness of a structural design is assessed in terms of its structural reliability and its resource efficiency.

In a world of constant growth with limited resources [2–8] and countless ecological [9–12], economical [12–15], sociological [12, 16–20], and many potential future crises due to this growth, it is one of the most challenging tasks of our generation to use resources efficiently. The building sector within the European Union uses 1200 to 1400 million tons of building materials per year [21]. This means every inhabitant of the European Union consumes about 3 tons of building materials per year. In general, an inhabitant of an industrialized country consumes between 10 and 20 tons of materials per year in total (excluding water and air, as well as indirect material use, e.g., through induced soil erosion) [8]. Hence, the building sector is responsible for a major percentage of material consumption and plays a key role when it comes to resource sustainability. However, reducing the consumption of resources can – but does not have to – conflict with the safety of structures, and an appropriate balance must be found. When trying to find an optimal solution, typically two stages are necessary: First, the optimization of each structure and second, the optimization of design codes, which are the constraints placed on the first [22]. This thesis tackles the optimization of design codes.

In general, a distinction can be made between three different levels of probabilistic structural design codes: The risk-informed approach, the reliability-based approach, and the semi-probabilistic approach.

The risk-informed approach (e.g., [23]) is the most general approach, leading to the most optimal solution in finding a balance between resource consumption and the safety of structures. However, it requires a full risk analysis, including knowledge about the probability of system failure and knowledge about the respective consequences of failure. This approach is rarely applied.

The reliability-based approach (e.g., [24]) differs from the risk-informed approach in that it does not require any knowledge of the consequences of structural failure. A reliability analysis is conducted such that a structural system or elements of a structural system meet a target reliability. This leads to a less optimal balance between resource consumption and the safety of structures compared to the risk-informed approach; however, if the consequences of structural failure of the considered portfolio are within the same order of magnitude, the difference between the risk-informed and the reliability-based approach are rather small.

The semi-probabilistic approach is a further simplification of the reliability-based approach (e.g., [25]). In this thesis, the semi-probabilistic approach is referred to as the partial safety factor (PSF) concept. The PSF concept is the most common design concept for structures. All probabilistic quantities of the reliability-based approach are translated to deterministic values (i.e., as mean or quantile values). These values are called characteristic values. In order to achieve sufficient safety, PSFs and combination factors are applied to the characteristic values, resulting in so-called design values (design action effects and design resistances). Multiple design values are derived for a set of well-defined failure modes of structural elements. The system as a whole is typically not analyzed. If all design resistances are greater or equal to the respective design action effects, a structural system is considered safe; however, the reliability of individual structural elements/systems designed following this concept vary. A target reliability is only achieved on average for the full portfolio of structures. The transition from the reliability-based approach to the semi-probabilistic approach further reduces the optimality between resource consumption and the safety of structures. How much the optimality is reduced strongly depends on the level of detail of the PSF concept, i.e., how case-specific the safety components (characteristic values, PSFs, and combination factors) are determined. However, a higher level of detail can be negative regarding the ease-of-use of a standard.

This thesis investigates three possible adaptations of the PSF concept: First, the explicit inclusion of hidden safety effects within the PSF concept (Sec. 3). This becomes especially necessary if standard models are replaced by more advanced models. Second, the extension of the PSF concepts to the system-level by considering the amount of redundancy of a structural system (Sec. 4). Third, possible improvements on how to include non-linear structural response functions within the PSF concept (Sec. 5). All three possible adaptations lead to a homogenization of the safety level (decrease the variability of the reliabilities within the portfolio structures) and improve the resource efficiency. All three adaptions are analyzed on the reliability level. The risk level is not included within this thesis. Each of the three sections (Sec. 3-5) can be read independently; however, the background section (Sec. 2) should be read beforehand.

2. Background

In this section, the historical (Sec. 2.1) and the philosophical background (Sec. 2.2) are presented. Sec. 2.3 gives a general introduction to the PSF concept and thus lays the foundation for the three main parts of this thesis about hidden safeties (Sec. 3), redundancies (Sec. 4), and non-linear effects (Sec. 5). A reader in a hurry may skip Sec. 2.1 and Sec. 2.2.

2.1. Historical background

The first historical records on structural design stem from ancient Egypt and ancient Babylonia. In those times, structures were built using the trial and error method, intuition, and experiments on scale models. No record exists of any theoretical consideration, neither of the strength of structural members nor of the behavior of structural materials. Through the trial and error process, more and more empirical knowledge was acquired, which was passed from generation to generation [26].

With the rise of natural science, the ancient Greeks and later the ancient Romans began to develop models and theories to understand the phenomena of nature (e.g., *Archimedes* (287-212 BC) discovered the principle of the lever). However, these newly discovered laws of physics were mostly of scientific interest and rarely applied in building practice. E.g., the stone in an Ancient Greek temple or the arch ring of an Ancient Roman masonry bridge was designed at a level one or two orders of magnitude below its crushing strength. Thus, the shape and not the material strength governed its stability. For this reason all ancient and medieval writings on buildings are concerned precisely with geometrical rules [27]. *Vitruvius* (75-15 BC), for example, gives geometric proportions for the construction of temples: *"The distance between columns should be two and a quarter of their diameter and their length should be nine and a half of the diameter."* If a structure had novel geometric forms (e.g., Gothic churches), often multiple attempts were needed to achieve a design that did not collapse [28].

In the Renaissance, great minds like *Leonardo da Vinci* (1452-1519 AC), *Stevin* (1548-1620 AC), and *Galilei* (1564-1641 AC) rediscovered the achievements of ancient civilization, expanded them, and started to apply them in building practice. With the help of *Newton* (1642-1726 AC), *Hooke* (1635-1702 AC), *Bernoulli* (1654-1705 AC), *Navier* (1785-1836 AC), and many more, the classical mechanics and the theory of material strength were developed such that in the 18th century they became standard in practice [27, 29–31]. With this, a fundamental shift in the building culture took place: The design of structures became less based on experience and more on physical models and theories.

The new models were standardized and formed the base of various building codes: To guarantee the safety of structures – designed according to these new building codes – the global safety factor format was developed in the 19th century. Structures were designed such that the resistances were scaled by a single global safety factor to be greater than the action effects. The values of the resistances and the action effects were either based on expert knowledge or on the average values of statistical tests. Choosing the value of the global safety factor was not straightforward. Various authors and different building codes recommended different values for different materials and their respective resistance types [32]. Over time, these values were iteratively adapted to achieve a level of safety which was accepted by society. E.g., in the early 20th century, the safety factor for reinforcing steel in the UK was 2.0 [33]. In 1939, the British Standards Institution decreased the safety factor, considering the shortage of steel during world war II. The new safety factor was 1.6 for members in bending and 1.8 for members in direct tension. After the war, the lower safety factors were considered to be reasonable and a safety factor of 1.7 for both bending and direct tension was established [34].

In the 1960s, probabilistic modeling became increasingly popular [35]. However, the full probabilistic approach was considered to be too complicated to be used in practice [36]. Instead, the semi-probabilistic PSF concept was developed [36–38]. In contrast to the global safety factor format, multiple PSFs are applied to various actions and various resistances. The PSF concept is the main issue of this thesis. Sec. 2.2 gives a philosophical foundation and Sec. 2.3 gives a detailed description of the PSF concept.

2.2. Philosophical foundation

As stated in Sec. 2.1, the standard approach to design structures shifted from experience-based design to model-based design during the Renaissance. This section tries to philosophically describe such models and incorporates this description into a general definition of the designing process of a structure.

The concept of modeling proves to be fundamental for the scientific description and the technical manipulation possibilities based on it. Models mediate between the abstract theory and the concrete phenomenon to be described (i.e., the aspect of reality to be described) by idealizing certain aspects of the phenomenon and concretizing abstract assumptions of the theory. A model is an interpretation of an empirical phenomenon that facilitates intellectual access to this phenomenon, e.g., by analogizing, idealizing, and simplifying it [39]. There are many different types of models: scale models represent enlarged or reduced imitations of the modeled object, analog models (e.g., the planetary model of the atom) aim at its structure, theoretical models want to describe the essential properties of an object or system in a bundle of assumptions and equations [40].

An essential characteristic of models is that they always model only a certain aspect of the empirical phenomenon, i.e., the description is always necessarily partial, while other aspects that are not relevant to the respective research question are methodically excluded. The aspects that are addressed in the modeled description are therefore always dependent on the research interest and the respective research question. In addition, the thematized

aspects are often addressed in an idealized form that does not occur in reality. This also leads to different, inconsistent models being used within certain branches of science, which nevertheless fulfill their purpose for the respective sub-aspects [41].

When it comes to the design of structures, various models and theories are needed to describe the actions and resistances at hand. The selection process of these models often leads to questions such as: *How precise are these models?* or *What is the true value of some phenomenon described via these models?*. Such questions cannot be answered satisfactorily within the field of civil engineering. They are covered by the philosophical research area of epistemology. In epistemology, various approaches deal with such questions (e.g., [42–45]). These different approaches would answer such questions differently, and there is no consensus on which concept is the right one. One possible approach – which is well suited to structural design – is formulated by Cartwright [46–48]. The approach formalized in this thesis is inspired by her approach.

Cartwright's approach focuses on the description of a single phenomenon $\mathcal{P}$ of an object $\mathcal{O}$. She distinguishes between two fundamentally different ways to derive the value $\mathcal{V}$ of a phenomenon. If the value is determined purely empirically, it is called the true value $\mathcal{V}_{true}$ of a phenomenon. Hence, truth is equivalent to empirical adequateness. Alternatively, the value can be determined by describing the object with a model $\mathcal{M}$ that is suitable such that a theory $\mathcal{T}$ can be applied to the model to determine a value. A value that is derived this way is called nominal value $\mathcal{V}_{nom}$. Fig. 2.1 gives an overview of the difference in the determination of the true value and the nominal value of a phenomenon.
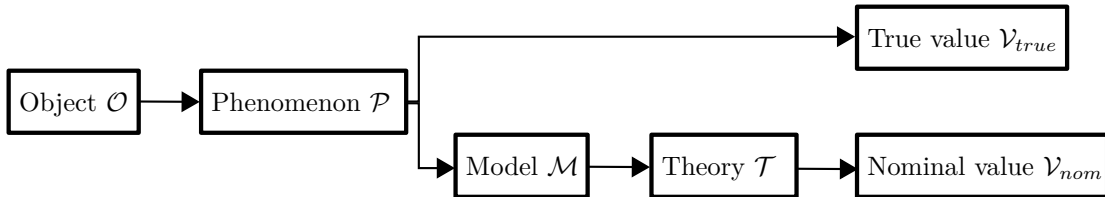
Fig. 2.1.: Difference in the determination of the true value and the nominal value of a phenomenon.

An example of Cartwright's approach is the determination of the maximal force until failure of a simple supported beam in bending if the force is applied in the middle of the beam. A three-point bending test [49] can be performed to determine the value of the force at failure. Since the three-point bending test is an empirical method, the resulting value is called the true value. Alternatively, a nominal value of the force at failure can be determined via a model and a theory. One possible model consists of a simply supported isotopic cubic mass and an idealized point load. A possible theory is Euler-Bernoulli beam theory.

In the following, Cartwright's approach is transferred to structural design methods. However, the subsequent aspects of the approach should be noted beforehand:

- The nominal value and the true value of a phenomenon generally do not coincide. Hence, nominal values can be wrong to some extent. Or – in the words of Cartwright – this is "how the laws of physics lie" [46]. This raises the question of

where – in the chain from the phenomenon of an object to the model and theory to the value of a phenomenon – this "lie" takes place. Cartwright answers this question with the so-called *simulacrum account of explanation*: The simulacrum account of explanation states that theories are always true within the limits of the model and the "lying" is due to the model's incorrect description of the phenomenon. This is in contrast to the more conventional picture of the deductive-nomological model of Hempel and Oppenheimer [50] where the "lying" is due to an insufficient theory.

- There is a trade-off by how much the value of a phenomenon is true and how good one is able to explain the value: Purely empirical values are true in the sense of empirical adequateness; however, they are purely descriptive and, therefore, do not explain anything. In contrast, a physical theory can give some explanation of the value of a phenomenon. E.g., in the above example, the true value derived via the three-point-bending test does not give any explanation of itself. In contrast, the nominal value is derived via beam theory, which provides a mathematical relationship between the variables involved. From this, an engineer can derive some understanding of the problem and draw conclusions, such as that it is more efficient to adjust the height of the beam than the width to increase its bending resistance.

- In some cases, it is arguable to what extent the value of a phenomenon can be derived purely empirically, thus, to what extent the determination of the true value is possible. This is especially the case if the value of a phenomenon can not be measured directly, but only indirectly. E.g., in order to determine the Young's modulus of a truss member, multiple other quantities are required (cross-section area, amount of an applied force, and the strain caused by the force). Given these, the Young's modulus can be calculated. This calculation can be interpreted as the application of a model and a theory. In this sense, the determined value of the Young's modulus may be interpreted as a nominal value. However, it is based on empirical measurements only and the phenomenon Young's modulus can simply be interpreted as a mathematical combination of these empirical measurements without any model or theory being involved. Thus, it can also be interpreted as a true value. In this thesis, the latter interpretation is used.

- Another important aspect of the true value of a phenomenon is that it can only be determined retrospectively (since it can only be observed empirically). In contrast, physical theories can also forecast the value of a phenomenon. This is of special importance in the design of structures, since we want to forecast values of structural phenomena like the state of failure.

- It should be noted that values of phenomena (nominal or true) can be an input to models used to derive other nominal or true values of phenomena, leading to a tree-like structure.

- In the scope of this thesis, statistical models play an important part. Formally, a statistical model consists of the triplet of a sample space $\mathcal{S}$, an event space $\mathcal{A}$ and a set of probability distributions $\mathcal{P}$ on $\mathcal{A}$ [51]. Such a model can be used to describe the – assumed to be possible – values of a phenomenon probabilistically. It is typically paired with data of true values of phenomena of similar but different objects.

Probability theory can be applied to determine which probability distribution of the set $\mathcal{P}$ to choose. This includes methods like the methods of moments, maximum likelihood estimation or Bayesian parameter estimation. The resulting value of the phenomenon at hand is a random variable. The random variable itself can be interpreted as a nominal value. Alternatively, the random variable can be reduced to a deterministic value (e.g., the mean or a quantile value). Fig. 2.2 illustrates the derivation of a nominal value in case of a statistical model being involved.
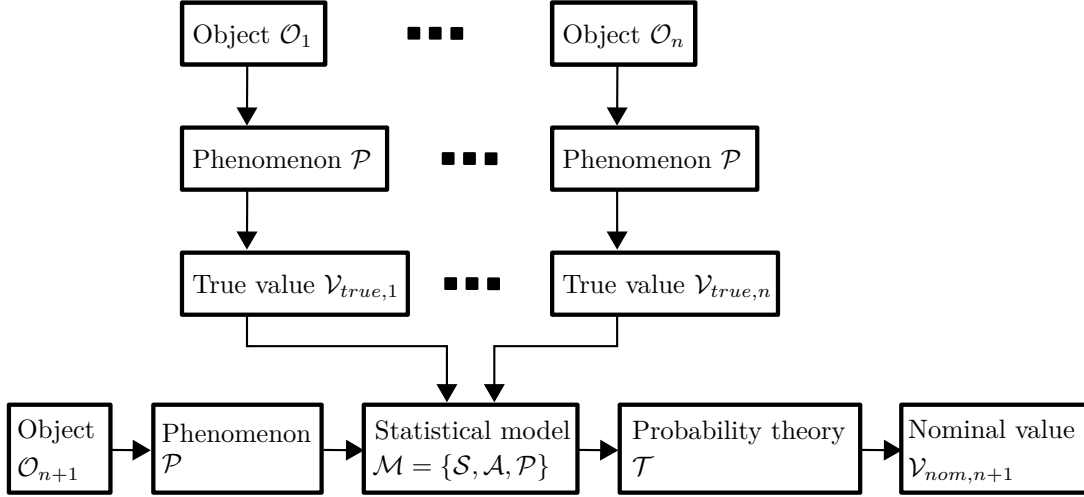
Fig. 2.2.: Determination of a nominal value via a statistical model.

An example may again be the strength of a beam in bending. A possible statistical model is given by the sample space $\mathcal{S} = [0,\infty)$, the event space $\mathcal{A}$ defined as the Borel σ-algebra on $\mathcal{S}$ and the set of probability distributions $\mathcal{P}$ defined by the log-normal distribution with undefined parameters. This model can be combined with data, namely the empirically derived true values of the bending strength of $1, \dots, n$ beams which are considered to be the similar, however, not identical. From this, the parameters of the log-normal distribution can be determined, e.g., through maximum likelihood estimation. The resulting random variable can be used to predict the bending strength of a beam $n + 1$.

The above mentioned trade-off between the amount of "lying" and the ability to explain a value can be well observed when it comes to statistical models. Since statistical models are based on empirically derived data, the amount of "lying" is rather small. However, almost no explanatory insight is provided.

- As already mentioned, the nominal value and the true value of a phenomenon generally do not coincide and Cartwright refers to this difference as "lying" of the model. In the context of this work, the difference between the nominal value and the true value is described probabilistically and referred to as model uncertainty. It can be distinguished between two types of uncertainty: Aleatoric and epistemic uncertainty. Following [52], aleatoric uncertainty is defined as uncertainty that cannot be eliminated within the confines of the current state of science. In contrast, epistemic uncertainty is due to limited knowledge. Epistemic uncertainty could be reduced by

collecting information, e.g., through tests, improved models, etc.

If the nominal value of a phenomenon is a random variable, the involved epistemic uncertainty can have the following sources: The choice of the sample space, the event space, the probability distribution type of the used statistical model, the fitting method of the applied probability theory and limited or wrong data. If all those sources are eliminated – which is only hypothetically possible – the probability distribution of the resulting random variable is called a purely aleatoric distribution. If the derivation of a value of a phenomenon only includes aleatoric uncertainties, this value is called a purely aleatoric value. This nomenclature is in contrast with most other authors, who typically refer to it as the true distribution and the true value, which – in the nomenclature of this thesis – is considered a purely aleatoric distribution and a purely aleatoric value [53]. This thesis strictly follows the approach inspired by Cartwright. Therefore, true values are defined as the empirically and retrospectively observed values. The true distribution of a value is a Dirac delta distribution at the empirically and retrospectively observed true value; hence, the true distribution reduces to a deterministic value.

- An important quantity in the context of uncertainty is the probability of failure. The following three probabilities of failure are distinguished within this thesis: The nominal probability of failure (including epistemic as well as aleatoric uncertainties), the purely aleatoric probability of failure (including only aleatoric uncertainties), and the true probability of failure which – following Cartwrights approach – is a retrospectively and empirically observed value, namely the value if failure happened or not. Hence, the true probability of failure is either 1 or 0. In this context, it is important to distinguish between the probability of failure and the failure rate. The true failure rate is the retrospectively and empirically observed ratio of a number of failures to the total number of observations. This number can be between 1 or 0.

Based on Cartwright's approach to describe models, a structural design method can be defined via a tree like structure. This tree can typically be split into an action and a resistance side. Fig. 2.3 illustrates a mask version of such a tree. Each vertex of the tree represents the determination of a value of a phenomenon. If the vertex consists only of an object, a phenomenon, and a value, then the determined value is a true value. This is typically the case for leaves. If the vertex consists only of an object, a phenomenon, a model, a theory, and a value, then the determined value is a nominal value. The root of the tree represents the quantity that needs to be verified. If the verification is at the element-level, the root-object is the associated structural element. If the verification is at the system-level, the root-object is the whole structure. The root-phenomenon is the failure mode of the respective element or system. The model of the root vertex consists of the two quantities of the action effect and the resistance of the considered failure mode. The theory of the root vertex is either – in case of a deterministic verification – a mathematical metric comparing the action effect to the resistance or – in case of a probabilistic verification – probability theory in order to calculate the nominal probability that the action effect is greater than the resistance. This probability can then be classified as sufficient or not. Hence, the value assigned to the phenomenon of the root has either the value "verification fulfilled" or "verification not fulfilled". Fig. 2.4 shows an example instantiation of the mask from Fig. 2.3 illustrating the structural design of a beam subjected to snow load.
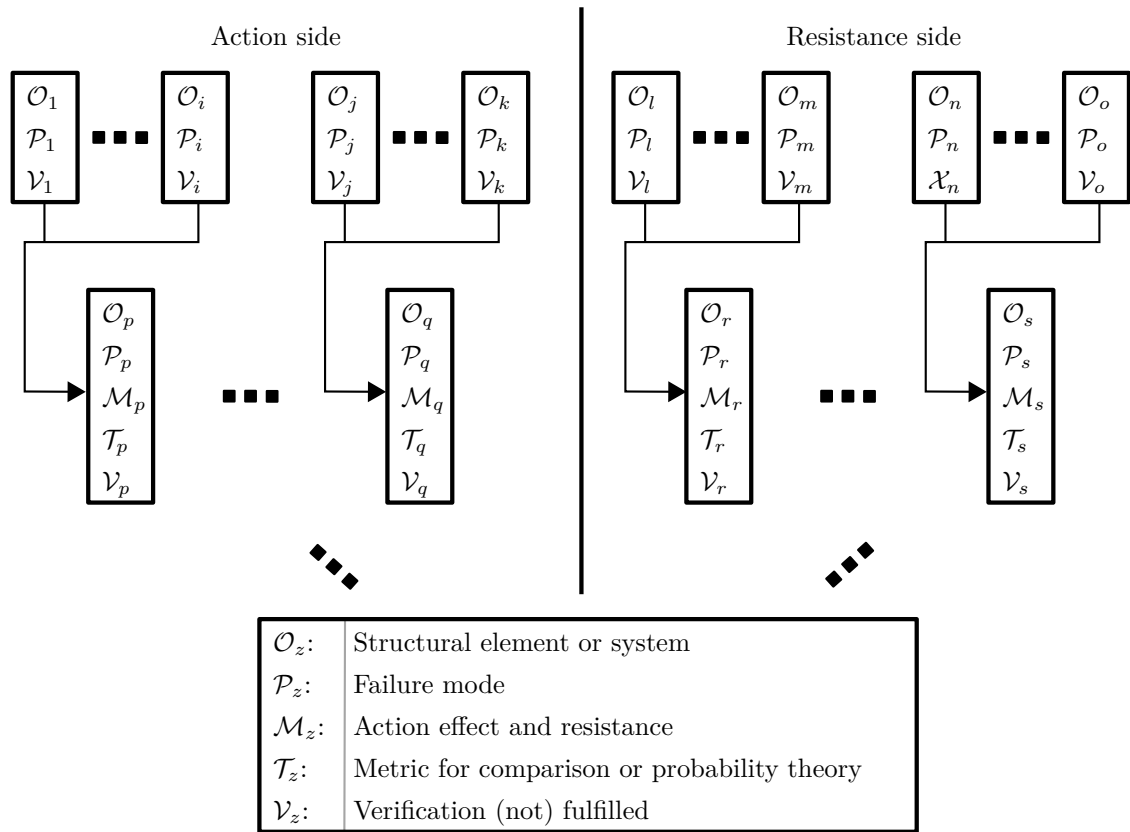
Fig. 2.3.: Mask version of a tree representing a structural design method.

Remark: In some cases, the resistance model can depend on actions and the structural model can depend on material properties. Moreover, the resistance model and the structural model may be combined into a single model. Such cases are not covered within the scope of this thesis.

$\mathcal{O}$: Snow year #1
$\mathcal{P}$: Maximal snow depth
$\mathcal{V}$: 540 [mm]

$\blacksquare\blacksquare\blacksquare$

$\mathcal{O}$: Snow year #t
$\mathcal{P}$: Maximal snow depth
$\mathcal{V}$: 700 [mm]

$\mathcal{O}$: Beam #1
$\mathcal{P}$: Bending strength
$\mathcal{V}$: 71 [N/mm^2]

$\blacksquare\blacksquare\blacksquare$

$\mathcal{O}$: Beam #n
$\mathcal{P}$: Bending strength
$\mathcal{V}$: 75 [N/mm^2]

$\mathcal{O}$: Snow in year # t+1
$\mathcal{P}$: Maximal snow depth
$\mathcal{M}$: Statistical model
$\mathcal{T}$: Probability theory
$\mathcal{V}$: 950 [mm]

$\mathcal{O}$: Hypothetical beam in bending
$\mathcal{P}$: Bending moment
$\mathcal{M}$: Statistical model
$\mathcal{T}$: Probability theory
$\mathcal{V}$: 65 [N/mm^2]

$\mathcal{O}$: Beam #n+1
$\mathcal{P}$: Bending moment
$\mathcal{M}$: Structural model with planned beam length
$\mathcal{T}$: Newton's Mechanic
$\mathcal{V}$: $9.5 \cdot 10^6$ [Nmm]

$\mathcal{O}$: Beam #n+1
$\mathcal{P}$: Maximal bending resistance
$\mathcal{M}$: Cross-section area with planned dimensions
$\mathcal{T}$: Euler Bernoulli beam theory
$\mathcal{V}$: $10.8 \cdot 10^6$ [Nmm]

$\mathcal{O}$: Beam #n+1
$\mathcal{P}$: Bending failure
$\mathcal{M}$: Bending moment and maximal bending resistance
$\mathcal{T}$: Metric for comparison: $\leq$
$\mathcal{V}$: Verification fulfilled

Fig. 2.4.: Example of the structural design verification procedure of a beam under snow load visualized as a tree.

2.3. The Partial safety factor concept

The PSF concept is the most popular concept in modern structural design codes. It is a semi-probabilistic concept, i.e., it is based on probabilistic models. From these probabilistic models, three different safety components are derived: The characteristic values, the PSF, and the combination factors. Characteristic values are usually determined from statistics as lower quantile values of material strengths and higher quantile values of actions. The PSFs are typically values greater than 1 increasing the actions via multiplication and decreasing resistances via division; hence, they increase the resulting design resistances. The combination factors are applied multiplicatively to variable actions. Their values are typically less than 1, hence, they decrease the resulting design resistances. They are justified by the fact that multiple variable actions may not act simultaneously, hence, their maxima may occur at different points in time. Both, the PSFs and the combination

factors are derived via code calibration processes. With the help of these three safety components, structural design in practice requires deterministic calculations only.

In this thesis, the nomenclature of the PSF concept implemented in Eurocode 0 [25] is used; however, all investigations and results can be transferred to other semi-probabilistic design codes (e.g., [54–57]). Various points of view of the PSF concept are outlined. This includes the deterministic view (Sec. 2.3.1), the probabilistic view (Sec. 2.3.2), the portfolio view (Sec. 2.3.3), the system-level view (Sec. 2.3.4), and the calibration view (Sec. 2.3.5).

2.3.1. Deterministic view

Verification of an element failure mechanism is typically conducted by proving that the design resistance against that failure mechanism $r_{d,EC}$ is greater than or equal to the action effect on that failure mechanism $e_{d,EC}$:

$$r_{d,EC} \geq e_{d,EC} \tag{2.1}$$

The subscript EC is added to the design values and also to several subsequent values, functions, and distributions to emphasize that these quantities are nominal quantities, including epistemic uncertainties of the Eurocode models.

In the derivation of $e_{d,EC}$ and $r_{d,EC}$, one can identify four different models being involved: The action models, the material models, the structural model, and the resistance model. Fig. 2.6 illustrates these models using the nomenclature of Sec. 2.2.

The action models represent permanent and variable actions. This is typically done via statistical models, which – in a second step – provide deterministic values: The so-called characteristic actions $l_{k,EC}$. Those values are the input to a structural model which provides a function $t_{S,EC}$ to calculate the action effect of the considered element failure mechanism. Typically, multiple load case combinations need to be checked to find the ultimately relevant load case combination.

The material models represent various material strengths. This is again typically done via statistical models, which – in a second step – provide deterministic values: The characteristic material strengths $m_{k,EC}$. Those values are the input to a resistance model which provides a function $t_{R,EC}$ to calculate the resistance against the considered element failure mechanism.

On the basis of these four models, the design action effect and the design resistance of

Action side

$\mathcal{O}$:	Action #1
$\mathcal{P}$:	Action phenomenon #1
$\mathcal{M}$:	Action model #1
$\mathcal{T}$:	Action theory #1
$\mathcal{V}$:	Characteristic action $l_{k,EC,1}$

$\vdots$

$\mathcal{O}$:	Action #n
$\mathcal{P}$:	Action phenomenon #n
$\mathcal{M}$:	Action model #n
$\mathcal{T}$:	Action theory #n
$\mathcal{V}$:	Characteristic action $l_{k,EC,n}$

Apply PSFs $\gamma_{f,1...n}$ and combination factors ψ_0, ψ_1, ψ_2

$\mathcal{O}$:	Structural element
$\mathcal{P}$:	Action effect
$\mathcal{M}$:	Structural model
$\mathcal{T}$:	Structural theory
$\mathcal{V}$:	Action effect value

Apply PSF γ_{Sd}

Design action effect $e_{d,EC}$

Resistance side

$\mathcal{O}$:	Material #1
$\mathcal{P}$:	Material phenomenon #1
$\mathcal{M}$:	Material model #1
$\mathcal{T}$:	Material theory #1
$\mathcal{V}$:	Characteristic strenght $m_{k,EC,1}$

$\vdots$

$\mathcal{O}$:	Material #m
$\mathcal{P}$:	Material phenomenon #m
$\mathcal{M}$:	Material model #m
$\mathcal{T}$:	Material theory #m
$\mathcal{V}$:	Characteristic strenght $m_{k,EC,m}$

Apply PSFs $\gamma_{m,1...n}$

$\mathcal{O}$:	Structural element
$\mathcal{P}$:	Resistance
$\mathcal{M}$:	Resistance model
$\mathcal{T}$:	Resistance theory
$\mathcal{V}$:	Resistance value

Apply PSF γ_{Rd}
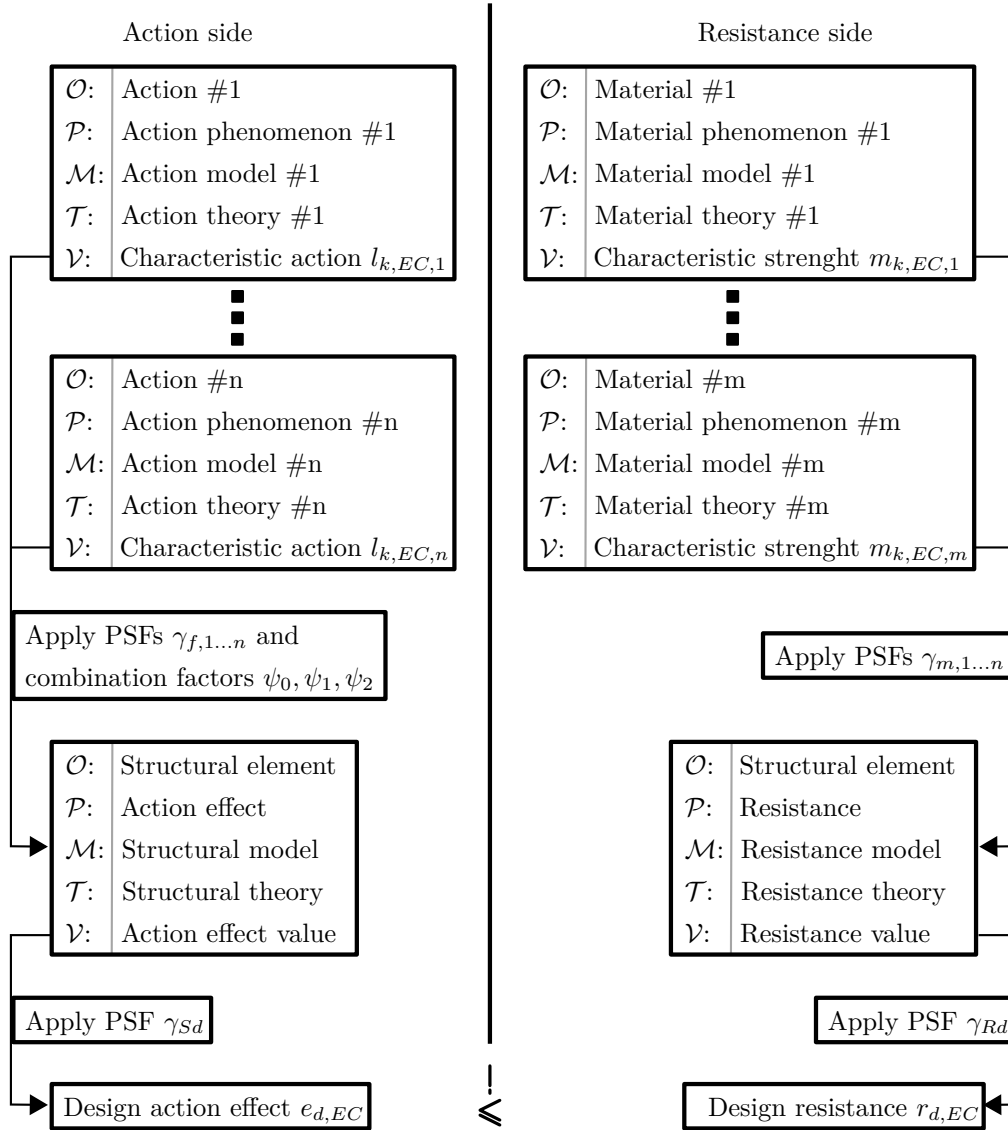
Design resistance $r_{d,EC}$

Fig. 2.5.: Illustration of the derivation of the design actions and design resistances following the nomenclature of Sec. 2.2.

Eqn. 2.1 can be calculated as

$$e_{d,EC} = \gamma_{Sd} \cdot t_{S,EC}(\gamma_{f,1} \cdot l_{k,EC,1}, \cdots, \gamma_{f,i} \cdot l_{k,EC,i}, \quad \text{Permanent actions} \tag{2.2}$$
$$\gamma_{f,i+1} \cdot l_{k,EC,i+1}, \quad \text{Leading variable action}$$
$$\left.\begin{array}{l}\gamma_{f,i+2} \cdot \psi_{i+2} \cdot l_{k,EC,i+2}, \ldots, \\ \gamma_{f,n} \cdot \psi_n \cdot l_{k,EC,n}\end{array}\right\} \quad \text{Accompanying variable actions}$$

$$r_{d,EC} = \frac{t_{R,EC}\left(\frac{m_{k,EC,1}}{\gamma_{m,1}}, \ldots, \frac{m_{k,EC,i}}{\gamma_{m,i}}\right)}{\gamma_{Rd}} \tag{2.3}$$

where γ_f, γ_{Sd}, γ_m, and γ_{Rd} are PSF accounting for the model uncertainties of the action, structural, material, and resistance model. ψ_i are the combination factors considering the unlikely event of simultaneously high variable loads.

Typically, the design action effect $e_{d,EC}$ is calculated first and then the design parameters of the resistance model (e.g., the height and width of a beam) are chosen such that the design resistance $r_{d,EC}$ is greater or equal to $e_{d,EC}$. If they are equal, this usually corresponds to the most material-efficient solution. In some cases, the structural model depends on the resistance model (e.g., cross-section dimensions influence the bending stiffness of beams, which affects the action effects in the statically overdetermined case). In those cases, the determination of the design values becomes an iterative process.

Assuming that only a single action is present and only a single material is included in the resistance calculation, Eqns. 2.2 and 2.3 can be simplified to

$$e_{d,EC} = \gamma_{Sd} \cdot t_{S,EC}(\gamma_f \cdot l_{k,EC}) \tag{2.4}$$

$$r_{d,EC} = \frac{t_{R,EC}\left(\frac{m_{k,EC}}{\gamma_m}\right)}{\gamma_{Rd}} \tag{2.5}$$

In the following, this simplified case is further illustrated.

To make the application of PSF user-friendly, the Eurocode merges the PSFs of the action and the resistance side:

$$\gamma_F = \gamma_f \times \gamma_{Sd} \tag{2.6}$$
$$\gamma_M = \gamma_m \times \gamma_{Rd} \tag{2.7}$$

Although this merge simplifies the design process, it raises the question if γ_F and γ_M should be applied to the characteristic values l_k and m_k directly or to $t_S(l_k)$ and $t_R(m_k)$. As long as t_S and t_R are linear functions through the origin, both options lead to the same design values; however, if t_S and t_R are non-linear functions or do not pass through the origin, the two alternatives result in different design values and, therefore, in different structural reliabilities. The two respective basic design options regarding the structural model are

Design option (1) (prior to $t_{S,EC}$): $\qquad e_{d,EC} = t_{S,EC}(\gamma_F \cdot l_{k,EC})$ (2.8)

Design option (2) (posterior to $t_{S,EC}$): $\qquad e_{d,EC} = \gamma_F \cdot t_{S,EC}(l_{k,EC})$ (2.9)

and analogously for the resistance model

Design option (1) (prior to $t_{R,EC}$): $\qquad r_{d,EC} = t_{R,EC}(\gamma_M \cdot m_{k,EC}) \qquad$ (2.10)

Design option (2) (posterior to $t_{R,EC}$): $\qquad r_{d,EC} = \gamma_M \cdot t_{R,EC}(m_{k,EC}) \qquad$ (2.11)

Eurocode provides simplified rules on how to choose between the two basic design options when it comes to the structural model. Those rules and their effects on the structural reliability will be discussed in depth in Sec. 5.

The basic design options of the resistance model are not mentioned/covered by Eurocode. In practice, design option (1) is typically chosen. This thesis does not further investigate the two basic design options of the resistance model.

2.3.2. Probabilistic view

The choice of the three safety components – the characteristic values, the PSFs, and the combination factors – should be based on reliability analysis. A reliability analysis also includes the four models mentioned above: The action model, the structural model, the material model, and the resistance model. In fact, these models are typically used twice. Once in a deterministic manner to determine a design and a second time in a probabilistic manner to determine the probability of failure given the design. The models used to determine the design and the models used to calculate the probability of failure can differ. The following sections illustrate the application of the various models within a structural reliability analysis of codified design structures.

2.3.2.1. Simplified probabilistic view

Fig. 2.6 illustrates the common probabilistic view of the resistance model and the action effect model. The material model and the action model are only implicitly included as inputs to the resistance model and the action effect model. Eurocode itself does not provide the distributions R_{EC} and E_{EC} corresponding to the resistance model and the action effect model but only the corresponding characteristic values and the PSFs. The distribution can be implicitly inferred from background documentations (e.g., [58–60]) and from the distributions used in the calibration of the Eurocode safety components (e.g., [61]).
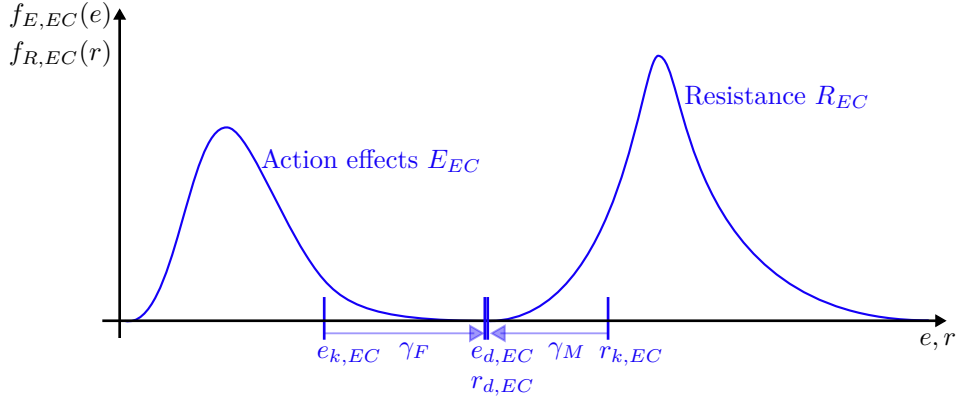
Fig. 2.6.: Basic reliability problem according to Eurocode models.

To calculate the nominal probability of failure according to Eurocode models given a Eurocode design, the following limit state function (LSF) can be formulated:

$$g = R_{EC} - E_{EC} \tag{2.12}$$

The corresponding nominal probability of failure is calculated as

$$\Pr(F; \mathcal{D}_{EC}, \mathcal{R}_{EC}) = \int_{\{g<0\}} f_{R_{EC}E_{EC}}(r,e) \, \mathrm{d}r \, \mathrm{d}e \tag{2.13}$$

where $f_{R_{EC}E_{EC}}$ is the joint PDF of R_{EC} and E_{EC}, $\mathcal{D}_{EC}$ represents the design choices according to Eurocode and $\mathcal{R}_{EC}$ represents the probabilistic choices within the reliability analysis according to Eurocode. Hence, as mentioned above, the probability of failure is conditional on the models used in the design and in the reliability analysis. Unless it is important for the context, this condition is omitted in the rest of this thesis.

Given the probability of failure, the corresponding reliability index β is calculated as

$$\beta = -\Phi^{-1}\left(\Pr(F)\right) \tag{2.14}$$

where Φ^{-1} is the inverse cumulative distribution function (CDF) of the standard normal distribution.

The integral of Eqn. 2.13 can not always be solved analytically. Within this thesis, non-analytically solvable cases are covered by estimating the probability of failure either through numerical integration methods, crude Monte Carlo estimation (MC) [62,63], Subset Simulation (SuS) [64–66] or the First Order Reliability Method (FORM) [38,67–69]. MC is a sampling-based method suitable for high dimensional LSFs; however, it is only applicable for high or medium probabilities of failure. SuS is an adaptive sampling method that is suitable for high-dimensional LSFs and small probabilities of failure. FORM is the method that forms the historical basis of the PSF concept. FORM transforms the limit state surface into standard normal space and approximates it by its tangent hyperplane at the point closest to the origin (called the FORM design point). The design point resulting from a PSF design (e_d, r_d) is ideally close to the FORM design point [38]. The definition of

the reliability index is closely related to the FORM method: The reliability index is equal to the distance of the FORM design point from the origin in case of uncorrelated standard normal random variables and a linear LSF; however, in other cases, the reliability index may differ from this distance depending on the non-linearity of the limit state surface in standard normal space. If multiple LSFs are investigated, representing multiple failure modes of one structure, FORM for series systems can be applied to estimate the system reliability index [70].

2.3.2.2. Detailed probabilistic view

A more in-depth view (compared to the classic view illustrated in Fig. 2.6) is illustrated in Fig. 2.7. This illustration explicitly includes all four models within a structural design: The action model and the material model are included via PDFs of the action $f_{L,EC}$ and the material strength $f_{m,EC}$, the structural model and the resistance model are represented via functions $t_{S,EC}$ and $t_{R,EC}$ which transform actions and material strength into action effects and resistances.
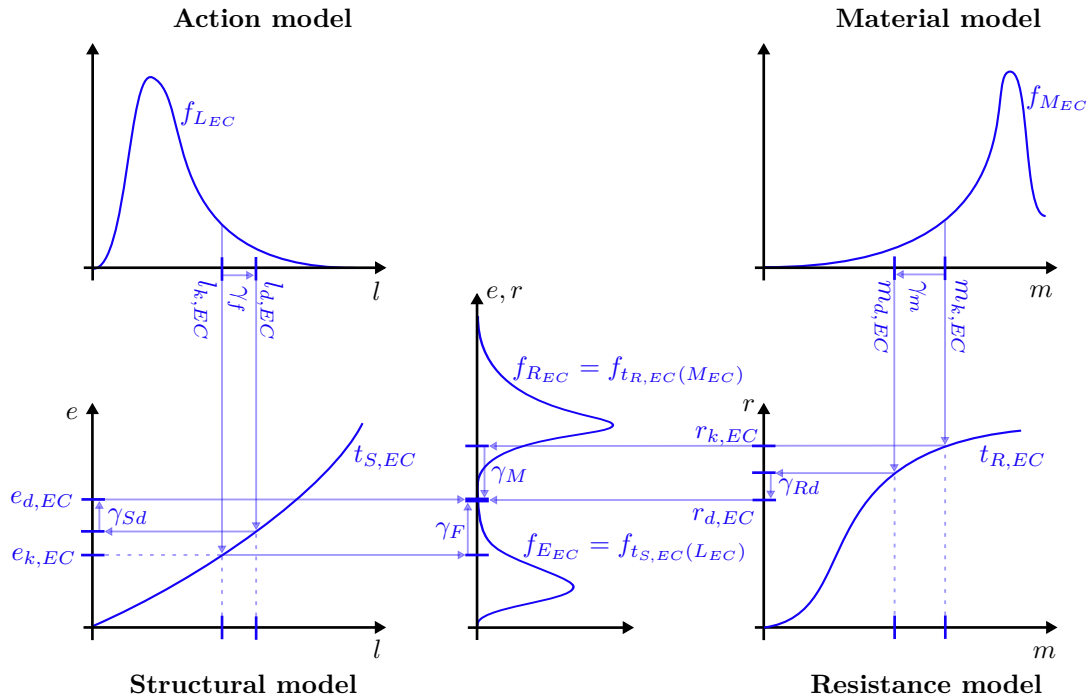
Fig. 2.7.: Illustration of the basic reliability problem and its relation to Eurocode models.

In the context of this in-depth consideration, the LSF of Eqn. 2.12 can be reformulated with explicit consideration of all four models:

$$g = t_{R,EC}(M_{EC}, \mathcal{D}_{EC}) - t_{S,EC}(L_{EC}) \tag{2.15}$$

where $\mathcal{D}_{EC}$ represents the design choices within the resistance model (e.g., cross-section dimensions or positioning of steel reinforcements). The space of possible $\mathcal{D}_{EC}$ follows from

the requirement that the design resistance is greater or equal to the design action effect (see Eqn. 2.1):

$$r_{d,EC} \overset{!}{\geq} e_{d,EC} \tag{2.16}$$

$$\Leftrightarrow \quad \frac{1}{\gamma_{Rd}} \cdot t_{R,EC}\left(\frac{m_{k,EC}}{\gamma_m}, \mathcal{D}_{EC}\right) \geq \gamma_{Sd} \cdot t_{S,EC}\left(\gamma_f \cdot l_{k,EC}\right)$$

A design can be considered optimal (in the sense of the PSF concept) if equality holds in Eqn. 2.16. Assuming such an optimal choice and further assuming that $\mathcal{D}_{EC}$ can be expressed through a single design parameter $\mathcal{P}_{EC}$ (e.g., the cross-section area), it follows that

$$\mathcal{P}_{EC} = t_{R,EC}^{-1}\left(\frac{m_{k,EC}}{\gamma_m}, \gamma_{Rd} \cdot \gamma_{Sd} \cdot t_{S,EC}\left(\gamma_f \cdot l_{k,EC}\right)\right) \tag{2.17}$$

where $t_{R,EC}^{-1}$ is the inverse function of $t_{R,EC}$ with respect to its second variable (design parameter). This inverse function only exists if $t_{R,EC}$ is a strictly monotone function with respect to its second variable; however, this is a reasonable assumption since the resistance typically increases with increasing design parameters. Thus, the LSF of Eqn. 2.15 can be reformulated as

$$g = t_{R,EC}\left(M_{EC}, t_{R,EC}^{-1}\left(\frac{m_{k,EC}}{\gamma_m}, \gamma_{Rd} \cdot \gamma_{Sd} \cdot t_{S,EC}\left(\gamma_f \cdot l_{k,EC}\right)\right)\right) - t_{S,EC}(L_{EC}) \tag{2.18}$$

Given this LSF, the nominal probability of failure according to Eurocode given an Eurocode design can be determined. This includes the epistemic uncertainties associated with the Eurocode models. To calculate purely aleatoric values and the purely aleatoric probability of failure, the purely aleatoric models need to be known. Fig. 2.8 re-illustrates Fig. 2.7 including the aleatoric distribution of the load L and the material property M and the functions t_E (aleatoric relationship between action and action effect) and t_R (aleatoric relationship between material property and resistance). From L and M, the corresponding characteristic values l_k and m_k can be obtained, and, by applying the PSFs, the design values l_d and m_d are obtained. Using the functions t_S and t_R, the characteristic values e_k and r_k, and the associated design values e_d and r_d are derived. These are the values to which the respective Eurocode values converge when all epistemic uncertainties vanish. In this sense, they can be interpreted as target values of the Eurocode models.
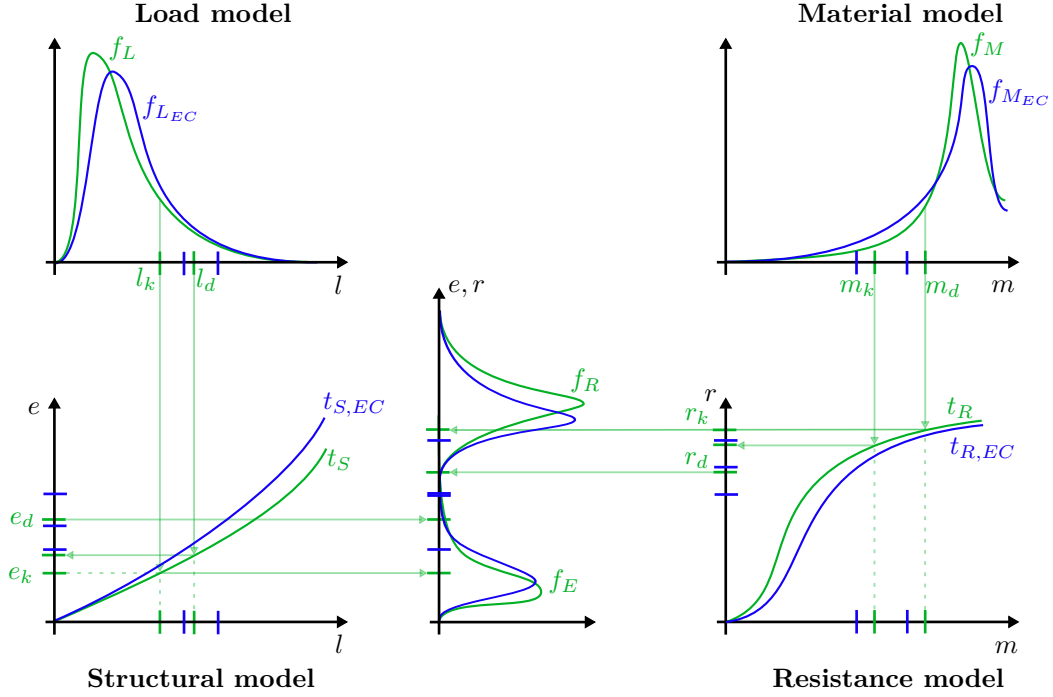
Fig. 2.8.: Illustration of the Design approach of the Eurocode (blue) compared to the purely aleatoric models (green) for one specific design situation.

Applying the purely aleatoric models, the following LSF can be formalized

$$g = t_R(M, \mathcal{D}_{EC}) - t_S(L) \tag{2.19}$$

Following Eqn. 2.17, this can be rewritten as

$$g = t_R\left(M, t_{R,EC}^{-1}\left(\frac{m_{k,EC}}{\gamma_m}, \gamma_{Rd} \cdot \gamma_{Sd} \cdot t_{S,EC}\left(\gamma_f \cdot l_{k,EC}\right)\right)\right) - t_S(L) \tag{2.20}$$

Given this LSF, the purely aleatoric probability of failure given a Eurocode design can be calculated.

The LSF of Eqn. 2.20 can be simplified if certain assumptions about the functions t_R, $t_{R,EC}$, t_S and $t_{S,EC}$ can be made. In the following, various possible assumptions are demonstrated:

- One possible assumption regarding the resistance side is that t_R and $t_{R,EC}$ are multiplicatively separable functions, hence, can be written as

$$t_R(m,p) = t_{R,m}(m) \cdot t_{R,p}(p) \tag{2.21}$$
$$t_{R,EC}(m,p) = t_{R,EC,m}(m) \cdot t_{R,EC,p}(p) \tag{2.22}$$

where $t_{R,p}$ and $t_{R,EC,p}$ are functions of the design choices and $t_{R,m}$ and $t_{R,EC,m}$ are

functions of the material strength. This simplifies Eqn. 2.20 to

$$g = t_{R,p} \left(t_{R,EC,p}^{-1} \left(\frac{\gamma_{Rd} \cdot \gamma_{Sd} \cdot t_{S,EC} \left(\gamma_f \cdot l_{k,EC} \right)}{t_{R,EC,m} \left(\frac{m_{k,EC}}{\gamma_m} \right)} \right) \right) \cdot t_{R,m} \left(M \right) - t_S(L) \quad (2.23)$$

If one additionally assumes that the functions $t_{R,p}$ and $t_{R,EC,p}$ are the same, the LSF can be further simplified to

$$g = \frac{\gamma_{Rd} \cdot \gamma_{Sd} \cdot t_{S,EC} \left(\gamma_f \cdot l_{k,EC} \right)}{t_{R,EC,m} \left(\frac{m_{k,EC}}{\gamma_m} \right)} \cdot t_{R,m} \left(M \right) - t_S(L) \quad (2.24)$$

- A special case of the multiplicative separability is the assumption that t_R and $t_{R,EC}$ are linear with respect to p and go through the origin, hence, can be written as

$$t_R(m,p) = t_{R,m}(m) \cdot p \cdot c \qquad\qquad c \in \mathbb{R}^+ \qquad (2.25)$$
$$t_{R,EC}(m,p) = t_{R,EC,m}(m) \cdot p \cdot c_{EC} \qquad\qquad c_{EC} \in \mathbb{R}^+ \qquad (2.26)$$

This simplifies Eqn. 2.20 to

$$g = \frac{\gamma_{Rd} \cdot \gamma_{Sd} \cdot t_{S,EC} \left(\gamma_f \cdot l_{k,EC} \right) \cdot c}{t_{R,EC,m} \left(\frac{m_{k,EC}}{\gamma_m} \right) \cdot c_{EC}} \cdot t_{R,m} \left(M \right) - t_S(L) \quad (2.27)$$

If one additionally assumes that $c = c_{EC}$, the LSF can be further simplified to

$$g = \frac{\gamma_{Rd} \cdot \gamma_{Sd} \cdot t_{S,EC} \left(\gamma_f \cdot l_{k,EC} \right)}{t_{R,EC,m} \left(\frac{m_{k,EC}}{\gamma_m} \right)} \cdot t_{R,m} \left(M \right) - t_S(L) \quad (2.28)$$

- Another special case of the multiplicative separability is the assumption that t_R and $t_{R,EC}$ are linear with respect to m and through the origin:

$$t_R(m,p) = t_{R,p}(p) \cdot m \cdot c \qquad\qquad c \in \mathbb{R}^+ \qquad (2.29)$$
$$t_{R,EC}(m,p) = t_{R,EC,p}(p) \cdot m \cdot c_{EC} \qquad\qquad c_{EC} \in \mathbb{R}^+ \qquad (2.30)$$

This simplifies Eqn. 2.20 to

$$g = t_{R,p} \left(t_{R,EC,p}^{-1} \left(\frac{\gamma_m \cdot \gamma_{Rd} \cdot \gamma_{Sd} \cdot t_{S,EC} \left(\gamma_f \cdot l_{k,EC} \right)}{m_{k,EC} \cdot c_{EC}} \right) \right) \cdot M \cdot c - t_S(L) \quad (2.31)$$

If one additionally assumes that the functions $t_{R,p}$ and $t_{R,EC,p}$ are the same, the LSF can be further simplified to

$$g = \frac{\gamma_m \cdot \gamma_{Rd} \cdot \gamma_{Sd} \cdot t_{S,EC} \left(\gamma_f \cdot l_{k,EC} \right)}{m_{k,EC}} \cdot M - t_S(L) \quad (2.32)$$

- A possible assumption regarding the action side is that t_S and $t_{S,EC}$ are linear:

$$t_S(l) = c_1 \cdot l + c_2 \qquad\qquad c_1, c_2 \in \mathbb{R}^+ \qquad\qquad (2.33)$$
$$t_{S,EC}(l) = c_{1,EC} \cdot l + c_{2,EC} \qquad\qquad c_{1,EC}, c_{2,EC} \in \mathbb{R}^+ \qquad\qquad (2.34)$$

This simplifies Eqn. 2.20 to be

$$g = t_R\left(M, t_{R,EC}^{-1}\left(\frac{m_{k,EC}}{\gamma_m}, \gamma_{Rd} \cdot \gamma_{Sd} \cdot (c_{1,EC} \cdot \gamma_f \cdot l_{k,EC} + c_{2,EC})\right)\right) - (c_1 \cdot L + c_2) \qquad (2.35)$$

- A common form of the LSF follows from the combination of the assumptions that $t_R = t_{R,EC}$ is linear with respect to m and goes through the origin as well as $t_S = t_{S,EC}$ is linear and goes trough the origin. From this Eqn. 2.20 can be written as

$$g = \frac{\gamma_m \cdot \gamma_{Rd} \cdot \gamma_{Sd} \cdot \gamma_f \cdot l_{k,EC}}{m_{k,EC}} \cdot M - L \qquad (2.36)$$

Applying the merge of the PSF according to Eqn. 2.6 and 2.7, the LSF can be rewritten as

$$g = \frac{\gamma_M \cdot \gamma_F \cdot l_{k,EC}}{m_{k,EC}} \cdot M - L \qquad (2.37)$$

This LSF is often used in code (re)calibrations to represent design situations of the PSF concept in a general way (e.g., in [61]). It can also be found in Eurocode 0 [25]. However, if this LSF is used, one should be aware of the numerous assumptions that are necessary to reach this simplified form.

It should be noted that – under specific assumptions – the probability of failure is invariant to scaling of t_S, $t_{S,EC}$, t_R or $t_{R,EC}$. This signifies that t_S and $t_{S,EC}$ or t_R and $t_{R,EC}$ can be redefined and replaced without effecting the resulting probability of failure as follows

$$\widetilde{t}_S(x) := c \cdot t_S(x) \qquad\qquad c \in \mathbb{R} \qquad\qquad (2.38)$$
$$\widetilde{t}_{S,EC}(x) := c \cdot t_{S,EC}(x) \qquad\qquad\qquad\qquad (2.39)$$

or

$$\widetilde{t}_R(x) := c \cdot t_R(x) \qquad\qquad c \in \mathbb{R} \qquad\qquad (2.40)$$
$$\widetilde{t}_{R,EC}(x) := c \cdot t_{R,EC}(x) \qquad\qquad\qquad\qquad (2.41)$$

The assumptions necessary for such a replacement are those needed in the formulation of the LSFs 2.24, 2.27, 2.28, 2.32, and 2.37. The invariance to scaling is the reason why normalized random variables (random variables with a mean of 1) can be used in numerous investigations of the PSF concept (e.g., [61, 71, 72]).

2.3.3. Portfolio view

The previous sections (Sec. 2.3.1, 2.3.2.1, and 2.3.2.2) focus on a single design situation; however, the PSF is developed to be applicable in a wide range of design situations. Hence, LSFs like Eqn. 2.12 to Eqn. 2.37 slightly differ for different application cases of the same models. The portfolio view tries to capture this variability. A portfolio can, in principle, be formalized in two different ways:

The first approach covers the variability of the portfolio via multiple LSFs representing the full spectrum of the considered portfolio. The LSFs can be combined with weighting factors to cover their respective relative occurrence rates within the portfolio. This approach is applied in Sec. 3.4.1 to formalize a portfolio of road bridges.

The second approach uses a single but generic LSF. Such a generic LSF can be derived by generalizing one variation of the LSFs of Sec. 2.3.2.2. Such a generalization should distinguish between aleatoric quantities and nominal quantities. The generalization of the aleatoric quantities modifies t_S, t_R, M, and L. The generalization of the nominal quantities modifies $t_{S,EC}$, $t_{R,EC}$, $m_{k,EC}$, and $l_{k,EC}$. How these modifications can be conducted is discussed in the following:

- The random variables M and L can be modified such that they cover not only the material strength and the action of a specific design situation but the material strength and the action of the full spectrum of the portfolio. E.g., the distribution of the strengths of a certain type of timber can be generalized to cover various types of timber or the distribution of the wind load of a specific location can be generalized to represent the wind load of a larger area.

- The characteristic material strength $m_{k,EC}$ and the characteristic action $l_{k,EC}$ can be represented probabilistically within a generic LSF. This seems to be counter-intuitive since structural design codes require the same characteristic values for various design situations within a portfolio, hence, those values are deterministic. However, the relationship of the nominal characteristic value to the purely aleatoric distributions M and L per design situation may differ in the sense that they represent different quantile values of their respective purely aleatoric distributions. The distributions of $m_{k,EC}$ and $l_{k,EC}$ can be included by studying the relationship between the nominal characteristic values according to the code and the purely aleatoric characteristic value. The relationship is typically represented by the following relative error:

$$\Theta^{-1} = \frac{\text{Nominal characteristic value}}{\text{Aleatoric characteristic value}} \tag{2.42}$$

  In literature, this error is typically defined the other way around, namely, as the error of the aleatoric value relative to the nominal value. To be consistent with literature, Eqn. 2.42 denotes the error as an inverse relative error.

  If the distribution of Θ^{-1} and the distribution of the aleatoric characteristic value are determined, Eqn. 2.42 can be rearranged to determine the distribution of the nominal characteristic value.

The issue of a probabilistic representation of $m_{k,EC}$ and $l_{k,EC}$ is especially important when it comes to investigations of hidden safeties. An example is given in Sec. 3.3.3.1 and Sec. 3.3.3.2 for the case of the characteristic values of the Eurocode wind load model and advanced wind load modeling techniques.

- If the structural model or the resistance model differ over the domain of all possible design situations, the functions t_S, t_R, $t_{S,EC}$ or $t_{R,EC}$ can be modified. They are either replaced by a functional that covers each design situation of the considered portfolio individually or a probabilistic component is added (e.g., a multiplicative model uncertainty) that covers the variability of the models within the portfolio. The structural and resistance models on portfolio-level are denoted by T_S and T_R, respectively.

In some cases, the two above approaches to represent a portfolio of design situations (either via multiple LSFs or via a single generic LSF) can be combined, meaning that a portfolio may be represented via multiple generic LSFs, each representing a subset of the portfolio. One example is the portfolio utilized in the revision of the Eurocode [61]. This portfolio is summarized in Annex A and applied in Sec. 3.3.5 and Sec. 4.5.

2.3.4. System-level view

In general, the PSF concept verifies structural safety at the element-level. For each structure, various element failure mechanisms (e.g., bending failure of a beam, punching shear of a column or maximum tensile strength of a membrane) need to be taken into account. Some elements require multiple verifications (e.g., a beam may be verified against bending failure, shear failure, and failure due to stability reasons). A verification at the system-level is not conducted. However, in some cases, the failure of an element directly leads to the failure of the system; therefore, the system reliability can be lower than the one at the element-level. In other cases, element failure does not directly lead to system failure because of redundancies. The system reliability can therefore be higher than the reliability at the element-level. Back when the PSF concept was introduced, the research community was aware of this issue: "Since the knowledge of system reliability is incomplete and not sufficiently documented for practice, a quantitative assessment of different structural systems is not intended" [36]. Therefore, a system-level view of the PSF concept does not exist.

Today, system reliability is well studied and applicable outside the scope of the PSF concept. Various methods exist to evaluate system reliability and determine a robust structural design [38, 73–75]. However, none of these methods can be transferred to be applicable within the PSF concept. Sec. 4 addresses this problem and derives an additional PSF to include system effects within the PSF concept.

2.3.5. Calibration view

There are many different reasons for the calibration of the PSF concept, including new modeling approaches, changes in safety requirements, the incorporation of experience gained since the last calibration, changes on the load side or the development of new types of construction materials. In general, two calibration approaches of the PSF concept can be distinguished: The risk-based approach and the reliability-based approach [76].

Out of the two, the risk-based approach is the higher-level approach. A full risk analysis includes the reliability of a structure and the consequences of its failure to minimize the overall risk. ISO 2394:2015 [23] provides principles for performing such an analysis. A risk-based code calibration of the PSF concept adapts the safety components of the PSF concept such that the overall risk of a portfolio of considered design situations is minimized [77]. A generic framework of risk-based code calibration is given in [78]. Overall, the consideration of consequences makes the risk-based code calibrations rather complex; therefore, applications are limited. Examples can be found in [79–81]. In this thesis, risk-based code calibration is not considered.

The reliability-based calibration approach ensures that a certain target reliability is – on average – achieved within a portfolio of considered design situations [82–84]. Applications can be found in [71, 72, 85–88]. A reliability-based code calibration can be divided into two main steps. In the first step, a target value needs to be defined. In the second step, the safety components of the PSF concept need to be adjusted to match this target value. Both steps are described in the following two sections.

2.3.5.1. Defining a target reliability for reliability-based code calibration

Typically, a target reliability is defined as the average reliability of the status quo (e.g., [61, 84]). This value is found by investigating the reliability of the current design choices (if no calibration has been conducted yet) within a representative portfolio of design situations. If the portfolio is described via a set of multiple LSFs, the target probability of failure can be defined as the weighted average of the aleatoric probability of failure

$$\Pr(F)_{TRG} = \frac{1}{\sum_i w_i} \cdot \sum_i w_i \cdot \Pr\left(F; \mathcal{D}_{EC,i}, \mathcal{R}_i\right) \tag{2.43}$$

where $\Pr\left(F; \mathcal{D}_{EC,i}, \mathcal{R}_i\right)$ is the aleatoric probability of failure given the design choices $\mathcal{D}_{EC,i}$ of the i-th limit state according to the current code and derived via a purely aleatoric reliability analysis $\mathcal{R}_i$. w_i are the weights of the i-th design situation. Similarly, a target reliability index can be defined as

$$\beta_{TRG} = \frac{1}{\sum_i w_i} \cdot \sum_i w_i \cdot \left(-\Phi^{-1}\left(\Pr\left(F; \mathcal{D}_{EC,i}, \mathcal{R}_i\right)\right)\right) \tag{2.44}$$

Note that the target probability of failure derived via Eqn. 2.43 transformed to the reliability index is unequal to the target reliability index derived via Eqn. 2.44 ($\beta_{TRG} \neq$

$-\Phi^{-1}\left(\Pr(F)_{TRG}\right)$). Both approaches are viable as long as the respective subsequent calibration is conducted using the same approach. If this is the case, the results in calibration differ only marginally.

Remark: If the portfolio is represented by a single but general LSF, the calculation of the weighted average is not necessary and the target values are obtained directly.

2.3.5.2. Performing the calibration to match the target reliability

Given a target reliability, the calibration can be performed in various ways. The most straightforward way follows from the requirement to preserve the same level of safety as prior to the calibration, hence, to fulfill the following equation:

$$\frac{1}{\sum_i w_i} \cdot \sum_i w_i \cdot \Pr\left(F; \mathcal{D}_{ADP,i}, \mathcal{R}_i\right) \overset{!}{=} \Pr(F)_{TRG} \tag{2.45}$$

or – in case of a target reliability index – to fulfill

$$\frac{1}{\sum_i w_i} \cdot \sum_i w_i \cdot \left(-\Phi^{-1}\left(\Pr\left(F; \mathcal{D}_{ADP,i}, \mathcal{R}_i\right)\right)\right) \overset{!}{=} \beta_{TRG} \tag{2.46}$$

where $\mathcal{D}_{ADP,i}$ represents the design choices following the adapted PSF concept.

Eqns. 2.45 and 2.46 can be fulfilled by solving the following minimization problems:

$$v_{ADP} = \min_{v_{ADP}} \left\{ \left\| \left[\frac{1}{\sum_i w_i} \cdot \sum_i w_i \cdot \Pr\left(F; \mathcal{D}_{ADP,i}, \mathcal{R}_i\right) \right] - \Pr(F)_{TRG} \right\| \right\} \tag{2.47}$$

or

$$v_{ADP} = \min_{v_{ADP}} \left\{ \left\| \left[\frac{1}{\sum_i w_i} \cdot \sum_i w_i \cdot \left(-\Phi^{-1}\left(\Pr\left(F; \mathcal{D}_{ADP,i}, \mathcal{R}_i\right)\right)\right) \right] - \beta_{TRG} \right\| \right\} \tag{2.48}$$

where v_{ADP} is the safety component of the PSF that is adjusted and enters $\mathcal{D}_{ADP,i}$. This can, e.g., be a quantile value defining a characteristic value or the value of a PSF. In practice it may be numerically convenient to reformulate this minimization problem as a root finding problem (by deleting the absolute values).

v_{ADP} could also be a set of multiple values that are calibrated simultaneously (e.g., multiple PSFs). In this case the solution of Eqns. 2.47 and 2.48 will not be uniquely defined anymore. Some of the solutions might be very suboptimal with respect to the homogenization of the level of safety. This issue can be overcome by shifting the absolute value function to the inner of the sum.

$$v_{ADP} = \min_{ADP} \left\{ \frac{1}{\sum_i w_i} \cdot w_i \cdot \sum_i \left| \Pr\left(F; \mathcal{D}_{ADP,i}, \mathcal{R}_i\right) - \Pr(F)_{TRG} \right| \right\} \tag{2.49}$$

or

$$v_{ADP} = \min_{ADP} \left\{ \frac{1}{\sum_i w_i} \cdot w_i \cdot \sum_i \left| -\Phi^{-1} \left(\Pr \left(F; \mathcal{D}_{ADP,i}, \mathcal{R}_i \right) \right) - \beta_{TRG} \right| \right\} \qquad (2.50)$$

Eqns. 2.49 and 2.50 lead to slightly different result than Eqns. 2.47 and 2.48. As a consequence, the achieved probabilities of failure or reliability indices do not match the target values on average (Eqns. 2.45 and 2.46 are not fulfilled).

The difference between the approach of Eqns. 2.49 and 2.50, and Eqns. 2.47 and 2.48 can be understood from the following interpretation: Eqns. 2.47 and 2.48 ensure that the difference of the average of the whole portfolio to the target value is minimized; hence, they optimize the adaptation from a macro perspective. Eqns. 2.49 and 2.50 ensure that the average of the difference of the individual limit states to the target value is minimized; hence, they optimize the adaptation from a micro perspective. In the case of code calibration, the macro perspective may be more meaningful. However, Eqns. 2.49 and 2.50 have the advantage of being easily adjustable in order to give more weight to values further away from the target values, e.g., by replacing the absolute value function with a quadratic function, as follows:

$$v_{ADP} = \min_{ADP} \left\{ \frac{1}{\sum_i w_i} \cdot w_i \cdot \sum_i \left(\Pr \left(F; \mathcal{D}_{EC,ADP,i}, \mathcal{R}_i \right) - \Pr(F)_{TRG} \right)^2 \right\} \qquad (2.51)$$

or

$$v_{ADP} = \min_{ADP} \left\{ \frac{1}{\sum_i w_i} \cdot w_i \cdot \sum_i \left(-\Phi^{-1} \left(\Pr \left(F; \mathcal{D}_{ADP,i}, \mathcal{R}_i \right) \right) - \beta_{TRG} \right)^2 \right\} \qquad (2.52)$$

The approach of Eqn. 2.52 is commonly applied in code calibration (e.g. [61, 84]).

The approach of Eqns. 2.51 and 2.52 can be interpreted as an approach that minimizes the variance of the probability of failure/reliability within the portfolio. Similarly, the approach of Eqns. 2.47 and 2.48 may be interpreted as the minimization of the mean error (bias) within the portfolio. Both is desirable and may possibly be combined in the case where v_{ADP} is a set of multiple values that are calibrated simultaneously.

Eventually, the difference between the various approaches differs only marginally and the resulting calibrated values hardly differ. Within this thesis, the approach of Eqn. 2.47 is applied in Sec. 3.3.5 and the approach of Eqn. 2.48 is applied in Sec. 4.5.

3. Hidden safety in structural design codes

"Hidden safety" is a term that most engineers have a rough idea of but usually lack detailed knowledge of. The idea is typically related to the conservatism of models and the effect of this conservatism on design and structural safety. This already points in the right direction, and, in fact, a deeper understanding of the effects of hidden safety is not necessary as long as the design choices only follow the standard models provided by a structural design code (e.g. the Eurocode). In this case, hidden safety is an implicit safety component that can remain hidden from the user. This, however, changes if standard models get replaced by different – presumably more advanced and less conservative – models. Then hidden safety needs to be treated explicitly and the PSF concept needs to be adapted. This section is about the explicit inclusion of hidden safety within the PSF concept.

The challenges related to hidden safety have not received much attention in the scientific literature. Only a small number of publications explicitly mention the challenges related to hidden safety. These include Byfield and Nethercot [89], who examined various constructional steelwork resistance models (e.g., the bending resistance of restrained beams or the shear-buckling resistance of plate girders) and adapted the respective PSFs in order to homogenize the safety level. Milan et al. [90] investigated the influence of different probabilistic models (distribution choices and distribution fitting techniques) of the time-variant and time-invariant wind load model components on the probability of failure. Nowak et al. [91] calculated the probability of failure of bridges and compared it to the probability of failure including measurements of inner forces. Gomes and Beck [92] proposed a conservatism index to classify structural models. Other publications involving hidden safety include Toft et al. [93], Hanninen et al. [94], and Gazetas et al. [95]. However, none of these publications provides a general framework on how to consider hidden safety in the PSF concept.

A general framework to investigate the effects of hidden safety and how to adapt the PSF concept is given by Teichgräber et al. [96]. The framework is exemplarily applied to the wind action model of the Eurocode replacing several components of the model with more advanced modeling approaches by Teichgräber et al. [96–98]. Moreover, the framework is applied to the traffic action model LM1 of the Eurocode which is replaced by a traffic action simulation by Teichgräber et al. [99–101]. In the following, these publications are summarized (which partly includes direct copies) and reformulated to be consistent with the theoretical background of Sec. 2.3.

3.1. General framework to investigate the effects of hidden safety and to adapt the partial safety factor concept

The general framework to investigate the effects of hidden safeties and to adapt the PSF concept is based on the LSF of Eqn. 2.18 and Eqn. 2.20. It is separated into three main steps: The first step deals with the effects of hidden safety on the structural design (Sec. 3.1.1), the second step is about the effects of hidden safety on structural reliability (Sec. 3.1.2), and the third step performs the adaptation of the PSF concept (Sec. 3.1.3).

The first two steps can, in principle, be performed on individual design situations. However, the third step is only meaningful when a representative portfolio of design situations is considered. Therefore, the first two steps are considered at the portfolio level as well.

A special case in the investigation of hidden safeties are existing structures. In these cases, it is no longer possible to adjust the design decisions because they have already been made. Rather, the issue is the classification of a particular design and whether hidden safeties can be exploited to classify a particular design as sufficient. This issue is investigated in Sec 3.1.4.

3.1.1. Effects of hidden safety to the structural design

Following Eqn. 2.17 the design choices according to Eurocode can be represented via

$$\mathcal{P}_{EC} = t_{R,EC}^{-1} \left(\frac{m_{k,EC}}{\gamma_m}, \gamma_{Rd} \cdot \gamma_{Sd} \cdot t_{S,EC} \left(\gamma_f \cdot l_{k,EC} \right) \right) \tag{3.1}$$

If – instead of the Eurocode – the purely aleatoric models would be used the following purely aleatoric design choices would be obtained

$$\mathcal{P} = t_R^{-1} \left(\frac{m_k}{\gamma_m}, \gamma_{Rd} \cdot \gamma_{Sd} \cdot t_S \left(\gamma_f \cdot l_k \right) \right) \tag{3.2}$$

The purely aleatoric design is of interest for the following reason: More advanced models typically reduce the amount of epistemic uncertainty compared to standard models. Hence, if Eurocode models get replaced by more advanced models, the resulting design choices changes presumably into the direction of the purely aleatoric design choices. Hence, the purely aleatoric design can be interpreted as a converging value of a process eliminating epistemic uncertainties.

A replacement of a Eurocode model with a more advanced model can be done for the material model, the action model, the structural model, and the resistance model, resulting

in one of the following advanced design choices:

$$
\mathcal{P}_{adv} = \begin{cases} t_{R,EC}^{-1}\left(\frac{m_{k,adv}}{\gamma_m},\gamma_{Rd}\cdot\gamma_{Sd}\cdot t_{S,EC}\left(\gamma_f\cdot l_{k,EC}\right)\right) & \text{advanced material model} \\ t_{R,EC}^{-1}\left(\frac{m_{k,EC}}{\gamma_m},\gamma_{Rd}\cdot\gamma_{Sd}\cdot t_{S,EC}\left(\gamma_f\cdot l_{k,adv}\right)\right) & \text{advanced action model} \\ t_{R,EC}^{-1}\left(\frac{m_{k,EC}}{\gamma_m},\gamma_{Rd}\cdot\gamma_{Sd}\cdot t_{S,adv}\left(\gamma_f\cdot l_{k,EC}\right)\right) & \text{advanced structural model} \\ t_{R,adv}^{-1}\left(\frac{m_{k,EC}}{\gamma_m},\gamma_{Rd}\cdot\gamma_{Sd}\cdot t_{S,EC}\left(\gamma_f\cdot l_{k,EC}\right)\right) & \text{advanced resistance model} \end{cases} \tag{3.3}
$$

Eqns. 3.1, 3.2, and 3.3 each cover an individual design situations and, therefore, are deterministic values. If, instead of individual design situation, a full portfolio of design situations is investigated (see Sec. 2.3.3), $\mathcal{P}_{EC}$, $\mathcal{P}$, and $\mathcal{P}_{adv}$ are either represented via multiple deterministic values representative of different design situations within the portfolio, or $\mathcal{P}_{EC}$, $\mathcal{P}$, and $\mathcal{P}_{adv}$ become random variables representing the variability of design choices within the considered portfolio. In the second case Eqns. 3.1, 3.2, and 3.3 can be rewritten as

$$
\mathcal{P}_{EC} = T_{R,EC}^{-1}\left(\frac{M_{k,EC}}{\gamma_m},\gamma_{Rd}\cdot\gamma_{Sd}\cdot T_{S,EC}\left(\gamma_f\cdot L_{k,EC}\right)\right) \tag{3.4}
$$

$$
\mathcal{P} = T_R^{-1}\left(\frac{M_k}{\gamma_m},\gamma_{Rd}\cdot\gamma_{Sd}\cdot T_S\left(\gamma_f\cdot L_k\right)\right) \tag{3.5}
$$

$$
\mathcal{P}_{adv} = \begin{cases} T_{R,EC}^{-1}\left(\frac{M_{k,adv}}{\gamma_m},\gamma_{Rd}\cdot\gamma_{Sd}\cdot T_{S,EC}\left(\gamma_f\cdot L_{k,EC}\right)\right) & \text{advanced material model} \\ T_{R,EC}^{-1}\left(\frac{M_{k,EC}}{\gamma_m},\gamma_{Rd}\cdot\gamma_{Sd}\cdot T_{S,EC}\left(\gamma_f\cdot L_{k,adv}\right)\right) & \text{advanced action model} \\ T_{R,EC}^{-1}\left(\frac{M_{k,EC}}{\gamma_m},\gamma_{Rd}\cdot\gamma_{Sd}\cdot T_{S,adv}\left(\gamma_f\cdot L_{k,EC}\right)\right) & \text{advanced structural model} \\ T_{R,adv}^{-1}\left(\frac{M_{k,EC}}{\gamma_m},\gamma_{Rd}\cdot\gamma_{Sd}\cdot T_{S,EC}\left(\gamma_f\cdot L_{k,EC}\right)\right) & \text{advanced resistance model} \end{cases}
$$

$$\tag{3.6}$$

where $T_{R,EC}$, $T_{S,EC}$, T_R, T_S, $M_{k,EC}$, $L_{k,EC}$, M_k, and L_k are the extensions to portfolio level of $t_{R,EC}$, $t_{S,EC}$, t_R, t_S, $m_{k,EC}$, $l_{k,EC}$, m_k, and l_k, following the approach of Sec. 2.3.3.

Eqns. 3.4, 3.5, and 3.6 are formalized such that the individual design situations of Eqns. 3.1, 3.2, and 3.3 are expanded to portfolio level with respect to the material model, the action model, the structural model, and the resistance model. Alternatively, the expansion to portfolio level can also be done with respect to just one of the models. Moreover, various assumptions can be made to simplify those generic representations of the design choices at the portfolio level. Those assumptions closely follow the assumptions made in Sec. 2.3.2.2 to simplify the representation of the LSF and the design choices. This includes assumptions about the linearity of the structural and the resistance model and the assumption that nominal models are equal to purely aleatoric models. Typically, it is not critical to apply those assumptions to the models that are not replaced by advanced models. E.g., if the Eurocode action model is replaced by a more advanced model, assumptions about the material model, the structural model, and the resistance model are not critical. The reason for this is that those assumptions enter the calculation of $\mathcal{P}_{EC}$, $\mathcal{P}$, and $\mathcal{P}_{adv}$ equally. This makes a relative comparison of those quantities still valid. In contrast, assumptions about the model that is replaced by a more advanced model should be introduced carefully.

After $\mathcal{P}_{EC}$, $\mathcal{P}$, and $\mathcal{P}_{adv}$ are derived, they can be compared in order to estimate the effect of the respective models on the design choices. The ratios $\frac{\mathcal{P}_{EC}}{\mathcal{P}}$, and $\frac{\mathcal{P}_{adv}}{\mathcal{P}}$ indicate how much the epistemic uncertainties of the applied models lead to a deviation of a more

ideal design choice purely based on aleatoric uncertainties. In case $\mathcal{P}_{EC}$, $\mathcal{P}$, and $\mathcal{P}_{adv}$ are random variables derived via a portfolio, the ratio of the respective means $\frac{\mathrm{E}[\mathcal{P}_{EC}]}{\mathrm{E}[\mathcal{P}]}$, and $\frac{\mathrm{E}[\mathcal{P}_{adv}]}{\mathrm{E}[\mathcal{P}]}$ can be derived.

In this context, the term *conservative model* is defined as follows: A model is conservative in a specific design situation if it leads to a larger design resistance than the design resistance one would obtain with purely aleatoric models; hence, if the ratios $\frac{\mathcal{P}_{EC}}{\mathcal{P}}$ and $\frac{\mathcal{P}_{adv}}{\mathcal{P}}$ are greater 1.

It can be challenging to derive $\mathcal{P}$. If this is the case, the ratios $\frac{\mathcal{P}_{adv}}{\mathcal{P}_{EC}}$ and $\frac{\mathrm{E}[\mathcal{P}_{adv}]}{\mathrm{E}[\mathcal{P}_{EC}]}$ can be calculated instead to indicate how much the advanced model changes the design choices compared to the Eurocode model.

The ratios of the design choices indicate the material consumption of the respective models. However, it should be noted that the relationship between the design choices and the material consumption is not necessarily linear. Moreover, serviceability limit states are not considered in this comparison.

3.1.2. Effects of hidden safety on the structural reliability

Given a design choice (see Sec. 3.1.1) the aleatoric probabilities of failure can be calculated via a reliability analysis $\mathcal{R}$ that only uses purely aleatoric distributions. The nominal probability of failure according to Eurocode can be calculated via a reliability analysis $\mathcal{R}_{EC}$ using the probabilistic bases of Eurocode models. The nominal probability of failure according to advanced models can be calculated via a reliability analysis $\mathcal{R}_{adv}$ using the probabilistic bases of the advanced models. Tab. 3.1 summarizes the various combinations of design choices and choices within the reliability analysis to calculate the aleatoric and nominal probability of failure.

		Design choice following		
		aleatoric models	Eurocode	advanced models
Reliability	aleatoric models	$\Pr(F; \mathcal{P}, \mathcal{R})$	$\Pr(F; \mathcal{P}_{EC}, \mathcal{R})$	$\Pr(F; \mathcal{P}_{adv}, \mathcal{R})$
analysis	Eurocode	$\Pr(F; \mathcal{P}, \mathcal{R}_{EC})$	$\Pr(F; \mathcal{P}_{EC}, \mathcal{R}_{EC})$	$\Pr(F; \mathcal{P}_{adv}, \mathcal{R}_{EC})$
following	advanced models	$\Pr(F; \mathcal{P}, \mathcal{R}_{adv})$	$\Pr(F; \mathcal{P}_{EC}, \mathcal{R}_{adv})$	$\Pr(F; \mathcal{P}_{adv}, \mathcal{R}_{adv})$

Tab. 3.1.: Possible combinations of design choices and choices within the reliability analysis to calculate the probability of failure.

If a portfolio of design situations is considered, the probability of failure can either be calculated conditionally on the design choices, resulting in a distribution of the probability of failure or the variability of the portfolio can be included, resulting in the mean of the conditional version.

To investigate the effects of various design choices, the different probabilities of failure of Tab. 3.1 can be compared. Alternatively, the respective reliability indies can be cal-

culated (see Eqn. 2.14) and compared. A comparison of reliability indices is often more meaningful because failure probabilities can differ by several orders of magnitude, making a comparison difficult to interpret. This is not the case for reliability indices. The reason for this is the non-linear transformation via the standard normal CDF. However, exactly this non-linear transformation should be kept in mind when comparing reliability indices.

When it comes to the subsequent adaptation of the PSF concept with respect to hidden safeties (see Sec. 3.1.3) the aleatoric probabilities of failure given design choices following Eurocode and following advanced modeling techniques $\Pr(F; \mathcal{P}_{EC}, \mathcal{R})$ and $\Pr(F; \mathcal{P}_{adv}, \mathcal{R})$ are of special interest. The difference between those two probabilities of failure is caused by two counteracting effects:

- Standard models typically include conservative assumptions and parameter specifications.[1] This adds a conservative bias of $\mathcal{P}_{EC}$ in comparison to $\mathcal{P}$. More advanced models may be less conservative. Hence, if standard models are replaced by more advanced models, the decrease in bias increases the probability of failure.

- Standard models typically include larger epistemic uncertainties than more advanced models. If standard models get replaced by more advanced models, the reduction of model uncertainty decreases the probability of failure.

Depending on which of these effects dominates, structural reliability can either increase or decrease. In order to preserve the same level of safety, an adaptation of the PSF concept is needed.

Similar to the purely aleatoric design choices, it can be challenging to find the purely aleatoric models to perform a purely aleatoric reliability analysis $\mathcal{R}$. Typically, simplifying assumptions must be made, which add epistemic uncertainty; hence, the purely aleatoric reliability analysis $\mathcal{R}$ is not purely aleatoric anymore. Nevertheless, such a reliability analysis is called to be purely aleatoric within this thesis. As already stated, such simplifying assumptions are not critical when it comes to the comparison of the aleatoric probabilities of failure (in particular the comparison of $\Pr(F; \mathcal{P}_{EC}, \mathcal{R})$ and $\Pr(F; \mathcal{P}_{adv}, \mathcal{R})$ used within the subsequent adaption of the PSF concept), since those assumptions enter the respective reliability analyses equally, hence, making a relative comparison valid.

3.1.3. Adaptation of the partial safety factor concept with respect to hidden safeties

The adaptation of the PSF concept with respect to hidden safeties follows Sec. 2.3.5. Thereby, the target probability of failure or the target reliability index follow from the design choices made by Eurocode (see Eqn. 2.43 and 2.44). The adaptation can either be performed by introducing an additional PSF that is applied to the quantity resulting from the advanced model or – in case of an advanced material model or an advanced action model – by adapting the quantile value used to define the characteristic value. The

---

[1]For a formal definition of the term *conservative model* see Sec.3.1.1

adaptation follows Eqns. 2.47-2.52. This ensures that the application of advanced models leads – on portfolio level – to the same level of safety as the Eurocode models.

Depending on which of the two counteracting effects (the elimination of a conservative bias vs. the decrease of model uncertainty as described in Sec. 3.1.2) is stronger, the adapted safety components increase or decrease the design choices. I.e., if the effect of the elimination of a conservative bias dominates, an additional partial is greater than 1 and an adapted quantile value to define the characteristic value is smaller than the previous one in the case of a material model and greater than the previous one in the case of an action model. If the effect of the decreased model uncertainty dominates, then the opposite follows.

Once the adaptation is conducted, the first step to investigate the effect of the design choices (Sec. 3.1.1) can be repeated, including the adaptation within the design choices and compared to the design choices without the adaptation. Moreover, the second step to investigate the effects on structural reliability (Sec. 3.1.2) can be repeated with respect to the adapted design choices. However, this is not very meaningful, since the resulting level of safety is already known from the adaptation procedure, namely, the utilized target reliability. It may only differ slightly, depending on the exact recalibration procedure (Sec. 2.3.5). Nevertheless, it may be useful to perform such a calculation to check whether the recalibration has been performed correctly.

3.1.4. Hidden safeties in the context of existing structures

Hidden safeties are important not only in the context of the application of advanced models to design new structures but also in the context of the application of advanced models to reassess existing structures. In many instances, the safety of existing structures can no longer be demonstrated by standard code-based assessments. Reasons for this include changes in the code, changes in the demands on the structures and deterioration. This issue is formalized as follows: Let $\mathcal{P}_{exist}$ be the design choice of an existing structure and let $\mathcal{P}_{EC}$ be the design choice one would obtain if one would redesign the structure following the current standard code (see Eqn. 3.1). Then the existing structure is in compliance with the current standard if $\mathcal{P}_{exist} \geq \mathcal{P}_{EC}$ and not in compliance with the current standard if $\mathcal{P}_{exist} \leq \mathcal{P}_{EC}$.

If an existing structure is not in compliance with the current standard, it is common practice to perform a more detailed assessment utilizing advanced models. Let $\mathcal{P}_{adv}$ be the design choice one would obtain if one would redesign the structure following the advanced model (see Eqn. 3.3). If $\mathcal{P}_{exist} \geq \mathcal{P}_{adv}$ the existing design is sufficient according to the advanced model and if $\mathcal{P}_{exist} \leq \mathcal{P}_{adv}$ the existing design is not sufficient according to the advanced model. In this way, many structures can be shown to comply with safety requirements, even if they cannot be verified by standard assessments.

Such an application of advanced models in replacement of standard models leads to the same two effects on reliability as the application within the design of new structures (see Sec. 3.1.2):

- Standard models typically include more conservative assumptions and parameter specifications in comparison to advanced models; hence, $\mathcal{P}_{EC} > \mathcal{P}_{adv}$ on average. Therefore, the application of advanced models accepts – on average – more existing design choices. Hence, if standard models get replaced by more advanced models, the decrease in bias increases the average probability of failure of the accepted existing structures.

- Standard models typically include larger epistemic uncertainties than more advanced models. Hence, the uncertainty of $\mathcal{P}_{EC}$ is larger than the uncertainty of $\mathcal{P}_{adv}$. This decreases the average probability of failure of the accepted design choices.

Similar to the case of new structures, these two effects counteract each other in their effect on structural reliability and should be balanced out via an adaptation of the PSF concept. The adapted PSF concept would – obviously – not be used in a design of an actual new structure, but only to derive the design value one would obtain using the advanced model $\mathcal{P}_{adv}$ if one would redesign the existing structure. $\mathcal{P}_{adv}$ is then compared to $\mathcal{P}_{EC}$. The choice of a target probability of failure or the target reliability to perform such an adaptation is not as straightforward as in the case of new structures for the following reason: Increasing the resistance of existing structures is often associated with high construction costs, as this usually includes modification or even partly deconstruction of the existing building. The increase of resistances of new structures typically only includes the increase of materials costs. This difference in cost to increase resistance should justify a slightly lower target reliability [102]. However, the determination of such a target reliability should include the cost associated to failure. This basically leads to a risk based code calibration, which is not part of this thesis.

3.2. Formal definition of hidden safety

The framework of Sec. 3.1 does not include a formal definition of the term "hidden safety", but only covers the effects arising from hidden safety and how to compensate those effects via adaptations of the PSF concept. In fact, a definition is not needed in practice; however, it is of philosophical/theoretical interest. In the following, a more formal definition is attempted.

In literature, the words "hidden safety" occur in different contexts with slightly different meanings, e.g., in [89–95]. In these publications, hidden safety is usually understood as a conservative bias of a model. While this points in the right direction, it does not cover the full complexity of hidden safety for the following reasons:

The word "safety" in the term "hidden safety" indicates that the term should be expressed by a measure of safety, such as the probability of failure. The bias of a model itself cannot be directly expressed by such a measure, but only its effect. Moreover, the bias only captures the mean error of a model. Higher order moments (variance, skewness, etc.) are not considered, however, should be included. The word "hidden" in the term "hidden safety" indicates that this part of the safety is not visible from the perspective of the model that contains the hidden safety. To determine which part of the safety

is hidden, the safety according to the model that includes the hidden safety should be compared to the model excluding the hidden safety. From a prospective point of view, the purely aleatory model is suitable for this purpose. The following failure probabilities from Tab. 3.1 should therefore be compared to determine the hidden safety of a standard model: $\Pr(F; \mathcal{P}_{EC}, \mathcal{R}_{EC})$ versus $\Pr(F; \mathcal{P}_{EC}, \mathcal{R})$. Note that these values can be different for different given design choices $\mathcal{P}_{EC}$ resulting from different design situations. Hence, hidden safety is not just a property of a model but also depends on the design situation the model is applied to. This dependency can be overcome via the portfolio perspective.

3.3. Case study 1: Hidden safety in the Wind load model of the Eurocode

This case study investigates the effects of hidden safety in the wind load model of Eurocode 1 [103]. An exchange of the Eurocode wind load model with more advanced modeling techniques is considered. The case study follows the three steps of Sec. 3.1.1, 3.1.2, and 3.1.3: First, the effect on the design choices and the material usage are studied. Second, the effect on structural reliability is derived. Third, an adaptation of the PSF concept is conducted. Considering this adaptation, the design choices are re-evaluated.

The case study uses the portfolio defined in Annex A, excluding snow actions and imposed actions, only considering wind actions according to Eurocode and the advanced wind action modeling techniques as follows. The case study is only valid under the assumptions of this portfolio.

3.3.1. Wind load model of the Eurocode

The wind load model of the Eurocode is based on five components [58, 104]: The wind climate, the terrain, the aerodynamic response, the mechanical response, and the design criteria. Accordingly, Eurocode 1 [103] and its background documentations (e.g., [105]) define the characteristic wind load pressure $q_{k,EC}$ as:

$$q_{k,EC} = q_{b,k,EC} \cdot c_{e,k,EC} \cdot c_{f,k,EC} \cdot c_{s,k,EC} \cdot c_{d,k,EC} \tag{3.7}$$

These coefficients are characteristic values of the wind load components:

- $q_{b,k,EC}$ is the characteristic value of the wind velocity pressure: It is defined as the 10-minute mean velocity pressure at a height of $10\,\mathrm{m}$ above ground with a roughness length of $0.05\,\mathrm{m}$ and a return period of 50 years.

- $c_{e,k,EC}$ is the characteristic value of the exposure coefficient: It considers the roughness of the terrain and the height of the structure and is based on empirically determined formulas. Eurocode assumes that these formulas are unbiased estimators of the expected exposure coefficient and thus the characteristic value is the mean.

- $c_{f,k,EC}$ is the characteristic value of the force coefficient: It addresses the geometry of the structure. Its values are based on investigations of [59] and obtained as the 78 % quantile of the yearly maxima of the force coefficient, which are assumed to follow a Gumbel distribution [106].

- $c_{sd,k,EC} = c_{s,k,EC} \cdot c_{d,k,EC}$ is the characteristic value of the structural factor: It accounts for the fact that wind peak pressures do not occur simultaneously on the total surface of the structure (represented through $c_{s,k,EC}$) and for the dynamical effect caused by wind turbulences exciting the structure at its eigenfrequencies (represented through $c_{d,k,EC}$). Eurocode assumes that these formulas are unbiased estimators of the expected structural factor and thus the characteristic value is the mean.

In summary, the characteristic values are defined as

$$q_{b,k,EC} = F_{Q_{b,EC}}^{-1}(0.98) \tag{3.8}$$

$$c_{e,k,EC} = \mathrm{E}[C_{e,EC}] \tag{3.9}$$

$$c_{f,k,EC} = F_{C_{f,EC}}^{-1}(0.78) \tag{3.10}$$

$$c_{sd,k,EC} = \mathrm{E}[C_{sd,EC}] \tag{3.11}$$

where $Q_{b,EC}$, $C_{e,EC}$, $C_{f,EC}$, and $C_{sd,EC}$ represent the respective random variables according to Eurocode. The distributions of these random variables are not given by Eurocode and background documents are mostly opaque. However, these distributions are not needed in the following, but only the respective purely aleatoric distributions are defined and used in the subsequent reliability analysis (see Sec. 3.3.4). $q_{b,k,EC}$, $c_{e,k,EC}$, $c_{f,k,EC}$, $c_{sd,k,EC}$ are intended to be estimates of the receptive purely aleatoric characteristic values. The uncertainty within this estimation is induced by representing $q_{b,k,EC}$, $c_{e,k,EC}$, $c_{f,k,EC}$, $c_{sd,k,EC}$ as random variables. The distribution of those random variables is determined in Sec. 3.3.3.1.

3.3.2. Advanced wind load model

The advanced wind load model consists of the same wind load model components as the Eurocode model. The characteristic wind load pressure is defined as

$$q_{k,adv} = q_{b,k,adv} \cdot c_{e,k,adv} \cdot c_{f,k,adv} \cdot c_{sd,k,adv} \tag{3.12}$$

where $q_{b,k,adv}$, $c_{e,k,adv}$, $c_{f,k,adv}$, and $c_{sd,k,adv}$ are the advanced counterparts of the respective Eurocode characteristic values. In accordance with the Eurocode, these are defined similar to the Eurocode model as

$$q_{b,k,adv} = F_{Q_{b,adv}}^{-1}(0.98) \tag{3.13}$$

$$c_{e,k,adv} = \mathrm{E}[C_{e,adv}] \tag{3.14}$$

$$c_{f,k,adv} = F_{C_{f,adv}}^{-1}(0.78) \tag{3.15}$$

$$c_{sd,k,adv} = \mathrm{E}[C_{sd,adv}] \tag{3.16}$$

It is assumed that the distributions $Q_{b,adv}$, $C_{e,adv}$, $C_{f,adv}$, and $C_{sd,adv}$ are derived using long-term on-site wind data and wind tunnel tests on scale models of the structure. A more detailed description of these advanced models is given in the subsequent Sec. 3.3.3.2.

Similar to the Eurocode model, the distributions of $Q_{b,adv}$, $C_{e,adv}$, $C_{f,adv}$, and $C_{sd,adv}$ are not given; however, they are also not needed. Instead, the distributions of $q_{b,k,adv}$, $c_{e,k,adv}$, $c_{f,k,adv}$, and $c_{sd,k,adv}$ representing the uncertainty in the determination of the advanced characteristic values are derived in Sec.3.3.3.2.

3.3.3. Effects of the wind load model to design choice

Adopting the portfolio of Annex A, the design choices of a given material i following Eurocode are

$$
\mathcal{P}_{i,EC} = \frac{\gamma_{R_i}}{\theta_{R_i,k} \cdot r_{i,k}} \cdot [(1 - a_{Q,i}) \cdot (a_G \cdot \gamma_S \cdot g_{S_i,k} + (1 - a_G) \cdot \gamma_P \cdot g_{P,k}) +
$$
$$
+ a_{Q,i} \cdot \gamma_Q \cdot Q_{b,k,EC} \cdot C_{e,k,EC} \cdot C_{f,k,EC} \cdot C_{sd,k,EC}] \tag{3.17}
$$

where γ_{R_i} is the PSF of the resistance side, γ_S is the PSF of the self weight, γ_P is the PSF of the permanent action, γ_Q is the PSF of wind action, $r_{i,k}$ is the characteristic material strength, $\theta_{R_i,k}$ is the model uncertainty in the estimation of the characteristic material strength, $g_{S_i,k}$ is the characteristic self weight, $g_{P,k}$ is the characteristic permanent action, and $a_{Q,i}$ and a_G are action proportion factors. The respective values are listed in Annex A.

$Q_{b,k,EC}$, $C_{e,k,EC}$, $C_{f,k,EC}$, $C_{sd,k,EC}$ are random variables representing the characteristic values of the wind action model components according to Eurocode. Technically, the characteristic values are deterministic values estimating the mean or certain quantile values of the respective underling purely aleatoric distributions. Following Sec. 2.3.3, a probabilistic description is used taking its relative error into account. Following Eqn. 2.42, the distribution of the characteristic values is derived via the distribution of the relative error in the estimation of the characteristic values. A detailed derivation of the respective distributions is skipped here and described in detail in Sec. 3.3.3.1.

Analogously, the design choices of a given material i following advanced wind action modeling techniques are

$$
\mathcal{P}_{i,adv} = \frac{\gamma_{R_i}}{\theta_{R_i,k} \cdot r_{i,k}} \cdot [(1 - a_{Q,i}) \cdot (a_G \cdot \gamma_S \cdot g_{S_i,k} + (1 - a_G) \cdot \gamma_P \cdot g_{P,k}) +
$$
$$
+ a_{Q,i} \cdot \gamma_Q \cdot Q_{b,k,adv} \cdot C_{e,k,adv} \cdot C_{f,k,adv} \cdot C_{sd,k,adv}] \tag{3.18}
$$

where $Q_{b,k,adv}$, $C_{e,k,adv}$, $C_{f,k,adv}$, $C_{sd,k,adv}$ are random variables representing the characteristic values of the wind action model components according to advanced wind action modeling techniques. The detailed derivation of their distribution is again skipped and described in detail in Sec. 3.3.3.2.

Additionally, four more cases $\mathcal{P}_{i,Q_{b,k,adv}}$, $\mathcal{P}_{i,C_{e,k,adv}}$, $\mathcal{P}_{i,C_{f,k,adv}}$, and $\mathcal{P}_{i,C_{sd,k,adv}}$ are considered where only one of the wind action components is replaced with advanced wind action

modeling techniques:

$$\mathcal{P}_{i,Q_{b,k,adv}} = \frac{\gamma_{R_i}}{\theta_{R_i,k} \cdot r_{i,k}} \cdot [(1 - a_{Q,i}) \cdot (a_G \cdot \gamma_S \cdot g_{S_i,k} + (1 - a_G) \cdot \gamma_P \cdot g_{P,k}) + \tag{3.19}$$
$$+ a_{Q,i} \cdot \gamma_Q \cdot Q_{b,k,adv} \cdot C_{e,k,EC} \cdot C_{f,k,EC} \cdot C_{sd,k,EC}]$$

$$\mathcal{P}_{i,C_{e,k,adv}} = \frac{\gamma_{R_i}}{\theta_{R_i,k} \cdot r_{i,k}} \cdot [(1 - a_{Q,i}) \cdot (a_G \cdot \gamma_S \cdot g_{S_i,k} + (1 - a_G) \cdot \gamma_P \cdot g_{P,k}) + \tag{3.20}$$
$$+ a_{Q,i} \cdot \gamma_Q \cdot Q_{b,k,EC} \cdot C_{e,k,adv} \cdot C_{f,k,EC} \cdot C_{sd,k,EC}]$$

$$\mathcal{P}_{i,C_{f,k,adv}} = \frac{\gamma_{R_i}}{\theta_{R_i,k} \cdot r_{i,k}} \cdot [(1 - a_{Q,i}) \cdot (a_G \cdot \gamma_S \cdot g_{S_i,k} + (1 - a_G) \cdot \gamma_P \cdot g_{P,k}) + \tag{3.21}$$
$$+ a_{Q,i} \cdot \gamma_Q \cdot Q_{b,k,EC} \cdot C_{e,k,EC} \cdot C_{f,k,adv} \cdot C_{sd,k,EC}]$$

$$\mathcal{P}_{i,C_{sd,k,adv}} = \frac{\gamma_{R_i}}{\theta_{R_i,k} \cdot r_{i,k}} \cdot [(1 - a_{Q,i}) \cdot (a_G \cdot \gamma_S \cdot g_{S_i,k} + (1 - a_G) \cdot \gamma_P \cdot g_{P,k}) + \tag{3.22}$$
$$+ a_{Q,i} \cdot \gamma_Q \cdot Q_{b,k,EC} \cdot C_{e,k,EC} \cdot C_{f,k,EC} \cdot C_{sd,k,adv}]$$

Fig. 3.1 shows violin plots of the distributions of the design choices. Those distributions take the relative frequency of the different materials and load compositions of the considered portfolio into account, as well as the uncertainty in the estimation of the characteristic wind action values. Ratios of the expected values of the design choices according to the advanced model cases to the Eurocode model case are reported in Tab. 3.2.
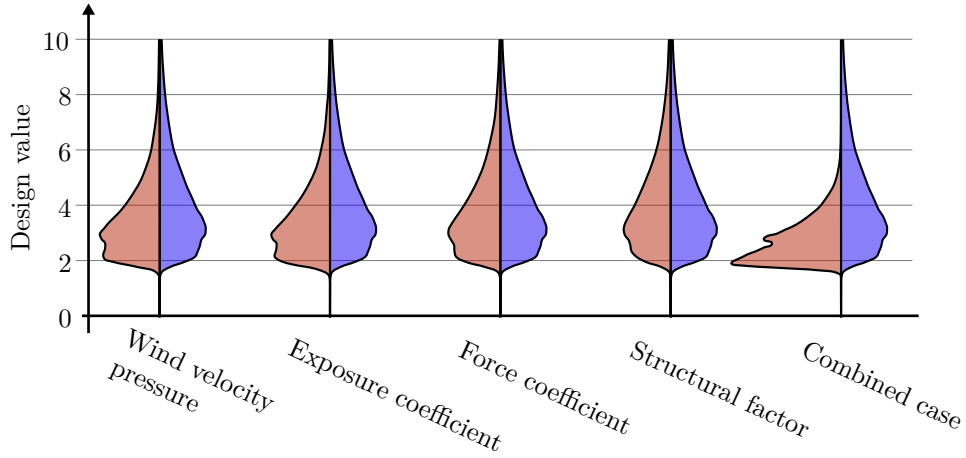
Fig. 3.1.: Violin plots showing the distribution of design values obtained with Eurocode models (blue) and advanced models (red).

3.3.3.1. Distributions of the characteristic wind load model components according to Eurocode

The characteristic values in the Eurocode are estimates of the quantile values of the respective underlying aleatoric distributions. However, the underlying aleatoric distributions vary from case to case. E.g. Fig. 3.2 illustrates this for the wind velocity pressure. Similar holds for the other wind load model components.

The derivation of the characteristic wind load model components according to Eurocode

Material i	1	2	3	4	5	6	1-6
Wind velocity pressure	0.79	0.81	0.81	0.79	0.79	0.81	0.80
Exposure coefficient	0.83	0.84	0.84	0.83	0.83	0.84	0.84
Force coefficient	0.91	0.92	0.92	0.91	0.91	0.92	0.92
Structural factor	1.00	1.00	1.00	1.00	1.00	1.00	1.00
Combined case	0.60	0.63	0.62	0.60	0.60	0.63	0.62

Tab. 3.2.: Average design values obtained with the use of advanced modeling techniques relative to those obtained with Eurocode models, calculated as $\frac{\mathrm{E}[\mathcal{P}_{i,x,adv}]}{\mathrm{E}[\mathcal{P}_{i,EC}]}$ with x representing the respective advanced model case. Results are listed for the six material properties separately and for the full portfolio.
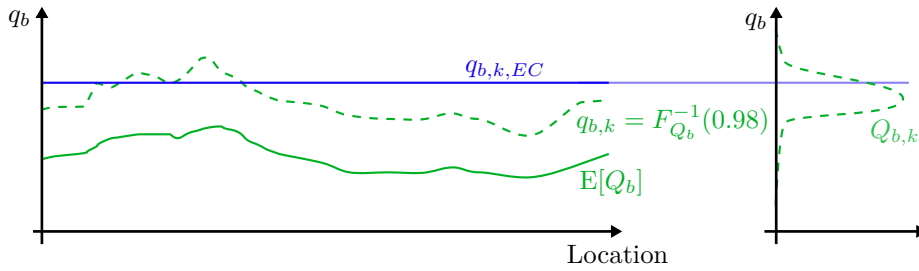
Fig. 3.2.: Derivation of the distribution of the characteristic value $Q_{b,k}$ resulting from the aleatoric distribution of the wind velocity pressure Q_b (green) and its relationship to the characteristic value according to Eurocode $q_{b,k,EC}$ (blue).

is based on the relative errors of the Eurocode characteristic value $q_{k,EC}$ relative to the aleatoric characteristic value q_k. Fig. 3.3 illustrates the situation in the case of wind velocity pressure. In contrast to Fig. 3.2, the perspective is changed by standardizing every quantity relative to $q_{b,k}$. Mathematically, this new perspective is equivalent to the previous one, however, it more clearly reflects how advanced modeling techniques affect the design process. Fig. 3.3 additionally includes the characteristic wind velocity pressure according to advanced modeling techniques $q_{b,k,adv}$, which is needed in the subsequent Sec. 3.3.3.2.

Fig. 3.3.: Re-illustration of Fig. 3.2, whereby the wind velocity pressure Q_b (green) and the characteristic value according to Eurocode $q_{b,k,EC}$ (blue) are standardized by the characteristic value of the aleatoric distribution. The characteristic value according to advanced modeling techniques $q_{b,k,adv}$ is added in red.

Hence, the relative error in the estimation of the characteristic values are defined as

$$\Theta_{q_{b,k,EC}} = \frac{q_{b,k,EC}}{Q_{b,k}} \tag{3.23}$$
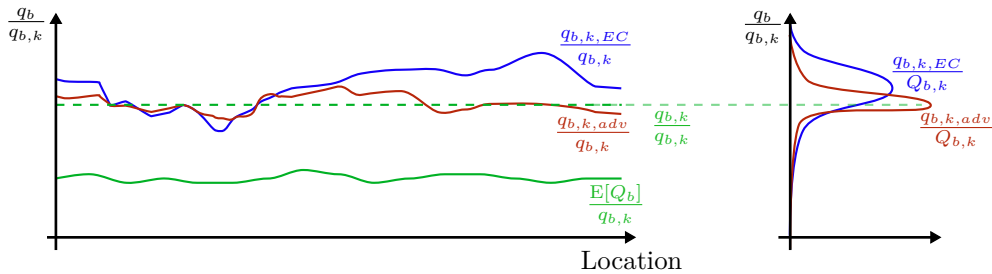
$$\Theta_{c_{e,k,EC}} = \frac{c_{e,k,EC}}{C_{e,k}} \tag{3.24}$$

$$\Theta_{c_{f,k,EC}} = \frac{c_{f,k,EC}}{C_{f,k}} \tag{3.25}$$

$$\Theta_{c_{sd,k,EC}} = \frac{c_{sd,k,EC}}{C_{sd,k}} \tag{3.26}$$

In literature, typically the inverse of this error, $\Theta^{-1}_{q_{b,k,EC}}$, is specified. Tab. 3.3 summarizes the distributions of these inverse relative errors. Following Davenport [107] and the JCSS probabilistic modeling code [108], they follow a log-normal distribution. The distribution parameters are based on [107] and justified as follows:

	Mean	c. o. v.
$\Theta^{-1}_{q_{b,k,EC}} \sim \mathcal{LN}$	0.8	0.30
$\Theta^{-1}_{c_{e,k,EC}} \sim \mathcal{LN}$	0.8	0.15
$\Theta^{-1}_{c_{f,k,EC}} \sim \mathcal{LN}$	0.9	0.20
$\Theta^{-1}_{c_{sd,k,EC}} \sim \mathcal{LN}$	1.0	0.15

Tab. 3.3.: Distribution of the relative errors $\frac{\text{Characteristic value of aleatoric distribution}}{\text{Characteristic value of EC}}$.

- $\Theta^{-1}_{q_{b,k,EC}}$: Davenport [107] suggests a mean value of 0.8 and a coefficient of variation of 0.2–0.3. To verify these numbers, the wind velocity v_b at $10\,[\text{m}]$ above ground is investigated at 265 meteorological stations of the German Meteorological Service [109]. Each of the stations is located in open space. Only stations between 0–1100 [m] above sea level (range of validity of the Eurocode) and only stations with at least 20 years of recording are considered. The wind velocity is converted to the wind velocity pressure via

$$q_b = \frac{1}{2} \cdot \rho \cdot v_b^2 \tag{3.27}$$

where $\rho = 1.25 \left[\frac{\text{kg}}{\text{m}^3}\right]$ is the air density. From the time histories of q_b, the yearly maxima at all stations are obtained and used to fit a Gumbel distribution through a maximum likelihood estimator. Moreover, the statistical uncertainty is accounted for via a normal approximation of the posterior [110]. Finally, $q_{b,k,Data}$ is obtained as the 98 [%] quantiles of each Gumbel distribution and divided by the characteristic values of the respective location specified in the Eurocode. The resulting ratios are shown in Fig. 3.4. The sample mean of these ratios is 0.82, which confirms the choice of $\mathrm{E}[\Theta^{-1}_{q_{b,k,EC}}] = 0.8$. The sample coefficient of variation is 0.36, hence the upper bound of the values suggested by Davenport is choosen [107].

- $\Theta^{-1}_{c_{e,k,EC}}$: Davenport [107] suggests a mean of 0.8 and a coefficient of variation of 0.1-0.2. No data could be found to justify these numbers.
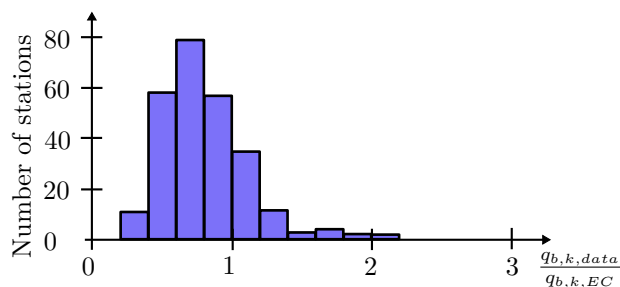
Fig. 3.4.: Histogram of the ratios of the characteristic values $q_{b,k,Data}$ obtained from data of the German Meteorological Service [109] and the characteristic values $q_{b,k,EC}$ of the respective location specified in the Eurocode [103].

- $\Theta^{-1}_{c_{f,k,EC}}$: Davenport [107] suggests a mean of 0.9 and a coefficient of variation of 0.1-0.2. Measurements done by Svend Ole Hansen et al. [111] on a benchmark model of a tall building [112] confirmed these values with a tendency towards the upper bound.

- $\Theta^{-1}_{c_{sd,k,EC}}$: Davenport [107] suggests a mean of 1.0 and a coefficient of variation of 0.1-0.2. No data could be found to justify these numbers.

Solving the Eqns. 3.23-3.26 for the characteristic values, the distribution of $Q_{b,k,EC}$, $C_{e,k,EC}$, $C_{f,k,EC}$, $C_{sd,k,EC}$ can be derived. This requires the aleatoric characteristic values. These are taken as the respective mean values and the respective quantile values of the purely aleatoric distributions defined in the subsequent Sec. 3.3.4. Tab. 3.4 shows the resulting distributions.

	Mean	c. o. v.
$Q_{b,k,EC} \sim \mathcal{LN}$	2.56	0.30
$C_{e,k,EC} \sim \mathcal{LN}$	1.28	0.15
$C_{f,k,EC} \sim \mathcal{LN}$	1.23	0.20
$C_{sd,k,EC} \sim \mathcal{LN}$	1.02	0.15

Tab. 3.4.: Distributions of the characteristic wind load model components according to Eurocode.

3.3.3.2. Distributions of the characteristic wind load model components according to advanced modeling techniques

By analogy with Sec. 3.3.3.1, the distributions of the characteristic wind load model components according to advanced modeling techniques are described through the distributions of the respective inverse relative errors. Tab. 3.5 summarizes these distributions.

	Mean	c. o. v.
$\Theta^{-1}_{q_{b,k,adv}} \sim \mathcal{LN}$	1.0	0.10
$\Theta^{-1}_{c_{e,k,adv}} \sim \mathcal{LN}$	1.0	0.05
$\Theta^{-1}_{c_{f,k,adv}} \sim \mathcal{LN}$	1.0	0.15
$\Theta^{-1}_{c_{sd,k,adv}} \sim \mathcal{LN}$	1.0	0.10

Tab. 3.5.: Distribution of the relative errors $\frac{\text{Characteristic value of aleatoric distribution}}{\text{Characteristic value of Adv}}$.

The advanced models are presumed to be the most accurate state-of-the-art models. Hence, no reference model serving as a reference truth is available. Instead, measurement data has to be evaluated to justify the parameters of the error distributions. This is conducted following the ISO/IEC guide [113]:

- $\Theta^{-1}_{q_{b,k,adv}}$: It is assumed that advanced wind load modeling techniques utilize on-site wind data to estimate the characteristic wind velocity pressure. It is postulated that such an analysis leads to an unbiased estimator. Based on the data from the German Meteorological Service [109] described in Sec. 3.3.3.1, the coefficient of variation of $\Theta^{-1}_{q_{b,k,adv}}$ is estimated as 0.1. This estimate is based on the assumption that extreme wind pressures follow a Gumbel distribution.

- $\Theta^{-1}_{c_{e,k,adv}}$: It is presumed that advanced wind modeling techniques utilize on-site wind data to predict $c_e(z)$ [114, 115]. According to Eurocode 1 [103] the characteristic exposure coefficient is calculated as

$$c_e(z) = 0.19 \cdot \left(\frac{z_0}{0.05} \right)^{0.07} \cdot \ln \left(\frac{z}{z_0} \right) \tag{3.28}$$

where z is the height above ground and z_0 is the roughness length of the terrain. Kelly and Jørgensen [116] determine the uncertainty in the prediction of z_0 through on-site data. They find that z_0 can be estimated with a coefficient of variation 5 [%], given one year of on-site wind data. This leads to an uncertainty in the order of 2 [%] in the estimate of $c_e(z)$. Considering the inherent uncertainty of Eqn. 3.28, it is assumed that the advanced modeling technique results in a coefficient of variation of 5 [%] on the $c_e(z)$ estimate.

- $\Theta^{-1}_{c_{f,k,adv}}$: It is presumed that advanced wind modeling techniques utilize wind tunnel tests to predict the force coefficient. Wind tunnels can be calibrated such that they lead to unbiased results [117], hence $\mathrm{E}[\Theta^{-1}_{c_{f,k,adv}}] = 1$. The coefficient of variation of $\Theta^{-1}_{c_{f,k,adv}}$ is deduced from calculations done by Long [118], who evaluates wind tunnel data of a simple rectangular building and compares it with results from the full scale test reported in [119, 120]. From the results of [118], a coefficient of variation of $\Theta^{-1}_{c_{f,k,adv}}$ equal to 0.15 is derived.

- $\Theta^{-1}_{c_{sd,k,adv}}$: No data could be found to estimate the distribution of the relative error in the estimation of the characteristic structural factor following advanced wind load modeling techniques. Since the estimation of the structural factor according to Eurocode is already unbiased, the estimation according to advanced wind load

modeling techniques is also assumed to be unbiased. Hence, $\mathrm{E}[\Theta_{c_{sd,k,adv}}^{-1}] = 1$. The coefficient of variation of $\Theta_{c_{sd,k,adv}}^{-1}$ is presumed to be 0.1.

By analogy with Sec. 3.3.3.1, the distributions of $Q_{b,k,adv}$, $C_{e,k,adv}$, $C_{f,k,adv}$, $C_{sd,k,adv}$ are derived. Tab. 3.6 shows the resulting distributions.

	Mean	c. o. v.
$Q_{b,k,adv} \sim \mathcal{LN}$	1.90	0.10
$C_{e,k,adv} \sim \mathcal{LN}$	1.00	0.05
$C_{f,k,adv} \sim \mathcal{LN}$	1.09	0.15
$C_{sd,k,adv} \sim \mathcal{LN}$	1.01	0.10

Tab. 3.6.: Distributions of the characteristic wind load model components according to advanced wind load modeling techniques.

3.3.4. Effects of the wind load model to the reliability

Given the distributions of the design values (see Sec. 3.1.1), it can be investigated how the aleatoric probability of failure changes when moving from Eurocode models to advanced models. Following the portfolio of Annex A, the LSF given material i is defined as

$$
\begin{aligned}
g(\mathcal{P}, \Theta_{R_i}, R_i, G_{S,i}, G_P, Q, a_{Q,i}, a_G) = & \mathcal{P} \cdot \Theta_{R_i} \cdot R_i - \\
& - (1 - a_{Q,i}) \cdot [a_G \cdot G_{S,i} + (1 - a_G) \cdot G_P] - \\
& - a_{Q,i} \cdot Q_b \cdot C_e \cdot C_f \cdot C_{sd}
\end{aligned}
\tag{3.29}
$$

where $\mathcal{P} \in \left\{ \mathcal{P}_{i,EC}, \mathcal{P}_{i,adv}, \mathcal{P}_{i,Q_{b,k,adv}}, \mathcal{P}_{i,C_{e,k,adv}}, \mathcal{P}_{i,C_{f,k,adv}}, \mathcal{P}_{i,C_{sd,k,adv}} \right\}$, Θ_{R_i} is the resistance model uncertainty, R_i is the material strength, $G_{S,i}$ is the self-weight, and G_P is the permanent load. The respective distributions are listed in Annex A.

Q_b, C_e, C_f, and C_{sd} are the assumed aleatoric distributions of the wind action model components. The respective distributions follow [108] and [61] and are listed in Tab. 3.7.

	Mean	c. o. v.
$Q_b \sim \mathcal{G}$	1	0.25
$C_e \sim \mathcal{LN}$	1	0.15
$C_f \sim \mathcal{G}$	1	0.10
$C_{sd} \sim \mathcal{LN}$	1	0.10

Tab. 3.7.: Standardized aleatoric distributions of wind load model components. The maximum wind velocity pressure Q_b refers to an annual reference period.

The aleatoric probability of failure is calculated with the first-order reliability method (FORM) [68]. Fig. 3.5 shows box plots of the resulting reliability indices. Ratios of the

expected values of the aleatoric probabilities of failure of the advanced model cases to the ones of the Eurocode model case are reported in Tab. 3.8.
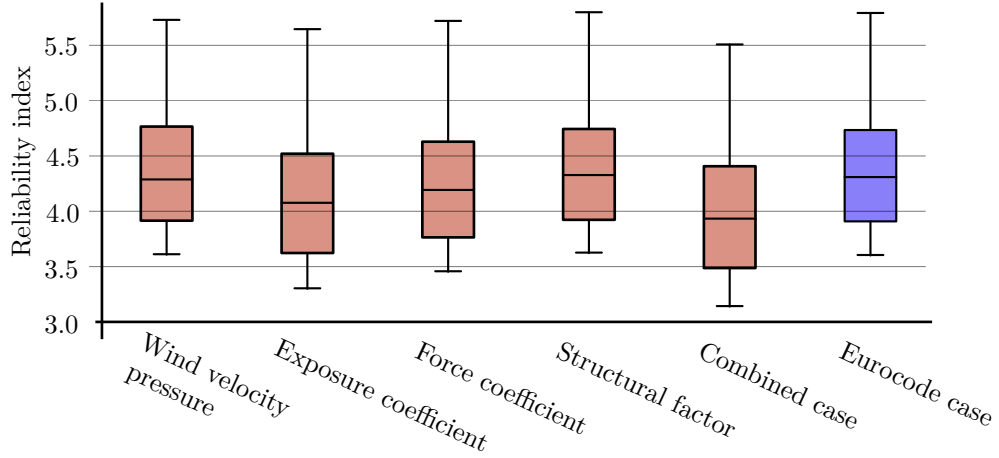
Fig. 3.5.: Boxplots of the annual reliability indices according to Eurocode (blue) and advanced modeling techniques (red).

Wind velocity pressure	1.08
Exposure coefficient	3.05
Force coefficient	1.50
Structural factor	0.80
Combined case	4.22

Tab. 3.8.: Ratios of the weighted average annual probabilities of failure of the design following Eurocode and advanced modeling techniques.

3.3.5. Adaptation of the partial safety factor concept with respect to advanced wind load modeling

To compensate for the lost hidden safety through the application of advanced modeling techniques, the PSF concept needs to be adjusted. Two possible adjustments are demonstrated in the following: The adjustment of the PSF of the wind action via an additional PSF $\gamma_{Q,add}$ (applied additionally to γ_Q) and the adjustment of the characteristic values of the wind action model component; however, the latter is only demonstrated for the characteristic wind velocity pressure.

Following Eqn. 2.43 an annual target probability of failure is calculated as

$$\Pr(F)_{TRG} = \frac{1}{\sum_i w_i} \cdot \sum_i w_i \cdot \Pr(F; \mathcal{P}_{adv}(\gamma_{Q,add}), \mathcal{R}_i) = 3 \cdot 10^{-5} \tag{3.30}$$

where w_i are the weights given in Annex A considering the relative frequencies of the different materials and action compositions of the considered portfolio.

The additional PSF $\gamma_{Q,add}$ is found following Eqn. 2.47

$$\gamma_{Q,add} = \min_{\gamma_{Q,add}} \left\{ \left| \frac{1}{\sum_i w_i} \cdot \sum_i w_i \cdot \Pr\left(F; \mathcal{P}_{i,adv}(\gamma_{Q,add}), \mathcal{R}_i\right) - \Pr(F)_{TRG} \right| \right\} \quad (3.31)$$

where $\mathcal{P}_{i,adv}(\gamma_{Q,add})$ represents the advanced design choice including $\gamma_{Q,add}$ defined as

$$\mathcal{P}_{i,adv}(\gamma_{Q,add}) = \frac{\gamma_{R_i}}{\theta_{R_i,k} \cdot r_{i,k}} \cdot [(1 - a_{Q,i}) \cdot (a_G \cdot \gamma_S \cdot g_{S_i,k} + (1 - a_G) \cdot \gamma_P \cdot g_{P,k}) +$$
$$+ a_{Q,i} \cdot \gamma_{Q,add} \cdot \gamma_Q \cdot Q_{b,k,adv} \cdot C_{e,k,adv} \cdot C_{f,k,adv} \cdot C_{sd,k,adv}] \quad (3.32)$$

Analogously, values of $\gamma_{Q,add}$ are derived for the four design variations of Eqns. 3.19-3.22 where only one of the wind action components is replaced with advanced wind action modeling techniques. Tab. 3.9 shows the resulting additional PSFs. Values above 1 result in an increase of γ_Q, values below 1 decrease γ_Q.

Wind velocity pressure:	1.01
Exposure coefficient:	1.19
Force coefficient:	1.06
Structural factor:	0.97
Combined case:	1.20

Tab. 3.9.: Additional PSF $\gamma_{Q,add}$ regarding each advanced wind load modeling technique and the combined case.

The adaptation of the quantile value defining the characteristic wind velocity pressure $v_{Q_{b,k,adv}}$ again follows Eqn. 2.47 and is calculated as

$$v_{Q_{b,k,adv}} = \min_{\gamma_{Q,add}} \left\{ \left| \frac{1}{\sum_i w_i} \cdot \sum_i w_i \cdot \Pr\left(F; \mathcal{P}_{i,Q_{b,k,adv}}(v_{Q_{b,k,adv}}), \mathcal{R}_i\right) - \Pr(F)_{TRG} \right| \right\} \quad (3.33)$$

where $\mathcal{P}_{i,Q_{b,k,adv}}(v_{Q_{b,k,adv}})$ represents the design choice including advanced wind velocity pressure modeling defined as

$$\mathcal{P}_{i,Q_{b,k,adv}}(v_{Q_{b,k,adv}}) = \frac{\gamma_{R_i}}{\theta_{R_i,k} \cdot r_{i,k}} \cdot [(1 - a_{Q,i}) \cdot (a_G \cdot \gamma_S \cdot g_{S_i,k} + (1 - a_G) \cdot \gamma_P \cdot g_{P,k}) +$$
$$+ a_{Q,i} \cdot \gamma_Q \cdot Q_{b,adv}^{-1}(v_{Q_{b,k,adv}}) \cdot C_{e,k,EC} \cdot C_{f,k,EC} \cdot C_{sd,k,EC}] \quad (3.34)$$

The resulting quantile value is $v_{Q_{b,k,adv}} = 0.9817$ which is a slight increase from the original quantile value of 0.98.

3.3.6. Effects of the adaptation to the design choices

The adaptation of the safety factors is introduced in order to ensure that the overall reliability achieved with the advanced model is the same as that achieved with the Eurocode

model. Here, the effect of this adaptation on the material usage achieved with advanced models is investigated.

Tab. 3.10 shows the ratio of weighted averaged expected values of design values with an adapted PSF. Comparing these values to the ratios without adaptation (last row in Tab. 3.2), it can be seen that the adaptation leads to a (albeit limited) reduction of the material savings from the use of advanced wind load modeling techniques.

Wind velocity pressure	0.81
Exposure coefficient	0.95
Force coefficient	0.95
Structural factor	0.97
Combined case	0.70

Tab. 3.10.: Average design values obtained with the use of advanced modeling techniques relative to those obtained with Eurocode models with adapted PSFs, calculated as $\frac{\mathrm{E}[P_{i,x,adv}]}{\mathrm{E}[P_{i,EC}]}$ with x representing the respective advanced model case. Results are listed for the full portfolio only.

If the quantile value that defines the characteristic wind velocity pressure is adapted, the material saving potential is marginally better than in the case of an additional PSF with respect to an advanced model regarding the wind velocity pressure: The ratio of the averaged design values decreases from 0.81 to 0.80.

3.4. Case study 2: Hidden safety in the traffic load model of the Eurocode

This case study investigates the hidden safety associated with the traffic load model $LM1$ of road bridges defined in the Eurocode [103]. The Eurocode model is compared to a direct simulation of the traffic load. Hidden safety is investigated within the domain of reinforced concrete T-beam bridges. The case study investigates the effect on the design choices (following Sec. 3.1.1) and the effect on the probability of failure (following Sec. 3.1.2). Moreover, the effects of hidden safeties within the traffic load model are investigated regarding existing bridges assuming a hypothetical increase in traffic loads (following Sec. 3.1.4).

This case study differs from case study 1 in several ways: The structural model t_S and the resistance model t_R are not assumed to be linear but are explicitly modeled, which allows for a much higher level of detail. The portfolio is not represented via a generic LSF but through multiple LSF representing various bridges. Furthermore, in contrast to the first case study, no adaptation of the PSF concept is conducted.

3.4.1. Considered portfolio of road bridges

The portfolio of road bridges considered within this case study is the domain of two-lane reinforced concrete highway bridges. Both lanes have the same direction of travel. Fig. 3.6 shows the cross-section of the bridge.
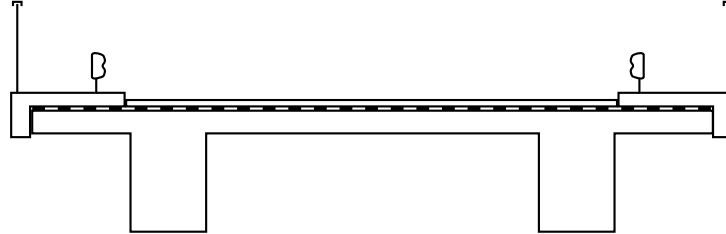

Fig. 3.6.: Cross-section of the bridges considered within the portfolio.

The portfolio of bridges consists of combinations of the following three parameters:

- The number of spans $n_{fields} \in \{1, 2, 3\}$.

- The length of the spans $l_{span} \in \{15, 20, 25\}$ [m]. This corresponds to the cost-efficient range of span-lengths of reinforced concrete bridges. For simplicity, the lengths of all spans are assumed to be equal.

- The traffic load intensity on the bridge is either light, medium or heavy. The different intensities of the traffic load are based on the simulation model described in Sec. 3.4.2 using data from three different highway sections with light, medium, and heavy traffic load intensities.

Thus, a total of $3 \cdot 3 \cdot 3 = 27$ variants of bridges are considered within the portfolio.

3.4.2. Traffic load model of the Eurocode

The traffic load model of the Eurocode consists of four parts $LM1$-$LM4$ [103]. However, only $LM1$ (axle loads and uniformly distributed loads) is considered within this case study. $LM2$ (verification of single-axle loads) and $LM3$ (special vehicle loads) are excluded by NA of Germany [121]. $LM4$ (crowd loading) is not considered in this case study.

$LM1$ gives multiple characteristic values covering the surface loads per traffic lane $q_{i,k}$, surface loads on the remaining areas $q_{r,k}$, and point loads of two double axles of a heavy truck per traffic lane Q_i. In the case of the bridges within the considered portfolio, the

following values are given:

$$q_{1,k} = 27.00 \left[\frac{\text{kN}}{\text{m}}\right] \tag{3.35}$$

$$q_{2,k} = 7.5 \left[\frac{\text{kN}}{\text{m}}\right] \tag{3.36}$$

$$q_{r,k} = 8.75 \left[\frac{\text{kN}}{\text{m}}\right] \tag{3.37}$$

$$Q_{1,k} = 600 \,[\text{kN}] \tag{3.38}$$

$$Q_{2,k} = 400 \,[\text{kN}] \tag{3.39}$$

The characteristic loads are increased with adjustment factors α. The adjustment factors are taken from the German national annex of the Eurocode [121]. Other countries have different values.

$$\alpha_{q_{1,k}} = 1.\overline{33} \tag{3.40}$$

$$\alpha_{q_{2,k}} = 2.4 \tag{3.41}$$

$$\alpha_{q_{r,k}} = 1.2 \tag{3.42}$$

$$\alpha_{Q_{1,k}} = 1 \tag{3.43}$$

$$\alpha_{Q_{2,k}} = 1 \tag{3.44}$$

The $LM1$ model was calibrated by traffic load measurements on European bridges. The magnitude of the uniform and concentrated loads of $LM1$ were adjusted so that the internal forces produced by $LM1$ correspond to the 99.9 [%] quantile of the internal forces produced by the measured traffic load [122, 123]. The resulting uniform and concentrated loads were chosen as characteristic loads.

3.4.3. Simulation of traffic load

The simulation Sim of the traffic load is carried out in collaboration with the chair of concrete structures of the Technical University of Munich [124]. The simulation is based on measurement data of the traffic on the A92 at a lightly trafficked location, the A92 at a normally trafficked location, and the A61 at a heavily trafficked location are statistically evaluated and probability distributions of various traffic parameters are fitted. Those distributions are used to simulate 100 years of traffic flow on the bridges of the considered portfolio. The internal forces at the critical cross-section of each bridge are evaluated every second. The structural model representing the bridge is a multi-span Euler-Bernoulli beam. A general extreme value distribution of the annual maxima is fitted from the time histories of the internal forces using the maximum likelihood method. The 99.9 [%] quantiles of the fitted extreme value distributions are chosen as the characteristic loads.

The determined characteristic values are increased by a factor α_{Sim}, which corresponds to the increase due to the fitting factors of the $LM1$ model. α_{sim} is determined separately for each load-effect. Its value is determined as the quotient of the respective load-effect due to

the characteristic traffic loads of the $LM1$ model increased with and without adjustment factors.

3.4.4. Effects of the traffic model on the design choice

The bridge is designed with respect to bending failure in the support area and in the field area and with respect to shear failure next to the supports. Following Eqn. 2.2 the design action effect $e_{d,EC}$ per considered element failure mechanism following Eurocode is calculated as

$$e_{d,EC} = t_{S,EC}(\gamma_G \cdot (l_{k,EC,1} + \cdots + l_{k,EC,6}),$$
$$\gamma_Q \cdot \left(\alpha_{q_{1,k}} \cdot q_{1,k} + \alpha_{q_{2,k}} \cdot q_{2,k} + \alpha_{q_{r,k}} \cdot q_{r,k} \right),$$
$$\gamma_Q \cdot \left(\alpha_{Q_{1,k}} \cdot Q_{1,k} + \alpha_{Q_{2,k}} \cdot Q_{2,k} \right)) \tag{3.45}$$

where $t_{S,EC}$ is the structural model representing a single/two/three-span beam calculated with Euler-Bernoulli beam theory. $\gamma_G = 1.35$ is the PSF with respect to permanent loads, $l_{k,EC,1-6}$ are the characteristic values of the permanents defined as

$$l_{k,EC,1} = 132.5 \left[\frac{kN}{m} \right] \qquad \text{Dead weight of the supporting structure} \tag{3.46}$$

$$l_{k,EC,2} = 0.002 \left[\frac{kN}{m} \right] \qquad \text{Double layer of bitumen} \tag{3.47}$$

$$l_{k,EC,3} = 13.48 \left[\frac{kN}{m} \right] \qquad \text{Asphalt} \tag{3.48}$$

$$l_{k,EC,4} = 17.87 \left[\frac{kN}{m} \right] \qquad \text{Bridge caps} \tag{3.49}$$

$$l_{k,EC,5} = 0.08 \left[\frac{kN}{m} \right] \qquad \text{Guardrails} \tag{3.50}$$

$$l_{k,EC,6} = 0.02 \left[\frac{kN}{m} \right] \qquad \text{Railing} \tag{3.51}$$

$\gamma_Q = 1.35$ is the PSF regarding traffic loads. Different load case combinations regarding the application of $q_{1,k}$, $q_{2,k}$, $q_{r,k}$, $Q_{1,k}$, and $Q_{2,k}$ on the different fields of the multi-span bridge are considered.

The design action effects $e_{d,Sim}$ following the simulation model are calculated as

$$e_{d,Sim} = t_{S,EC} \left(\gamma_G \cdot (l_{k,EC,1} + \cdots + l_{k,EC,6}) \right) + \gamma_Q \cdot e_{k,Sim} \tag{3.52}$$

where $e_{k,Sim}$ are the inner forces of the respective failure mechanism directly resulting from the simulation of the traffic (see Sec. 3.4.3). The simulation used the same structural model $t_{S,EC}$ as the Eurocode design. Hence, the effects on the design and subsequently on reliability only arise from the difference in traffic load modeling and not from different structural models being used.

The design resistances $r_{d,EC,B}$ against bending and $r_{d,EC,S}$ against shear failure are chosen

such that they are equal to the respective design action effects. The determination of the resistances follows Eqn. 2.2, where the resistance models regarding bending and shear failure from which $t_{R,EC}$ results follow Eurocode 2 [125]. The underlying models are visualized in Fig. 3.7 and 3.8. From this, the $r_{d,EC,B}$ and $r_{d,EC,S}$ are calculated following

$$r_{d,B} = A_{s1} \cdot \frac{f_y}{\gamma_S} \cdot (h - d_1) \cdot \left(1 - \frac{k_a \cdot \left(A_{s1} \cdot \frac{f_y}{\gamma_S} - A_{s2} \cdot \frac{f_y}{\gamma_S}\right)}{\alpha_R \cdot \alpha_{cc} \cdot \frac{f_c}{\gamma_C} \cdot b \cdot (h - d_1)}\right) + \qquad (3.53)$$
$$+ A_{s2} \cdot \frac{f_{y2}}{\gamma_S} \cdot \left(\frac{k_a \cdot \left(A_{s1} \cdot \frac{f_y}{\gamma_S} - A_{s2} \cdot \frac{f_y}{\gamma_S}\right)}{\alpha_R \cdot \alpha_{cc} \cdot \frac{f_c}{\gamma_C} \cdot b} - d_2\right)$$

and

$$r_{d,S} = \min\{V_{Rd,sy,Rd,max}\} \qquad (3.54)$$

where $V_{Rd,sy}$ is the tensile strength defined as

$$V_{Rd,sy} = \frac{A_S}{S_W} \cdot \frac{f_y}{\gamma_S} \cdot z \cdot (\cot(\theta) + \cot(\alpha)) \cdot \sin(\alpha) \qquad (3.55)$$

and $V_{Rd,max}$ is the compression strength defined as

$$V_{Rd,max} = b \cdot z \cdot \nu_1 \cdot \alpha_{cc} \cdot \frac{f_c}{\gamma_C} \cdot \frac{\cot(\theta) + \cot(\alpha)}{1 + \cot^2(\alpha)} \qquad (3.56)$$

The respective variables are defined as follows:

A_{S1} and A_{S2}	Steel cross-section area of the longitudinal reinforcement
A_S	Steel cross-section area of the shear reinforcement
f_y	Characteristic steel tensile strength
f_c	Characteristic concrete compression strength
S_W	Distance of the shear reinforcements
$\gamma_S = 1.15$	PSF steel tension
$\gamma_C = 1.5$	PSF concrete compression
$k_a = 0.416$	
$\alpha_R = 0.8095$	
$\alpha_{cc} = 0.85$	
$z = 0.9 \cdot (h - d_1)$	
$\nu_1 = 0.75 \cdot \left(1.1 - \frac{f_c}{500}\right)$	
h	Heigh
b	Effective width of the pressure zone
d_1 and d_2	Effective height of tension or compression reinforcement
α	Tension angle
θ	Compression angle

The compression angle can be calculated by solving the following inequality

$$1 \leq \cot(\theta) = \frac{1.2}{\left(1 - \frac{0.24 \cdot f_c^{1/3} \cdot b \cdot z}{e_d}\right)} \leq 3 \tag{3.57}$$
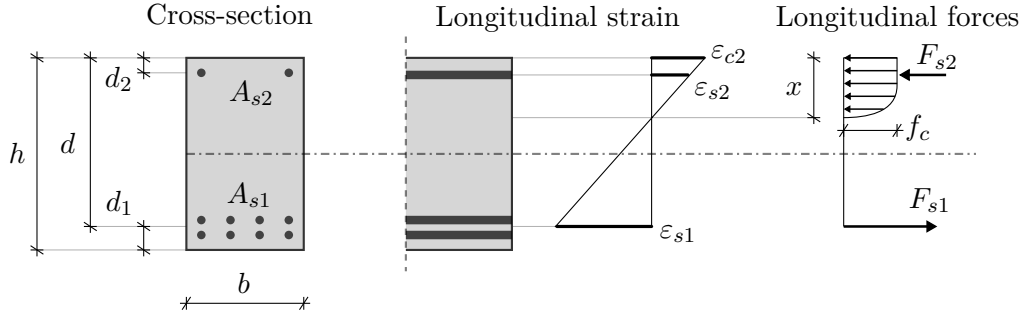
Fig. 3.7.: Bending resistance model of the Eurocode.
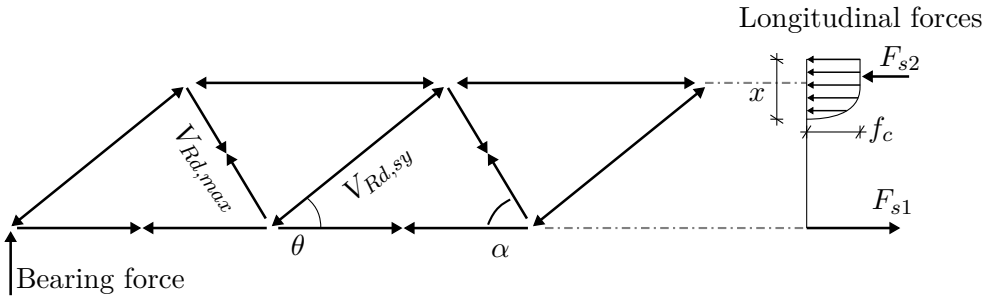
Fig. 3.8.: Shear resistance model of the Eurocode.

The design selection (steel reinforcement cross-section areas) is determined by calculating the design effects of the actions and the design resistances. Tab. 3.11 shows the resulting design choices. On average, the replacement of $LM1$ with Sim results in 29 [%] less steel volume.

n_{fields}	l_{span}	Traffic load model used to design	$A_{S,1}$ [cm^2]	$A_{S,2}$ [cm^2]	A_S [cm^2]
1	15	$LM1$	112.93	–	28.14
		Sim_{light}	78.56	–	20.10
		Sim_{medium}	83.47	–	20.10
		Sim_{heavy}	108.02	–	24.12
	20	$LM1$	181.67	–	31.67
		Sim_{light}	132.57	–	24.12
		Sim_{medium}	137.48	–	28.14
		Sim_{heavy}	152.21	–	28.14

		$LM1$	265.14	–	40.20
	25	Sim_{light}	201.31	–	32.16
		Sim_{medium}	206.22	–	32.16
		Sim_{heavy}	216.04	–	32.16
2	15	$LM1$	$\begin{bmatrix} 73.65 & 73.65 \end{bmatrix}$	88.38	32.16
		Sim_{light}	$\begin{bmatrix} 49.10 & 49.10 \end{bmatrix}$	63.83	24.12
		Sim_{medium}	$\begin{bmatrix} 54.01 & 54.01 \end{bmatrix}$	63.83	24.12
		Sim_{heavy}	$\begin{bmatrix} 63.83 & 68.74 \end{bmatrix}$	63.83	28.14
	20	$LM1$	$\begin{bmatrix} 117.84 & 117.84 \end{bmatrix}$	157.12	40.20
		Sim_{light}	$\begin{bmatrix} 83.47 & 83.47 \end{bmatrix}$	112.93	32.16
		Sim_{medium}	$\begin{bmatrix} 88.38 & 88.38 \end{bmatrix}$	117.84	32.16
		Sim_{heavy}	$\begin{bmatrix} 98.20 & 98.20 \end{bmatrix}$	117.84	32.16
	25	$LM1$	$\begin{bmatrix} 166.94 & 166.94 \end{bmatrix}$	265.14	44.22
		Sim_{light}	$\begin{bmatrix} 112.93 & 112.93 \end{bmatrix}$	171.85	36.18
		Sim_{medium}	$\begin{bmatrix} 127.66 & 132.57 \end{bmatrix}$	186.58	36.18
		Sim_{heavy}	$\begin{bmatrix} 142.39 & 137.48 \end{bmatrix}$	191.49	40.20
3	15	$LM1$	$\begin{bmatrix} 78.56 & 49.10 & 78.56 \end{bmatrix}$	$\begin{bmatrix} 78.56 & 78.56 \end{bmatrix}$	32.16
		Sim_{light}	$\begin{bmatrix} 54.01 & 34.37 & 54.01 \end{bmatrix}$	$\begin{bmatrix} 54.01 & 54.01 \end{bmatrix}$	24.12
		Sim_{medium}	$\begin{bmatrix} 58.92 & 34.37 & 58.92 \end{bmatrix}$	$\begin{bmatrix} 58.92 & 58.92 \end{bmatrix}$	24.12
		Sim_{heavy}	$\begin{bmatrix} 54.01 & 34.37 & 54.01 \end{bmatrix}$	$\begin{bmatrix} 54.01 & 54.01 \end{bmatrix}$	24.12
	20	$LM1$	$\begin{bmatrix} 127.66 & 78.56 & 7127.66 \end{bmatrix}$	$\begin{bmatrix} 137.48 & 137.48 \end{bmatrix}$	40.20
		Sim_{light}	$\begin{bmatrix} 93.29 & 49.10 & 93.29 \end{bmatrix}$	$\begin{bmatrix} 88.38 & 88.38 \end{bmatrix}$	28.14
		Sim_{medium}	$\begin{bmatrix} 93.29 & 49.10 & 93.29 \end{bmatrix}$	$\begin{bmatrix} 93.29 & 93.29 \end{bmatrix}$	32.16
		Sim_{heavy}	$\begin{bmatrix} 98.20 & 54.01 & 98.20 \end{bmatrix}$	$\begin{bmatrix} 93.29 & 93.29 \end{bmatrix}$	32.16
	25	$LM1$	$\begin{bmatrix} 181.67 & 108.02 & 181.67 \end{bmatrix}$	$\begin{bmatrix} 220.95 & 220.95 \end{bmatrix}$	48.24
		Sim_{light}	$\begin{bmatrix} 147.8 & 44.19 & 147.8 \end{bmatrix}$	$\begin{bmatrix} 152.21 & 152.21 \end{bmatrix}$	40.20
		Sim_{medium}	$\begin{bmatrix} 147.8 & 49.10 & 147.8 \end{bmatrix}$	$\begin{bmatrix} 157.12 & 157.12 \end{bmatrix}$	40.20
		Sim_{heavy}	$\begin{bmatrix} 152.21 & 49.10 & 152.21 \end{bmatrix}$	$\begin{bmatrix} 162.03 & 162.03 \end{bmatrix}$	48.24

Tab. 3.11.: Reinforcement cross-sectional areas of all bridges within the considered portfolio.

3.4.5. Effects of the traffic model to the probability of failure

The effect of the traffic model $LM1$ and Sim to the system probability of failure is investigated. System failure is defined as a combination of bending or shear failures such that the system becomes kinematic. Only failure mechanisms with negative virtual work regarding the action side are considered. Fig. 3.9 exemplary illustrates the 10 considered system failure mechanisms in the case of the three-span bridge.
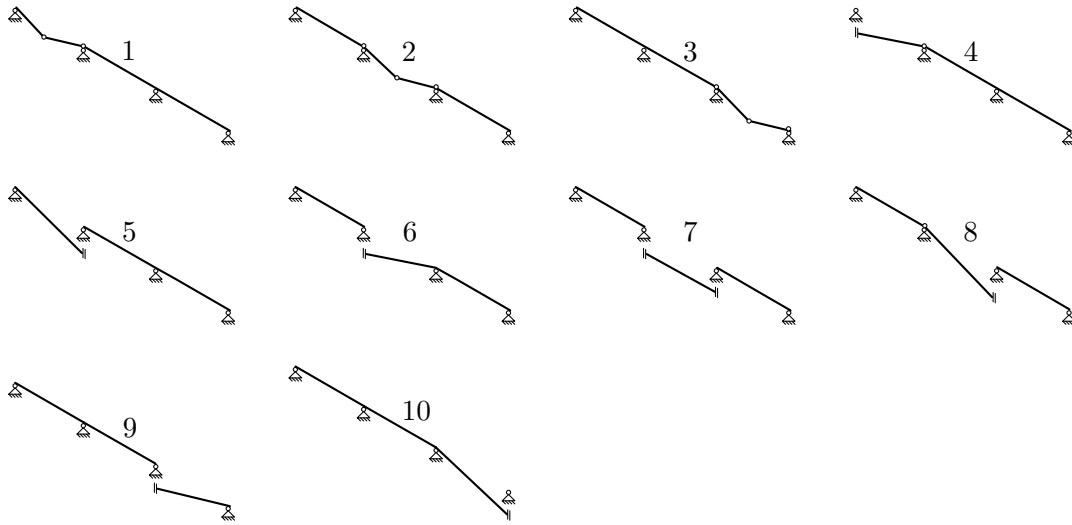
Fig. 3.9.: System failure mechanisms 1-10 of the three span version of the bridge.

For each failure mechanism, a LSF can be determined using the principle of virtual work. E.g., the LSF of the first failure mechanism is

$$
g_{Sys1,1}(\mathbf{x}) = \frac{1}{6} \cdot R_{d,S,F1} \cdot U_B + \frac{1}{15} \cdot R_{d,S,S1} \cdot U_B + \tag{3.58}
$$

$$
+ \left(-LC_1 - 12{,}5 \cdot L_1 \cdot U_1 - 12.5 \cdot \sum_{i=2}^{6} L_i \cdot U_{2-6}\right) \cdot U_S
$$

where $R_{d,S,F1}$ and $R_{d,S,S1}$ are the bending resistance in the middle of the first field and at the first inner support following Eqn. 3.53 including all its parameters as random variables and applying respective model uncertainties. U_B, U_1, U_{2-6}, U_S are the model uncertainties of the bending resistance model, the permanent self-weight, the variable self-weight, and the structural model. L_1-L_6 are random variables representing the actions defined in Eqn. 3.46-3.51. Their respective distributions are listed in Tab. 3.12. LC_1 represents the traffic load following the traffic load simulation, which is acting towards the first failure mechanism. It is derived as follows: The time series of the internal forces involved in the respective failure mechanism are weighted and summed with respect to the

factors of virtual work (in the case of the first failure mechanism, this is the sum of the first rock moment and the first support moment weighted by 1/6 and 1/15). A general extreme value distribution is fitted to the yearly maxima of the resulting time series. The statistical uncertainty is included via a multivariate normal distribution of the distribution parameters of the general extreme value distribution derived by means of the curvature of the profile log-likelihood evaluated at the parameter estimators of the general extreme value distribution [110]. This results in the following:

$$
(\xi_{LC_1}, \sigma_{LC_1}, \mu_{LC_1}) \sim \mathcal{N}\left(\begin{bmatrix} -0{,}22 \\ 29{,}73 \\ 674{,}11 \end{bmatrix}, \begin{bmatrix} 1 & -0{,}49 & -0{,}32 \\ -0{,}49 & 1 & 0{,}04 \\ -0{,}32 & 0{,}04 & 1 \end{bmatrix}\right) \ [\text{kN}] \tag{3.59}
$$

where ξ_{LC_1} is the shape parameter, σ_{LC_1} is the sale parameter and μ_{LC_1} is the location parameter. Finally, LC_1 is defined via the inverse CDF of the general extreme value distribution as

$$
LC_1 = GEV^{-1}\left(x_{LC_1}; \xi_{LC_1}, \sigma_{LC_1}, \mu_{LC_1}\right) \tag{3.60}
$$

where x_{LC_1} is the function parameter following a uniform distribution between 0 and 1.

Some traffic load situations act in the direction of multiple failure mechanisms, which makes the various failure mechanisms statistically dependent. This dependence is included via the correlation matrix of the function parameters $x_{LC_1} - x_{LC_{10}}$ which is numerically determined as

$$
\Sigma_{xx} = \begin{bmatrix}
1 & 0{,}94 & 0{,}86 & 0{,}73 & 0{,}71 & 0{,}79 & 0{,}27 & 0{,}72 & 0{,}80 & 0{,}73 \\
0{,}94 & 1 & 0{,}92 & 0{,}63 & 0{,}75 & 0{,}69 & 0{,}32 & 0{,}76 & 0{,}70 & 0{,}77 \\
0{,}86 & 0{,}92 & 1 & 0{,}51 & 0{,}84 & 0{,}58 & 0{,}33 & 0{,}85 & 0{,}59 & 0{,}84 \\
0{,}73 & 0{,}63 & 0{,}51 & 1 & 0{,}43 & 0{,}98 & 0{,}15 & 0{,}43 & 0{,}96 & 0{,}44 \\
0{,}71 & 0{,}75 & 0{,}84 & 0{,}43 & 1 & 0{,}49 & 0{,}32 & 0{,}99 & 0{,}51 & 0{,}97 \\
0{,}79 & 0{,}69 & 0{,}58 & 0{,}98 & 0{,}49 & 1 & 0{,}20 & 0{,}50 & 0{,}98 & 0{,}50 \\
0{,}27 & 0{,}32 & 0{,}33 & 0{,}15 & 0{,}32 & 0{,}20 & 1 & 0{,}32 & 0{,}23 & 0{,}27 \\
0{,}72 & 0{,}76 & 0{,}85 & 0{,}43 & 0{,}99 & 0{,}50 & 0{,}32 & 1 & 0{,}51 & 0{,}98 \\
0{,}80 & 0{,}70 & 0{,}59 & 0{,}96 & 0{,}51 & 0{,}98 & 0{,}23 & 0{,}51 & 1 & 0{,}51 \\
0{,}73 & 0{,}77 & 0{,}84 & 0{,}44 & 0{,}97 & 0{,}50 & 0{,}27 & 0{,}98 & 0{,}51 & 1
\end{bmatrix} \tag{3.61}
$$

A reliability analysis using FORM results in the probabilities of failure listed in Tab. 3.13. On average, the probability of system failure of bridges designed following $LM1$ is 6.8 orders of magnitude lower than the probability of system failure of bridges designed following Sim.

Variable	Type	Mean	Standart deviation/c.o.v.
Density of reinforced concrete	$\mathcal{N}$	$25 \left[\frac{\text{kN}}{\text{m}^3}\right]$	$1 \left[\frac{\text{kN}}{\text{m}^3}\right]$
Weight of caps	$\mathcal{N}$	$25 \left[\frac{\text{kN}}{\text{m}^3}\right]$	$1 \left[\frac{\text{kN}}{\text{m}^3}\right]$
Weight of asphalt	$\mathcal{N}$	$24 \left[\frac{\text{kN}}{\text{m}^3}\right]$	$0.96 \left[\frac{\text{kN}}{\text{m}^3}\right]$
Weight of railings	$\mathcal{N}$	$77 \left[\frac{\text{kN}}{\text{m}^3}\right]$	$1 \left[\frac{\text{kN}}{\text{m}^3}\right]$
A_S	$\mathcal{N}$	NV	$4\,[\%]$
f_y	$\mathcal{N}$	$f_{yk} + 60 \left[\frac{\text{N}}{\text{mm}^2}\right]$	$30 \left[\frac{\text{N}}{\text{mm}^2}\right]$
f_c	$\mathcal{N}$	$f_{ck} + 8 \left[\frac{\text{N}}{\text{mm}^2}\right]$	$4.5 \left[\frac{\text{N}}{\text{mm}^2}\right]$
k_a	$\mathcal{N}$	0.416	$5\,[\%]$
α_R	$\mathcal{N}$	0.8095	$5\,[\%]$
α_{cc}	$\mathcal{N}$	0.85	$10\,[\%]$
h	$\mathcal{N}$	$\begin{cases} 0{,}003 \cdot \text{NV} & \text{if NV} \leq 1000[\text{mm}] \\ 3 & \text{if NV} > 1000[\text{mm}] \end{cases}$	$\begin{cases} 4 + 0.006 \cdot \text{NV} & \text{if NV} \leq 1000[\text{mm}] \\ 10 & \text{if NV} > 1000[\text{mm}] \end{cases}$
b	$\mathcal{N}$	$\begin{cases} 0{,}003 \cdot \text{NV} & \text{if NV} \leq 1000[\text{mm}] \\ 3 & \text{if NV} > 1000[\text{mm}] \end{cases}$	$\begin{cases} 4 + 0.006 \cdot \text{NV} & \text{if NV} \leq 1000[\text{mm}] \\ 10 & \text{if NV} > 1000[\text{mm}] \end{cases}$
d	$\mathcal{N}$	$\begin{cases} 2.5 & \text{if NV} \leq 200[\text{mm}] \\ -7 & \text{if NV} > 200[\text{mm}] \end{cases}$	$6\,[\text{mm}]$
U_1	$\mathcal{N}$	1	$6\,[\%]$
U_{2-6}	$\mathcal{N}$	1	$10\,[\%]$
U_S	$\mathcal{N}$	1	$1\,[\%]$
U_B	$\mathcal{N}$	1.025	$7\,[\%]$
U_Q	$\mathcal{LN}$	1	$10\,[\%]$
U_C	$\mathcal{LN}$	1.1	$15\,[\%]$
U_P	$\mathcal{N}$	1	$15\,[\%]$

Tab. 3.12.: Random variables of the probabilistic resistance models. A_S and f_y are correlated with correlation coefficient 0.5. All other variables are assumed to be uncorrelated. f_{yk} and f_{ck} are the characteristic values (98 [%] quantiles) of the steel and the concrete strength respectively. NV is respective nominal value

n_{fields}	l_{span}	Traffic load model used in the reliability analysis	Traffic load model used to design	$P(F)$
1	15	Sim_{low}	$LM1$	10^{-17}
			Sim_{low}	10^{-9}
		Sim_{mid}	$LM1$	10^{-17}
			Sim_{mid}	10^{-9}
		Sim_{heavy}	$LM1$	10^{-17}
			Sim_{heavy}	10^{-11}
	20	Sim_{low}	$LM1$	10^{-14}
			Sim_{low}	10^{-8}
		Sim_{mid}	$LM1$	10^{-14}
			Sim_{mid}	10^{-9}
		Sim_{heavy}	$LM1$	10^{-14}
			Sim_{heavy}	10^{-10}
	25	Sim_{low}	$LM1$	10^{-15}
			Sim_{low}	10^{-10}
		Sim_{mid}	$LM1$	10^{-15}
			Sim_{mid}	10^{-10}
		Sim_{heavy}	$LM1$	10^{-15}
			Sim_{heavy}	10^{-10}
2	15	Sim_{low}	$LM1$	10^{-17}
			Sim_{low}	10^{-8}
		Sim_{mid}	$LM1$	10^{-16}
			Sim_{mid}	10^{-10}
		Sim_{heavy}	$LM1$	10^{-16}
			Sim_{heavy}	10^{-9}
	20	Sim_{low}	$LM1$	10^{-17}
			Sim_{low}	10^{-9}
		Sim_{mid}	$LM1$	10^{-17}
			Sim_{mid}	10^{-9}
		Sim_{heavy}	$LM1$	10^{-16}
			Sim_{heavy}	10^{-10}
	25	Sim_{low}	$LM1$	10^{-16}
			Sim_{low}	10^{-7}

		Sim_{mid}	$LM1$	10^{-16}
			Sim_{mid}	10^{-9}
		Sim_{heavy}	$LM1$	10^{-15}
			Sim_{heavy}	10^{-9}
		Sim_{low}	$LM1$	10^{-17}
			Sim_{low}	10^{-9}
	15	Sim_{mid}	$LM1$	10^{-17}
			Sim_{mid}	10^{-8}
		Sim_{heavy}	$LM1$	10^{-16}
			Sim_{heavy}	10^{-9}
		Sim_{low}	$LM1$	10^{-16}
			Sim_{low}	10^{-8}
3	20	Sim_{mid}	$LM1$	10^{-16}
			Sim_{mid}	10^{-8}
		Sim_{heavy}	$LM1$	10^{-16}
			Sim_{heavy}	10^{-9}
		Sim_{low}	$LM1$	10^{-15}
			Sim_{low}	10^{-10}
	25	Sim_{mid}	$LM1$	10^{-15}
			Sim_{mid}	10^{-10}
		Sim_{heavy}	$LM1$	10^{-15}
			Sim_{heavy}	10^{-10}

Tab. 3.13.: Probability of failure of all bridges within the considered portfolio.

3.4.6. Effects of hidden safeties within the traffic load model in the context of existing bridges

In this section, the studies from the previous section are adapted and applied to a hypothetical portfolio of existing bridges whose traffic loads have increased since the bridges were built. For this purpose, the structural and resistance models are no longer presented in detail as in Eqn. 3.53 and 3.54, but simplified assuming that the structural and resistance models according to Eurocode $t_{S,EC}$ and $t_{R,EC}$ are both linear and through the origin and equal to the true structural models t_S and t_R. This simplifies the calculations and allows more general results. The LSF can be formalized following Eqn. 2.37 as

$$g = \mathcal{P}_{EC} \cdot M - f_{inc} \cdot L \tag{3.62}$$

with

$$\mathcal{P}_{EC} = \frac{\gamma_F \cdot \gamma_M \cdot L_{k,EC}}{m_{k,EC}} \qquad (3.63)$$

Following Eurocode [126] γ_F is 1.35. Further, γ_M is set to be 1.1. $m_{k,EC}$ is set to be the 5% quantile of M and assumed to be equal to the purely aleatoric value. The traffic load increase since the construction day is assumed to be 30% and included via the load increase factor $f_{inc} = 1.3$. This value is not based on any data and should be interpreted as a hypothetical increase. In an actual application case, f_{inc} must be derived respectively. f_{inc} is varied between 1 and 2 in a subsequent sensitivity analysis. M, L and $L_{k,EC}$ are random variables representing the material strength, the traffic load and characteristic value of the traffic load.

The distribution of M is chosen to be follow a log-normal distribution with $\mathrm{E}[M] = 1$ and $\mathrm{c.\,o.\,v.}[M] = 0.1$. $\mathrm{c.\,o.\,v.}[M]$ is varied between 0.05 and 0.3 in a subsequent sensitivity analysis to cover the full range of various materials. The distribution of L to be follow a Gumbel distribution with $\mathrm{E}[L] = 1$ and $\mathrm{c.\,o.\,v.}[L] = 0.08$. The choice is based on the simulated traffic load model of the previous sections as follows: Generalized extreme value distributions are fitted to the action effects of the bridges of the portfolio described in Sec. 3.4.1 similar to Eqn. 3.59; however, this was done on element-level and not – as in the previous sections – on system-level. The resulting extreme value distributions have shape parameters that are close to 0, in which case the generalized extreme value distribution converges to the Gumbel distribution. The sample mean of the coefficient of variation of the field moments is 0.06, of the supporting moments is 0.08 and of the shear forces at the supports is 0.08. This justifies the choice of $\mathrm{c.\,o.\,v.}[L] = 0.08$.

The distribution of $L_{k,EC}$ is found following the approach of Eqn. 2.42 by defining the relative error in the estimation of the characteristic value as

$$\Theta_{EC} = \frac{l_k}{l_{k,EC}} \qquad (3.64)$$

where l_k is the characteristic value of the purely aleatoric traffic load. Equivalently, the error in the estimation of the characteristic value following the simulation model is defined as

$$\Theta_{adv} = \frac{l_k}{l_{k,adv}} \qquad (3.65)$$

Θ_{adv} is required in the later selection procedure to determine whether a bridge can withstand the increased load. Θ_{adv} and Θ_{EC} are chosen to follow a log-normal distributions with $\mathrm{E}[\Theta_{adv}] = 1$, $\mathrm{c.\,o.\,v.}[\Theta_{adv}] = 0.1$, $\mathrm{E}[\Theta_{EC}] = 0.7$ and $\mathrm{c.\,o.\,v.}[\Theta_{EC}] = 0.2$. The choices of the distribution parameters are justified as follows:

- $\mathrm{E}[\Theta_{adv}] = 1$: Since the simulation is based on real data, it is reasonable to assume that it estimates the characteristic value without bias.

- $\mathrm{c.\,o.\,v.}[\Theta_{adv}] = 0.1$: The coefficient of variation comprises three different uncertainties: The statistical uncertainty due to a limited simulation time, the uncertainty of the chosen distribution type and the uncertainty of incomplete modeling (e.g. con-

struction sites on the highway may change the traffic load but are not included in the simulation). The statistical uncertainty is included via the multivariate normal distribution of the parameter estimates of the fitted extreme value distributions of the inner forces [110]. The resulting coefficients of variation due to statistical uncertainty are in the range of 0.02-0.04. Unfortunately, no data is available to estimate the two other sources; hence, the overall uncertainty of c. o. v.$[\Theta_{adv}] = 0.1$ is based on a subjective assessment. c. o. v.$[\Theta_{adv}]$ is altered between 0.05 and 0.2 in a subsequent sensitivity analysis.

- $E[\Theta_{EC}] = 0.7$: Within the portfolio of bridge structures, the sample mean of the relative error is 0.76 regarding field moments, 0.70 regarding supporting moments, and 0.79 regarding the shear forces at the supports. A value of 0.7 is applied and altered between 0.4 and 1.0 in a subsequent sensitivity analysis.

- c. o. v.$[\Theta_{EC}] = 0.2$: Θ_{EC} can be rewritten as $\Theta_{EC} = \frac{l_k}{l_{k,adv}} \cdot \frac{l_{k,adv}}{l_{k,EC}} = \Theta_{adv} \cdot \frac{l_{k,adv}}{l_{k,EC}}$. The distribution parameters of Θ_{adv} is already known/estimated. The distribution of $\frac{l_{k,adv}}{l_{k,EC}}$ is also log-normal. The mean coefficient of variation of $\frac{l_{k,adv}}{l_{k,EC}}$ is 0.17 regarding field moments, 0.13 regarding supporting moments and 0.14 regarding the shear forces at the supports. Taking the highest value of 0.17 into account, a coefficient of variation of Θ_{EC} of approximately 0.2 is derived. c. o. v.$[\Theta_{EC}]$ is altered between 0.1 and 0.3 in the subsequent sensitivity analysis.

Eventually, the distributions of $L_{k,EC}$ and $L_{k,adv}$ are

$$
\begin{aligned}
L_{k,EC} \sim \mathcal{LN} \qquad\qquad & \mu_{\ln L_{k,EC}} = \ln(l_k) - \mu_{\ln\Theta_{EC}} \\
& \sigma_{\ln L_{k,EC}} = \sigma_{\ln\Theta_{EC}} \qquad\qquad\qquad (3.66) \\
L_{k,adv} \sim \mathcal{LN} \qquad\qquad & \mu_{\ln L_{k,adv}} = \ln(f_{inc} \cdot l_k) - \mu_{\ln\Theta_{adv}} \\
& \sigma_{\ln L_{k,adv}} = \sigma_{\ln\Theta_{EC}} \qquad\qquad\qquad (3.67)
\end{aligned}
$$

where $\mu_{\ln}$ and $\sigma_{\ln}$ are the location and the scale parameter of the respective log-normal distribution.

From $L_{k,EC}$ and $L_{k,adv}$ $n = 10\,000$ samples $l_{k,EC,i}$ and $l_{k,adv,i}$ are drawn. This is needed, since some of the subsequent calculations are sample-based. Apart from the statistical error originating from the sampling, the results are not effected by n.

Fig. 3.10 shows the probabilities of failure (annual reference period) of the bridges designed by Eurocode loaded with the original traffic load ($f_{inc} = 1$). The mean annual probability of failure is $E[\Pr(F \mid \text{EC-Design}, f_{inc} = 1)] = 4.9 \cdot 10^{-8}$. Following Sec. 2.3.5, this probability can be interpreted as the target probability of failure.

Fig. 3.11 shows how the probabilities of failure of the bridges designed according to Eurocode change if the traffic load is increased by 30 % ($f_{inc} = 1.3$). The increased traffic load raises the mean probability of failure from $4.9 \cdot 10^{-8}$ to $1.1 \cdot 10^{-5}$.

To decide whether a bridge is still in compliance with the standard, even if the traffic load is increased, the following procedure is performed: Given a sample-pair $l_{k,EC,i}$ and $l_{k,adv,i}$
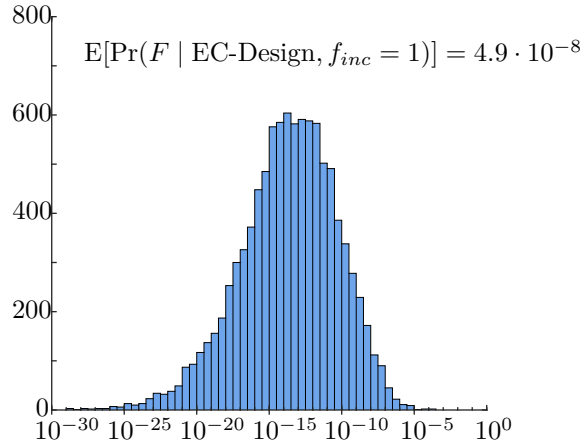
Fig. 3.10.: Histogram of the probability of failure $\Pr(F \mid \text{EC-Design}, f_{inc} = 1)$ of bridge structures designed following Eurocode.
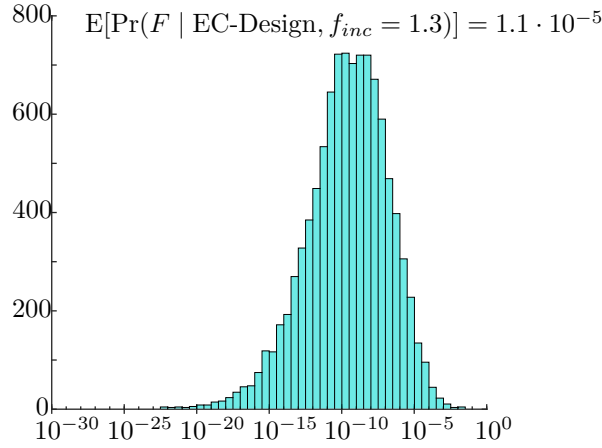

Fig. 3.11.: Histogram of the probability of failure $\Pr(F \mid \text{EC-Design}, f_{inc} = 1.3)$ of bridge structures designed following Eurocode loaded by a 30 % higher traffic load.

a bridge is accepted/rejected if:

$$l_{k,adv,i} \leq l_{k,EC,i} \Rightarrow \text{accept} \tag{3.68}$$

$$l_{k,adv,i} > l_{k,EC,i} \Rightarrow \text{reject} \tag{3.69}$$

This acceptance/rejection rule is based on the following train of thought: Advanced traffic load modeling may estimate a characteristic traffic load that is lower than the characteristic traffic load according to Eurocode (even when an increased traffic load is present). If this lower characteristic value would be used to design the bridge, it would result in smaller resistances; therefore, the reassessment according to advanced traffic load modeling would deem the existing Eurocode design to be sufficient.

Fig. 3.12 subdivides the histogram of Fig. 3.11 into accepted/rejected cases. 68.8 % of the bridge structures are accepted and 31.1 % are rejected. The mean probability of failure of the accepted bridges is $\text{E}[\Pr(F \mid \text{EC-Design}, f_{inc} = 1.3), \text{accepted}] = 1.7 \cdot 10^{-8}$ is smaller than the target probability of failure of $4.87 \cdot 10^{-8}$; hence, the reassessment leads to sufficiently safe structures.
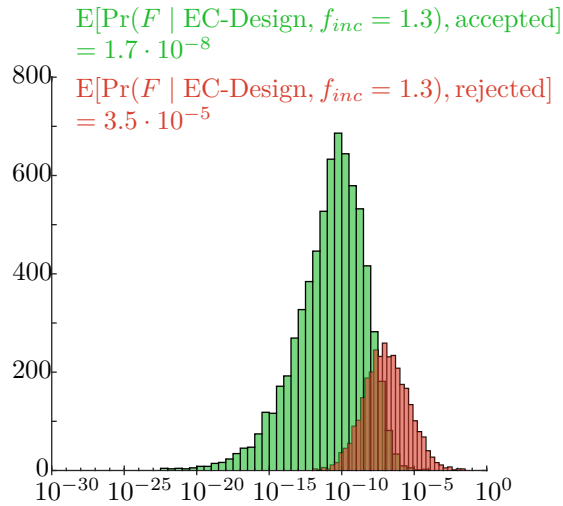
Fig. 3.12.: Histogram of the probability of failure $\Pr(F \mid \text{EC-Design}, f_{inc} = 1.3)$ of bridge structures designed following Eurocode loaded by a 30% increased traffic load divided into accepted (green) and rejected (red) bridges according to advanced traffic load modeling.

To illustrate the difference between the effect of advanced modeling in the evaluation of existing structures and the design of new structures, the traffic load simulation is also used to design the bridges loaded with the original traffic load $f_{inc} = 1^2$. Fig. 3.13 shows the resulting probabilities of failure. The mean probability of failure $\text{E}[\Pr(F \mid \text{adv-Design}, f_{inc} = 1)] = 3.1 \cdot 10^{-7}$ is below the target of $4.9 \cdot 10^{-8}$. This shows, that the negative effect on the structural reliability of the lost conservative bias is stronger than the positive effect of the reduced model uncertainty. An additional safety factor would be needed if advanced traffic load models were to be used for bridge design. Here, such a calibration is not performed.
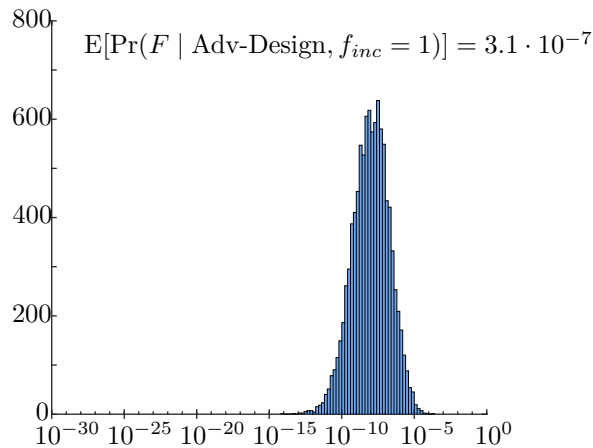

Fig. 3.13.: Histogram of the probability of failure $\Pr(F \mid \text{Adv-Design}, f_{inc} = 1)$ of bridge structures designed following advanced traffic load modeling.

---

[2]Remark: The resulting probabilities of failure of the advanced designs with an increased load ($f_{inc} > 1$) would be exactly the same as in Fig. 3.13, as long as the load increase is also considered within the design. f_{inc} would appear twice and cancel each other out: Once within the design (a factor applied on $l_{k,adv,i}$) and once as a factor applied on the load L.

In conclusion, the use of advanced models for the reassessment of existing structures appears justified without further adjustment of the safety factors within this hypothetical setup. This is in contrast to the design of new structures. The difference can be understood by comparing the histogram of the probability of failure of the accepted bridge structures (green histogram in Fig. 3.12) to the histogram of the probability of failure of bridge structures designed by advanced traffic load modeling (blue histogram in Fig. 3.13): Following Fig. 3.68, a structure is accepted if $L_{k,adv} \leq L_{k,EC}$. If equality holds, the accepted Eurocode design and the advanced design are equal; hence, both histograms coincide. The greater the difference $L_{k,EC} - L_{k,adv}$, the more hidden safety remains, which decreases the probability of failure in the reassessment case.

The setup of this study is, of course, only one possible setup. Other setups obviously lead to different results. Therefore, an additional sensitivity analysis is performed. Fig. 3.14 shows the resulting probabilities of failure and the resulting acceptance rates, when altering selected parameters of the case study one at a time.

The potentially critical cases of the sensitivity analysis carried out – which should be identified – are the cases in which the mean probability of failure of the assumed structures is greater than the mean probability of failure of the bridge structures under the original load (target probability of failure). The results show that this is the case when

- the load strongly increases ($f_{inc} > 1.6$). However, this case is not critical, since the target probability of failure is not exceeded by much and the acceptance rate simultaneously drops to a very low level.

- the coefficient of variation of the material property is rather large (c.o.v.$[M] > 0.2$). This is also not critical since the target probability of failure is only marginally exceeded.

- the coefficient of variation of the traffic load is rather large (c.o.v.$[M] > 0.15$). Again, this is not critical, since the target probability of failure is only marginally exceeded.

- the estimation of the characteristic traffic load according to Eurocode is very biased ($E[\Theta_{EC}] < 0.65$). This is also not concerning since, in this case, the Eurocode design includes high amounts of hidden safety, which leads to very low probabilities of failure. This hidden safety can serve as a reserve against increased traffic loads.

- the estimation of the characteristic traffic load according to Eurocode is associated with low uncertainty (c.o.v.$[\Theta_{EC}] < 0.18$). In this case, the coefficient of variation in the estimation of the characteristic value of the Eurocode model and the advanced traffic load model match closely. Hence, the reassessment does not reduce the uncertainty significantly but reduces the bias (hidden safety). This case can be critical and should be prevented; however, this case is rare since the uncertainty of advanced models is typically much smaller than the uncertainty of standard models.

- the estimation of the characteristic traffic load according to advanced models is relatively uncertain (c.o.v.$[\Theta_{adv}] > 0.18$). As in the previous bullet point, the

coefficient of variation in the estimation of the characteristic value of the Eurocode model and the advanced traffic load model are close. This case can also be critical and should be prevented; however, it is again rather rare.

Overall, the reassessment of bridges through advanced modeling in most cases leads to sufficiently safe structures. It is only critical if c. o. v.$[\Theta_{EC}]$ and c. o. v.$[\Theta_{adv}]$ are very similar. However, the conducted sensitivity analysis only varies one parameter at a time. A case in which multiple parameters are varied simultaneously may lead to a more critical outcome.
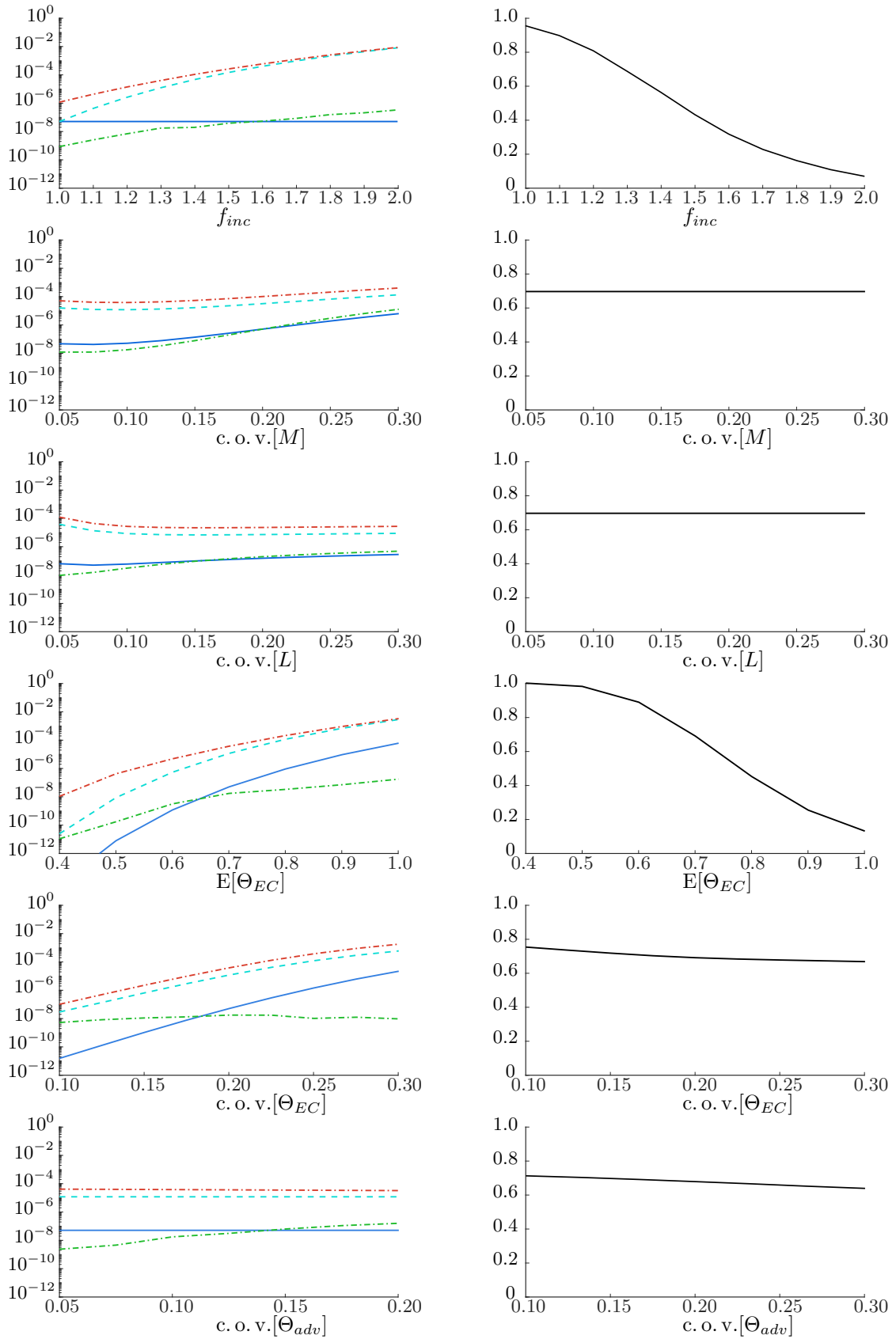
Fig. 3.14.: Mean probability of failure (left) and acceptance rate (right) of bridge structures altering setup parameters one at a time. The blue lines represent the mean probability of failure when the original load is applied (target probability of failure), the teal dashed lines represent the mean probability of failure when the increased load is applied and the dash doted green and red lines represent the mean probability of failure of the accepted and the rejected bridge structures.

3.5. Discussion

The proposed framework can be used to account for hidden safety within the partial safety concept when advanced modeling techniques replace standard models. This will typically result in – on average – lower design values while still achieving the same level of safety. It may seem counter-intuitive that the average reliability remains unchanged if the resistances are reduced on average; however, this is due to the more targeted designs (i.e., the design is strengthened where it is needed and relaxed where it is not). This translates into a higher material efficiency. The results are more sustainable and economic structures. Since the building industry is one of the main material and energy consumers and is responsible for a high amount of greenhouse gas emissions, it is crucial to exploit this material saving potential [127].

The decrease of the average design value does not directly correspond to the same reduction of the material effort for two reasons: First, the relationship between the design value and the material effort depends on the design situation (e.g., for trusses under pure tension, the relationship is a one-to-one mapping, but the bending resistance of a rectangular beam has a quadratic relationship with the material effort). Second, the design values within the framework are calculated only with respect to ultimate limit states. Serviceability limit states are not included, but are often decisive for the design.

The application of the proposed framework ideally uses only purely aleatoric models. This, however, is unrealistic in most cases and certain model assumptions have to be made. These assumptions might not be fully correct; hence, the resulting calibration may not be perfect. However, it is still a step in the right direction and preferable to the applications of advanced models without a calibration through the proposed framework.

The most challenging model assumptions that have to be made are the accuracy of the standard and advanced models. The probabilistic description of these accuracies is challenging because they characterize the model prediction relative to the "truth". However, the truth is unknown. Empirical data and expert knowledge must be taken into account carefully. The quantification of the effect of hidden safety and the calibration of the PSF concept are sensitive to the probability distributions describing model accuracies.

The choice of a representative portfolio of design situations and an adequate probabilistic description of all random variables within the portfolio may seem to be another critical point. However, the calibration of safety components is not sensitive to the portfolio choices. This is because the portfolio is used for the investigation of both the standard model and the advanced model. This validates a relative comparison – which is the basis of the calibration – of the two models, even if the portfolio is not perfectly accurate.

Overall, adapting the PSF concept using the proposed framework is not a trivial task and probably not worth the effort in most individual design cases. However, it is also not intended to be used in individual design cases but is aimed at code writers or developers of advanced models who perform this work once. The resulting adaptation of the PSF concept can then be applied by every engineer who wants to use the respective advanced model.

3.6. Conclusion

Structural design codes are the result of a long evolutionary adaptation process (see. Sec. 2.1). This adaptation is partly empirical (through the inclusion of new experience) and partly deductive (through the use of new and advanced models). The empirical adaptation of design codes mostly retains the hidden safety arising from conservative choices in model parameters. In contrast, a deductive adaptation typically changes the amount of hidden safety. The proposed framework compensates for this and ensures a consistent overall safety level.

Investigations of the effects of hidden safety are necessary if advanced models – which are not covered by the codes – are applied. With the rapid developments in computational engineering, such use is becoming increasingly frequent. Engineers who use these newly developed models may have the impression that their designs have increased reliability because the advanced models are more precise. However, because of hidden safety, this is not necessarily the case. The exchange of existing standard models with advanced and potentially more accurate models can have two counteractive effects on structural reliability: On the one hand, existing models typically include hidden safety due to conservative assumptions and parameter specifications. More advanced models may be less conservative; hence, (hidden) safety might get lost. On the other hand, more advanced models typically include less model uncertainty, which increases structural reliability.

If one of the two effects on the reliability of structures is dominant, the safety concept should be calibrated accordingly. This can be done via the proposed framework. The framework ensures that the advanced models and the established models lead to the same level of safety. The higher accuracy of advanced models is still utilized, which translates into higher material efficiency. This results in more sustainable and economical structures that are just as safe as the current status quo, which follows standard models.

4. System effects in codified design

The PSF concept in structural design codes has been developed and is applied at the level of structural elements. Safety factors are calibrated such that a target reliability is – on average – achieved for each element failure mechanism. System effects are not taken into account. Resulting system reliabilities can be below as well as above the target reliability, depending on the system. This section addresses this problem and derives an additional PSF that decreases the resistance of systems with high system reliability and increases the resistance of systems with low system reliability. The values of the additional PSF γ_{Sys} are derived via a link to a generalized version of the Daniels system. The generalization includes probabilistic action modeling, material models, correlation among members, and non-equal load-sharing among members. For each generalization, efficient reliability evaluation methods are proposed and numerical investigations are conducted.

The proposed principle behind the use of the Daniels system for deriving γ_{Sys} is, in a nutshell, the following: First, a link between general structural systems and the generalized version of the Daniels system is established, such that one is able to approximate the reliability of any structural system in terms of the reliability of a generalized Daniels system. Second, a recalibration of the PSF concept is performed with respect to the design of different variations of the Daniels system. This homogenizes the reliability level of the Daniels system with respect to system effects. Third, γ_{Sys} can be translated back and applied to general structural systems. Due to the necessary simplifications, the derived PSF does not completely homogenize the reliability level of general structural systems, however, it is a step in the right direction.

Within this section, it is assumed that the nominal structural model and the nominal resistance model are equal to the respective purely aleatoric models; hence, $t_{S,EC} = t_S$ and $t_{R,EC} = t_R$. Moreover, it is assumed that the nominal material models and the nominal action models are equal to the respective purely aleatoric models; hence, $M_{EC} = M$ and $L_{EC} = L$ and, therefore, $m_{k,EC} = m_k$ and $l_{k,EC} = l_k$.

Parts of this section are taken from Teichgräber et al. [128].

4.1. Motivating example

The following example illustrates two aspects and potential improvements regarding these aspects when designing structural systems according to the PSF concept. The first aspect is resource efficiency, i.e., that the same level of safety could be achieved with fewer resources. The second aspect is the homogenization of the safety level, i.e., that the

element-based design can lead to both too high and too low safety and how this can be homogenized. In this example, both aspects will be illustrated and two ideas will be introduced on how to tackle those aspects; however, only the second idea is feasible within the PSF concept, so only this idea will be pursued.

Fig. 4.1 (left) illustrates the example structure. It is a L-shaped frame structure with a horizontal force H and a vertical force V. For the sake of simplicity, only bending failure is considered. Following the PSF concept, the design bending resistances M_{1,R_d} and M_{2,R_d} of the horizontal and vertical members result from the maximum bending moment per member at the design load level (see Fig. 4.1 (right)). Numerical values of the characteristic and the design actions/ resistances, as well as the respective distributions, are omitted in the following example as they do not contribute to the understanding of the problem at hand.
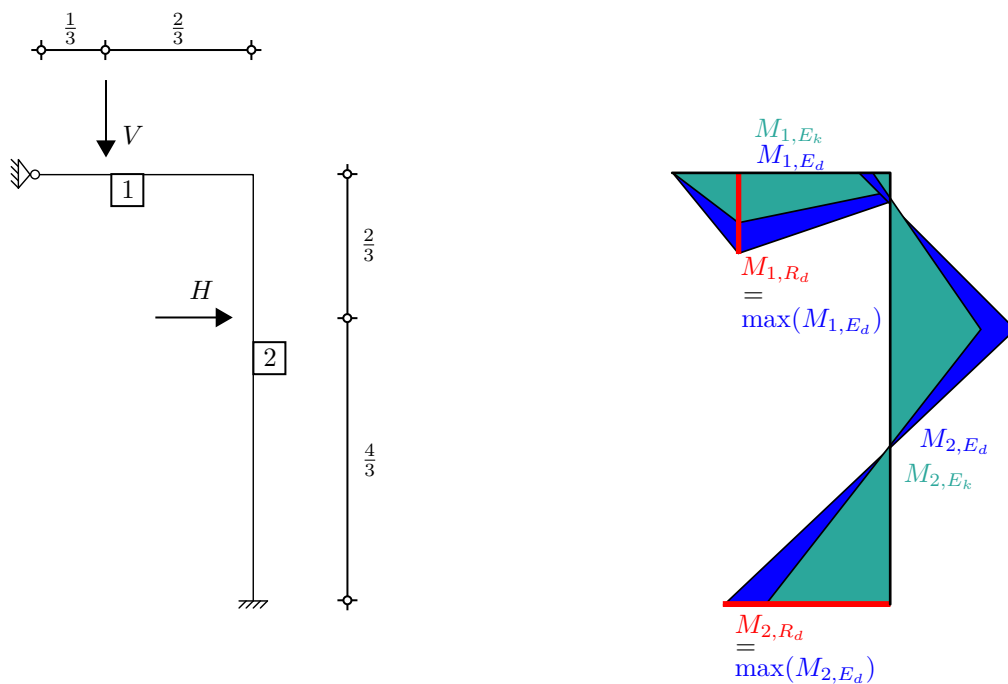

Fig. 4.1.: Example structure (left) and the bending moments due to the actions V and H at characteristic (cyan) and design (blue) load level (right).

To illustrate the effects of element-based design, a reliability analysis at the system-level needs to be conducted. This requires the analysis of the failure mechanisms of the system. The failure mechanisms are obtained by iteratively adding joints at the locations of maximum bending moment per element until the system becomes kinematic. Fig. 4.2 illustrates this procedure. This results in three failure mechanisms FM_1, FM_2 and FM_3.

When determining the failure mechanisms in the general case (this example only considers bending failure), failure in tension, compression, shear force, etc. have to be considered too. For larger systems with numerous element failure mechanisms, finding the failure mechanisms can become a non-trivial combinatorial problem. Methods for effectively
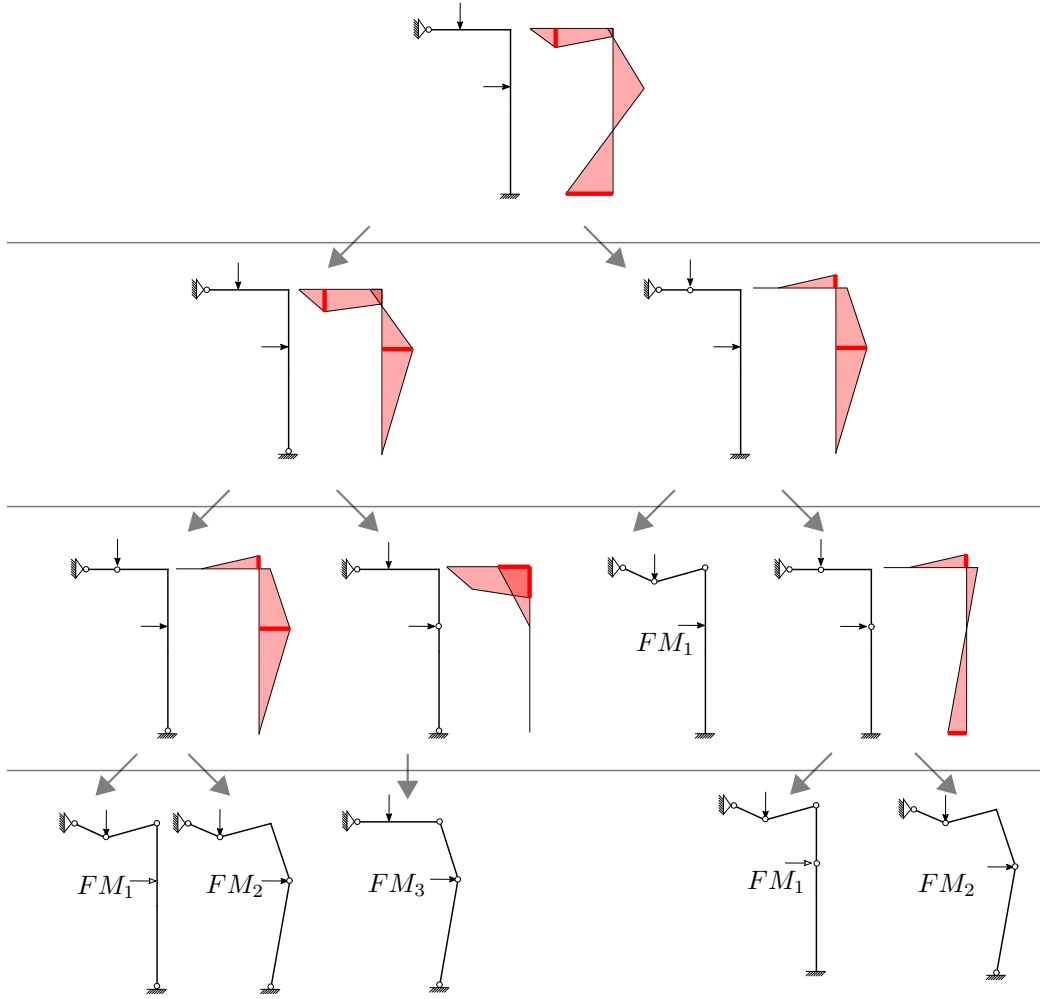
Fig. 4.2.: Illustration of the determination of failure mechanisms with respect to bending failure by iteratively adding joints at the locations of maximum moments per element.

finding all (relevant) failure mechanisms are described, e.g., in [69].

Once the failure mechanisms have been determined, a LSF can be obtained for each failure mechanism using the principle of virtual work (assuming ideal plastic material behavior). Fig. 4.3 illustrates this for the second failure mechanism FM_2. This results in the following three LSFs, each of which describes a system failure mechanism:

$$g_1 = \frac{9}{2} \cdot R_1 + \frac{3}{2} \cdot \min\left(R_1, R_2\right) - V \tag{4.1}$$

$$g_2 = \frac{9}{2} \cdot R_1 + \frac{12}{4} \cdot R_2 - V - H \tag{4.2}$$

$$g_3 = \frac{3}{2} \cdot \min\left(R_1, R_2\right) + \frac{12}{4} \cdot R_2 - H \tag{4.3}$$

The location parameters of the distributions of R_1 and R_2 directly follow from the chosen design values (M_{1,R_d} and M_{2,R_d}). Hence, different design choices will result in different

limit state functions and, therefore, different reliabilities. The system reliability can be obtained by considering the series system of failure events $\{g_1 < 0\}$, $\{g_2 < 0\}$ and $\{g_3 < 0\}$. The application of FORM for series systems results in a system reliability of $\beta_{Sys} = 4.9$.
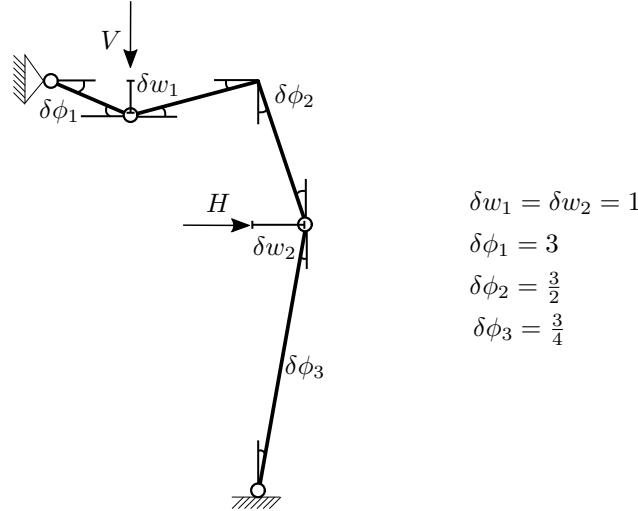
$$\delta w_1 = \delta w_2 = 1$$
$$\delta \phi_1 = 3$$
$$\delta \phi_2 = \frac{3}{2}$$
$$\delta \phi_3 = \frac{3}{4}$$

Fig. 4.3.: Virtual displacement figure of the second failure mechanism FM_2.

Fig. 4.4 plots potential design choices (including the above design choices of M_{1,R_d} and M_{2,R_d}) and the isolines of their respective system reliability indices. The green area indicates design choices that are valid according to the PSF concept and the red area indicates design choices that are not valid according to the PSF concept. The questions to be answered in this context are: Should the range of valid design resistances be changed and is such a change possible within the PSF concept? Two different ideas of how the ranges of valid design values could be adjusted are illustrated in Fig. 4.5.

The first idea (left illustration of Fig. 4.5) is to allow certain design resistances to be below the threshold set by the PSF concept as long as this is compensated through other design resistances that are above their respective threshold, resulting in the overall same level of safety. This may be desirable since some design resistances can only be achieved with a greater use of resources than others. Hence, this idea tackles the above-mentioned aspect of resource efficiency. The other above-mentioned aspect of homogenizing the safety level is not addressed by this idea. In practice, the implementation of this idea requires a system reliability analysis of the structure to ensure that the level of safety remains unchanged. However, this idea can not be implemented within the PSF concept. Instead, a full probabilistic design must be conducted. Since this work focuses on adjustments of the PSF concept, this idea is not further investigated.

The second idea (right illustration of Fig. 4.5) is to adjust the design resistances via the application of an additional PSF γ_{Sys}. The value of γ_{Sys} can be above or below 1, thereby either increasing or decreasing the threshold of possible design resistances set by the PSF concept. γ_{Sys} is – ideally – below 1 if the respective system reliability is above the target reliability and vice versa. This idea mainly tackles the aspect of homogenizing
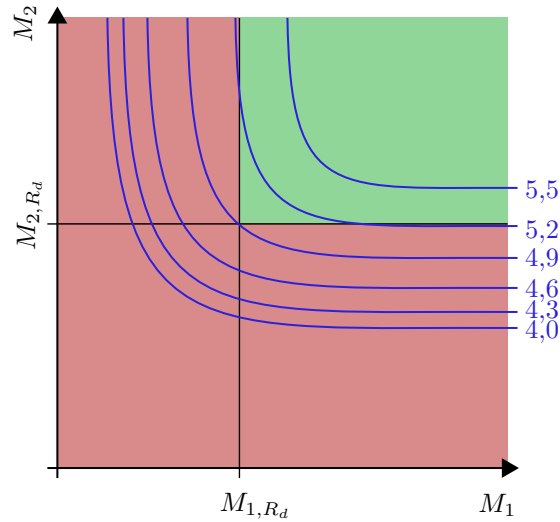
Fig. 4.4.: Valid (green area) and non-valid design values (red area) for a design of the example system following the PSF concept. Isolines of the system reliability are in blue.
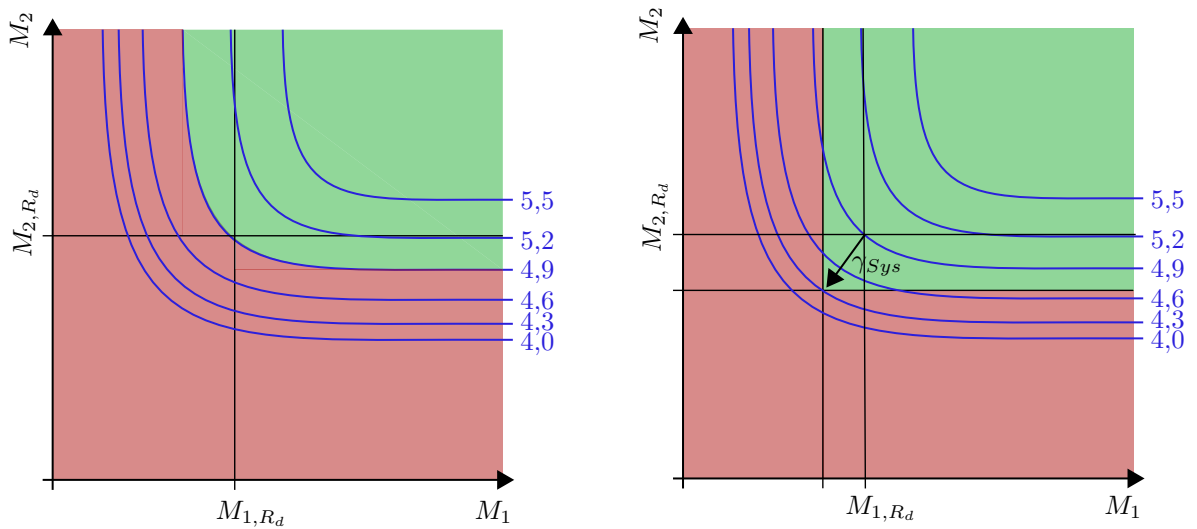

Fig. 4.5.: Two possible adjustments of the ranges of valid design resistances (green areas). The left figure allows one of the design resistances to be below the valid threshold according to the PSF concept if this is compensated for by the other design resistance above the respective threshold. In the right figure, the valid ranges of the design resistances are adjusted via an additional PSF γ_{Sys}, resulting in a different safety level, ideally closer to a certain target safety level.

the safety level. The aspect of resource efficiency may also be addressed since the relationship between design resistance and probability of failure is not linear (doubling the design resistance typically reduces the failure probability by more than half), and thus

homogenization of the safety level can have a positive effect on resource efficiency.

In the following, the second idea is realized. The values of γ_{Sys} are derived in dependence on various system properties of general structural systems. Within this derivation, the Daniels system plays a key role, which is introduced in the next section.

4.2. Original Daniels system

The Daniels system (Fig. 4.6) is named after Henry Ellis Daniels. His Ph.D., which was founded by the Wool Industries Research Association, investigates the strength of a bundle of textile threads [129]. He derived analytical expressions for the probability distribution of the strength of such bundles under deterministic load. His findings were later applied to study the system effects of structural systems (e.g. [130–132]). The key characteristic of the Daniels system is that all members are subjected to the same action. If one or more members fail, the load is redistributed evenly among the remaining members.
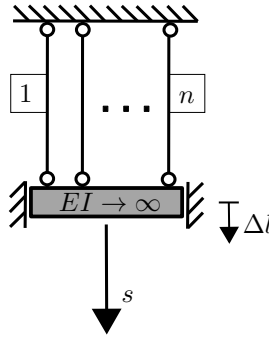

Fig. 4.6.: Daniels system.

The original formulation of the Daniels system (Fig. 4.6) has the following properties:

- Deterministic and equal cross-sections A_i.

- Deterministic and equal Young's modulus E_i.

- Deterministic action s. The horizontal bar distributes the action equally among all members that have not failed.

- The ultimate strengths $\sigma_{max,i}$ $(i = 1, \ldots, n)$ of the members are random variables. All $\sigma_{max,i}$ are independent and identically distributed.

- Members exhibit linear-elastic brittle material behavior according to Fig. 4.7.

For simplification purposes and without loss of generality, all cross-sections are here set to one: $A_i := 1$ $(i = 1, \ldots, n)$. Consequently, the maximal resistance R_i of the ith bar is equal to $\sigma_{max,i}$.
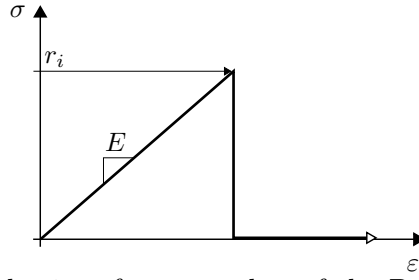
Fig. 4.7.: Brittle material behavior of one member of the Daniels system: Linear-elastic material behavior until element strength $\sigma_{max,i} = r_i$ is reached. Once r_i is exceeded, the resistance drops to zero.

The resistance of the Daniels system is determined from the following train of thought: The system resistance until the first member fails is n times the resistance of the weakest member. The system resistance until the second member fails is $n-1$ times the resistance of the second-weakest member. And so on. It follows that the system resistance $R_{Sys,n}$ of a Daniels system with n members is

$$R_{Sys,n} = \max_{i=1}^{n} \left\{ (n-i+1) \cdot R_{(i)} \right\} \tag{4.4}$$

where $R_{(i)}$ is the resistance of the ith strongest member, i.e., it is the ith order statistic of R_i. Fig. 4.8 illustrates the principle behind Eqn. 4.4 for a Daniels system with 3 members.
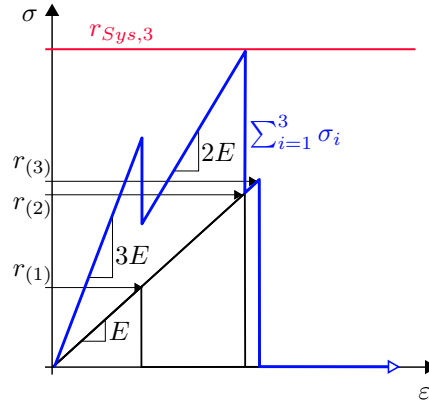

Fig. 4.8.: Illustration of the system resistance $R_{Sys,3}$ of a Daniels system with three members. The maximum system resistance is reached before failure of the second-weakest member $r_{Sys,3} = 2 \cdot r_{(2)}$.

For a Daniels system with three members (as in Fig. 4.8) the probability of system failure $\Pr(F_{Sys,3})$ can be calculated as

$$\Pr(F_{Sys,3}) = \sum_{i=1}^{3} \sum_{\substack{j=1 \\ j \neq i}}^{3} \sum_{\substack{k=1 \\ k \neq i,j}}^{3} \Pr\left(R_i < \frac{s}{3} \cap R_i < R_j < \frac{s}{2} \cap R_j < R_k < s \right) = \tag{4.5}$$

$$= 3! \cdot \int_{0}^{\frac{s}{3}} f_R(r_3) \int_{r_3}^{\frac{s}{2}} f_R(r_2) \int_{r_2}^{s} f_R(r_1) \mathrm{d}r_1 \, \mathrm{d}r_2 \, \mathrm{d}r_3$$

71

where f_R is the PSF of the member resistance R. Hence, the probability of failure is calculated by solving a three-dimensional integral. In the general case of a Daniels system with n members, the probability of failure is calculated as

$$\Pr(F_{Sys,n}) = n! \cdot \int_0^{\frac{s}{n}} \int_{r_n}^{\frac{s}{n-1}} \cdots \int_{r_2}^{s} f_R(r_n) \cdot f_R(r_{n-1}) \ldots f_R(r_1) \, \mathrm{d}r_1 \ldots \mathrm{d}r_{n-1} \, \mathrm{d}r_n \quad (4.6)$$

Daniels [129] found multiple analytical expressions to calculate this integral. The most well-known one is derived via a Taylor series expansion of the multidimensional integral in terms of the lower bound of the first integral and via a recursive relation of the n-folded integral and its derivative. From this, the following recursive formula of the CDF of the system resistance can be derived [130, 132]:

$$F_{R_{Sys,n}}(s) = (-1)^{n+1} \cdot F_R^n \left(\frac{s}{n} \right) - \sum_{i=1}^{n-1} \left[(-1)^i \cdot \binom{n}{i} \cdot F_R^i \left(\frac{s}{n} \right) \cdot F_{R_{Sys,n-i}}(s) \right] \quad (4.7)$$

where F_R is the CDF of the resistance of a single member.

For an intuitive understanding of Eqn. 4.7, one can interpret the formula as a sophisticated application of the principle of inclusion and exclusion, which exploits the symmetry of the failure domain. Fig. 4.9 illustrates this for the case of $n = 2$. The failure domain is the union of two rectangles.

$$\Pr(F_{Sys,2}) = \ldots$$
$$= F_R(s) \cdot F_R(\tfrac{s}{2}) + F_R(\tfrac{s}{2}) \cdot F_R(s) - F_R(\tfrac{s}{2}) \cdot F_R(\tfrac{s}{2})$$
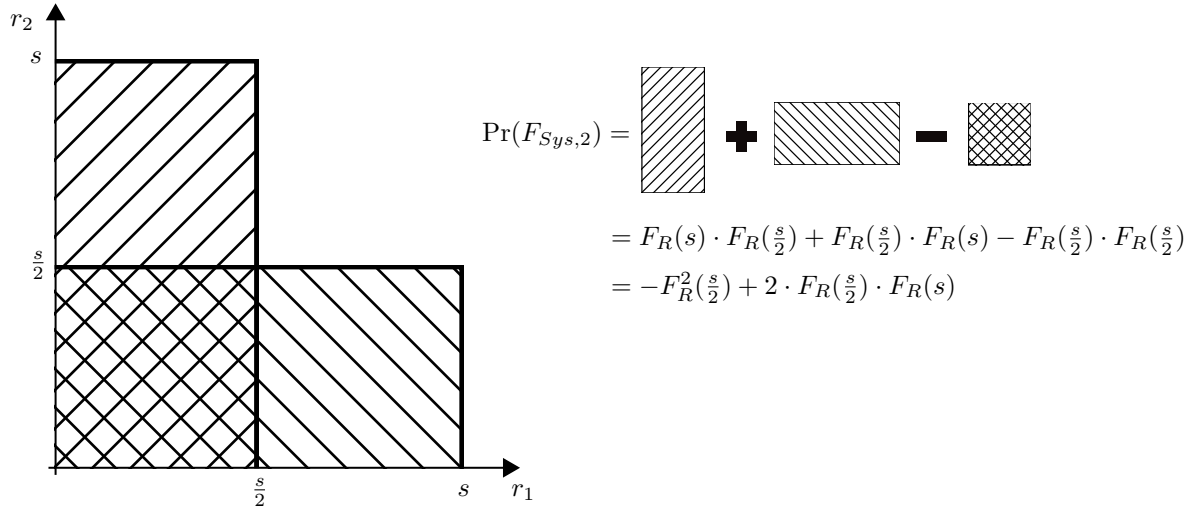$$= -F_R^2(\tfrac{s}{2}) + 2 \cdot F_R(\tfrac{s}{2}) \cdot F_R(s)$$

Fig. 4.9.: Illustration of the failure domain of a Daniels system with two bars (left) and the calculation of the probability of system failure via the principle of inclusion and exclusion.

In the general case, the union of $n!$ hypercubes defines the failure domain. Their edge lengths are defined via all possible permutations of s, $\frac{s}{2}$, $\ldots$ $\frac{s}{n}$. Since the resistances of the members are independent, the evaluation of the probability of each hypercube and their respective intersections is possible via evaluations of the member resistances' CDF.

Besides the exact formula to calculate the probability of failure, Daniels also found that $R_{Sys,n}$ is asymptotically normally distributed [129]. This finding was improved in [133] and

extended, such that correlation among members [130,134], more general force-deformation curves [135], local load-sharing (stress concentrations of members next to failed members) [136–138] and time-dependent deterioration [139] can be considered. Different, and not necessarily Gaussian, asymptotic behavior was deduced for these different extensions. However, the convergence to the asymptotic result is slow; this holds for the original formulation as well as for all extensions [140]. This means that the limiting distribution of the system resistance is only suitable for systems with a large number of members n.

If the number of members n is smaller, a more exact evaluation of the system resistance is necessary. In this regard, the author is not aware of any research other than the works of Gollwitzer, Hohenbichler, and Rackwitz [70, 131, 132, 141]. They utilized an order-statistics approach and reinterpreted system failure as the intersection of failure events [141]. The probability of this intersection can be approximated via FORM for parallel systems [70]. The approximation error of this approach is not negligible but represents a major improvement over the asymptotic approach. This approach allows the relaxation of some of Daniel's original assumptions. Gollwitzer and Rackwitz utilized this to carry out numerous numerical studies covering probabilistic action modeling, material modeling, and correlation [131, 132].

Inspired by the works of Gollwitzer et al., the subsequent Sec. 4.3 extends the Daniels system with respect to four aspects: probabilistic action modeling, material modeling of the members, correlation among members, and non-equal load-sharing among members. For all extensions, efficient algorithms for reliability evaluations are developed and numerical studies are provided.

Three of these four extensions of the Daniels system coincide with the extensions of Gollwitzer et al., namely, action modeling, material modeling, and correlation. However, the approaches within this work differ fundamentally: They are not based on FORM for parallel systems, but either analytical, based on standard FORM, or sampling methods. The proposed material model is simpler than the one of Gollwitzer [132] which is based on a material model for timber with multiple parameters to calibrate. The proposed model is less specialized and therefore possibly less accurate, but it is more generally applicable. Moreover, the proposed approach to include correlation is more general.

4.2.1. Relation to parallel and series system

When it comes to the reliability of structural systems, the two most extreme cases of structural behavior are represented by the ideal parallel and the ideal series systems. These two systems form a lower bound (ideal series system) and an upper bound (ideal parallel system) of the system reliability of any general structural system, including the Daniels system. For this reason, they are important in the classification of the subsequent investigations. Fig. 4.10 shows a mechanical interpretation of an ideal parallel system and an ideal series system.

System failure of the ideal parallel system is defined as the state where all members fail. In most application cases, the definition of system failure of the parallel system is not very meaningful. The ideal series system fails if at least one of the members fails. The
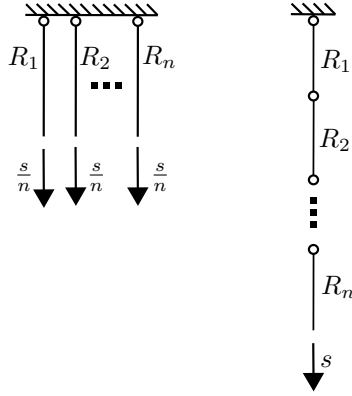
Fig. 4.10.: Mechanical representation of an ideal parallel system (left) and an ideal series system (right).

respective probabilities of system failure are

$$\Pr(F_{Sys,n;\text{Parallel}}) = \left[F_R \left(\frac{s}{n} \right) \right]^n \tag{4.8}$$

$$\Pr(F_{Sys,n;\text{Series}}) = 1 - \left[1 - F_R \left(s \right) \right]^n \tag{4.9}$$

where s is the action, n is the number of independent and identical distributed members, and F_R is the CDF of the member resistances.

4.2.2. Numerical investigations with the original Daniels system

Numerous numerical investigations of the original Daniels system exist in literature (e.g., [70, 129, 131, 132, 141]); however, for the sake of completeness and to improve the understanding of the subsequent extensions of the Daniels system, this section performs some numerical investigations.

The resistances R_i of the Daniels system are assumed to be independent and follow a log-normal distribution ($\text{E}[R_i] = 1$ and $\text{c.o.v.}[R_i] = 0.1$). The load s is deterministically chosen such that a certain target reliability index β_{TRG} is met for the case of a Daniels system with just one member. In the case of the Daniels systems with $n > 1$, s is scaled proportionally to the number of members n, such that the load per member (if no member fails) is the same for any investigated Daniels system.

Fig. 4.11 shows the reliability index with an increasing number of members for different target reliability indices. The number of members for which the minimum reliability index is obtained depends on the value of β_{TRG}. If β_{TRG} is small, the minimum is obtained for large n and the reliability behavior of the Daniels system is similar to the reliability behavior of the ideal series system. For larger β_{TRG}, the minimum is reached for smaller n. For the rest of this section, β_{TRG} is fixed at $= 4.3$, as this is in the common range of the nominal reliability index required for structural systems [61, 108]. All subsequent results are not sensitive to minor changes of the chosen target reliability index. However, if β_{TRG} deviates more strongly from 4.3 the subsequent results should be considered with
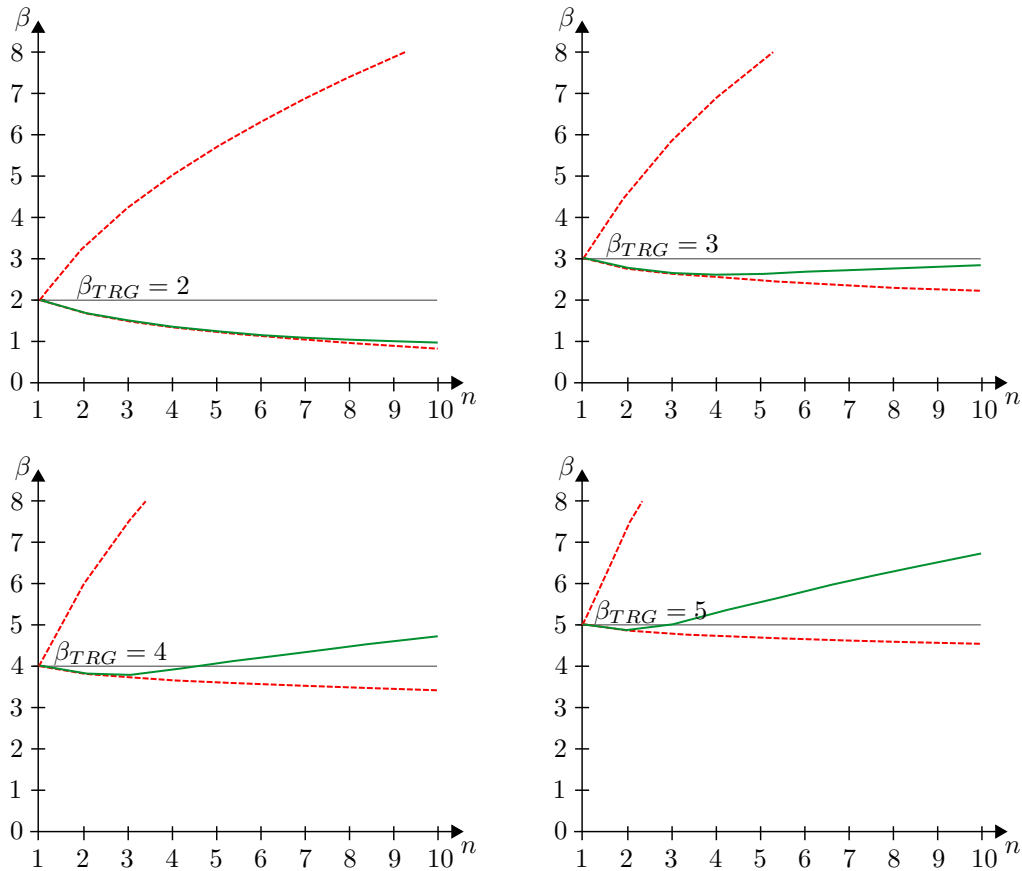
caution.

Fig. 4.11.: Reliability index of the Daniels system (green) and the ideal parallel/series system (dashed red) with 1 to 10 members for different target reliability indices β_{TRG} of 2, 3, 4, and 5.

Fig. 4.12 plots the reliability index for different coefficients of variation of R. The coefficient of variation of the member resistance R has a strong impact on the reliability behavior of the Daniels system. If c. o. v.$[R]$ is small, the reliability index of the Daniels system is closer to the one of a series system. For larger c. o. v.$[R]$, the reliability index of the Daniels system behaves more like a parallel system. The reliability indices of the ideal parallel/series system are independent of c. o. v.$[R]$.
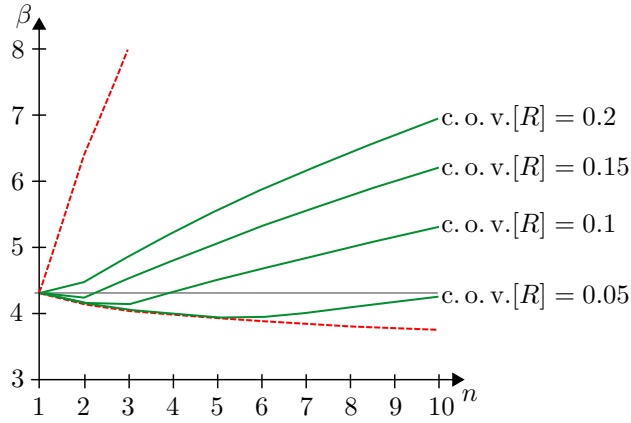
Fig. 4.12.: Reliability index of the Daniels system (green) and the ideal parallel/series system (upper/lower dashed red) with 1 to 10 members with different c. o. v. of R of 0.05, 0.1, 0.15, and 0.2.

4.3. Generalized Daniels system

In the following, the original formulation of Daniels is generalized in four directions to consider probabilistic load modeling, plastic and semi-plastic material modeling (however, without material mixing), modeling of correlation among members, and non-equal load-sharing among members. For all extensions, efficient algorithms for reliability evaluations are developed that are fast and accurate. The four extensions are presented separately, but they can partly be combined.

4.3.1. Probabilistic load modeling

Let $t_S(\mathbf{S})$ be a function modeling the resulting action effect on the Daniels System. $\mathbf{S}$ is a vector of action phenomena applied simultaneously (e.g., wind and snow), and the function t_S represents their combined effect. Assuming independence of the resistances and the action, the probability of system failure can be calculated by applying the total probability theorem:

$$\Pr(F_{Sys,n}) = \int_{\Omega_{\mathbf{S}}} F_{R_{Sys,n}}\left(t_S(\mathbf{S})\right) \cdot f_{\mathbf{S}}(\mathbf{s}) \mathrm{d}\mathbf{s} \tag{4.10}$$

where $\Omega_{\mathbf{S}}$ is the sample space of $\mathbf{S}$ and $f_{\mathbf{S}}$ is the joint PDF of $\mathbf{S}$.

As an alternative to direct numerical evaluation of the integral of Eqn. 4.10, FORM can be used. The way the LSF is formulated plays a crucial role here. An advantageous formulation is to represent the LSF as a one-component reliability problem [142, 143]:

$$g(P,\mathbf{S}) = P - \Pr(F_{Sys,n}) \tag{4.11}$$

where P is a random variable following a standard uniform distribution, and $\Pr(F_{Sys,n})$ can be calculated via the recursive formula of Eqn. 4.7. Transformation to standard normal

space results in

$$G(u_P,\mathbf{u_S}) = u_P - \Phi^{-1}\left(F_{R_{Sys,n}}(l(T_{U2X}(\mathbf{u_S})))\right) \tag{4.12}$$

where U_P is standard normally distributed, $\mathbf{u_S}$ is multivariate standard normally distributed, and T_{U2X} is the transformation from the standard normal space to the original space. $G(u_P,\mathbf{u_S})$ is suitable for application within FORM.

Alternatively, the LSF can be formulated as

$$g(R_{Sys,n},\mathbf{S}) = R_{Sys,n} - l(\mathbf{S}) \tag{4.13}$$

and transformed to the standard normal space as

$$G(u_R,\mathbf{u_S}) = F_{R_{Sys,n}}^{-1}\left(\Phi(u_R)\right) - l\left(T_{U2X}(\mathbf{u_S})\right) \tag{4.14}$$

This LSF is also suitable for application within FORM, however, it requires the numerical evaluation of $F_{R_{Sys,n}}^{-1}$, which is not available in closed form.

Remark: FORM should not be applied if the system resistance is formulated as in Eqn. 4.4. The LSF would be:

$$g(R_{Sys,n},\mathbf{S}) = \max_{i=1}^{n}\left\{(n-i+1)\cdot R_{(i)}\right\} - l(\mathbf{S}) \tag{4.15}$$

Applying FORM to this formulation of the LSF leads to incorrect results because the corresponding limit-state surface is highly non-linear.

4.3.1.1. Numerical investigations of the probabilistic load modeling

Numerical investigations are performed with a log-normally distributed resistance ($\mathrm{E}[R] = 1$ and c. o. v.$[R] = 0.1$) and a one-dimensional action following a Gumbel distribution with c. o. v.$[S] \in \{0.01, 0.02, \ldots, 0.05, 0.1, 0.2, \ldots, 0.5\}$. $\mathrm{E}[S]$ is chosen such that a target reliability index $\beta_{TRG} = 4.3$ is achieved in the case of a Daniels system with only one member.

Fig 4.13 illustrates how the reliability index changes in the case of $n > 1$ for different values of c. o. v.$[S]$. With increasing c. o. v.$[S]$, the reliability index of the Daniels system is less sensitive to n. Changes of c. o. v.$[S]$ in low ranges (0.01 to 0.05) have a stronger effect on the reliability index of the Daniels system. Values of c. o. v.$[S]$ in the range of (0.1 to 0.5) lead to similar reliability curves. In this range, the reliability of the Daniels system keeps decreasing with increasing n.
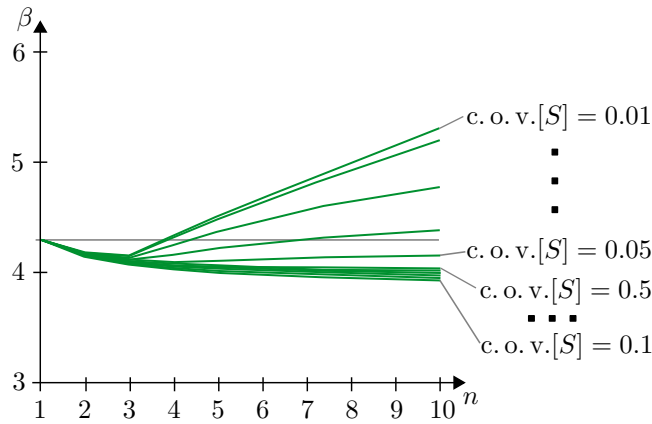
Fig. 4.13.: Reliability index of the Daniels system with 1 to 10 members with different c. o. v. of S of $0.01, 0.02, \ldots, 0.05$ and $0.1, 0.2, \ldots, 0.5$.

4.3.2. Material models

The original formulation of the Daniels system assumes brittle material behavior. In this section, an alternative, idealized material model is introduced that can also model plastic and semi-plastic material behavior. Two versions of this model are proposed and algorithms for the computation of the reliability index with these models are derived.

The stress-strain relationship of the considered material model is shown in Fig. 4.14. It is linear until a maximum stress σ_{max} is reached. If the strain increases further, the stress drops to a constant residual stress σ_{plast} [69].
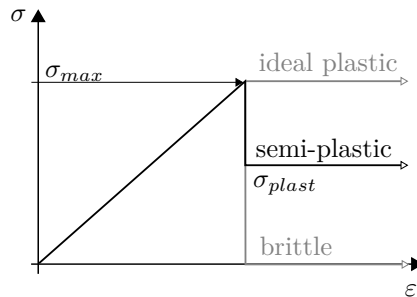
Fig. 4.14.: Stress-strain relationship for new material models.

The two different versions of the material models follow from different definitions of σ_{plast}. Either σ_{plast} is defined as a deterministic value:

$$\text{Material model 1: } \sigma_{plast,1} = f_{res} \cdot \mathrm{E}[\sigma_{max}] \qquad f_{res} \in [0;1] \qquad (4.16)$$

or probabilistically depending on σ_{max}:

$$\text{Material model 2: } \sigma_{plast,2} = f_{res} \cdot \sigma_{max} \qquad f_{res} \in [0;1] \qquad (4.17)$$

78

where f_{res} is a factor that quantifies the residual strength. If $f_{res} = 0$, both material models represent brittle material behavior. If $f_{res} = 1$, the second material model represents ideal plastic material behavior.

Both material models could be extended by also considering a probabilistic strain ϵ. For the sake of simplicity, this is included in this thesis.

The first material model can be "unrealistic" in the sense that $\sigma_{plast,1}$ can be greater than small instantiations of σ_{max} so that the stress-strain relationship would have an upward jump. However, this model has the advantage that Daniels' formula (Eqn. 4.7) can be adapted such that the probability of failure can still be calculated analytically. Thus, if a fast evaluation of the system resistance is needed and if f_{res} is sufficiently small, material model 1 may be advantageous.

The reason why the findings of the original Daniels system can be applied in case of the first version of the material model is illustrated in Fig. 4.15. It shows the failure domain of a Daniels system with two members modeled via material models 1 and 2. The failure domain of material model 1 is a union of two rectangles (as the failure domain of the original Daniels system is shown in Fig. 4.9). This form allows for the application of the findings of the original Daniels system. This is not the case for material model 2, since the failure domain is no longer a union of rectangles.
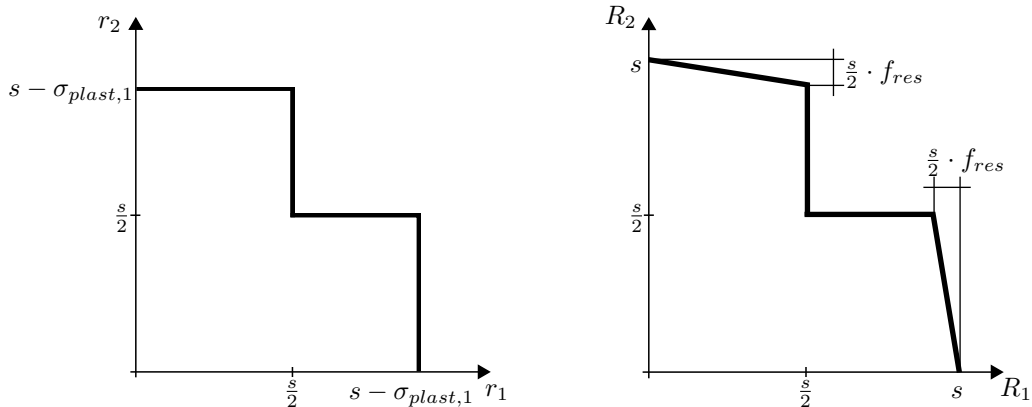
Fig. 4.15.: Failure domain of a Daniels system with two members of material model 1 (left) and material model 2 (right).

The adaptation of Daniels' formula (Eqn. 4.7) to make it suitable for material model 1 is as follows: The plastic resistance of the failed members can be reinterpreted as an additional negative action. Hence, the recursive formula to evaluate the CDF of the system resistance can be adapted to calculate the probability of system failure under a deterministic action

s as

$$F_{R_{Sys,m}}(s) = (-1)^{m+1} \cdot F_R^m \left(\frac{s - (n-m) \cdot \sigma_{plast,1}}{m} \right) \tag{4.18}$$

$$- \sum_{j=1}^{m-1} \left[(-1)^j \cdot \binom{m}{j} \cdot F_R^j \left(\frac{s - (n-m) \cdot \sigma_{plast,1}}{m} \right) \cdot \right.$$

$$\left. F_{R_{Sys,m-j}}(s - (n-m) \cdot \sigma_{plast,1}) \right]$$

where m is an auxiliary variable of the recursion. The recursion has to be conducted for $m = 1, \dots, n$.

Eqn. 4.18 only calculates the probability of system failure if the plastic resistance of the system is smaller than the action $\sigma_{plast,1} \cdot n < s$. If $\sigma_{plast,1} \cdot n > s$, the probability of system failure $\Pr(F_{Sys,n})$ is zero.

In the case of material model 2, the probability of failure can be calculated via the following n-fold parameter integral:

$$\Pr(F_{Sys,n}) = n! \cdot \int_0^{\frac{s}{n}} \int_{r_n}^{\frac{s}{n-1} - f_{res} \cdot r_n} \cdots \int_{r_2}^{s - \sum_{i=1}^{n-1} f_{res} \cdot r_i} \tag{4.19}$$

$$f_R(r_n) \cdot f_R(r_{n-1}) \dots f_R(r_1) \, \mathrm{d}r_1 \dots \mathrm{d}r_{n-1} \, \mathrm{d}r_n$$

For larger n, it is not feasible to evaluate the integral with classic numerical integration methods. Furthermore, FORM is not suitable because of the shape of the failure domain. Instead, MC [62, 63] or advanced sampling-based methods, such as SuS [64–66], can be applied to estimate $\Pr(F_{Sys,n})$.

In the special case of the full plastic material behavior (material model 2 with $f_{res} = 1$), the system resistance is the sum of the member resistances. The limit-state function is

$$g = \sum_{i=1}^{n} R_i - s \tag{4.20}$$

The corresponding limit-state surface is linear in the original space; hence, the application of FORM is suitable.

Remark: A sampling-based solution approach for material model 2 can also be combined with the analytic solutions provided in Eqn. 4.18. E.g., in the case of a Daniels system with two members of material 2, the probability of system failure can be calculated as

$$\Pr(F_{Sys,n}) = 2! \cdot \int_0^{\frac{s}{2}} \int_{r_2}^{s - f_{res} \cdot r_2} f_R(r_1) \cdot f_R(r_2) \mathrm{d}r_1 \mathrm{d}r_2 \tag{4.21}$$

This integral can be split as

$$\Pr(F_{Sys,n}) = 2! \cdot \left[\int_0^{\frac{s}{2}} \int_{r_2}^{s-f_{res}\cdot\frac{s}{2}} f_R(r_1) \cdot f_R(r_2) \mathrm{d}r_1 \mathrm{d}r_2 + \right. \tag{4.22}$$

$$\left. + \underbrace{\int_0^{\frac{s}{2}} \int_{s-r\cdot\frac{s}{2}}^{s-f_{res}\cdot r_2} f_R(r_1) \cdot f_R(r_2) \mathrm{d}r_1 \mathrm{d}r_2}_{=:I^+} \right]$$

The first integral of Eqn. 4.22 can be calculated analytically by applying Eqn. 4.18. Hence, only the error in the estimation of I^+ due to sampling-based integration remains. Since $I^+ < \Pr(F_{Sys,n})$, Eqn. 4.22 leads to a variance reduction of the estimator compared to a direct application of sampling based integration to Eqn. 4.21. This approach can be generalized to the case of a Daniels system with n members.

4.3.2.1. Numerical investigations with the alternative material model

Numerical investigations are performed with the same setup as in 4.3.1.1. Fig. 4.16 shows the reliability indices of Daniels systems with members modeled with material models 1 and 2 for different degrees of plasticity ($f_{res} = 0, 0.2, 0.4, 0.6, 0.8, 1.0$). For low values of f_{res}, the two material models lead to similar results. For larger f_{res}, the first material model leads to much larger reliability indices than the second material model. For this first material model, β eventually becomes infinite as $\sigma_{plast,1}\cdot n > s$. The reliability indices resulting from material model 2 are bounded by the ideal parallel system.

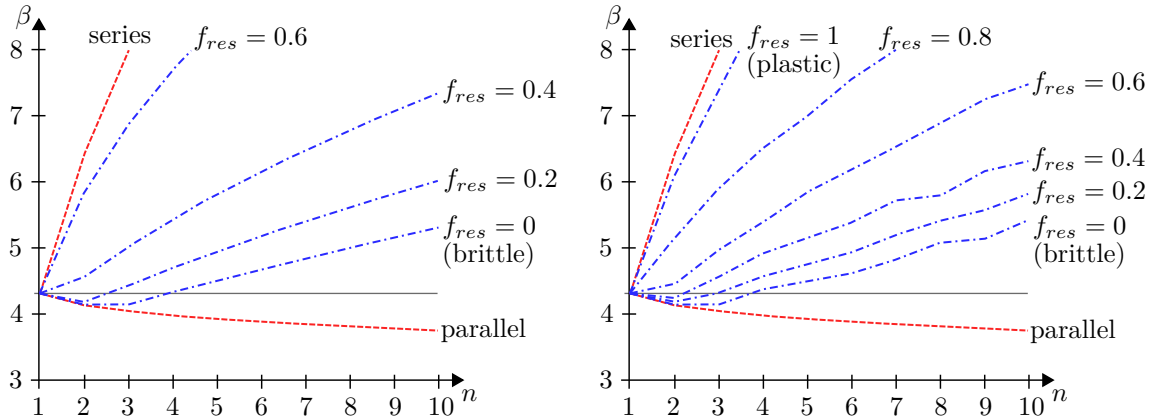Fig. 4.16.: Reliability index of the Daniels system with members modeled with material models 1 (left) and 2 (right) for different degrees of plasticity f_{res} (blue dash-dotted) and ideal series and parallel systems (red dashed). The reliability indices associated with material model 2 were calculated with the SuS-implementation of [144] with an intermediate probability per level of 0.1 and 10^4 samples per level.

4.3.3. Correlation among members

Daniels' original formulation assumed uncorrelated members. However, dependence among members is common, e.g., because of common manufacturing and environmental conditions. In this work, only equicorrelation is considered. This is reasonable since all members are typically dependent on the same phenomena. However, the approach can be generalized to unequal correlation among members.

The Daniels system is generalized to include equicorrelated members by means of a hierarchical model [73, 145, 146]. In the case of equicorrelation, a hierarchical model with only one hyperparameter α is required to represent the dependence structure (see Fig. 4.17). The approach can be extended to unequal correlation among members, as discussed further below.
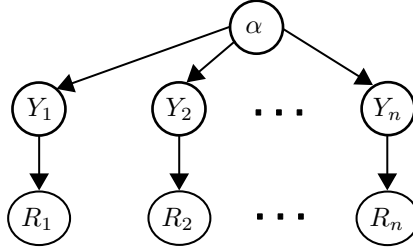

Fig. 4.17.: Hierarchical Bayesian network with hyperparameter α to model equicorrelation among member resistances.

It is mathematically convenient to choose a hyperparameter α that follows a standard normal distribution. Additionally, n standard normally distributed auxiliary random variables Y_i are introduced. The Y_i are equicorrelated jointly normal with a correlation coefficient ρ_Y, which follows from the correlation of the R_i transformed into the standard normal space [147, 148].

The conditional CDF $F_{R|\alpha}$ is given as [145]

$$F_{R|\alpha}\left(x \mid \alpha\right) = \Phi\left(\frac{\Phi^{-1}\left(F_R(x)\right) - \sqrt{\rho_Y} \cdot \alpha}{\sqrt{1 - \rho_Y}}\right) \tag{4.23}$$

The correlation model can be extended to resistances R_i with differing marginal distributions and varying mutual correlation coefficients. The only restriction is that the correlation matrix in standard normal space has to be of the Dunnett-Sobel class [73, 149].

The probability of failure is calculated via the total probability theorem as

$$\Pr(F_{Sys,n}) = \int_{-\infty}^{\infty} \varphi(\alpha) \cdot \Pr(F_{Sys,n} \mid \alpha)\mathrm{d}\alpha \tag{4.24}$$

where φ is the standard normal PDF. $\Pr(F_{Sys,n} \mid \alpha)$ is calculated with the original formula of Daniels (Eqn. 4.7), whereby the CDF of the member resistances is $F_{R_i|\alpha}$ defined via Eqn. 4.23. The integral in Eqn. 4.24 can be evaluated numerically. Alternatively,

$\Pr(F_{Sys,n})$ can be approximated by FORM. By analogy with Eqn. 4.11-4.12 FORM is applied to the following LSF:

$$G(U_P,\alpha) = U_P - \Phi^{-1}\left(F_{R_{Sys,n}|\alpha}(s)\right) \tag{4.25}$$

where U_P and α follow a standard normal distribution and $F_{R_{Sys,n}|\alpha}$ is the CDF of the system resistance following Eqn. 4.7, whereby the CDF of the member resistances is $F_{R_i|\alpha}$ defined via Eqn. 4.23.

4.3.3.1. Numerical investigations of the correlation model

Numerical investigations are performed with the same setup as in Sec. 4.3.1.1. Fig. 4.18 shows the influence of the correlation between member resistances of the Daniels system with ideal plastic, ideal brittle, and semi-plastic material modeled with material model 2 with $f_{res} = 0.5$. With increasing correlation, an increase in the number of members has less effect on reliability. If the members are fully correlated, the Daniels system degenerates into a single component system.

4.3.4. Modified load-sharing properties among members

The original Daniels system has the property of equal load-sharing among non-failed members. This property can mathematically be described via the following equation:

$$\forall_{i,j\in\{1,...,n\}}\forall_{\Lambda\subseteq\{1,...,n\}\setminus\{i,j\}} : \ s_{i,\Lambda} = s_{j,\Lambda} \tag{4.26}$$

where $s_{i,\Lambda}$ $i \in \{1,\ldots,n\}$ is the share of the total action s acting on the ith member of the Daniels system with failed members $\Lambda \subseteq \{1,\ldots,n\} \setminus i$ (the undamaged Daniels system is represented via $\Lambda = \varnothing$). The equal load-sharing property is a consequence of two assumptions of the original Daniels system: first, the postulate of equal cross-sections and Young's modulus, i.e., equal stiffnesses among all members. Second, the original Daniels system is modeled with a horizontal bar with infinite bending stiffness that is blocked against rotation on both sides. Altering any of these properties leads to non-equal load-sharing.

Fig. 4.19 shows three modifications of the Daniels system leading to different load-sharing properties.

Fig. 4.19 a): This modification includes varying cross-section areas per member. In this case Eqn. 4.26 does not hold anymore; however, another – slightly weaker – load-sharing property holds: The action is distributed proportional to the member stiffnesses:

$$\forall_{i,j\in\{1,...,n\}}\forall_{\Lambda\subseteq\{1,...,n\}\setminus\{i,j\}} : \ \frac{s_{i,\Lambda}}{A_i \cdot E} = \frac{s_{j,\Lambda}}{A_j \cdot E} \tag{4.27}$$

where E is the Young's modulus and A_i is the cross-section area of member i.
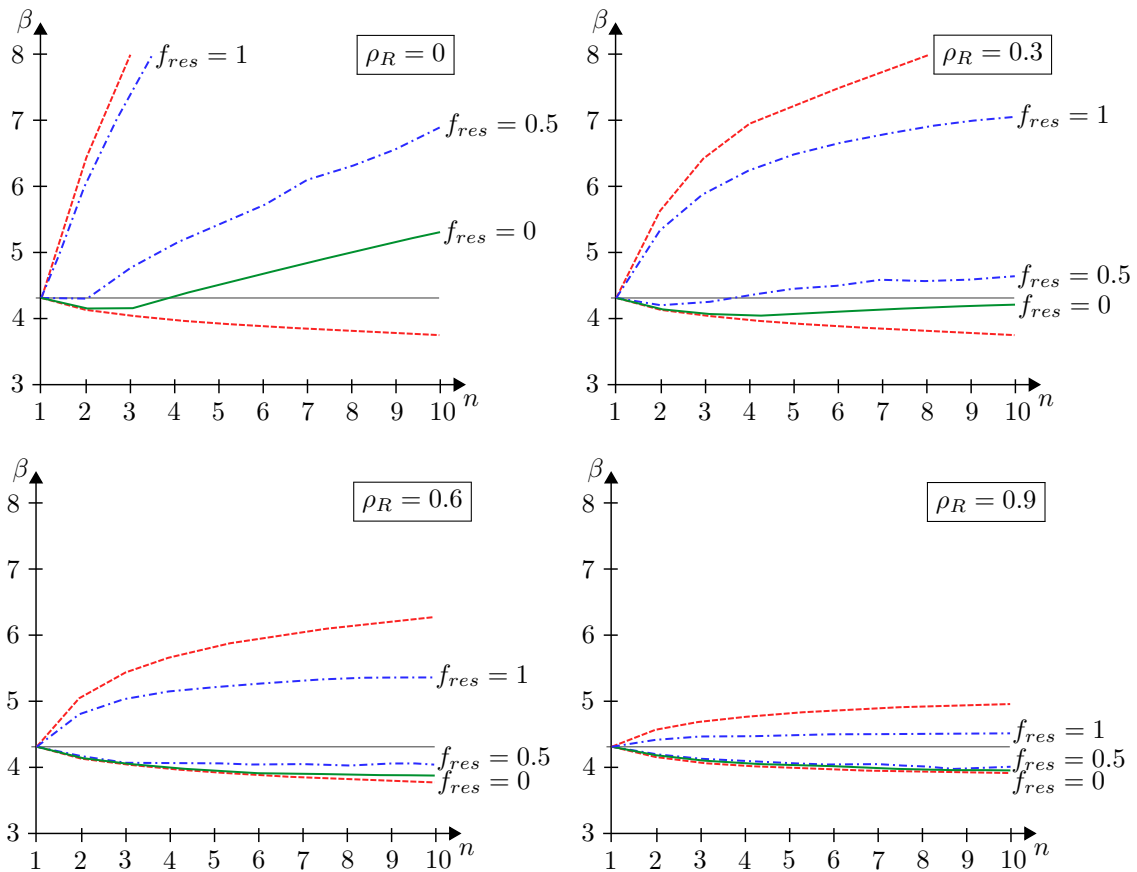
Fig. 4.18.: Reliability index of the ideal parallel and series system (dashed red) and the Daniels system with brittle material ($f_{res} = 0$, green), ideal plastic and semi-plastic material modeled with material model 2 ($f_{res} = 1, 0.5$, dash-doted blue). The members are uncorrelated (top left), equicorrelated with a correlation coefficient of 0.3 (top right), 0.6 (bottom left) and 0.9 (bottom right).

Fig. 4.19.: Modifications of the Daniels system that lead to different load-sharing properties.

Fig. 4.19 b): This modified Daniels system has a rotatable horizontal bar that is fixed at one end only. In this case Eqns. 4.26 and 4.27 do not hold; however, another – again slightly weaker – load-sharing property holds: After the failure of member k, the action redistributes proportionally:

$$\forall_{i,j\in\{1,\ldots,n\}}\forall_{\Lambda\subseteq\{1,\ldots,n\}\setminus\{i,j\}}\forall_{k\in\{1,\ldots,n\}\setminus(\Lambda\cup\{i,j\})}: \quad \frac{s_{i,\Lambda}}{s_{j,\Lambda}} = \frac{s_{i,\Lambda\cup k}}{s_{j,\Lambda\cup k}} \tag{4.28}$$
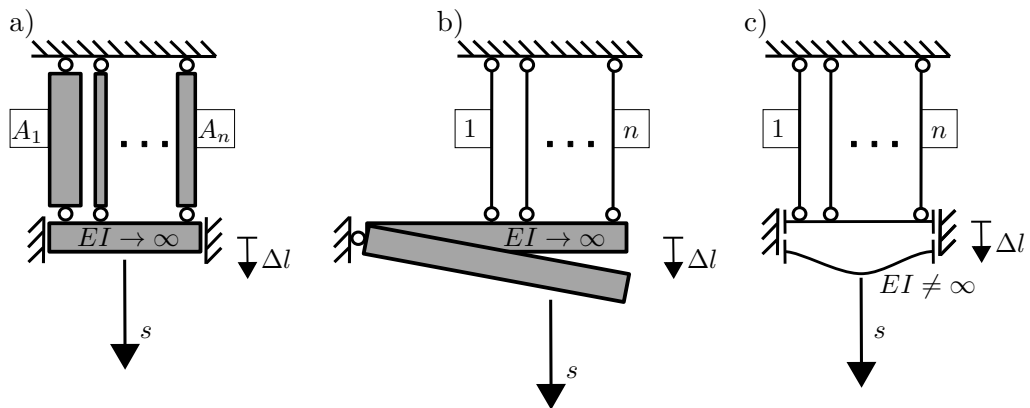
Fig. 4.19 c): This modified Daniels system has a horizontal bar with a finite bending stiffness. In this case, none of the properties (Eqns. 4.26-4.28) hold.

The three above-mentioned load-sharing properties (Eqns. 4.26-4.28) are logically related to each other as follows: Eqn.4.26 $\Rightarrow$ Eqn.4.27 $\Rightarrow$ Eqn.4.28; hence, they can be interpreted as three levels of load-sharing.

In order to derive a formula to calculate the system reliability of modified Daniels systems, it is helpful to compare the failure domains of the original Daniels system and the modified Daniels system. Fig. 4.20 visualizes this for the case of three members. The failure domain of the original Daniels system is the union of 6 cubes whose edge lengths are all possible combinations of s, $\frac{s}{2}$, and $\frac{s}{3}$. The recursive formula from Daniels (Eqn. 4.7) makes use of the symmetric shape of the failure domain and the fact that the member resistances are independent and identical distributed. The failure domain of modified Daniels systems also consists of 6 cubes; however, these are not necessarily symmetric anymore, and the member resistances are not necessarily identically distributed random variables.
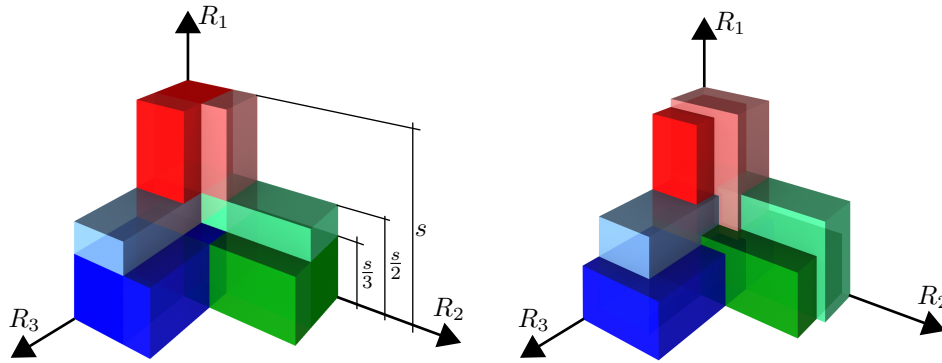
Fig. 4.20.: Failure domain of the original Daniels system (left) and a modified Daniels system (right) with 3 members.

In the general case of a Daniels system with modified load-sharing, the failure domain is described by $n!$ hypercubes H_j ($j = 1, \ldots, n!$). Each hypercube describes one possible ordering of member failures leading to system failure. The edge lengths of a hypercube are equal to the actionshare $s_{i,\Lambda}$ where i is the next member to fail and Λ are members that have already failed. In the case of a proportional redistribution after member failure (Eqn. 4.28), the calculation of all $s_{i,\Lambda}$ is straightforward. If Eqn. 4.28 does not hold, the calculation of each $s_{i,\Lambda}$ requires a structural analysis.

In the following, two analytical approaches to calculate the probability of failure of Daniels

systems with modified load-sharing are presented. The first approach is via the application of the principle of inclusion and exclusion. The second approach meshes the failure domain with disjoint hypercubes and sums up their respective probabilities. Both approaches are reasonable for moderately small numbers of members n. For larger n, MC [62, 63] or advanced sampling methods such as SuS [64–66] should be applied.

The first approach is based on the principle of inclusion and exclusion. The probability of system failure $F_{Sys,n}$ can be evaluated as

$$\Pr(F_{Sys,n}) = \sum_{k=1}^{n!} (-1)^{k-1} \sum_{\substack{I \subseteq \{1,\ldots,n!\} \\ |I|=k}} \Pr\left(\bigcap_{j \in I} H_j\right) \tag{4.29}$$

where the second summation is with respect to all possible index sets I of numbers from 1 to $n!$ and cardinality k.

With an increasing number of members n, the evaluation of Eqn. 4.29 becomes numerically infeasible, even for moderate n. This is not only because the number of hypercubes H_j grows with $\mathcal{O}(n!)$, but in particular since the number of m-tuples to describe the intersections grows with $\mathcal{O}(n!!)$. The largest numerically reasonable number of elements for applying the principle of inclusion and exclusion is $n = 4$. In this case, $4! = 24$ hypercubes H_j exist. This leads to $\binom{24}{2} = 276$ intersection pairs, $\binom{24}{3} = 2024$ intersection triplets, etc. Reaching the maximum at $\binom{24}{12} = 2\,704\,156$ intersection 12-tuples. If the system consists of 5 members, $5! = 120$ hypercubes H_j exist. The number of intersection tuples is already 10^{36}.

A numerically preferable alternative to the principle of inclusion and exclusion is the following meshing approach: First, the failure domain is divided into non-overlapping hypercubes. Then the probability of system failure is calculated as the sum of the probabilities of all events defined via these hypercubes. One possibility to define the hypercubes and calculate their respective probabilities is to envelop the system failure domain with the hypercube $[0,s] \times [0,s] \times \cdots \times [0,s]$ and mesh it per direction ($\hat{=}$member) i with the grid $s_{i,\Lambda}$ ($\hat{=}$ actionshare of member i regarding system state with failed members Λ). If all $s_{i,\Lambda}$ for all Λ differ, the meshing defines a maximum of $n!^n$ sub-hypercubes h_j.

Summing over the probability of all sub-hypercubes within the failure domain $\Omega_{F_{Sys,n}}$ gives the probability of system failure

$$\Pr(F_{Sys,n}) = \sum_{h_j \subseteq \Omega_{F_{Sys,n}}} \Pr(h_j) \tag{4.30}$$

This approach has complexity $\mathcal{O}\left(n!^n\right)$, hence, is more feasible than the application of the principle of inclusion and exclusion.

4.3.4.1. Numerical investigations of modified load-sharing among members

In the following, the meshing approach is applied to the modified Daniels systems a) and b) of Fig. 4.19. As for the original Daniels system, equal Young's modulus per member , deterministic action s (chosen such that the target reliability of $\beta_T = 4.3$ is met for $n = 1$), independent and identical distributed ultimate member strength $\sigma_{max,i}$ and linear-elastic brittle material behavior are assumed.

System a) of Fig. 4.19

The member strength $\sigma_{max,i}$ is assumed to be log-normally distributed with $\mathrm{E}[\sigma_{max,i}] = 1$ and c. o. v.$[\sigma_{max,i}] = 0.1$. The cross-section areas are varied linearly:

$$A_i = \begin{cases} 1 & n = 1 \\ 1 - f_s \cdot \left(2 \cdot \frac{i-1}{n-1} - 1 \right) & n \geq 2 \end{cases} \tag{4.31}$$

where n is the number of members of the modified Daniels system and $f_s \in [0,1)$ is a factor controlling the non-equality of the cross-section areas. The cross-section area of the first member is $A_1 = 1 - f_s$ and the cross-section area of the last member is $A_n = 1 + f_s$. The cross-section area of all other members is linearly interpolated between A_1 and A_n. If $f_s = 0$, the original Daniels system is obtained. The larger f_s, the more the cross-section areas differ, with a maximum inequality for $f_s = 1$.

Fig. 4.21 illustrates the resulting system reliability indices for a Daniels system with $n = 5$ members. The reliability index is not significantly influenced by the factor f_s. Similar results are obtained for other numbers of members n or different setups of the modified Daniels system (e.g., different c. o. v.$[\sigma_{max,i}]$ or semi-plastic material behavior). This indicates that, in general, the reliability index may not be sensitive to non-equal load-sharing if the load-sharing property of Eqn. 4.27 is fulfilled (proportionality to the mean member resistances).

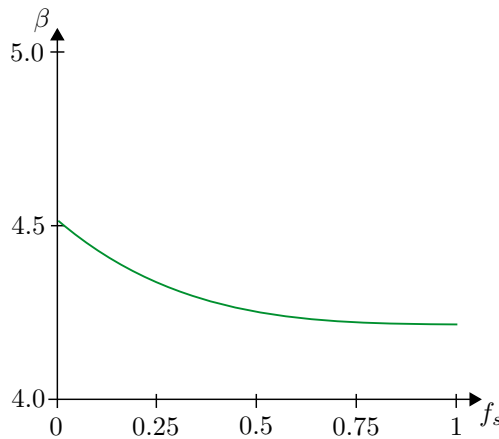Fig. 4.21.: System reliability index of the modified Daniels system a) with $n = 5$ brittle members and different levels of non-equal load-sharing controlled via f_s (the original Daniels system corresponds to $f_s = 0$).

System b) of Fig. 4.19

The member strength $\sigma_{max,i}$ is again assumed to be log-normally distributed with $\mathrm{E}[\sigma_{max,i}] = 1$ and c. o. v.$[\sigma_{max,i}] \in \{0.1, 0.2, 0.3\}$. All distances between members are assumed to be equal. Therefore, the action is linearly distributed among members. The inequality of load-sharing is described via the ratio of the deformation of the first member to the last member $\frac{\Delta l_1}{\Delta l_n}$. If $\frac{\Delta l_1}{\Delta l_n} = 1$, the support of the horizontal bar is infinitely far away from the first member of the modified Daniels system b). This is equivalent to the original Daniels system. With decreasing $\frac{\Delta l_1}{\Delta l_n} < 1$, the support moves closer to the first member, and the load-sharing becomes increasingly unequal. The maximum inequality in load-sharing is reached for $\frac{\Delta l_1}{\Delta l_n} = 0$.

Fig. 4.22 shows the resulting system reliability index with respect to the number of members n. The system reliability index first decreases with the increasing number of members, reaches a minimum and then increases. The smaller $\frac{\Delta l_1}{\Delta l_n}$ the lower the system reliability. The reason for this is the increasingly uneven load sharing between members: More heavily loaded members are more likely to fail, which favors a failure of the system due to cascading effects.

Fig. 4.23 illustrates the resulting system reliability with respect to different values of $\frac{\Delta l_1}{\Delta l_n}$ for systems with $n = 5$ members and c. o. v.$[\sigma_{max,i}] \in \{0.1, 0.2, 0.3\}$. Comparing the case of c. o. v.$[\sigma_{max,i}] = 0.1$ with Fig. 4.21 shows the much stronger effect to the system reliability of the non-proportional unequal load sharing case compared to the proportional case.
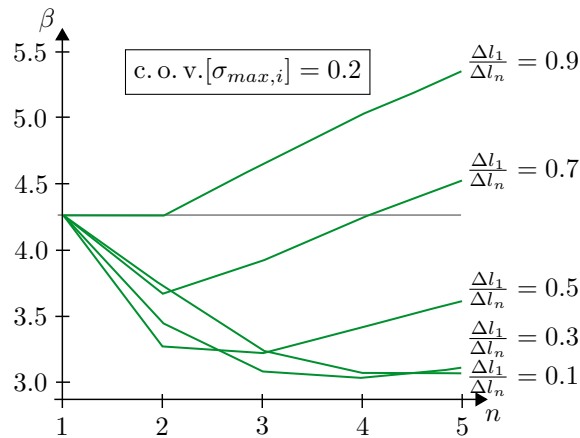

Fig. 4.22.: System reliability index of the modified Daniels system b) with n brittle members and different levels of non-equal load-sharing controlled via $\frac{\Delta l_1}{\Delta l_n}$.
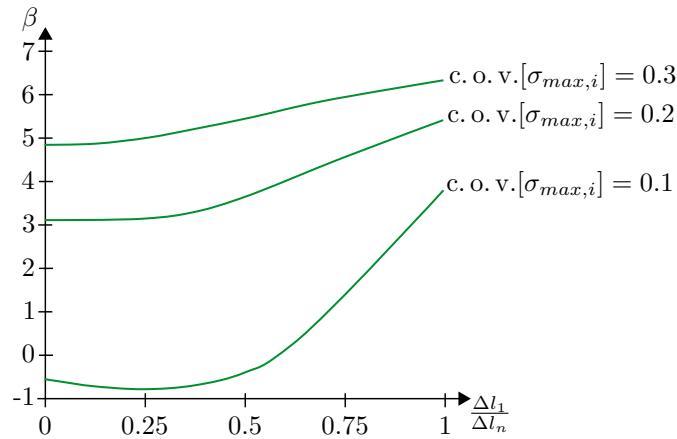
Fig. 4.23.: System reliability index of the modified Daniels system b) with $n = 5$ brittle members with varying c. o. v.$[\sigma_{max,i}] \in \{0.1, 0.2, 0.3\}$ and different levels of non-equal load-sharing controlled via $\frac{\Delta l_1}{\Delta l_n}$.

4.4. Link between general structural system and the generalized Daniels system

The PSF concept is a general design concept applicable to various kinds of structures. An adaptation of the PSF concept needs to take this variety into account. The generalized Daniels system is able to represent this variety. The link between the generalized Daniels System and general structural systems is illustrated in the following via an example structure taken from Madsen et al. [150].

Fig. 4.24 shows the example structure. It is a frame with a horizontal action H and a vertical action V. V is a log-normally distributed permanent action (E$[V] = 1$ and c. o. v.$[V] = 0.2$) and H is a Gumbel distributed variable action (E$[H] = 1$ and c. o. v.$[H] = 0.3$). Potential bending failure at the five different locations with the highest action-effects is considered. For reasons of simplification, other element failure mechanisms are not considered.

Fig. 4.24.: Example frame structure.

First, the example structure is designed following the standard PSF design, and second, a reliability analysis is conducted in order to establish a link to the generalized Daniels

system. This link will be used later (Sec.4.5) to derive the additional PSF γ_{Sys}.

4.4.1. Determination of the resistances according to the partial safety concept

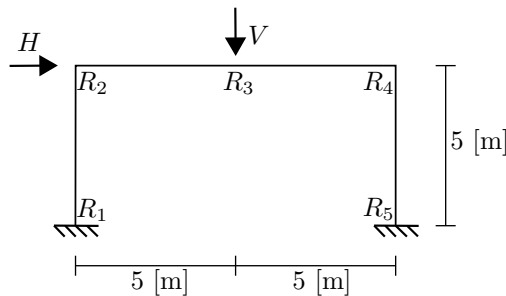The characteristic actions are $h_k = F_H^{-1}(0.98) = 1.78$, where F_H^{-1} is the inverse CDF of H, and $v_k = \mathrm{E}[V] = 1$. The corresponding PSFs are $\gamma_H = 1.5$ and $\gamma_V = 1.35$. The resulting design actions are $h_d = h_k \cdot \gamma_H = 2.67$ and $_d = v_k \cdot \gamma_V = 1.35$.

Two action cases are considered: $V \oplus H$ acting simultaneously and V acting alone. The design resistances $r_{d,i}$ are 3.49, 1.35, 2.03, 3.84, and 4.84 for $i = 1, \ldots, 5$. They result from the maximum absolute bending moments of the two action cases at the five different locations.

Choosing the PSF of the resistance as $\gamma_M = 1.3$, the characteristic resistances are calculated as $r_{k,i} = \gamma_M \cdot r_{d,i}$. The resistances are considered to be log-normally distributed with c.o.v.$[R_i] = 0.1$ and the characteristic values to be defined via the $5[\%]$ quantiles. This results in the distributions of the resistances R_i shown in Tab. 4.1. The resistances are chosen to be equicorrelated with a correlation coefficient of $\rho_{R_i, R_j} = 0.3$.

Tab. 4.1.: Distributions of the resistances R_i.

$V \sim \mathcal{LN}$	$\mathrm{E}[V] = 1$	c.o.v.$[V] = 0.2$
$H \sim \mathcal{G}$	$\mathrm{E}[H] = 1$	c.o.v.$[H] = 0.3$
$R_1 \sim \mathcal{LN}$	$\mathrm{E}[R_1] = 5.37$	c.o.v.$[R_1] = 0.1$
$R_2 \sim \mathcal{LN}$	$\mathrm{E}[R_2] = 2.08$	c.o.v.$[R_2] = 0.1$
$R_3 \sim \mathcal{LN}$	$\mathrm{E}[R_3] = 3.12$	c.o.v.$[R_3] = 0.1$
$R_4 \sim \mathcal{LN}$	$\mathrm{E}[R_4] = 5.93$	c.o.v.$[R_4] = 0.1$
$R_5 \sim \mathcal{LN}$	$\mathrm{E}[R_5] = 7.45$	c.o.v.$[R_5] = 0.1$

4.4.2. Reliability analysis and link to the Daniels system

All minimal cut sets of bending failures at the five different locations, which lead to a kinematic system, define the possible system failure modes. The author considers the four failure modes shown in Fig. 4.25.

The link between the frame and the generalized Daniels system depends on the material properties of the frame. Two cases are exemplarily investigated: ideal plastic and ideal brittle material behavior. If the material behavior is semi-plastic, a link to the generalized Daniels system could also be established; however, the action effects per damage state of the frame are not as straightforward to calculate, and yield hinge theory is required. This is not conducted within this example.
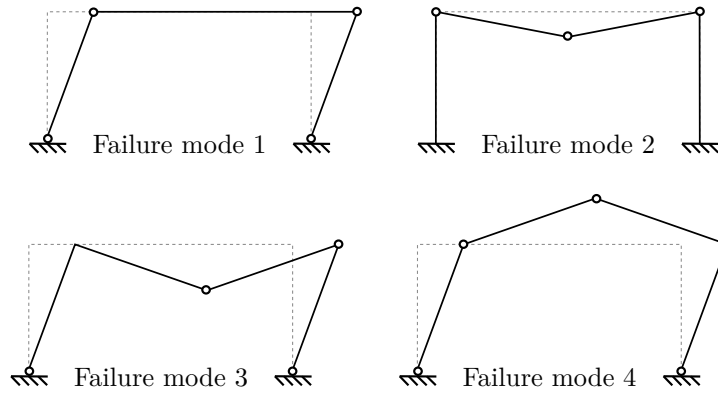
Fig. 4.25.: Considered failure modes of the frame.

4.4.2.1. Ideal plastic material behavior case

Utilizing the principle of virtual work (similar to the motivating example of Sec. 4.1), a LSF per failure mode can be derived. The inner virtual work represents the resistance of the system against a failure mode, and the outer virtual work represents the action acting in the direction of a failure mode. This leads to the following LSFs:

$$g_1 = R_1 + R_2 + R_4 + R_5 - 5 \cdot H \tag{4.32}$$

$$g_2 = R_2 + R_3 + R_4 - 5 \cdot V \tag{4.33}$$

$$g_3 = R_1 + 2 \cdot R_3 + 2 \cdot R_4 + R_5 - 5 \cdot H - 5 \cdot V \tag{4.34}$$

$$g_4 = R_1 + 2 \cdot R_2 + 2 \cdot R_3 + R_5 + 5 \cdot V - 5 \cdot H \tag{4.35}$$

System failure occurs if at least one failure mode occurs; hence, the system reliability is determined by means of a series system composed of the four LSFs. The reliability indices per failure mode are calculated with FORM:

$$\beta_{1,plast} = 4.66 \tag{4.36}$$

$$\beta_{2,plast} = 5.01 \tag{4.37}$$

$$\beta_{3,plast} = 5.28 \tag{4.38}$$

$$\beta_{4,plast} = 5.73 \tag{4.39}$$

and the system reliability with FORM for series systems:

$$\beta_{Sys,plast} = 4.62 \tag{4.40}$$

In the case of ideal plastic material behavior, it is possible to deduce a series system of generalized Daniels systems that is – from a reliability point of view – equivalent to the frame. The series system of generalized Daniels systems can be established as follows: The LSFs of Eqns. 4.32 to 4.35 do not only represent the failure mechanisms of the frame but all failure mechanisms of any structural system that have the same inner and outer virtual work. This means a generalized Daniels system with the same inner and outer virtual

work is – from a reliability point of view – equivalent to a failure mode of the frame. It is always possible to find such a Daniels system.

Fig. 4.26 shows the resulting Daniels systems in the case of the considered example structure. In contrast to the original Daniels system, the cross-sections areas of the members are chosen differently, resulting in different member stiffness (see modified Daniels system a) of Fig. 4.19.
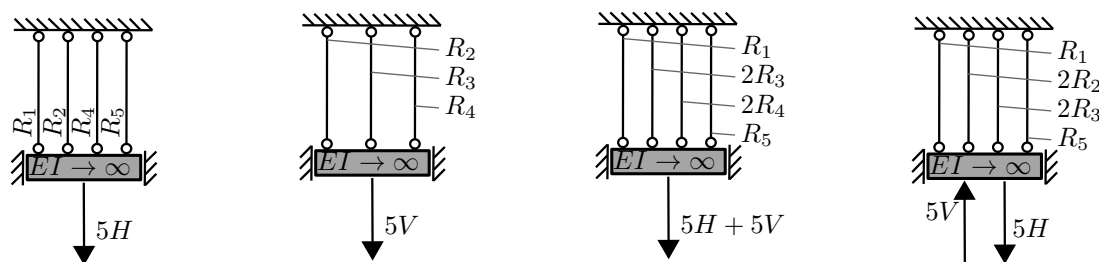
Fig. 4.26.: Generalized Daniels systems which are equivalent to the four failure modes of the example frame.

4.4.2.2. Ideal brittle material behavior case

The reliability analysis is carried out via MC as follows: For each sample of the actions, a structural analysis needs to be performed with respect to both action cases. If a resistance sample at one of the five locations of the frame is lower than the bending moment – caused by one of the action cases – a hinge is added at this location.[1] If multiple resistance samples are lower than the respective bending moments, the hinge is added at the location where the difference between resistance and bending moment is the greatest, whereby cases that occur in the action case of the permanent action only are added first. If a hinge is added, another structural analysis of the modified version of the frame is performed to add another joint. This procedure is repeated until the frame can either resist the actions or fails (becomes kinematic).

The resulting estimate of the system reliability index is:

$$\beta_{Sys,brit} = 3.20 \tag{4.41}$$

---

[1]It may seem unrealistic to only add a hinge in case of brittle failure, since brittle failure typically does not allow transmission of normal forces and shear forces anymore; however, in the example setup only bending failure is taken into account. In principle, the inclusion of normal force failure or shear force failure is possible. This would require an example with higher amounts of redundancy to derive meaningful results.

The reliability indices per failure mode are estimated as:

$$\beta_{1,brit} = 3.99 \tag{4.42}$$

$$\beta_{2,brit} = 3.22 \tag{4.43}$$

$$\beta_{3,brit} = \infty \tag{4.44}$$

$$\beta_{4,brit} = 4.74 \tag{4.45}$$

In the case of ideal brittle material behavior, it is not possible to establish a direct one-to-one equivalence to generalized Daniels systems, as in the case of ideal plastic material behavior. The main reason for this is the difference in action redistribution after one or more members fail. In the case of the Daniels system, the ratio between the action effects at each member and its stiffness is equal for all non-failed members (see Sec. 4.3.4). This is not the case for general structural systems with brittle members. There are two main reasons that cause member stiffnesses that are non-proportional to the action effects:

- The redistribution of inner forces after one or more members fail: If a member of a structural system fails, this may change the stress flow of the structure fundamentally. The action effects change while the stiffnesses of the undamaged members remain the same, leading to non-proportionality. This non-proportional redistribution of the action is critical since the stiffness of some members may now be lower than the stiffness that would result from a PSF design of an altered structure, including member failure.

- The consideration of multiple action cases: If the stiffnesses per member result from the maximum design stiffness of different action cases, member stiffnesses may not be proportional to the action effects caused by one of the action cases. However, this non-proportionality is not critical since it leads to an increase in stiffness compared to the cases where only one action case is considered; hence, it increases reliability.

For these reasons, one can only establish an equivalent generalized Daniels system for a given damage state of a structure. Following a member failure, a different generalized Daniels system is necessary to represent the new configuration.

First, the case of unequal load-sharing after member failure is illustrated. Therefore, the example frame is redesigned (analogously to Sec. 4.4.1) considering only the vertical action case. Since only one action case is considered, this initially leads to equal load-sharing between the members (see top of Fig. 4.27). After member failure occurs, the load-sharing becomes non-proportional to the member stiffnesses and the equivalent generalized Daniels system needs to be adapted. This can be done by modifying the horizontal bar to be rotatable and fixed against translations at one end (see bottom of Fig. 4.27 for failure at location 2). The non-proportional load-sharing results from the distance δl_i of the members to the fixed end of the horizontal bar for each member. δl_i is calculated as:

$$\delta l_i = \left| \frac{M_{i,\Lambda_2}(V = v_d)}{M_i(V = v_d)} \right| \tag{4.46}$$

where $M_i(V = v_d)$ and $M_{i,\Lambda_2}(V = v_d)$ are the inner moments at location i caused by the vertical design action v_d, if no failure or failure at location 2 is present. If failure at
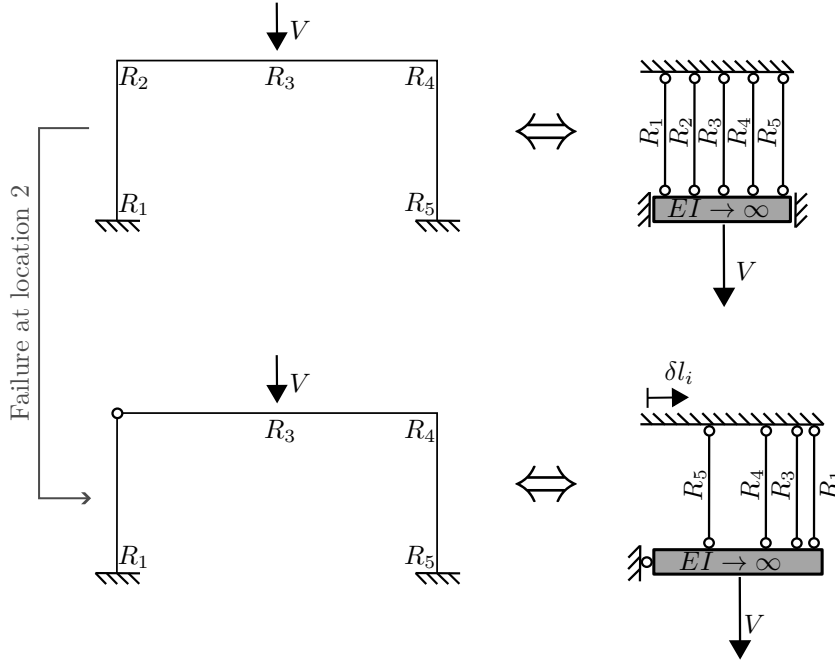
Fig. 4.27.: Example frame considering the action case of V only. The load-sharing is proportional to the member stiffnesses, as long as no member has failed. After a member failure occurs, the load-sharing is non-proportional to the member stiffnesses.

another location occurs, the equivalent generalized Daniels system needs to be adapted again by recalculating δl_i with respect to the new damage state of the frame. Hence, the positioning of the members of the generalized Daniels system keep shifting with each member failure.

Second, the case of unequal load-sharing due to the consideration of multiple load cases is illustrated. Therefore, the undamaged example frame is investigated considering both action cases V and $V \oplus H$. Because two actions are acting in two different directions, the generalized Daniels system needs to be modeled with two horizontal bars. The members are not directly attached to these horizontal bars anymore, but infinitely stiff connections transfer the action effects accordingly (see Fig. 4.28). $\delta l_{i,V}$ and $\delta l_{i,H}$ are calculated as

$$\delta l_{i,V} = \left| \frac{M_i(V = v_d)}{\max\left\{ M_i(V = v_d, h = h_d), M_i(V = v_d) \right\}} \right| \tag{4.47}$$

$$\delta l_{i,H} = \left| \frac{M_i(H = h_d)}{\max\left\{ M_i(V = v_d, h = h_d), M_i(V = v_d) \right\}} \right| \tag{4.48}$$

Some of the action effects do not induce tension but compression on the members of the Daniels system (modeled with the help of a rocker). This is because the inner moments caused by V and H at a specific location of the frame have opposing signs. Consequently, the members of the Daniels system cannot only fail due to tension but also due to compression. If the bending stiffness at a location of the frame is independent of the bending direction (e.g., for symmetric cross-sections), the resistance against compression of the

corresponding member of the Daniels system is equally distributed and fully correlated to their respective resistance against tension. If the bending stiffnesses differ with respect to the bending direction, the resistance against tension and compression of the corresponding member of the Daniels system also differs accordingly (however, they are still fully correlated).
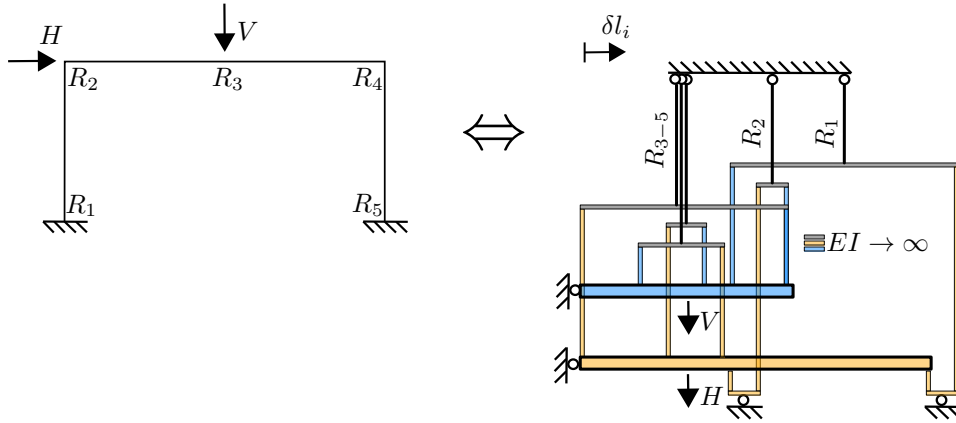
Fig. 4.28.: Undamaged frame loaded by $V \oplus H$ and Daniels system representing the equivalent system behavior until element failure occurs. R_1-R_5 are determined following the PSF concept, considering both action cases.

Remark: The equivalence of the frame and the generalized Daniels systems of Fig. 4.27 and 4.28 only hold since the relationship between actions and action effects is linear. If a structure behaves non-linearly, the shape of the horizontal bar needs to be adjusted (e.g., parabolic in the case of quadratic non-linearities).

4.4.3. List of entities to establish equivalence of the generalized Daniels system and general structural systems

The illustrations of the example frame show that it is always possible to define a series system of generalized Daniels systems (which – in the brittle and semi-plastic case – have to be adapted to a specific damage state of the structure) that describe the reliability of any structural system. The following list of entities describes this equivalence between the generalized Daniels system and general structural systems. The list is complete in the sense that no further entities need to be known to form generalized Daniels systems, which – from a reliability point of view – are equivalent to any arbitrary structural system.

1. Number of system failure mechanisms: equal to the number of generalized Daniels systems needed. These Daniels systems are connected as a series system. Failure of one Daniels system is equal to the occurrence of a failure mechanism, hence, system failure.

2. Number of element failures that lead to a system failure mechanism: Number of members in the corresponding Daniels system.

3. Resistance of each element of the structure: Directly corresponds to the material type and the maximal stiffness of the members of the Daniels system. If the material type is brittle of semi-plastic the corresponding generalized Daniels system needs to be adapted for each damage state of the general structural system, resulting in a sequence of generalized Daniels systems.

4. Correlation among the elements of the structure: Determines the correlation among members of the Daniels system.

5. Actions of the structure: Directly correspond to the action of each Daniels system.

6. Geometry of the structure: From the geometry, the action effects can be calculated, hence, the relation between actions and resistances of the Daniels system can be established. This determines the load-sharing properties of the Daniels system.

4.5. Adaptation of the PSF concept with respect to system effects

The possible combinations of the six entities of the list in Sec. 4.4.3 are endless. In order to derive the additional PSF γ_{Sys}, some necessary simplifications and assumptions have to be made. The derived PSF is only valid on that basis. The simplifications and assumptions of the six entities are the following:

1. It is assumed that one system failure mechanism is dominant and other system failure mechanisms can be neglected. No series system of Daniels systems has to be evaluated, but only a singular Daniels system.

2. Only global failure mechanisms are taken into account. Under this assumption, the number of element failures that lead to a system failure mechanism is equal to the static over-determination of the system plus one. Daniels systems with $n = 1, \ldots, 10$ members are investigated; hence, statically determined and $1, \ldots, 9$ times statically over-determined systems.

3. The material behavior of each element of the structure is assumed to be of the same type. No Daniels systems with mixed materials are considered. Further, different dimensions of the elements of the structure are neglected; hence, only Daniels systems with equal stiffnesses per member are investigated. The behavior of ideal plastic material ($f_{res} = 1$), ideal brittle material ($f_{res} = 0$), and semi plastic material behavior modeled following material model 2 with $f_{res} \in \{0.25, 0.5, 0.75\}$ is investigated.

4. Only positive equicorrelation among elements is considered.

5. The variability of the action side is taken into account by using the action combinations of the portfolio of Annex A.

6. The geometry of the structure is neglected and it is assumed that the actions evenly

distribute among the elements of the structure and also evenly redistribute in case of element failure. This includes changes in the load sharing due to local deformations. In the case of plastic material behavior, this assumption is always satisfied as shown in Sec. 4.4.2.1 (since equal element strength and dimensions is already assumed); however, in the case of brittle or semi-plastic material behavior, this assumption is critical (see Sec. 4.4.2.2). In these cases, the derived additional PSF should be applied with caution.

Given a specific Daniels system, the average reliability index is calculated with respect to the portfolio of action cases as follows:

$$\overline{\beta} = \frac{\sum_{i=1}^{3} \sum_{j=1}^{9} \beta_{Q_i, a_{Q,j}}}{27} \tag{4.49}$$

where $\beta_{Q_i, a_{Q,j}}$ is the reliability index of the Daniels system under the action case resulting from Q_i and $a_{Q,j}$ defined in Annex A. Fig. 4.29 shows the resulting average reliability indices.

To homogenize the reliability of Daniels systems, the additional PSF γ_{Sys} is introduced. γ_{Sys} is applied to the characteristic value of the resistance in addition to γ_M; hence, the design resistance is calculated as $r_d = \frac{r_k}{\gamma_M \cdot \gamma_{Sys}}$. The value of γ_{Sys} depends on the number of members of the Daniels system n, the plastic residual of the material r, the coefficient of variation of the member resistances c. o. v.$[R]$, and the correlation among members $\rho_{R_i R_j}$. To determine the values of γ_{Sys} the following equation is solved (in accordace with Eqn. 2.46):

$$\overline{\beta}(\gamma_{Sys}; n, r, \text{c. o. v.}[R], \rho_{R_i R_j}) \overset{!}{=} \beta_{TRG} \tag{4.50}$$

where $\beta_{TRG} = 4.3$ is the target reliability defined following Eqn. 2.44 as the average reliability index if $n = 1$.

Figuratively speaking, the application of γ_{Sys} moves all lines in Fig. 4.29 to be constant at the target reliability index. Note that only the average reliability, $\overline{\beta}$ is constant, but the individual cases of the considered portfolio still scatter; however, this scattering is not related to system effects anymore.

Tab. 4.2 shows the values of γ_{Sys}. The vast majority of the derived values are close to 1. The minimum value is $\gamma_{Sys} = 0.75$ (ideal plastic system with c. o. v.$[R] = 0.2$ and $\rho_{R_i R_j} = 0.0$). The maximum value is $\gamma_{Sys} = 1.10$ (c. o. v.$[R] = 0.2$ and $\rho_{R_i R_j} = 0.6$).
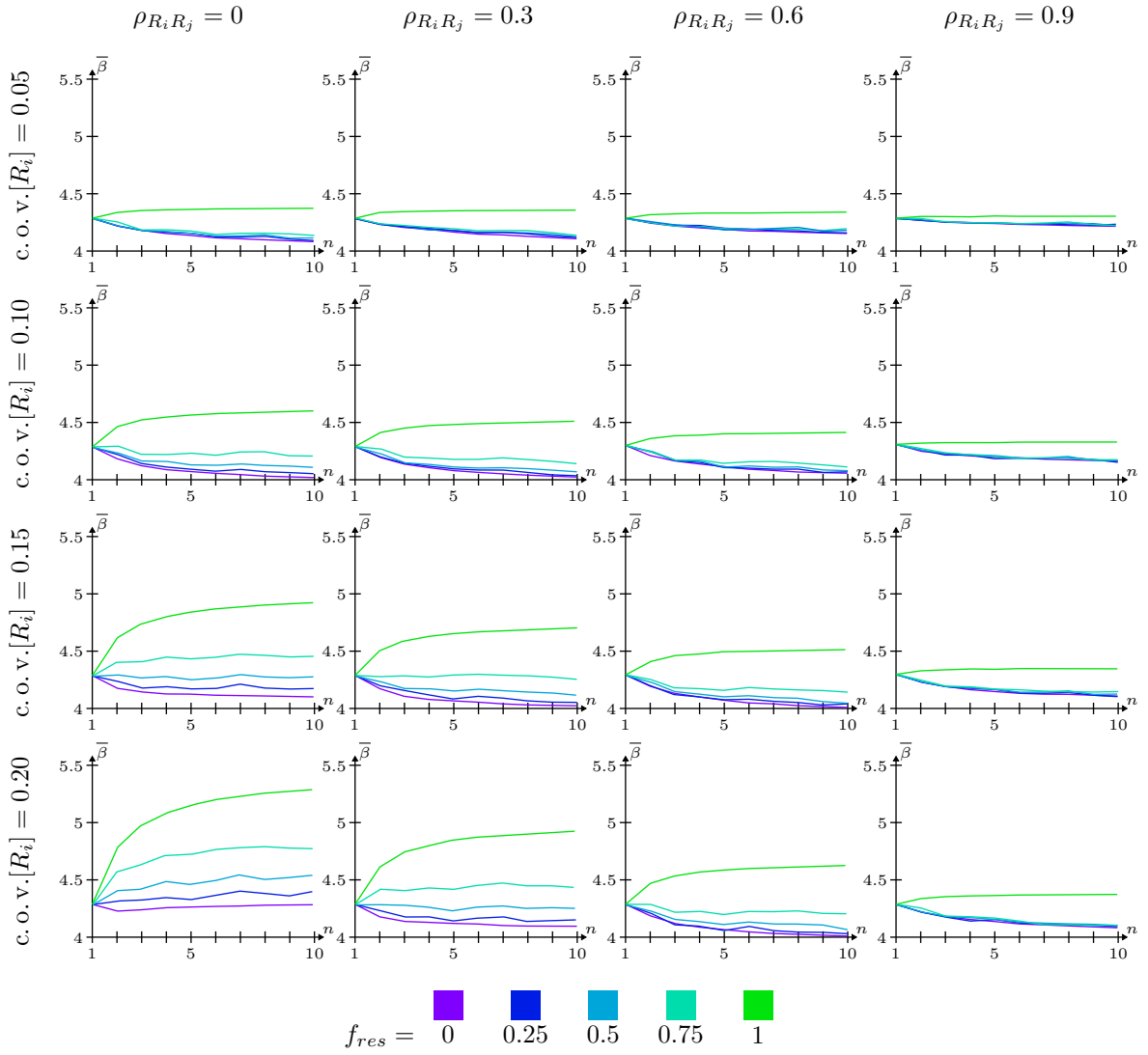
Fig. 4.29.: Average reliability indices of Daniels systems with $n = 1, \ldots, 10$ members, $f_{res} \in \{0, 0.25, 0.5, 0.75, 1\}$, c.o.v.$[R_i] \in \{0.05, 0.1, 0.15, 0.2\}$ and $\rho_{R_i R_j} \in \{0, 0.3, 0.6, 0.9\}$.

	n	1	2	3	4	5	6	7	8	9	10
Ideal plastic ($f_{res} = 1.00$)		1.00	0.99	0.98	0.98	0.98	0.98	0.98	0.98	0.97	0.97
Semi-plastic ($f_{res} = 0.75$)		1.00	1.00	1.03	1.03	1.03	1.03	1.03	1.03	1.04	1.04
Semi-plastic ($f_{res} = 0.50$)		1.00	1.01	1.03	1.03	1.04	1.04	1.04	1.04	1.05	1.05
Semi-plastic ($f_{res} = 0.25$)		1.00	1.01	1.03	1.04	1.04	1.04	1.04	1.04	1.05	1.06
Ideal brittle ($f_{res} = 0.00$)		1.00	1.02	1.03	1.04	1.04	1.05	1.05	1.06	1.06	1.06

	n	1	2	3	4	5	6	7	8	9	10
Ideal plastic ($f_{res} = 1.00$)		1.00	0.99	0.99	0.98	0.99	0.99	0.99	0.99	0.99	0.99
Semi-plastic ($f_{res} = 0.75$)		1.00	1.02	1.03	1.03	1.03	1.04	1.04	1.04	1.04	1.04
Semi-plastic ($f_{res} = 0.50$)		1.00	1.02	1.03	1.03	1.04	1.04	1.04	1.04	1.05	1.05
Semi-plastic ($f_{res} = 0.25$)		1.00	1.02	1.03	1.03	1.04	1.04	1.05	1.05	1.05	1.05

The left labels for the first table: c.o.v.$[R] = 0.05$, $\rho_{R_i R_j} = 0$.
The left labels for the second table: c.o.v.$[R] = 0.05$, $\rho_{R_i R_j} = 0.3$.

	1.00	1.02	1.03	1.03	1.04	1.04	1.05	1.05	1.05	1.05
Ideal brittle ($f_{res} = 0.00$)	1.00	1.02	1.03	1.03	1.04	1.04	1.05	1.05	1.05	1.05

c.o.v.$[R] = 0.05$, $\rho_{R_i R_j} = 0.6$

n	1	2	3	4	5	6	7	8	9	10
Ideal plastic ($f_{res} = 1.00$)	1.00	0.99	0.99	0.99	0.99	0.99	0.99	0.99	0.99	0.99
Semi-plastic ($f_{res} = 0.75$)	1.00	1.01	1.02	1.03	1.03	1.03	1.03	1.03	1.03	1.04
Semi-plastic ($f_{res} = 0.50$)	1.00	1.01	1.02	1.03	1.03	1.03	1.03	1.04	1.04	1.04
Semi-plastic ($f_{res} = 0.25$)	1.00	1.01	1.02	1.03	1.03	1.03	1.04	1.04	1.04	1.04
Ideal brittle ($f_{res} = 0.00$)	1.00	1.01	1.02	1.03	1.03	1.03	1.04	1.04	1.04	1.04

c.o.v.$[R] = 0.05$, $\rho_{R_i R_j} = 0.9$

n	1	2	3	4	5	6	7	8	9	10
Ideal plastic ($f_{res} = 1.00$)	1.00	1.00	1.00	1.00	1.00	1.00	1.00	1.00	1.00	1.00
Semi-plastic ($f_{res} = 0.75$)	1.00	1.01	1.01	1.01	1.02	1.02	1.02	1.02	1.02	1.02
Semi-plastic ($f_{res} = 0.50$)	1.00	1.01	1.01	1.01	1.02	1.02	1.02	1.02	1.02	1.02
Semi-plastic ($f_{res} = 0.25$)	1.00	1.01	1.01	1.01	1.02	1.02	1.02	1.02	1.02	1.02
Ideal brittle ($f_{res} = 0.00$)	1.00	1.01	1.01	1.01	1.02	1.02	1.02	1.02	1.02	1.02

c.o.v.$[R] = 0.1$, $\rho_{R_i R_j} = 0$

n	1	2	3	4	5	6	7	8	9	10
Ideal plastic ($f_{res} = 1.00$)	1.00	0.95	0.94	0.93	0.92	0.92	0.92	0.92	0.92	0.92
Semi-plastic ($f_{res} = 0.75$)	1.00	1.00	1.00	1.00	1.00	1.00	1.00	1.00	1.00	1.00
Semi-plastic ($f_{res} = 0.50$)	1.00	1.01	1.03	1.03	1.03	1.03	1.03	1.03	1.03	1.03
Semi-plastic ($f_{res} = 0.25$)	1.00	1.02	1.04	1.04	1.04	1.05	1.05	1.05	1.05	1.05
Ideal brittle ($f_{res} = 0.00$)	1.00	1.03	1.05	1.06	1.07	1.07	1.07	1.08	1.08	1.08

c.o.v.$[R] = 0.1$, $\rho_{R_i R_j} = 0.3$

n	1	2	3	4	5	6	7	8	9	10
Ideal plastic ($f_{res} = 1.00$)	1.00	0.97	0.96	0.95	0.95	0.95	0.94	0.94	0.94	0.94
Semi-plastic ($f_{res} = 0.75$)	1.00	1.01	1.02	1.02	1.02	1.02	1.02	1.02	1.02	1.03
Semi-plastic ($f_{res} = 0.50$)	1.00	1.02	1.04	1.04	1.05	1.05	1.05	1.05	1.05	1.06
Semi-plastic ($f_{res} = 0.25$)	1.00	1.02	1.05	1.05	1.06	1.06	1.06	1.06	1.07	1.07
Ideal brittle ($f_{res} = 0.00$)	1.00	1.03	1.05	1.06	1.06	1.07	1.07	1.08	1.08	1.08

c.o.v.$[R] = 0.1$, $\rho_{R_i R_j} = 0.6$

n	1	2	3	4	5	6	7	8	9	10
Ideal plastic ($f_{res} = 1.00$)	1.00	0.98	0.97	0.97	0.97	0.97	0.97	0.97	0.97	0.97
Semi-plastic ($f_{res} = 0.75$)	1.00	1.02	1.04	1.04	1.04	1.04	1.04	1.04	1.04	1.05
Semi-plastic ($f_{res} = 0.50$)	1.00	1.02	1.04	1.05	1.05	1.05	1.05	1.05	1.05	1.06
Semi-plastic ($f_{res} = 0.25$)	1.00	1.02	1.04	1.05	1.06	1.06	1.06	1.06	1.06	1.07
Ideal brittle ($f_{res} = 0.00$)	1.00	1.02	1.04	1.05	1.05	1.06	1.06	1.07	1.07	1.07

c.o.v.$[R] = 0.1$, $\rho_{R_i R_j} = 0.9$

n	1	2	3	4	5	6	7	8	9	10
Ideal plastic ($f_{res} = 1.00$)	1.00	0.99	0.99	0.99	0.99	0.99	0.99	0.99	0.99	0.99
Semi-plastic ($f_{res} = 0.75$)	1.00	1.01	1.02	1.03	1.03	1.03	1.04	1.04	1.04	1.04
Semi-plastic ($f_{res} = 0.50$)	1.00	1.01	1.02	1.03	1.03	1.03	1.04	1.04	1.04	1.04
Semi-plastic ($f_{res} = 0.25$)	1.00	1.01	1.02	1.03	1.03	1.03	1.04	1.04	1.04	1.04
Ideal brittle ($f_{res} = 0.00$)	1.00	1.01	1.02	1.03	1.03	1.03	1.04	1.04	1.04	1.04

c.o.v.$[R] = 0.15$, $\rho_{R_i R_j} = 0$

n	1	2	3	4	5	6	7	8	9	10
Ideal plastic ($f_{res} = 1.00$)	1.00	0.91	0.87	0.86	0.85	0.84	0.84	0.84	0.84	0.84
Semi-plastic ($f_{res} = 0.75$)	1.00	0.95	0.95	0.93	0.93	0.92	0.92	0.92	0.92	0.92
Semi-plastic ($f_{res} = 0.50$)	1.00	1.00	1.00	0.99	0.99	0.99	0.99	0.99	0.99	0.99
Semi-plastic ($f_{res} = 0.25$)	1.00	1.00	1.01	1.01	1.01	1.01	1.01	1.01	1.01	1.01
Ideal brittle ($f_{res} = 0.00$)	1.00	1.04	1.05	1.05	1.05	1.05	1.05	1.05	1.06	1.06

c.o.v.$[R] = 0.15$, $\rho_{R_i R_j} = 0.3$

n	1	2	3	4	5	6	7	8	9	10
Ideal plastic ($f_{res} = 1.00$)	1.00	0.94	0.91	0.90	0.89	0.89	0.89	0.89	0.89	0.89
Semi-plastic ($f_{res} = 0.75$)	1.00	0.99	0.99	0.99	0.99	0.98	0.98	0.98	0.98	0.98
Semi-plastic ($f_{res} = 0.50$)	1.00	1.02	1.02	1.02	1.02	1.02	1.02	1.02	1.03	1.03
Semi-plastic ($f_{res} = 0.25$)	1.00	1.02	1.03	1.04	1.05	1.05	1.05	1.05	1.05	1.06
Ideal brittle ($f_{res} = 0.00$)	1.00	1.04	1.06	1.06	1.07	1.07	1.08	1.08	1.08	1.08

c.o.v.$[R] = 0.15$, $\rho_{R_i R_j} = 0.6$

n	1	2	3	4	5	6	7	8	9	10
Ideal plastic ($f_{res} = 1.00$)	1.00	0.96	0.95	0.94	0.94	0.94	0.94	0.94	0.94	0.94

	n	1	2	3	4	5	6	7	8	9	10
Semi-plastic ($f_{res} = 0.75$)		1.00	1.02	1.03	1.03	1.03	1.03	1.03	1.03	1.03	1.03
Semi-plastic ($f_{res} = 0.50$)		1.00	1.03	1.05	1.05	1.05	1.05	1.05	1.06	1.06	1.06
Semi-plastic ($f_{res} = 0.25$)		1.00	1.04	1.06	1.06	1.07	1.07	1.07	1.07	1.07	1.08
Ideal brittle ($f_{res} = 0.00$)		1.00	1.03	1.05	1.06	1.07	1.08	1.08	1.09	1.09	1.09
c.o.v.$[R] = 0.15$, $\rho_{R_i R_j} = 0.9$	n	1	2	3	4	5	6	7	8	9	10
Ideal plastic ($f_{res} = 1.00$)		1.00	0.99	0.99	0.98	0.99	0.99	0.99	0.99	0.99	0.99
Semi-plastic ($f_{res} = 0.75$)		1.00	1.02	1.03	1.04	1.04	1.05	1.05	1.06	1.06	1.06
Semi-plastic ($f_{res} = 0.50$)		1.00	1.02	1.03	1.04	1.04	1.05	1.05	1.06	1.06	1.06
Semi-plastic ($f_{res} = 0.25$)		1.00	1.02	1.03	1.04	1.04	1.05	1.05	1.06	1.06	1.06
Ideal brittle ($f_{res} = 0.00$)		1.00	1.02	1.03	1.04	1.04	1.05	1.05	1.06	1.06	1.06
c.o.v.$[R] = 0.2$, $\rho_{R_i R_j} = 0$	n	1	2	3	4	5	6	7	8	9	10
Ideal plastic ($f_{res} = 1.00$)		1.00	0.86	0.81	0.79	0.78	0.77	0.76	0.75	0.75	0.75
Semi-plastic ($f_{res} = 0.75$)		1.00	0.91	0.89	0.86	0.85	0.84	0.83	0.83	0.83	0.83
Semi-plastic ($f_{res} = 0.50$)		1.00	0.95	0.95	0.92	0.92	0.91	0.90	0.90	0.90	0.89
Semi-plastic ($f_{res} = 0.25$)		1.00	0.99	0.98	0.96	0.96	0.94	0.93	0.93	0.93	0.93
Ideal brittle ($f_{res} = 0.00$)		1.00	1.03	1.02	1.01	1.01	1.01	1.01	1.01	1.01	1.01
c.o.v.$[R] = 0.2$, $\rho_{R_i R_j} = 0.3$	n	1	2	3	4	5	6	7	8	9	10
Ideal plastic ($f_{res} = 1.00$)		1.00	0.91	0.87	0.85	0.85	0.84	0.84	0.83	0.83	0.83
Semi-plastic ($f_{res} = 0.75$)		1.00	0.96	0.95	0.94	0.94	0.93	0.93	0.93	0.93	0.92
Semi-plastic ($f_{res} = 0.50$)		1.00	1.00	1.00	1.00	1.00	0.99	0.99	0.99	0.99	0.98
Semi-plastic ($f_{res} = 0.25$)		1.00	1.02	1.02	1.02	1.02	1.02	1.02	1.02	1.02	1.02
Ideal brittle ($f_{res} = 0.00$)		1.00	1.04	1.05	1.05	1.06	1.06	1.06	1.06	1.06	1.07
c.o.v.$[R] = 0.2$, $\rho_{R_i R_j} = 0.6$	n	1	2	3	4	5	6	7	8	9	10
Ideal plastic ($f_{res} = 1.00$)		1.00	0.94	0.93	0.92	0.91	0.91	0.91	0.90	0.90	0.90
Semi-plastic ($f_{res} = 0.75$)		1.00	1.01	1.02	1.02	1.02	1.02	1.02	1.02	1.02	1.02
Semi-plastic ($f_{res} = 0.50$)		1.00	1.02	1.05	1.05	1.05	1.05	1.05	1.06	1.06	1.06
Semi-plastic ($f_{res} = 0.25$)		1.00	1.03	1.06	1.06	1.07	1.07	1.07	1.08	1.08	1.08
Ideal brittle ($f_{res} = 0.00$)		1.00	1.04	1.06	1.07	1.08	1.09	1.09	1.09	1.10	1.10
c.o.v.$[R] = 0.2$, $\rho = 0.9$	n	1	2	3	4	5	6	7	8	9	10
Ideal plastic ($f_{res} = 1.00$)		1.00	0.99	0.98	0.98	0.98	0.98	0.98	0.98	0.97	0.98
Semi-plastic ($f_{res} = 0.75$)		1.00	1.03	1.04	1.05	1.06	1.06	1.07	1.07	1.08	1.08
Semi-plastic ($f_{res} = 0.50$)		1.00	1.03	1.04	1.05	1.06	1.06	1.07	1.07	1.08	1.08
Semi-plastic ($f_{res} = 0.25$)		1.00	1.03	1.04	1.05	1.06	1.06	1.07	1.07	1.08	1.08
Ideal brittle ($f_{res} = 0.00$)		1.00	1.03	1.04	1.05	1.06	1.06	1.07	1.07	1.08	1.08

Tab. 4.2.: Values of the additional PSF γ_{Sys} to take system effects into account within the PSF concept. γ_{Sys} needs to be applied to the material strength.

4.5.1. Example application of γ_{Sys}

To illustrate the application of γ_{Sys}, it is applied to the example frame of Sec. 4.4.2. The value of γ_{Sys} is determined through the following properties of the frame: The frame is 3 times statically overdetermined; therefore, 4 element failures make the frame kinematic ($n = 4$). The coefficient of variation of the member resistances is 0.1 and the members are equicorrelated with a correlation coefficient of 0.3; thus, the values of γ_{Sys} can be taken from the fourth column of Tab. 4.2 and the case of c.o.v.$[R] = 0.1$ and $\rho_{R_i R_j} = 0.3$. In the ideal plastic case, γ_{Sys} is 1.06. In the ideal brittle case, γ_{Sys} is 0.95.

The frame is redesigned using these values of γ_{Sys}. The distributions of the member

resistances R_{1-5} are determined analogously to Sec. 4.4.1; whereby, $\gamma_M \cdot \gamma_{Sys}$ is applied to the characteristic resistances. The system reliability is re-calculated as in Sec. 4.4.2. The resulting system reliability indices are:

$$\beta_{Sys,plast,\gamma_{Sys}} = 4.43 \qquad\qquad \beta_{Sys,brittle,\gamma_{Sys}} = 3.45 \qquad\qquad (4.51)$$

The previously calculated system reliabilities without the application of γ_{Sys} are $\beta_{Sys,plast} = 4.62$ and $\beta_{Sys,brittle} = 3.20$ (see Eqns. 4.40 and 4.41). Hence, both reliability indices are closer to the target reliability index of 4.3.

4.6. Discussion

As already mentioned, the calibration at hand is not perfect due to necessary simplifying assumptions; however, it is a step in the right direction. In the following, the most critical assumptions and their effect on system reliability are discussed. This includes the first, second, third, and sixth assumptions made in Sec. 4.5 to simplify the list of entities of equivalence of the generalized Daniels system and general structural systems. For each assumption, it is discussed whether it is conservative or not and whether the derived values of the additional PSF γ_{Sys} should therefore be higher or lower? The two assumptions (four and five) made in Sec. 4.5 are considered to be reasonable simplifications that do not need further discussion.

The first assumption (only one dominant failure mechanism is present), can be considered reasonable in most cases for the following reason: It is rarely the case that two or more similarly likely failure mechanisms exist. However, in the rare cases where two or more similarly likely failure mechanisms exist, these failure modes usually partly depend on the same element failures. Therefore, the respective failure domains overlap and the system failure probability is only slightly larger than the probability of the individual failure mechanisms. This is, e.g., the case in the example frame (see sec. 4.4.2.1 and 4.4.2.2). Hence, this assumption is critical only if two or more similarly likely failure modes exist that also do not depend on the same element failures. In the author's experience, this is rarely the case.

The second assumption (the consideration of global failure mechanisms only) is a conservative assumption if the corresponding γ_{Sys} is greater than 1, which is the case for predominantly brittle structures. It is a non-conservative assumption if the corresponding γ_{Sys} is smaller than 1, which is the case for predominantly plastic structures. This is for the following reason: Local failure mechanisms include fewer or equal numbers of element failures than global failure mechanisms. Therefore, the subsystem containing the local failure mechanism has a smaller or equal n than the whole system. In the case of predominantly brittle structures, γ_{Sys} is strictly monotonically increasing with increasing n and, therefore, the value of γ_{Sys} one would apply to the subsystem is smaller than the value of γ_{Sys} that is applied to the whole structure; hence, the subsystem is designed with a greater γ_{Sys} than intended. In the case of predominantly plastic structures, γ_{Sys} is strictly monotonically decreasing with increasing n. This leads to a design of the subsystem with a smaller γ_{Sys} than intended. However, the associated failure is "only" a local failure and

not a global failure mode of the whole structure.

The combination of the third and sixth assumptions is considered to be the most critical assumption. These assumptions include the assumption of a load distribution proportional to the element strength at all damage states of the structural system. When it comes to plastic material behavior, this assumption is always satisfied, as shown in Sec. 4.4.2.1. However, when the considered material is brittle or semi-plastic, this is a non-conservative simplification for the following reason: The PSF concept may lead to a load distribution that is proportional to the member strength in the undamaged state of the structure, but after a member fails, the load redistributes non-proportional to the member strength. This favors cascading failures of the system. The investigated frame structure takes this into account by making the horizontal bar of the Daniels system rotatable, allowing for non-proportional load distributions (see Fig. 4.27 and 4.28). However, such a modification of the Daniels system is not considered within the derivation of γ_{Sys}. Therefore, the values of γ_{Sys} are non-conservative in the case of predominantly brittle structures.

Overall, the values of γ_{Sys} are non-conservative. How much the values are non-conservative is difficult to determine. To answer this question, a large amount of real structures would have to be investigated. The author estimates the values of γ_{Sys} to be slightly non-conservative for predominantly plastic structures and slightly more but still not strongly non-conservative for predominantly brittle structures. For predominantly plastic structures, this non-conservatism is critical because the values of γ_{Sys} are below 1, reducing the system-resistance more than it should be compared to the design without the application of γ_{Sys}. For predominantly brittle structures, this non-conservatism is not critical because the values of γ_{Sys} are above 1, hence, the system resistance is increased compared to the standard case; however, it may not be as much as it should be.

4.7. Conclusion

An additional PSF γ_{Sys} is introduced to take system effects into account without leaving the framework of the PSF concept. It is derived by means of a generalized Daniels system. γ_{Sys} leads to a homogenization of the safety level. Due to necessary simplifications, the homogenization is not perfect; however, overall, it is a step in the right direction.

γ_{Sys} depends on the static over-determination of the system, its material behavior, the coefficient of variation of the material strength, and the correlation of the involved element failure mechanisms. The last two quantities may not be given within an PSF design and have to be determined separately. If γ_{Sys} would be included within a structural code, recommendations for these quantities for different structural systems need to be derived.

The majority of values of γ_{Sys} is close to 1. This is a reassuring result, as it shows that the majority of current PSF designs are not very far from the target reliability due to system effects. Neither material wastage due to overdesign nor unsafe structures usually occur. It should be noted, however, that the values of γ_{Sys} are slightly non-conservative, hence, the result is not as reassuring as one would wish for.

Overall, the application of γ_{Sys} may not be worth the effort in most cases. Exceptions may be larger or more critical structural systems (e.g., bridges) or structural systems that are built multiple times (e.g., prefabricated houses). In some cases γ_{Sys} has rather low values up to 0.75 (high static overdetermination, high plasticity of the material, high coefficient of variation of the material strength, and low correlation between element failure mechanisms). In these cases, a high saving potential of resources could be exploited; however, the application of γ_{Sys} is not needed due to safety issues. In other cases γ_{Sys} reaches values up to 1.10 (high static overdetermination, low plasticity of the material, low coefficient of variation of the material strength, and high correlation between element failure mechanisms). In these cases, the application of γ_{Sys} is recommended to ensure sufficient safety of the structure.

5. Effects of non-linearities in codified design

The PSFs of the Eurocode are intended to be used with linear models. They are calibrated such that, on average, the desired target reliability is achieved for the case of linear models [38, 61, 76]. In practice, they are also applied to non-linear models. This is in agreement with the PSF concept [38,69]. Except for extreme cases of non-linearities, the PSF concept would result in sufficiently safe structures if each quantity had its own calibrated PSF. However, in practice, PSFs cover the uncertainty of multiple quantities. In particular, Eurocode merges the PSFs of the action γ_f and the structural model γ_{Sd} and the PSFs of the material strength γ_m and the resistance model γ_{Rd} respectively (see Eqns. 2.6-2.7). This raises the questions of how these PSFs should be applied in the presence of non-linear models and if a sufficiently safe design can still be achieved.

The application of a PSF to a non-linear model can in principle be done in two different ways: The PSF can be applied to the argument or to the responses of the non-linear function. This refers to the two basic design options described in Eqns. 2.8-2.10. Both basic options can lead to a reliability below and above the target reliability. Structural design codes typically try to overcome this issue by choosing the more conservative of the two design options (e.g., [25]). In some cases, this may lead to overdesign. In other cases, the more conservative of the two options might still lead to insufficient reliability. This issue is the research question of this section: How do non-linear models affect structural reliability for the two basic design options? The question is investigated for one- or two-dimensional structural response functions t_S. The resistance model t_R is assumed to be linear and through the origin. Investigations of non-linear resistance models can be found, e.g., in [151–154].

Previous research on non-linear models applied within the PSF concept focuses mainly on reinforced concrete structures. The reinforced concrete research community has developed multiple methods to adapt PSF design and thereby provide alternatives to the two above-mentioned design options. The most popular method is the estimated coefficient of variation method (ECOV) [155]. It is based on an estimate of the coefficient of variation of the resistance via the mean and the characteristic material strength. Other methods can be found in [57, 151, 156, 157]. These methods are well investigated through various application studies (e.g., [152, 154, 158, 159]). More abstract and material independent investigations on the effects of non-linear models on reliability are not known to the author. Only a paper by Bakeer [160] partly covers this issue. The purpose of this section is to provide such abstract and material independent investigations. Thereby, the focus is on the two above-mentioned basic design options. Alternative design options, such as those offered by the reinforced concrete research community, could be generalized and investigated as well, but this is beyond the scope of this thesis.

Within this section, it is assumed that the nominal structural model and the nominal

resistance model are equal to the respective purely aleatoric models; hence, $t_{S,EC} = t_S$ and $t_{R,EC} = t_R$. Moreover, it is assumed that the nominal material models and the nominal action models are equal to the respective purely aleatoric models; hence, $M_{EC} = M$ and $L_{EC} = L$ and, therefore, $m_{k,EC} = m_k$ and $l_{k,EC} = l_k$.

In summary, the research question of this section focuses on the two LSF (one- and two-dimensional action cases)

$$g(M,L) = \frac{\gamma_M \cdot e_d}{m_k} \cdot M - t_S(L_1) \tag{5.1}$$

$$g(M,L_1,L_2) = \frac{\gamma_M \cdot e_d}{m_k} \cdot M - t_S(L_1,L_2) \tag{5.2}$$

derived following Sec. 2.3.2.2. L, L_1, L_2 are actions, M is the material strength, γ_M is the PSF of the resistance side, m_k is the characteristic value of the material strength and e_d is the design action effect.

In the one-dimensional action case, e_d is determined following Eqns. 2.8-2.9 as

Design option (1) (prior to t_S): $\qquad\qquad\qquad e_d = t_S(\gamma_F \cdot l_k) \tag{5.3}$

Design option (2) (posterior to t_S): $\qquad\qquad\qquad e_d = \gamma_F \cdot t_S(l_k) \tag{5.4}$

where γ_F is the PSF of the action side and l_k is the characteristic value of the action.

In the two-dimensional action case, design option (1) directly follows from the one-dimensional case and is defined as

Design option (1) (prior to t_S): $\qquad\qquad e_d = t_S(\gamma_{F1} \cdot l_{k1}, \gamma_{F2} \cdot l_{k2}) \tag{5.5}$

where γ_{F1} and γ_{F2} are the PSFs of the action side and l_{k1} and l_{k2} are the characteristic values of the actions. Design option (2) is not as straightforward to be transferred to the two-dimensional case. Hereby, the German national annex of Eurocode 0 [161] is used, which applies the PSF of the dominating action to the action effect and applies the remaining PSFs directly to the action; however, scaled by the PSF of the dominating action. Hence, design option (2) in the two-dimensional case is defined as

Design option (2) (posterior to t_S): $\tag{5.6}$

$$e_d = \max \left\{ \gamma_{F1} \cdot t_S \left(l_{k1}, \frac{\gamma_{F2}}{\gamma_{F1}} \cdot l_{k2} \right), \right.$$
$$\left. \gamma_{F2} \cdot t_S \left(\frac{\gamma_{F1}}{\gamma_{F2}} \cdot l_{k1}, l_{k2} \right) \right\}$$

To answer the research question of how these design options affect reliability, this section is structured as follows: First, it is explained how the Eurocode decides between design options (1) and (2) (Sec. 5.1). Second, existing measures of non-linearities and their effect on structural reliability are reviewed and a novel measure is introduced (Sec. 5.2). Next, a generic general parameter study (Sec. 5.3) on the effects of non-linear structural models is conducted. Eventually, two example applications 5.4 are conducted. The investigations are mainly based on the following publications of the author: [162–165]. Various proposals

on how the novel measure of non-linearity could potentially be included in the PSF concept are given in the conclusions of this section.

5.1. Eurocode approach for non-linear structural models

Eurocode [25] does not give clearly defined mathematical instructions when to use design option (1) or (2). It only states to use design option (1) if "the action effect increases more than the action" and option (2) if "the action effect increases less than the action". The background document *Designers' Guide to Eurocode: Basis of Structural Design* [166] specifies this mathematically as follows:

use option (1) if: $$t_S(\gamma_F \cdot l_k) > \gamma_F \cdot t_S(l_k) \tag{5.7}$$

use option (2) if: $$t_S(\gamma_F \cdot l_k) < \gamma_F \cdot t_S(l_k) \tag{5.8}$$

The instructions of Eurocode lead to some open questions when it comes to the classification of non-linearities:

One question is how to deal with initial actions such as prestress: The relationship between actions and their effects might be linear for values of actions above 0; however, under initial actions, t_S is highly non-linear at the origin (see Fig. 5.1). According to Eurocode [25] this case is interpreted as linear. The background document of Eurocode [166] implies a non-linearity, leading to design option (2).
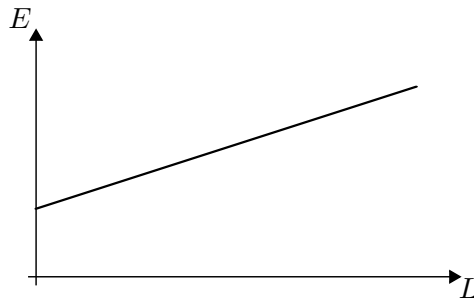

Fig. 5.1.: Relationship between actions and their effects in the presence of an initial action.

Another ambiguity arises if t_S has a change of curvature (see Fig. 5.2). This can, e.g., be the case when a structure is dominated by softening effects at lower load levels, but is dominated by hardening effects at higher loads. Here, the Eurocode [25] does not provide a classification of t_S. The background document of Eurocode [166] can lead to both design options, depending on the value at which the function has the change of curvature.

A third question is how to treat the case of multiple actions. This case is not covered by Eurocode 0 [25] nor the background document [166]. The German national annex [161] provides two design options defined analogously to the design option for the 2-dimensional action case of Eqns. 5.5-5.6 for the 2-dimensional action case. A specific rule for when to
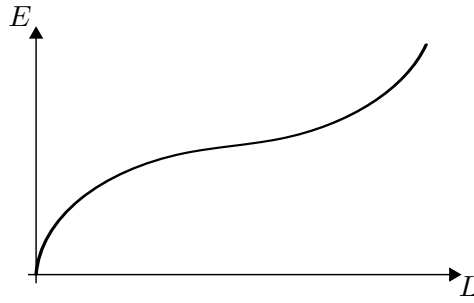
Fig. 5.2.: Relationship between actions and their effects in the presence of a change in curvature.

choose which design option is not given for the multidimensional case. Here, the author interprets the Eurocode such that the maximum e_d following from design options (1) and (2) should be chosen.

5.2. Proposal of new measures of non-linearity

Two new measures of non-linearity are proposed. The first measure is applicable within the semi-probabilistic setup of the PSF concept. The second measure is only applicable within a probabilistic setup and, therefore, not discussed in detail as the PSF concept is the main focus of this thesis. Existing measures are reviewed beforehand.

5.2.1. Review of existing measures of non-linearity

Multiple measures of the non-linearity of a function can be found in the literature, e.g., [167–171]; however, proposals for measures applicable within the PSF concept are sparse. The author is only aware of two measures: Two measures introduced by Uhlemann [172] and Bakeer [160].

The measure n introduced by Uhlemann was further investigated by [173] and eventually included in the background document of the Eurocode *Prospect for European Guidance for the Structural Design of Tensile Membrane Structures* [174] as follows:

$$n = \frac{t_S(f \cdot l_k)}{f \cdot t_S(l_k)} \tag{5.9}$$

Here, f is an arbitrary load increase factor. Based on the value of n different design options are recommended [174]:

$$n \begin{cases} = 1 & \text{use option (1) or option (2) (linear case)} \\ > 1 & \text{use option (1)} \\ < 1 & \text{use option (2)} \end{cases} \tag{5.10}$$

107

If $f = \gamma_F$, the rules for which design option to choose are equivalent for the Designers' Guide (Eqns. 5.7 and 5.8) and Uhlemann (Eqn. 5.9).

The measure n_F introduced by Bakeer is called the degree of homogeneity. It is derived via a first order Taylor series expansion of t_S mapped into log-space at the design point. This results in a measure of the relative change of the effect of action to the relative change of the action at the design point:

$$n_F = \frac{\gamma_F \cdot l_k}{t_S(\gamma_F \cdot l_k)} \cdot \frac{\mathrm{d}t_S(\gamma_F \cdot l_k)}{\mathrm{d}l} \tag{5.11}$$

which can be approximated via

$$n_F \approx \frac{1}{\ln(\gamma_F)} \cdot \ln\left(\frac{t_S(\gamma_F \cdot l_k)}{t_S(l_k)}\right) \tag{5.12}$$

If $n_F = 1$ the measure indicates t_S to be linear. If $n_F > 1$ the measure indicates $\gamma_F \cdot t_S(l_k) < t_S(\gamma_F \cdot l_k)$ which is linked to design option (1). If $0 < n_F < 1$ the measure indicates $t_S(\gamma_F \cdot l_k) < \gamma_F \cdot t_S(l_k)$ which is linked to design option (2).

The measure can analogously be defined on the resistance side to measure the non-linearity of t_R. Moreover, the measure is also applicable in the case of multiple actions, leading to a measure of the partial degree of homogeneity per applied action.

Both measures struggle with the prediction of reliability. If the measures have the same value, they can be related to very different reliabilities. To visualize this issue, Fig. 5.3 shows different t_S, which share the same measure n and n_F respectively. These different t_S may result in very different structural reliabilities. However, in defense of both measures, it should be noted that it is impossible to fully satisfy this requirement. Why this is the case can be seen from the parameter studies in Sec. 5.3.
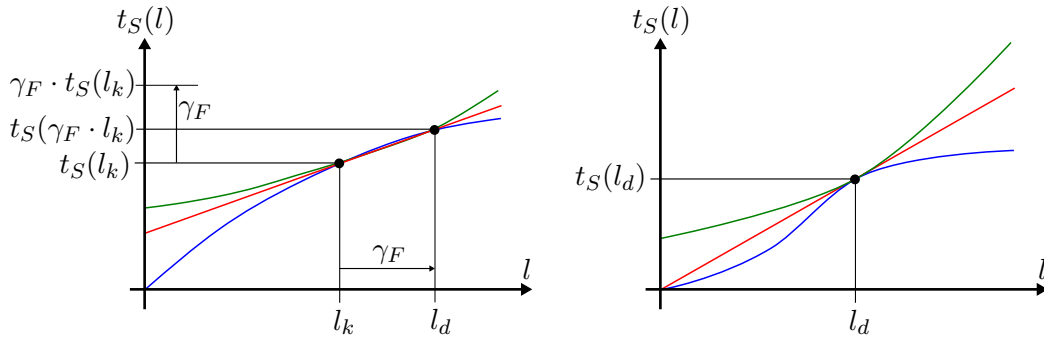

Fig. 5.3.: Different non-linear t_S that share the same measure of non-linearity n (left) and n_F (right). The t_S in the left illustration results in the same measure n since they share the same action effect at characteristic and design actions. The t_S in the right illustration results in the same measure n_F since they share the same action effect and the same gradient at design action.

5.2.2. Semi-probabilistic measure of non-linearity

The new proposed semi-probabilistic measure of non-linearity is based on the values of the PSF concept, namely the characteristic actions and design actions and their respective action effects. The measure is defined in terms of limit states with one or two actions. The measure is defined such that it can be included in the PSF concept to provide assistance on what design option to choose. However, an explicit proposal for inclusion is not given, as this would require an in-depth code calibration that is beyond the scope of this thesis. Potential future inclusions are indicated in the discussion (Sec. 5.5).

In the case of a single action, the measure consists of two components, the offset measure y_0 and the curvature measure κ (Fig. 5.4 illustrates y_0 and κ):

$$y_0 = \frac{t_S(0)}{t_S(l_k)} \tag{5.13}$$

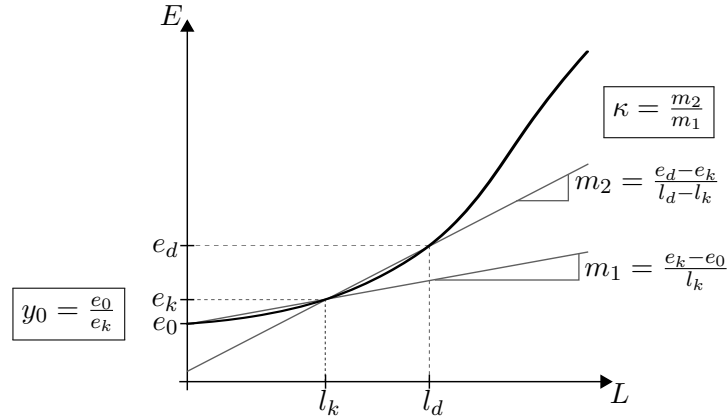$$\kappa = \frac{(t_S(l_d) - t_S(l_k)) \cdot l_k}{(t_S(l_k) - t_S(0)) \cdot (l_d - l_k)} \tag{5.14}$$

Fig. 5.4.: Measures y_0 and κ to classify the non-linearity of t_S in the case of one action.

In the case of two actions, the measure consists of six components, the offset measure y_0,

the curvature measures κ_1, κ_2, κ_{12}, and the ratio measures r_1, r_2:

$$y_0 = \frac{t_S(0,0)}{t_S(l_{1k},l_{2k})} \tag{5.15}$$

$$\kappa_1 = \frac{(t_S(l_{1d},0) - t_S(l_{1k},0)) \cdot l_{1k}}{(t_S(l_{1k},0) - t_S(0,0)) \cdot (l_{1d} - l_{1k})} \tag{5.16}$$

$$\kappa_2 = \frac{(t_S(0,l_{2d}) - t_S(0,l_{2k})) \cdot l_{2k}}{(t_S(0,l_{2k}) - t_S(0,0)) \cdot (l_{2d} - l_{2k})} \tag{5.17}$$

$$\kappa_{12} = \frac{(t_S(l_{1d},l_{2d}) - t_S(l_{1k},l_{2k}))}{(t_S(l_{1k},l_{2k}) - t_S(0,0))} \cdot \frac{\sqrt{l_{1k}^2 + l_{2k}^2}}{\sqrt{(l_{1d} - l_{1k})^2 + (l_{2d} - l_{2k})^2}} \tag{5.18}$$

$$r_1 = \frac{t_S(l_{1k},0) - t_S(0,0)}{t_S(l_{1k},l_{2k}) - t_S(0,0)} \tag{5.19}$$

$$r_2 = \frac{t_S(0,l_{2k}) - t_S(0,0)}{t_S(l_{1k},l_{2k}) - t_S(0,0)} \tag{5.20}$$

The interpretation of the components of the measures is as follows: y_0 is a measure of the amount of initial actions (e.g., due to prestress). If $y_0 = 0$ no initial action is present. If $y_0 = 1$ the action effect of the initial action is equal to the action effect of the characteristic action. κ is a measure of the curvature at the characteristic action. If $\kappa > 1$ then t_S is classified to be convex, if $\kappa = 1$ then t_S is classified to be without curvature and if $\kappa < 1$ then t_S is classified to be concave. Similar, κ_1 and κ_2 measures the curvature of t_S at $(l_{1k},0)$ and $(0,l_{2k})$ in the direction of the respective action. κ_{12} measures curvature of t_S at (l_{1k},l_{2k}) in the directions of the origin and the design point (l_{1d},l_{2d}), respectively. r_1 and r_2 measure the ratio of the action effect if only one characteristic action is applied, relative to the case where both characteristic actions are applied. If $r_1 = r_2$ the action effect of only action 1 or action 2 applied is the same. If $r_1 > r_2$ or $r_1 < r_2$ the action effect of action 1 or action 2 applied solely is greater than the respective other action applied solely. If $r_1 + r_2 = 1$ then t_S is approximately linear regarding actions below the characteristic value. If $r_1 + r_2 > 1$ then t_S is approximately convex in the perpendicular direction of the combined action regarding actions below the characteristic action level (the superposition of both actions is below the linear case). If $r_1 + r_2 < 1$ t_S is approximately concave in the perpendicular direction of the combined action regarding actions below the characteristic action level (the superposition of both actions is above the linear case).

The measure can be extended to more than two actions; however, this is not part of this thesis. It is rather intended to show that not all components of the two-dimensional dimension measure and, therefore, only two components of higher-dimensional measures are of primary interest. These two components are the measure of the initial load and the measure of the curvature in the direction of all actions. In the two-dimensional case, these are y_0 and κ_{12}. Sec. 5.3.2 investigates if this guess can be confirmed.

The proposed measure is straightforward to apply within the PSF concept for the following reason: It is exclusively based on evaluations of the structural response function t_S at the characteristic and design actions. Those evaluations are already necessary within a PSF design.

It would be desirable that similar structural reliabilities result from different limit states that share the same measure of non-linearity. However, this desire can unfortunately not be fulfilled for the proposed measure, as can be seen from the numerical investigations in Sec. 5.3. The main reason for this is that the probability of failure does not only depend on t_S but also on t_S interacting with (semi)-probabilistic properties, i.e., the choice of characteristic values, the PSFs, and the distributions of the actions and material strengths. However, one can argue that the proposed measure is a better predictor of reliability than the measures of Eqns. 5.9 and 5.11 for the following two reasons: First, κ is based on evaluations of t_S at three points (0, l_k and l_d). This captures the non-linear behavior of t_S more globally than the measure n which is based on evaluations at l_k and l_d only and the measure n_F which is based on evaluations (including the first derivative) at l_d only. Similar holds for the two-dimensional case. Secondly, y_0 accounts for different starting conditions at zero load level. In contrast, the measure n ignores different starting conditions and the measure n_F includes them only implicitly through the term $\frac{\gamma_F \cdot l_k}{t_S(\gamma_F \cdot l_k)}$.

5.2.3. Probabilistic measure of non-linearity

The proposed probabilistic measure of non-linearity is defined as the ratio of the approximated probability of failure calculated via FORM to the exact probability of failure ($\frac{\Pr(F)_{FORM}}{\Pr(F)}$). This measures the effect of non-linearity of the limit state surface in standard normal space on the probability of failure. The non-linearity of the limit state surface in standard normal space is influenced by the non-linearity of t_S as well as the distribution type of the load and the material strength. $\frac{\Pr(F)_{FORM}}{\Pr(F)}$ is 0 for linear t_S through the origin and normal distributed actions and material strengths. If $\frac{\Pr(F)_{FORM}}{\Pr(F)} < 1$, the limit state surface is dominated by a convex form. If $\frac{\Pr(F)_{FORM}}{\Pr(F)} > 1$, the limit state surface is dominated by a concave form.

This measure is not suitable for application within a design following the PSF concept but is more of a research interest. In contrast to the proposed measure of Sec.5.2.2 and the measures of Uhlemann [172] and Bakeer [160], non-linearity is not directly measured with respect to t_S but with respect to the limit state surface in standard normal space. Therefore, also the non-linearity of the resistance model t_R and the non-linearity due to the distribution types of the involved random variables in the original space is considered. The non-linearity is not measured in terms of function evaluations nor derivatives – as it is the case for the proposed measure and the measures of Uhlemann and Bakeer – but measured with respect to the probability mass within the failure domain defined via the limit state surface. For this reason, it can be argued that this measure is better when the quantity of interest is the reliability.

It should be noted, that $\frac{\Pr(F)_{FORM}}{\Pr(F)}$ is always equal to 1 if only one action is present. In this case the limit-state surface is just a point on a 1-dimensional axis. Therefore, the measure of non-linearity is not very meaningful in the one-dimensional action case.

5.3. Parameter studies on non-linear structural models

In the following, various studies are conducted to investigate how different amounts of non-linearity (measured via the newly proposed measure of non-linearity) affect structural reliability.

All considered studies are calibrated such that a target reliability index of $\beta_{TRG} = 4.3$ is achieved in the linear case. The calibration is conducted by adjusting the PSF of the resistance side γ_M such that β_{TRG} is met in the linear case. In the one-dimensional action case, the linear case is defined as any linear function with $\kappa = 1$ and $y_0 = 0$. Note that any linear structural response function leads to the same structural reliability because of the invariance of the structural reliability to scaling (see Eqn. 2.38-2.39). Therefore, any linear structural response function can be used for this calibration, resulting in the same γ_M. In the two-dimensional action case, the linear structural response function is defined as the structural response function that forms a plane spanned by two straight lines through the origin and the points $(l_{1k}, 0, t_S(l_{1k}, 0))$ and $(0, l_{2k}, t_S(0, l_{2k}))$. The six non-linear measures of this plane are $y_0 = 0$, $\kappa_1 = 1$, $\kappa_2 = 1$, $\kappa_{12} = 1$. The values of r_1 and r_2 depend on the angle of the plane. Hence, the values of r_1 and r_2 are not only varying for different non-linear t_S but also for different linear t_S. Therefore, γ_M is chosen differently for different values of r_1 and r_2. The reason for this is that – even in the linear case – two actions applied in various ratios can lead to the same design but different structural reliabilities. This effect occurs in practice but is filtered out in this work through the calibration of γ_M in order to isolate the non-linear effect.

$\beta_{TRG} = 4.3$ is in the common range of structural reliability index targets [61, 108]. Following [61] β_{TRG} is defined with respect to a reference period of 1 year. However, the subsequent parameter studies are not sensitive to the value of β_{TRG}. Similar results would be obtained, e.g., for the target reliability index following Eurocode 0 [25] of 4.7 (1 year) or 3.8 (50 years).

If the structural response functions t_S is non-linear, the resulting structural reliability can deviate from the target value. This can be the case for both design options (1) and (2). If the resulting reliability indices are above/below $\beta_{TRG} = 4.3$ one can consider the design to be conservative/non-conservative. The main focus of the subsequent studies is to investigate systematically under which conditions each design option is conservative or non-conservative.

5.3.1. One-dimensional action case

In the one-dimensional action case, first a base case is defined and investigated. Afterward, various other cases are investigated by varying one property of the base case at a time.

5.3.1.1. Base case

In the base case, a bi-linear functional form of t_S is defined with respect to different values of the curvature measure κ between 0 and 2. The offset measure y_0 is set to 0. The investigated t_S are shown in Fig. 5.5. Such bi-linear functional forms can, for example, occur in structures that are analyzed by first-order plastic hinge theory. In general, non-linear structural response functions typically have a much more complex functional form. However, as it will be shown in the subsequent Sec. 5.3.1.2 (where the bi-linear form is replaced with a quadratic one), the structural reliability is not very sensitive to the exact functional form. This is also confirmed by [164], where the structural response function of a membrane is compared to a quadratic approximation of the structural response function. Hence, it is not critical that the utilized functional forms do not exactly cover the structural response functions used in practice but only approximate their non-linear behavior.
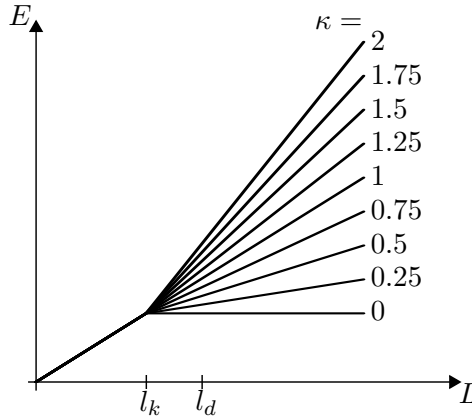

Fig. 5.5.: Bi-linear functional form of t_s of the base case for $\kappa = 0, 0.25, 0.5, \ldots, 2$.

In the base case, the material strength M follows a log-normal distribution with c.o.v.$[M] = 0.1$ and the action L follows a Gumbel distribution with c.o.v.$[L] = 0.3$.[1] The characteristic action l_k is chosen as the 98% quantile of L and the PSF of the action side γ_F is 1.5. The characteristic material strength m_k is chosen as the 5% quantile of M.

Fig. 5.6 shows the reliability indices for the base case designed following design options (1) or (2). The reliabilities are calculated via LSF of Eqn. 5.1. In the base case, both design options are conservative for $\kappa < 0$ and non-conservative for $\kappa > 0$. The approach of Eurocode 0 [25] chooses the more conservative of the two design options in both cases. For $\kappa < 0$ this would result in strong over-design and for $\kappa > 0$ in slight under-design.

Fig. 5.7 shows the limit state surfaces in standard normal space and compares the FORM design points to the design points implied by the PSF concept for different values of κ. Values of κ above 1 do not lead to strong non-linearities of the limit state surface. For values of κ below 1 the limit state surface becomes strongly non-linear.[2] The FORM

---

[1]The probability of failure is invariant to the choice of the mean values; hence, the mean values can be chosen arbitrary.

[2]Although the limit state surface looks linear in the case of $\kappa = 1$, it is slightly non-linear in standard
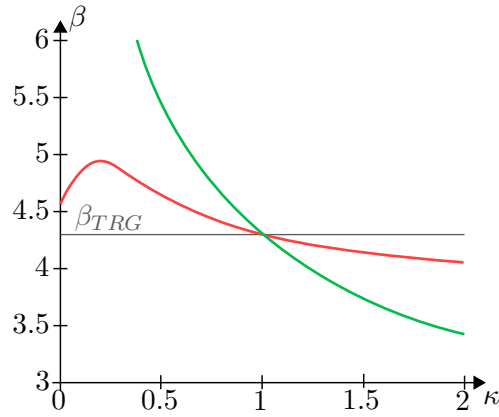
Fig. 5.6.: Reliability indices for the base case designed following design options (1) (red) or (2) (green).

design points and the design points implied by the PSF differ significantly in most cases, including the linear case. This hints at an imperfect choice of PSFs; however, PSFs are often suboptimal in specific design situations, hence, this is not unrealistic. The case of a more ideal PSF is studied below in Sec. 5.3.1.6.

5.3.1.2. Effect of the functional form of the structural response function

To investigate the effect of the structural response function, the functional form of t_S is altered from bi-linear to quadratic. Fig. 5.8 shows the resulting functions t_S for different values of κ. For $\kappa < 1$ the resulting t_S have a maximum and, therefore, drop to zero and become negative at higher load levels. If κ is only slightly below 1, the decreasing/negative part of t_S is at rather high load levels, which are too unlikely to be of interest. However, when κ becomes lower, the decreasing/negative part of t_S occurs at load levels likely enough to be of interest. These t_S might be unrealistic. However, for the sake of coherence and comparability with the bi-linear case, these cases are also covered.

Fig. 5.9 shows the resulting reliability indices. For $\kappa < 1$ both design options are more conservative than in the base case with bi-linear t_S and for $\kappa > 1$ less conservative; however, the differences are only marginal. Fig. 5.10 shows the limit state surfaces for different values of κ. The limit state surfaces are again almost linear for $\kappa > 1$ and highly non-linear for $\kappa < 1$.

Comparing Fig. 5.6 and 5.9 one can observe that the functional form of t_S seems to have little effect on the structural reliability for given κ and $e_0 = 0$. Similar can be observed for other functional forms of t_S.

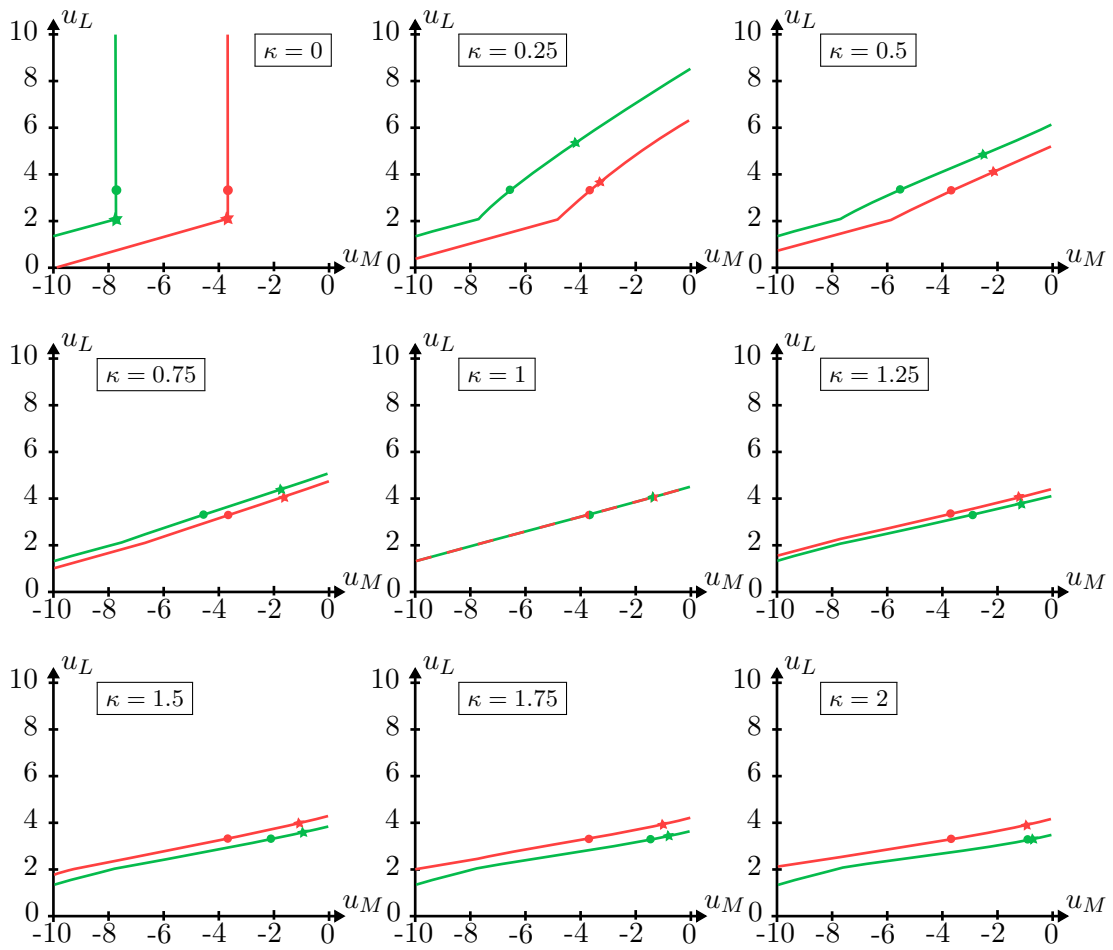normal space. In the original space, this LSF is exactly linear.

Fig. 5.7.: Limit state surfaces in standard normal space of the base case for different values of κ following design options (1) (red) or (2) (green). Stars represent the FORM design points and dots represent the design points implied by the PSF concept.
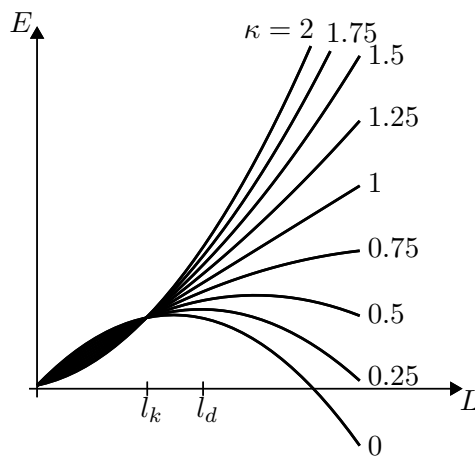

Fig. 5.8.: Quadratic functional form of t_s for $\kappa = 0, 0.25, 0.5, \ldots, 2$.
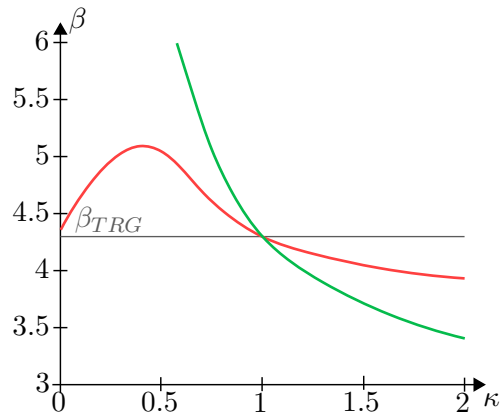
Fig. 5.9.: Reliability indices in the case of quadratic t_S following design options 1 (red) or 2 (green).
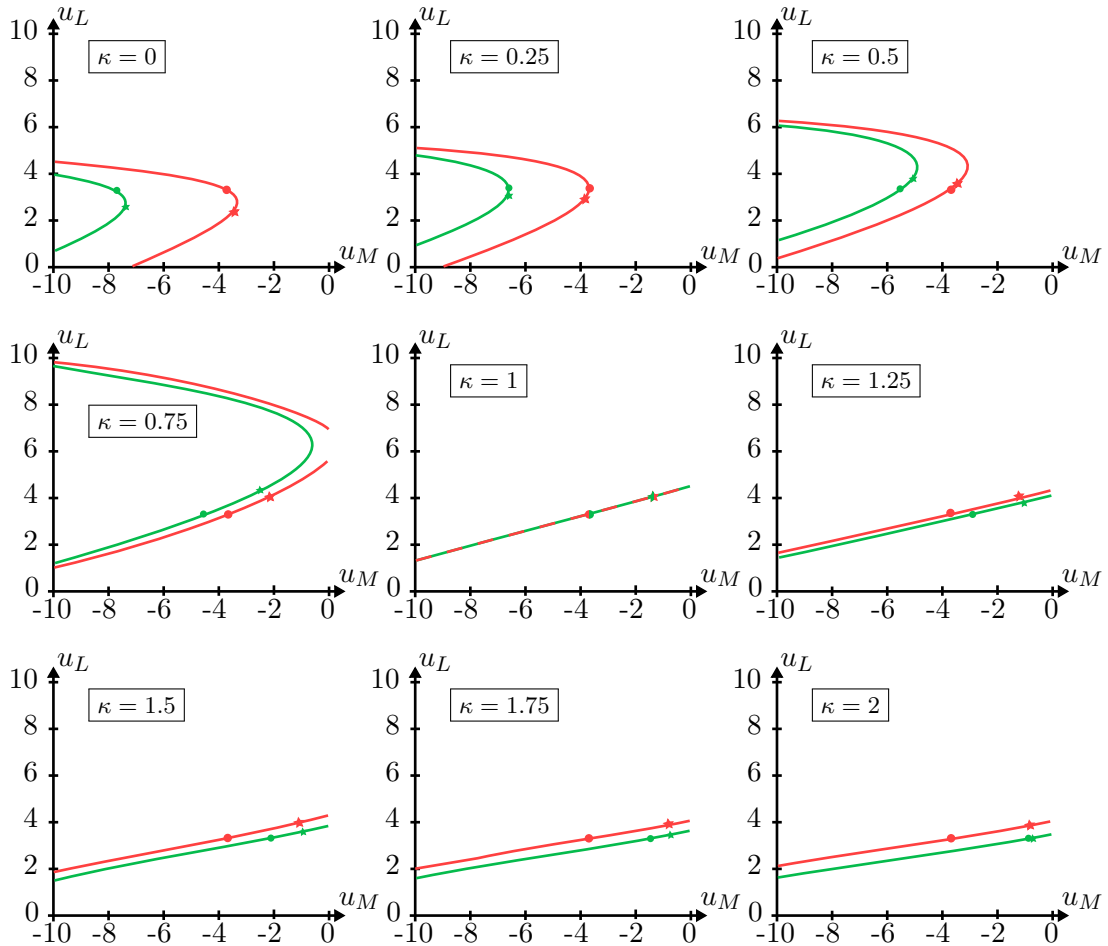

Fig. 5.10.: Limit state surfaces in standard normal space in the case of quadratic t_S for $\kappa = 0, 0.25, 0.5, \ldots, 2$ following design options 1 (red) or 2 (green). Stars represent the FORM design points and dots represent the design points implied by the PSF concept.

5.3.1.3. Effect of initial actions

To evaluate the effect of initial actions, different values of the offset measure $y_0 = 0.2, 0.4, 0.6$ or 0.8 are considered. Initial actions can, for example, be caused by prestressing. Moreover, deterministic permanent actions (e.g., dead weight) can be interpreted as initial actions. This includes permanent loads deterministically, which is in contrast to Eurocode 0 that includes permanent loads semi-probabilistically; however, since the uncertainties of permanent loads are typically small, this can be considered a good approximation.

It should be noted that the PSF γ_L is applied to the action effect when it comes to design option (2) and thus also to the initial load. In contrast, the γ_L is not applied to the initial load when it comes to design option (1).

Fig. 5.11 shows the resulting reliability indices. High values of y_0 indicate large initial actions. With increasing y_0, both design options become significantly more conservative, leading to strong over-design. The only exception occurs with design option (1) when the value of κ is rather low ($\kappa \lesssim 0.5$); however, this is only relative to the base case. In absolute terms, the resulting reliability indices are still conservative. Overall, the amount of initial actions has a significant effect on reliability. This issue is typically not covered by PSF codes (e.g., [25, 54]).
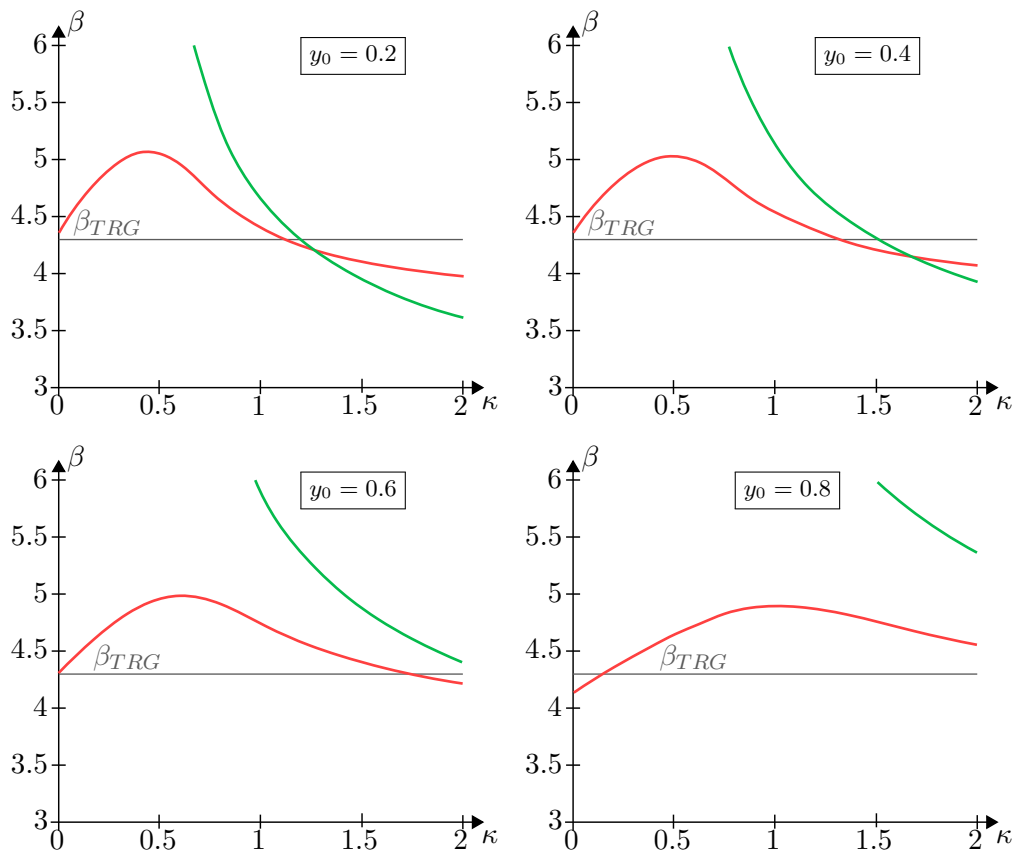

Fig. 5.11.: Reliability indices in case different y_0 following design options 1 (red) or 2 (green).

5.3.1.4. Effect of the distribution types

In this section, the distribution type of the action L and the material strength M of the base case are altered from Gumbel and log-normal to both being normal. The resulting reliability indices shown in Fig. 5.12 strongly differ from the base case. Now, design option (1) is non-conservative for $\kappa < 1$ and conservative for $\kappa > 1$. Design option (2) is still conservative for $\kappa < 1$ and non-conservative for $\kappa > 1$; however, the conservatism is significantly less than the base case for $\kappa < 1$. In this case, the approach of Eurocode 0 [25] to respectively choose the more conservative of the two design options is satisfactory.
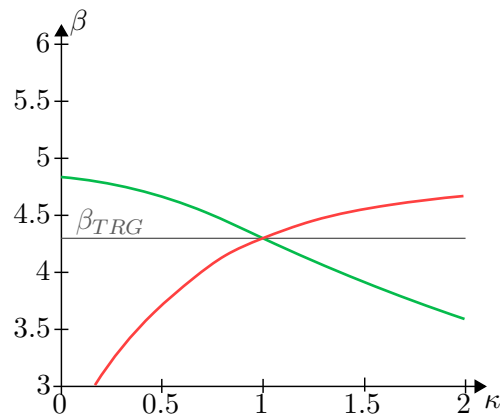

Fig. 5.12.: Reliability indices in the case of L and M being normally distributed (design options 1 (red) and 2 (green)).

5.3.1.5. Effect of the uncertainty of action and material

To investigate the uncertainty of action and material, the coefficient of variation of the action L is altered between 0.1, 0.3, and 0.5 and the coefficient of variation of the material strength M is altered between 0.05, 0.10, and 0.15. This covers the typical range of coefficients of variation of the action and resistance side [108]. The resulting reliability indices are very sensitive to these changes (see Fig. 5.13). In general, the more the design situation is dominated by the uncertainty of the action side (c. o. v.$[L] >>$ c. o. v.$[M]$), the greater the deviation from target reliability β_{TRG} is.

Especially the reliability resulting from design option (1) shows high sensitivity to the values of c. o. v.$[L]$ and c. o. v.$[M]$: The ranges of κ for which option (1) is conservative or non-conservative can switch: If the design situation is dominated by the uncertainty of the action design, option (1) is conservative for $\kappa < 1$ and non-conservative for $\kappa > 1$. With less domination of the action (e.g., graph in the left column of Fig. 5.13) this characteristic switches and design option (1) is non-conservative for $\kappa < 1$ and conservative for $\kappa > 1$.

Structural design codes typically only provide different PSF for different coefficients of variation of action and resistance but do not provide different non-linear design procedures [25, 54]. The next section shows the case if the PSF is adjusted.
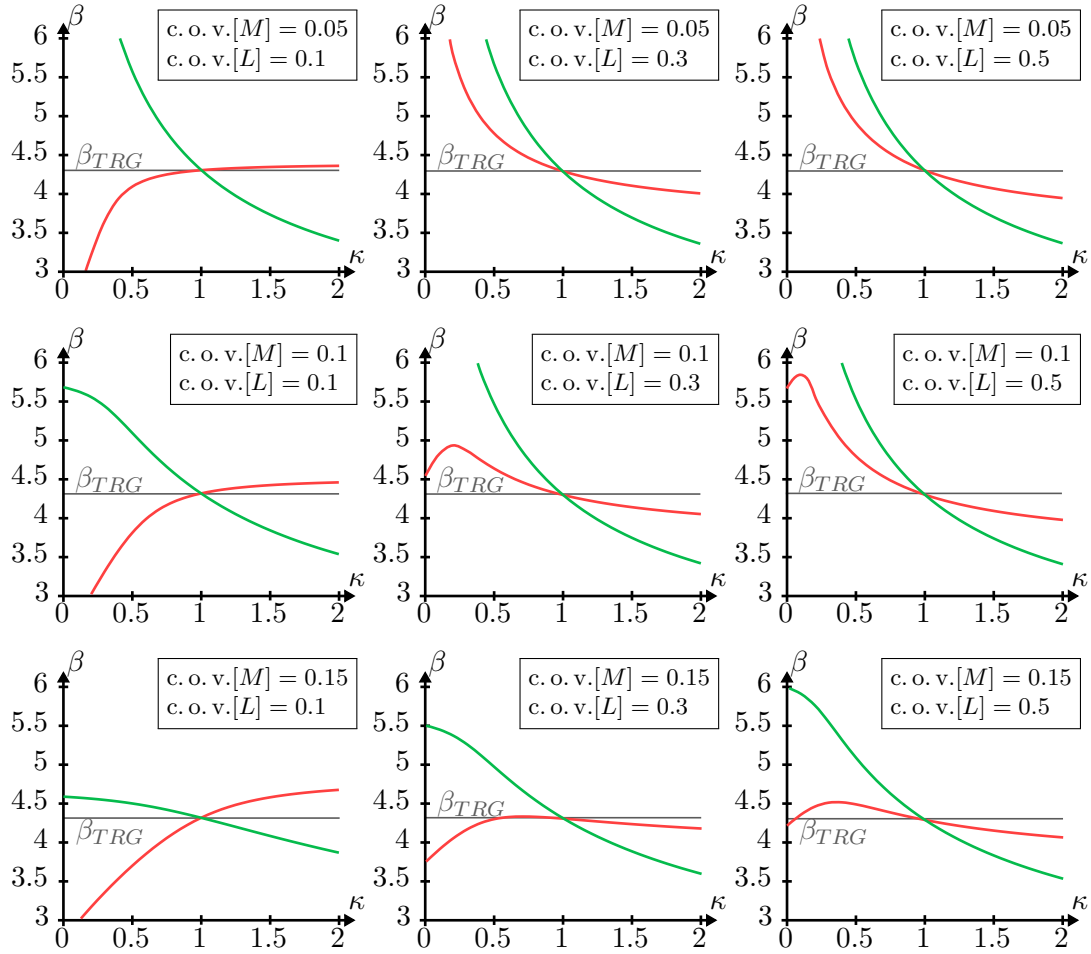
Fig. 5.13.: Reliability indices in the case of c. o. v.$[L] = 0.1, 0.2, ..., 0.5$ and c. o. v.$[M] = 0.05, 0.1, ..., 0.25$ (design options 1 (red) and 2 (green)).

5.3.1.6. Effect of the values of the partial safety factors

In this study, the values of the PSFs are altered – without changing the target reliability – such that the design point and the FORM design point coincide in the linear case; hence, the dot and the star in the middle row and middle column of Fig. 5.7 lie on top of each other. This can be interpreted as a more ideal choice of PSFs. The study is repeated for different combinations of the coefficients of variation of the action and the material strength, as in Sec. 5.3.1.5. Fig. 5.14 shows the resulting PSFs and the resulting reliability indices.

The resulting reliability indices of design option (1) differ significantly from those observed with fixed PSFs (Fig. 5.13). For $\kappa \lesssim 0.5$ design option (1) is non-conservative in all considered cases. If $\kappa \gtrsim 0.5$ the resulting reliability indices are very close to the target reliability index. This "convergence" is more rapid if c. o. v.$[L] >>$ c. o. v.$[M]$.

The resulting reliability indices of design option (2) are unaffected by the values of the PSFs compared to the case of less ideal PSFs (Fig. 5.13). This is because only the individual
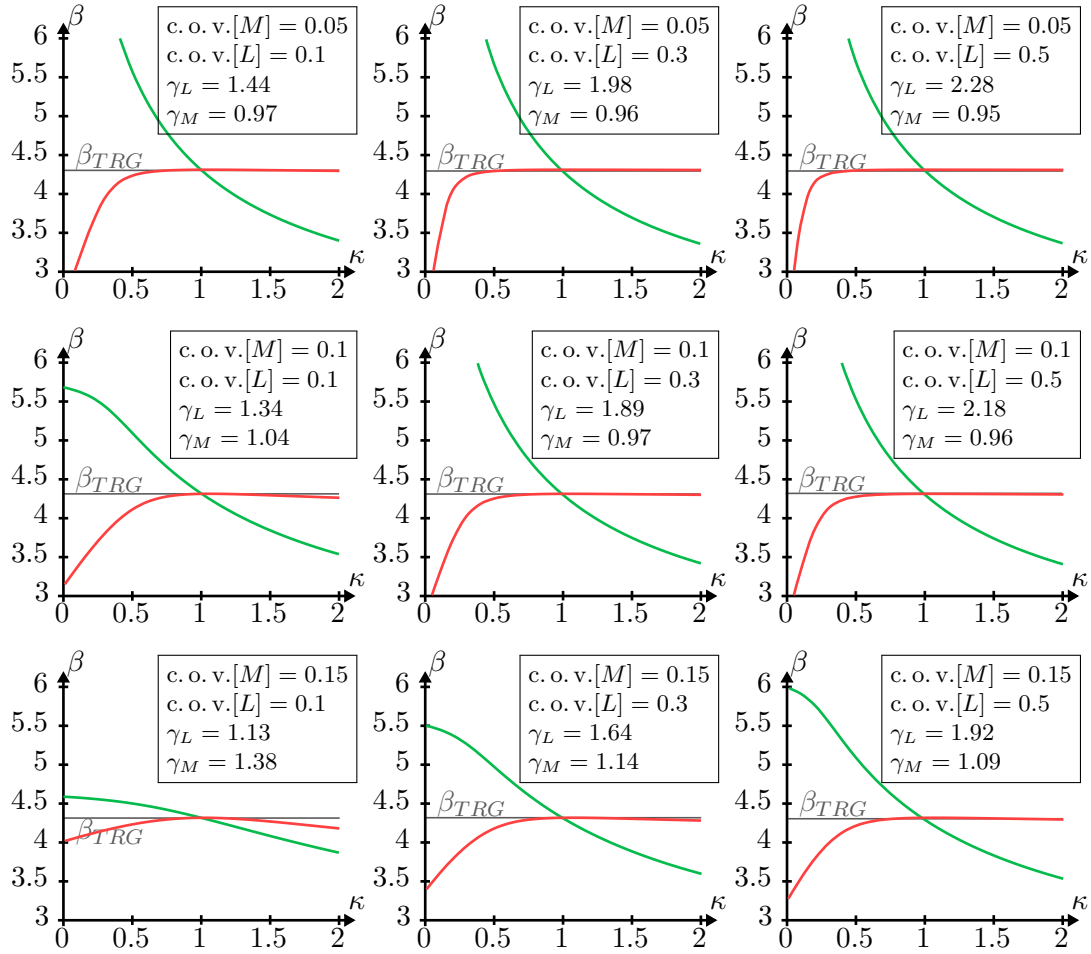
Fig. 5.14.: Reliability indices in the case of a PSF chosen such that the FORM design point and design point implied by the PSF concept coincide in the linear case (design options 1 (red) and 2 (green)).

values of γ_M and γ_L differ but not their product $\gamma_M \cdot \gamma_L$; hence, the design resulting from option (2) is unaffected.

5.3.2. Two-dimensional action case

This section investigates the two-dimensional action case. The material strength M is chosen to be log-normally distributed with $\text{COV}[M] = 0.1$ The actions L_1 and L_2 are chosen to be Gumbel distributions with $\text{COV}[L_1] = \text{COV}[L_2] = 0.3$. M, L_1 and L_2 are assumed to be independent.

Analogously to the one-dimensional action case, the characteristic actions l_{1k} and l_{2k} are defined as the 98% quantile values of L_1 and L_2, the characteristic material strength is defined as the 5% quantile of M and the PSFs associated with the actions are chosen as $\gamma_{L1} = 1.5$ and $\gamma_{L2} = 1.5$. The PSF on the material strength is chosen such that a target reliability of $\beta_{TRG} = 4.3$ is achieved in the corresponding linear LSF. The corresponding

linear LSF is defined by a t_S that is a plane spanned by two straight lines through the origin and the points $(l_{1k}, 0, t_S(l_{1k}, 0))$ and $(0, l_{2k}, t_S(0, l_{2k}))$. The offset measures and the curvature measures of this plane are $y_0 = 0$, $\kappa_1 = 1$, $\kappa_2 = 1$, and $\kappa_{12} = 1$. The values of r_1 and r_2 depend on the angle of the plane. Hence, the values of r_1 and r_2 are not only varying for different non-linear t_S but also for different linear t_S. Therefore, γ_M is chosen differently for different values of r_1 and r_2. The reason for this is that – even in the linear case – two actions applied in various ratios can lead to the same design but different structural reliabilities. This effect occurs in practice, but is filtered out in this work through the calibration of γ_M in order to isolate the non-linear effect.

A portfolio of non-linear structural response functions t_S is investigated. The portfolio is generated through various combinations of the measures of non-linearity as follows: $y_0 \in \{0, 0.2, \ldots, 0.8\}$, $\kappa_1 \in \{0, 0.25, \ldots, 2\}$, $\kappa_2 \in \{0, 0.25, \ldots, 2\}$, $\kappa_{12} \in \{0, 0.25, \ldots, 2\}$, $r_1 \in \{0.1, 0.3, \ldots, 0.9\}$, and $r_2 \in \{0.1, 0.3, \ldots, 0.9\}$. Since $r_1 < 1$ and $r_2 < 1$, only cases in which the combined action effect is greater than the individual action effect at the characteristic action level are considered; however, since κ_1 and κ_2 can be smaller than κ_{12}, the combined action effect might be lower than the individual action effect at higher action levels.

Given a combination of the measures of non-linearity, t_S is defined as a bi-linear function along each axis of action and the combined direction; hence, t_S is defined such that it forms three straight lines from $(0, 0, t_S(0, 0))$ towards the characteristic points $(l_{1k}, 0, t_S(l_{1k}, 0))$, $(0, l_{2k}, t_S(0, l_{2k}))$, and $(l_{1k}, l_{2k}, t_S(l_{1k}, l_{2k}))$, which then change direction towards $(l_{1d}, 0, t_S(l_{1d}, 0))$, $(0, l_{2d}, t_S(0, l_{2d}))$, and $(l_{1d}, l_{2d}, t_S(l_{1d}, l_{2d}))$. In between those lines t_S is linearly interpolated parallel to the non-dominating action direction. Fig. 5.15 shows possible variations of t_S.

The probability of failure of each structural response function within the considered portfolio is calculated via the LSF of Eqn. 5.2. Fig. 5.16 shows box-plots of the structural reliability indices resulting from design options (1) and (2). Moreover, it shows the structural reliability indices resulting from the maximum design values of options (1) and (2), which correspond to the design choice of Eurocode. In the majority of cases, Eurocode follows design option (2).

The smaller the range of a box-plot (i.e., ranges between maximum and minimum value or between the 25 % and 75 % quantile), the better the resulting structural reliability can be predicted via the respective measure of non-linearity. Box-plots that only marginally change with respect to varying values of a non-linearity measure indicate that the resulting structural reliability is not sensitive to this measure. This is the case for κ_1 and κ_2.

The influence of y_0, κ_1, κ_2, κ_{12}, r_1, and r_2 on the reliability index β is studied in detail via a variance-based global sensitivity analysis. The first-order Sobol indices S_i and the total order Sobol indices S_i^T are calculated as

$$S_i = \frac{\text{Var}\left[\text{E}\left[\beta | X_i = x_i\right]\right]}{\text{Var}\left[\beta\right]} \tag{5.21}$$

$$S_i^T = \frac{\text{Var}\left[\text{E}\left[\beta | \mathbf{X_{-i}} = \mathbf{x_{-i}}\right]\right]}{\text{Var}\left[\beta\right]} \tag{5.22}$$

where X_i represents one measure of non-linearity and the vector $\mathbf{X_{-i}}$ represents all but
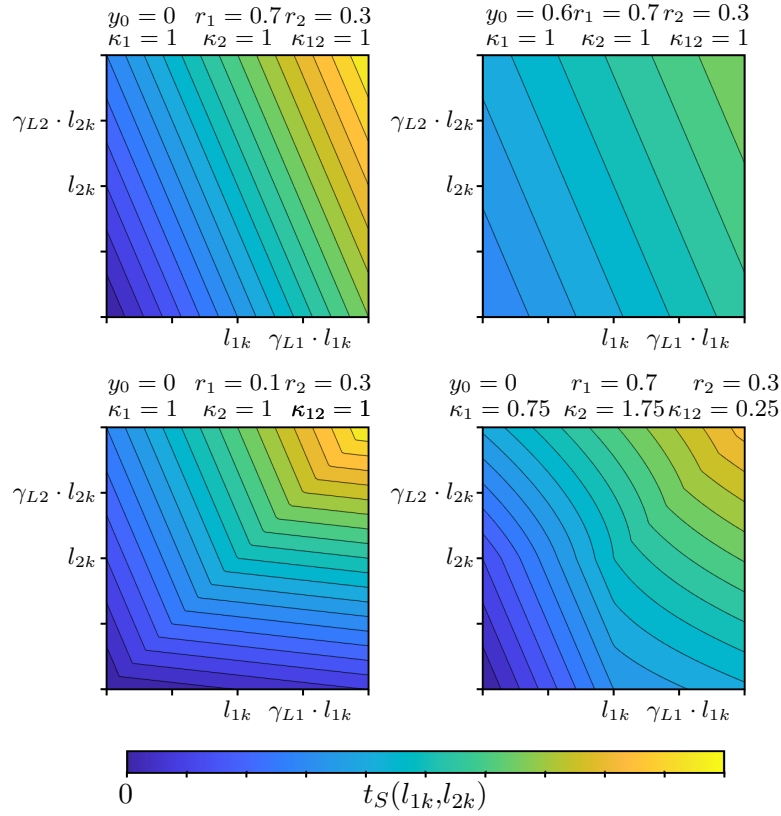
Fig. 5.15.: Measures y_0, κ_1, κ_2, κ_{12}, r_1, and r_2 to classify the non-linearity of t_S in the case of two actions.

one measure of non-linearity.

The first-order Sobol indices measure how much of the variance of the structural reliability is directly caused by each variance of the measures of non-linearity. The total-order Sobol additionally takes all variance with other measures of non-linearity into account. The resulting Sobol indices are shown in Tab. 5.1.

The first-order Sobol indices sum up to $\sum(S_i) = 0.95$ and $\sum(S_i) = 0.84$ for design options (1) and (2), respectively. In general, the first Sobol indices of independent input variables sum up to a maximum of 1. The difference $1 - \sum(S_i) = 0.05$ and $1 - \sum(S_i) = 0.16$ (for design options (1) and (2), respectively) measures the effect on structural reliability due to interactions of the measures of non-linearity. These numbers are low, indicating limited interaction. Which of the measures of non-linearity is responsible for the interaction can be understood by comparing the first-order Sobol indices to the total-order Sobol indices. This shows that r_1 and r_2 are the measures with the highest amount of interaction.

Remark: The uniform discretization of the measures of non-linearity to generate the portfolio mimics a uniform distribution of the measures of non-linearity. However, uniform distributions are certainly not a realistic assumption. The considered portfolio should therefore not be considered representative. Consequently, the box-plots shown in Fig. 5.16 are not representative. The parameter study should rather be understood as a gen-
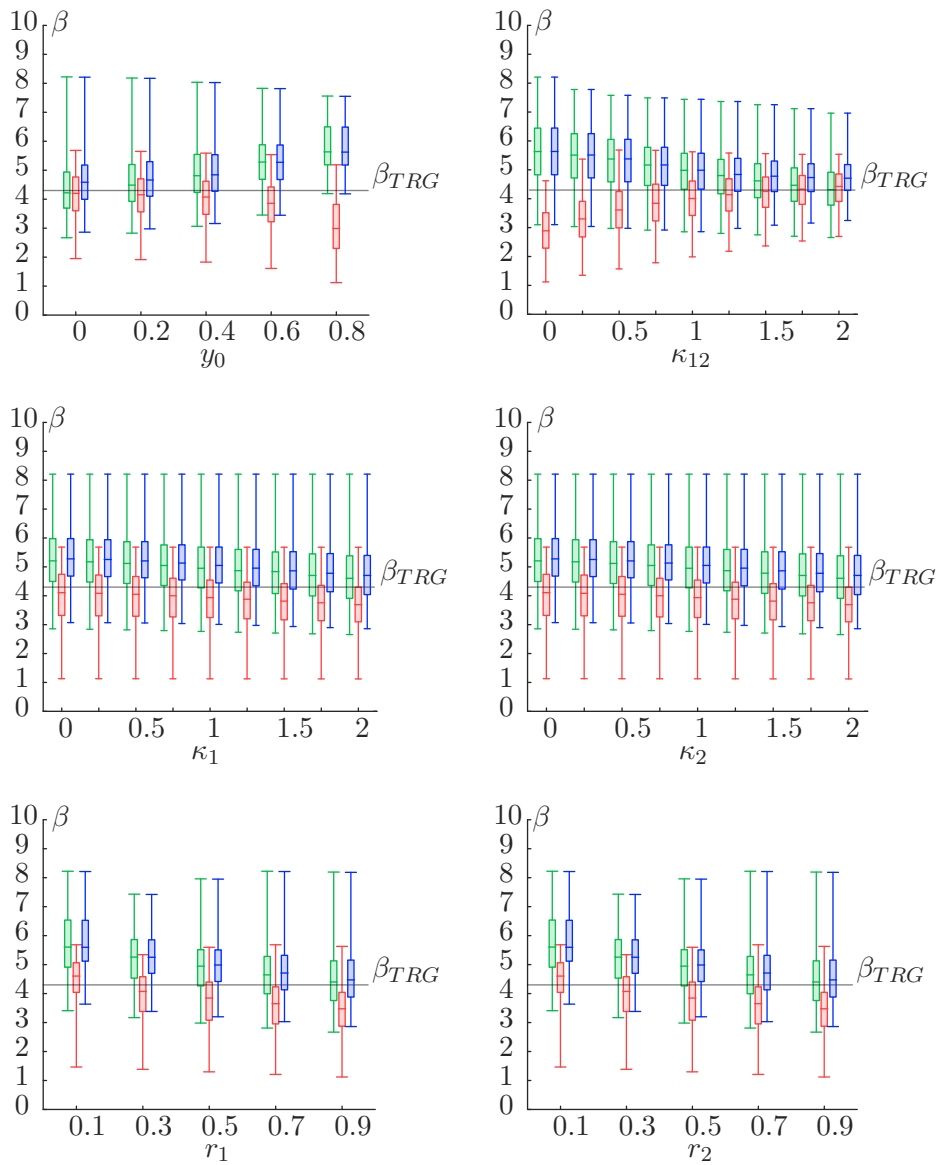
Fig. 5.16.: Box-plots of the structural reliability indices within the considered portfolio of non-linear structural response functions of design option (1) (red), design option (2) (green) and the design resulting from the maximum of design value of design option (1) or (2) (blue).

eral investigation of what can happen if non-linear structural models are used within the design.

Further remark: The two actions applied are symmetric, in the sense that they have the same mean, the same variance and the same distribution type. If the two actions would be asymmetrically, smaller Sobol indices for r_1 and r_2 are expected. Moreover, greater Sobol indices for κ_1 and smaller Sobol indices for κ_2 or vice versa are expected. The reason is the following: Changes in the ratio of the two considered action effects change the resulting structural reliability. Thereby, the structural reliability is specifically sensitive to changes of this ratio, if the ratio is close to 1. The symmetrically chosen actions lead to a ratio of 1

	i	S_i	S_i^T
Design option (1)	y_0	0.21	0.25
	κ_1	0.04	0.04
	κ_2	0.04	0.04
	κ_{12}	0.32	0.32
	r_1	0.17	0.27
	r_2	0.17	0.27
Design option (2)	y_0	0.22	0.24
	κ_1	0.06	0.10
	κ_2	0.06	0.10
	κ_{12}	0.20	0.26
	r_1	0.15	0.27
	r_2	0.15	0.27

Tab. 5.1.: First-order Sobol indices S_i and total-order Sobol indices S_i^T of the six measures of non-linearity with respect to the structural reliability.

between the actions and a ratio of 1 between the action effects considering the mean value of r_1 and r_2. Therefore, the structural reliability is sensitive to the values of r_1 and r_2. By contrast, if the ratio of the two action effects were far from 1, one of the two actions would be dominating. The action effect in the direction of the dominating action would be more sensitive to the respective κ-value.

5.3.3. Relation between the semi-probabilistic measure of non-linearity and the probabilistic measure of non-linearity

This section investigates the relation between the semi-probabilistic measure of non-linearity κ and the probabilistic measure of non-linearity in the one-dimensional action case. The offset of t_S and thus y_0 is set to 0 in this study. The study is performed for the base case of the parameter study defined in Sec. 5.3.1.1 and the quadratic case defined in Sec 5.3.1.2. The probability of failure using FORM is calculated to derive the probabilistic measure of non-linearity $\frac{\Pr(F)_{FORM}}{\Pr(F)}$. Fig. 5.17 shows the resulting values.

$\frac{\Pr(F)_{FORM}}{\Pr(F)}$ can be interpreted as a superior measure of non-linearity than the semi-probabilistic measure of non-linearity, since it includes the full probabilistic information and is formalized with respect to the probability of failure – rather than the functional form of t_S – what should be the quantity of interest. If the probabilistic measure of non-linearity and the semi-probabilistic measure of non-linearity would be equivalent (i.e. would provide the same amount of information), the graphs in Fig. 5.17 should be monotonously decreasing. This is not the case. The graphs decrease for small κ-values, then, however, become approximately constant. This indicates that κ values referring to concave non-linear behavior provide more complete information about the non-linearity effecting the probability of failure than κ values referring to convex non-linear behavior.
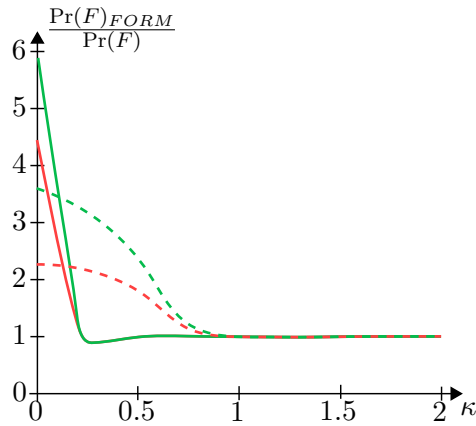
Fig. 5.17.: Values of the probabilistic measure of non-linearity $\frac{\Pr(F)_{FORM}}{\Pr(F)}$. Pulled through lines represent the bilinear case, dashed lines represent the quadratic case. Design options(1) is red and design option (2) is green.

Overall, the deviation of $\frac{\Pr(F)_{FORM}}{\Pr(F)}$ from 1 is relatively small. This indicates that FORM is still applicable in non-linear design, although it is based on a linearization of the limit state surface.

5.4. Example structures

This section applies the newly developed measure of non-linearity to two example structures: A dome space truss structure and a membrane structure. Both examples were developed in close collaboration with Martin Fußeder, who deserves a large part of the credit. Only the core aspects of both examples are given in this thesis. A detailed examination of the example structures can be found in [164] and [165].

5.4.1. 24-bar dome space truss structure

Dome-like space truss structures are regularly utilized as examples for investigations in the presence of geometrical non-linearity. The observed 24-bar dome truss (cf. Fig. 5.18) is a slightly modified version of the structure proposed in [175]. Most of the trusses (indicated as "truss 1" (solid lines) and "truss 3" (dashed-dotted lines) in Fig. 5.18) are tensioned and instability of the overall structure can be avoided. It is assumed that local buckling of the compressed members (indicated as "truss 2" (dashed lines) in Fig. 5.18) is prevented constructively.

For the ultimate limit state design, the situation is considered in which the maximal stress in the trusses exceeds the yield strength. Steel S355 with a characteristic yield strength of f_y=355 MPa is chosen. The action L is chosen to follow a Gumbel distribution with $\mathrm{E}[L] = 0.0375$ MN and c. o. v.$[L] = 0.3$. The yield strength M is chosen to follow a log-normal distribution with $\mathrm{E}[M] = 412.8$ MPa and c. o. v.$[M] = 0.07$ [108].
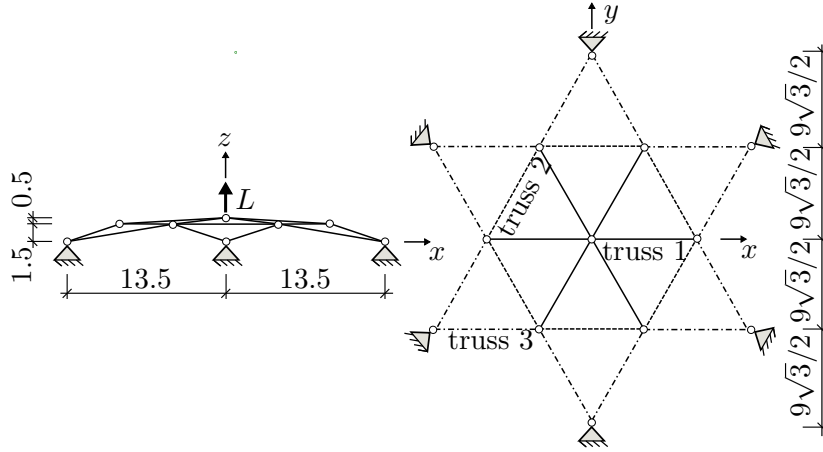
Fig. 5.18.: Observed 24-bar dome space truss structure shown in side view (left) and top view (right) with action L acting on the center node. The solid, dashed and dashed-dotted lines indicate the three different truss types. The dimensions are given in meters.

5.4.1.1. Partial safety factor design

The design choices follow the rules of Eurocode [25,176]. The PSF of the action is $\gamma_F = 1.5$ and the PSF of resistance is $\gamma_{M0} = 1.0$. The characteristic values are chosen based on [61] as $l_k = F_L^{-1}(0.98) = 0.0667$ MN and $m_k = f_y = E[M] - 2 \cdot \sigma_M = 355.0$ MPa with σ_M being the standard deviation of M.

Due to the symmetry of the structure and loading, only the cross-section of three trusses must be designed, which are indicated as "truss 1-3" in Fig. 5.18. Based on the two design options of Eqns. 5.7 and 5.8, the PSF design choices are

$$\text{Desing option (1):} \qquad A_i = \frac{\gamma_{M0} \cdot N_{truss\ i}\left(\gamma_F \cdot l_k, \mathbf{A}\right)}{f_y} \qquad (5.23)$$

$$\text{Desing option (2):} \qquad A_i = \frac{\gamma_{M0} \cdot \gamma_F \cdot N_{truss\ i}\left(l_k, \mathbf{A}\right)}{f_y} \qquad (5.24)$$

where $\mathbf{A} = [A_1, A_2, A_3]$ are the cross-sections of the respective trusses and $N_{truss\ i}$ is the normal force of the ith truss. For the structure at hand, the PSF design based on option (2) leads to larger absolute values of the normal forces for each truss.

5.4.1.2. Measure of non-linearity and classification in parameter study

Fig. 5.19 shows the action-effect of action diagrams. The non-linearity of each $N_{truss\ i}$ is measured via the curvature measure κ. Tab. 5.2 summarizes the values κ. The values of κ are slightly different when design options (1) or (2) are utilized.

The classification of the truss dome structure within the general parameter study is not
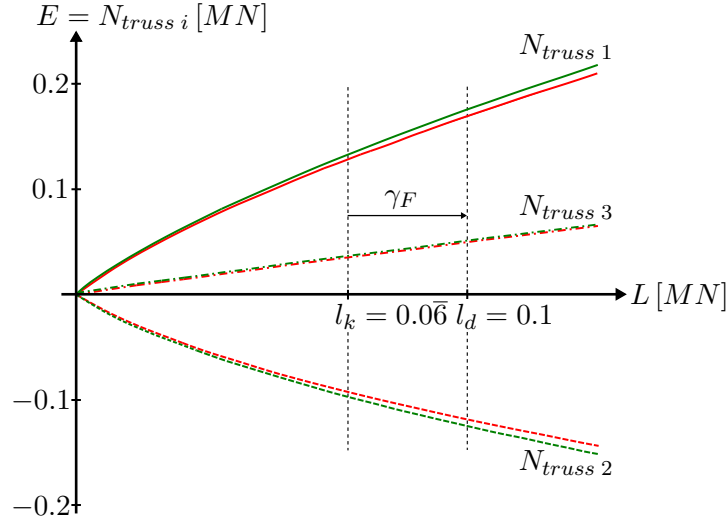
Fig. 5.19.: Action-effect of action diagrams of the truss dome normal forces $N_{truss\,i}$ (cf. Fig. 5.18). The red lines correspond to the design based on PSF option (1) and the green lines are according to design option (2).

| | κ | | |
Design option	truss 1	truss 2	truss 3
(1)	0.727	0.637	0.965
(2)	0.734	0.651	0.964

Tab. 5.2.: κ-values for the three observed truss members designed according to PSF options (1) and (2).

straightforward, since the parameter study of Sec. 5.3 only covers a finite set of possible structural designs. For the structure at hand, the following conditions differ from those in the parameter study: The PSF γ_{M0} was taken from the standard and was not specifically computed to achieve a target value for the linear case. The truss dome is therefore not at the same reliability level as the parameter study. Moreover, the characteristic material strength, the functions $N_{truss\,i}$ and the coefficient of variation of the material strength are not exactly covered by the parameter study.

The case of the parameter study that comes closest to the truss dome example is the case of bi-linear t_S with log-normally distributed M with c. o. v.$[M] = 0.05$ and Gumbel distributed L with c. o. v.$[L] = 0.3$ shown in Fig. 5.13 in the first row and the second column. The Fig. shows that both design options are conservative for $\kappa < 1$ compared to the linear case; hence, the parameter study suggests that all three trusses are conservative compared to the linear case. This is verified in the reliability analysis of the next Sec. 5.4.1.3.

Moreover, the probabilistic measure of non-linearity $\frac{\Pr(F)_{FORM}}{\Pr(F)}$ is calculated and listed in Tab. 5.3.

Design option	$\dfrac{\Pr(F)_{FORM}}{\Pr(F)}$		
	truss 1	truss 2	truss 3
(1)	1.013	1.019	1.008
(2)	1.016	1.025	1.008

Tab. 5.3.: FORM and analytic probability of failure ratios for the three observed truss members designed according to PSF options (1) and (2).

5.4.1.3. Reliability Analysis

Based on the cross-sections A_i (Eqns. 5.23 and 5.24), the LSF for the ith structural member can be formulated following Eqn. 5.1:

$$g_i = A_i \cdot M - N_{truss\,i}(L) = \begin{cases} \frac{\gamma_{M0} \cdot N_{truss\,i}(\gamma_F \cdot l_k)}{f_y} \cdot M - N_{truss\,i}(L) & \text{option (1)} \\ \frac{\gamma_{M0} \cdot \gamma_F \cdot N_{truss\,i}(l_k)}{f_y} \cdot M - N_{truss\,i}(L) & \text{option (2)} \end{cases} \quad (5.25)$$

Tab. 5.4 shows the resulting reliability indices. The difference between design options (1) and (2) is larger when the curvature measure κ differs from 1. This can be seen in particular by comparing the results of trusses 2 and 3. Furthermore, the reliability indices based on designs determined with PSF option (1) show less sensitivity to a varying degree of non-linearity than the designs according to option (2).

Design option	truss 1	truss 2	truss 3
(1)	3.79	3.83	3.72
(2)	4.18	4.40	3.76

Tab. 5.4.: Reliability indices β for the three observed truss members designed according to PSF options (1) and (2).

The limit state surface in standard normal space of both design options, together with the design points implied by the PSF concept and the FORM design points, are shown in Fig. 5.20. It can be seen that the difference between the limit state surfaces based on the two design options is higher the more κ differs from 1. Fig. 5.20 indicates also that all limit state surfaces are only marginally non-linear in standard normal space, despite the low κ values for trusses 1 and 2.

To verify the classification within the general parameter study (see Sec 5.4.1.2), the reliability analysis is repeated with the hypothetical case of linear functions for the normal forces. The resultant reliability index is 3.70 for all trusses. Since 3.70 is below all values of Tab. 5.4, the classification as a conservative design by the parameter study is confirmed.
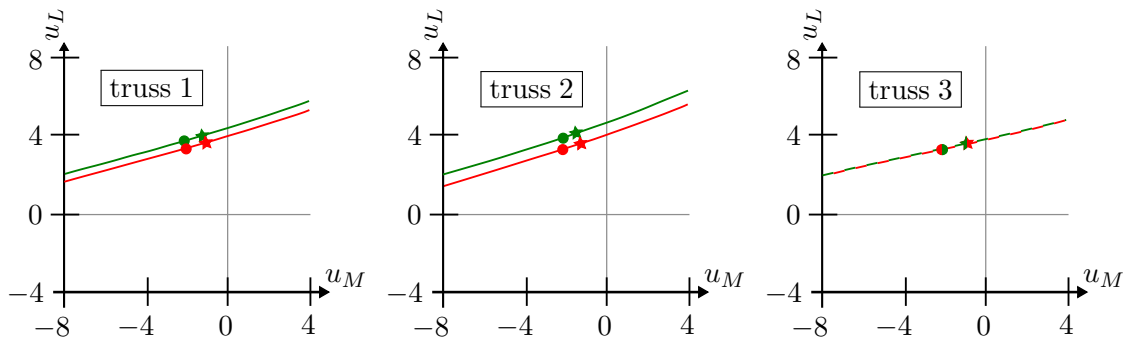
Fig. 5.20.: Limit state surface of the truss members 1-3 (cf. Fig. 5.18) designed following options (1) (red) and (2) (green) in standard normal space. The bullet points indicate the design points implied by the PSF concept. The stars indicate the FORM design points.

5.4.2. Membrane structure

The investigated membrane structure is a hyperbolic paraboloid, which is shown in Figure 5.21. It is a slightly modified version of the hypar presented in the Round Robin Exercise 4 of [177]. The structure has a base area of 6×6 [m] and a height of 2 [m] (cf. coordinates of edge points in Fig. 5.21) and is subjected to a snow load, which is acting in the negative z-direction. The membrane and its edge cables are fixed at the low and high points. The Young's moduli in warp and fill direction are $E_{warp/fill} = 600$ [kN/m] (pre-integrated over the thickness), the shear modulus is $G =$ [kN/m] (pre-integrated over the thickness) and the Poisson's ratio is $\nu = 0.4$. The edge cables have a Young's modulus of 205 [kN/mm^2] and a diameter of 12 [mm]. The membrane is subjected to an isotropic pre-stress of 3.0 [kN/m] and the edge cables are pre-stressed by 30 [kN].
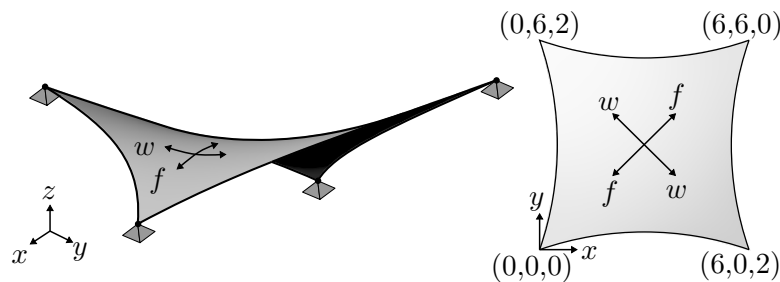

Fig. 5.21.: Observed membrane structure with indication of warp (w) and fill (f) direction.

The snow load L is chosen to follow a Gumbel distribution with mean $E[L] = 0.34$ [kN/m^2] and c. o. v.$[L] = 0.3$. The tensile strength M are chosen to follow a log-normal distribution with mean $E[M] = 1.0$ [kN/m^2] and c. o. v.$[M] = 0.1$.

5.4.2.1. Partial safety factor design

The design choices follow the rules of Eurocode [25] and the Technical Specification of CEN TC250 WG5 [178]. The PSFs of the The characteristic values are defined following [61] as the 98 [%] and 5 [%] fractile: $l_k = F_L^{-1}(0.98) = 0.60$ [kN/m²] and $m_k = F_M^{-1}(0.05) = 0.84$ [kN/m²].

For the ultimate limit state design, the situation is considered in which the maximal stress exceeds the tensile strength of the membrane. Because the snow load is acting in the negative z-direction on the membrane, the decisive stress is appearing in the warp direction. The progress of the maximal stress in warp direction for an increasing snow load is shown on the left-hand side of Fig. 5.22 (blue line). On the right-hand side of Fig. 5.22 the stress distribution in the warp direction due to design action $l_d = \gamma_F \cdot l_k$ and the position of the maximal stress is shown. It can be seen that the membrane is fully under tension at this stage, i.e., no wrinkling occurs. The final design choices directly follow from Eqns. 5.7 and 5.8.
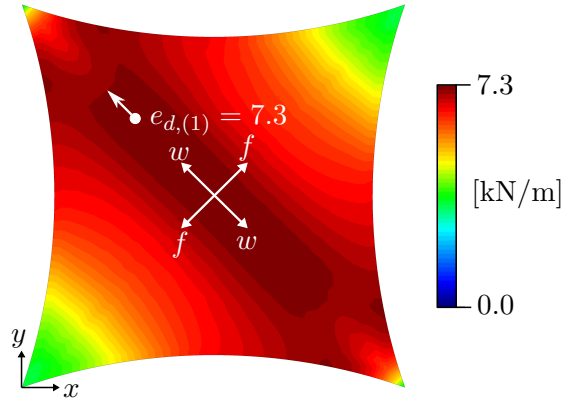

Fig. 5.22.: Left: Progress of maximal stress in the warp direction of the membrane due to increasing action (blue), its tangent at zero action (dashed). Right: Distribution of stress in the warp direction due to design action l_d.

5.4.2.2. Measure of non-linearity and classification in parameter study

The top left illustration in Fig. 5.23 shows the action-effect of action relationship of the membrane. The offset and the curvature measure of the membrane are $y_0 = 0.53$ and $\kappa = 1.19$.

Similar to the truss dome example of Sec 5.4.1, the membrane cannot be exactly classified in the parameter study shown in Sec 5.3. The case of the parameter study that is closest to the membrane example is the case of bi-linear t_S, log-normally distributed M with c. o. v.[M] = 0.1, Gumbel distributed L with c. o. v.[L] = 0.3, and an initial action of $y_0 = 0.6$, shown in Fig. 5.11 (bottom left). For the value of κ of the original membrane of
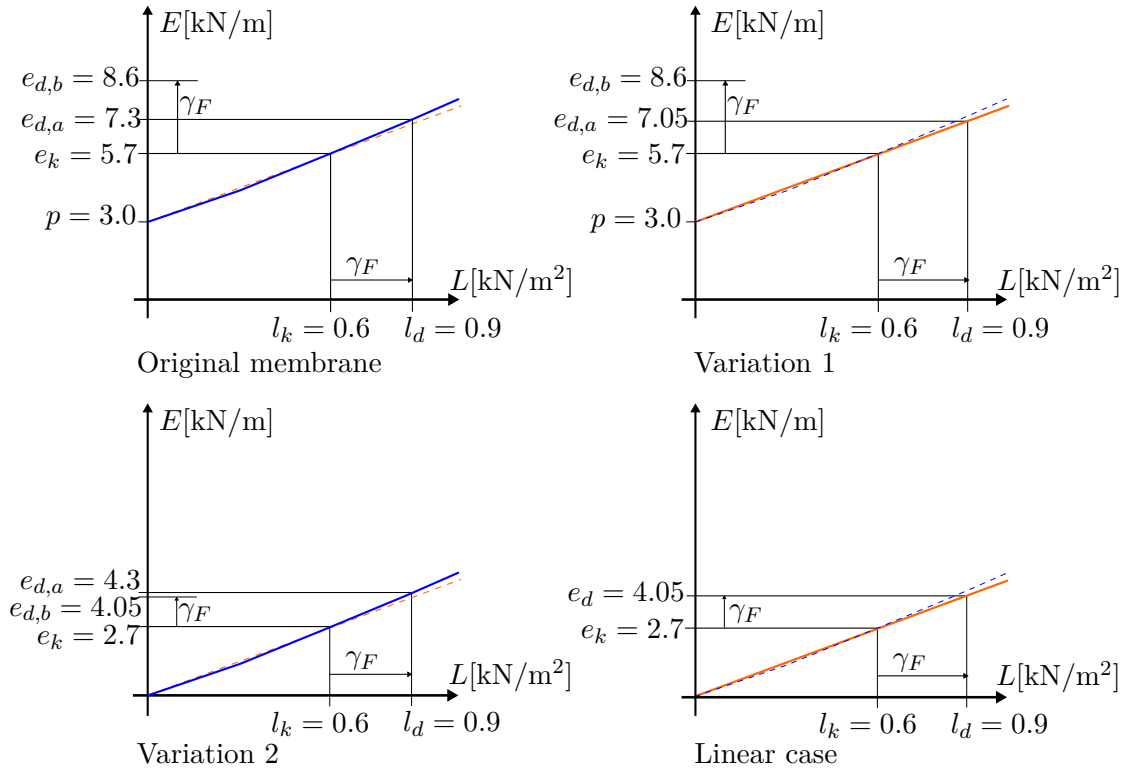
Fig. 5.23.: Observed options of linear (orange) and non-linear (blue) action - effect of action relations with and without pre-stress p.

1.19, this figure suggests that both design options are conservative compared to the linear case (variation 3).

To evaluate the effects of the two non-linearities (offset and curvature) separately, two more hypothetical cases are considered: In the first case, κ is set to 1 and y_0 remains as in the original membrane (variation 1 in Fig. 5.23). By comparing this case with the original case, the non-linear effect of the convex form of t_S is isolated. The classification within the general parameter study can be made within Fig. 5.11 (bottom left). The reliability indices of both design options decrease from $\kappa = 1$ to $\kappa = 1.19$, therefore, the parameter study suggests that both design options of the original structure are non-conservative compared to this hypothetical case. In conclusion, the convex form of t_S has a negative effect on reliability.

Second, the hypothetical case is investigated where κ remains the same as in the original structure but y_0 is set to 0 (variation 2 in Fig. 5.23). By comparing this case with the original case, the non-linear effect of the prestress can be isolated. The comparison can be done by comparing Fig. 5.11 (bottom left) to the base case (Fig. 5.6). This shows that both design options for the original structure are conservative compared to this hypothetical case. In conclusion, the prestress has a positive effect on reliability.

Overall, the positive effect of the prestress is greater than the negative effect of the convex form of t_S, since the comparison to the linear case showed an overall positive effect of the

non-linearity.

Finally, the probabilistic measure of non-linearity of the original membrane is calculated to be $\frac{\Pr(F)_{FORM}}{\Pr(F)} = 1.026$ for design option (1) and $\frac{\Pr(F)_{FORM}}{\Pr(F)} = 1.044$ for design option (2).

5.4.2.3. Reliability analysis

The LSF is again formalized following Eqn. 5.1. Tab. 5.5 shows the resulting reliability indices of the original membrane, its two variations and the corresponding linear case. This confirms the positive effect of the prestress and the negative effect of the convex form of t_S suggested by the parameter study. The limit state surface in the standard normal space of both design options and the design points according to the PSF concept and FORM of the original membrane, its two variations and the corresponding linear case are shown in Fig. 5.24.

Design option	Original membrane	Variation 1	Variation 2	Linear case
(1)	4.96	5.30	4.46	4.72
(2)	5.56	6.20	4.26	4.72

Tab. 5.5.: Reliability indices of the original membrane, its two variations and the corresponding linear case according to design options (1) and (2).
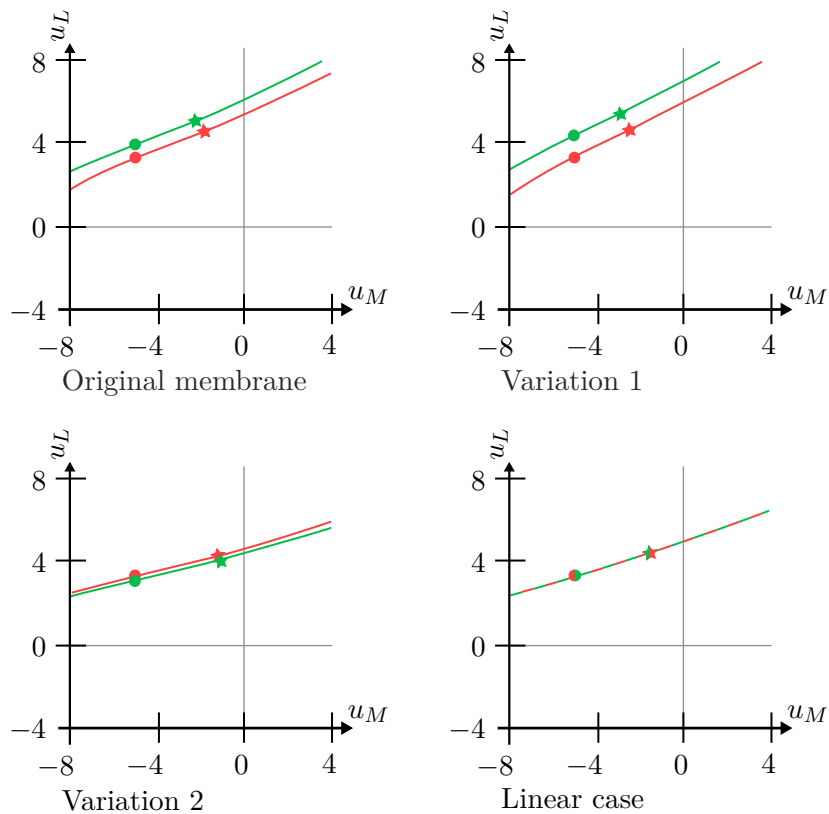
Fig. 5.24.: Limit state surface of the membrane designed with options (1) (red) and (2) (green) in standard normal space of the original membrane, its two variations and the corresponding linear case. The bullet points indicate the design points following the PSF concept. The stars indicate the FORM design points.

5.5. Discussion

As mentioned in Sec. 5.1, Eurocode chooses the more conservative alternative from design options (1) and (2) which, obviously, leads to greater structural reliability. This signifies that in Figs. 5.6, 5.9, 5.11, 5.12, 5.13 and 5.14 the design corresponding to the upper of the two curves is chosen. If this upper curve is below/above the linear reference reliability index β_{TRG} it is unsafe/safe but has low/high resource consumption.[3]

The question to be disused is how the introduced measure of non-linearity could be included in the PSF concept in order to homogenize the level of safety with respect to non-linearities. The determination of the measure does not complicate the designing process by much, since these values can be calculated as a side product of a PSF design. The values could provide guidance to the engineer in order to classify a design without the need of a reliability analysis. An engineer could classify its structure within the parameter study (see Sec. 5.3) and determine if the design is on the safe side or not, as it is

---

[3]In some design situations, this reliability index at the linear level inherently may be too high or too low; however, the reason for this is not related to the non-linearity of the structural response function but to something different (e.g., suboptimal PSFs) that should be considered separately.

done for the investigated example structures (see Sec. 5.4.1.2 and 5.4.2.2). However, such a classification is not straightforward and requires a deeper understanding of the issue. Alternatively, the measure could be used to modify design rules within the framework of the PSF concept. Simple design guidelines could be provided that do not require any understanding of the issue. Three possible adaptation approaches to provide such guidance are:

- The rule for choosing design option (1) or (2) could be based on ranges of values of y_0 and κ (in the one-dimensional action case) or κ_{12} (in the two-dimensional action case). In the two-dimensional case, κ_1, κ_2, r_1, and r_2 maybe also included; however, for the sake of simplicity, those parts of the two-dimensional measure could be ignored as those are of less significance (see sensitivity analysis of Sec. 5.3.2). Analogously, this approach could be transferred to the n-dimensional case, i.e., only the offset measure and the curvature measure in the direction of all actions combined could be used. In contrast to the current policy, the design option that leads to a smaller design value should also be valid in some cases. In particular, design option (1) can also be preferable for cases of $\kappa < 1$ or $\kappa_{12} < 1$. This could avoid drastic overdesign. Additionally, in extreme ranges of the measure, further analysis or even a full probabilistic analysis could be recommended or required.

- An additional PSF could be implemented. The value of the PSF could – analogously to the above approach – depend on the offset measure and the curvature measure in the direction of all actions combined. The more case-specific this additional PSF is (the smaller the respective ranges of offset measure and the curvature measure are), the better the homogenization of the reliability level will be.

- A split of the PSF with respect to the uncertainty of the action and the uncertainty of the structural response function could be conducted. This would reverse the merge of Eqn. 2.6 and values of γ_f and γ_{Sd} could be determined individually.

In general, the non-linearity of a structure cannot be quantified at system-level, but only the non-linearity of an action - effect of action relation corresponding to a certain limit state can be quantified. Hence, separate values of the measure need to be determined for each limit state. Therefore, each of the above adaptation approaches needs to be applied to each limit state of a structure separately.

All three adaptation approaches would homogenize the reliability level such that it would be closer to β_{TRG}. Moreover, all three adaptations would only depend on the values of the measure of non-linearity. As mentioned, this has the advantage of making the adaptations straightforward to apply within the PSF concept. A disadvantage is that the measure only describes the non-linearity of the structural response function directly and not the interaction of non-linear structural response functions with (semi)-probabilistic properties. However, those interactions have a great impact on the reliability, as shown in the parameter studies in Sec.5.3. Hence, all three approaches would only party homogenize the PSF-concept when it comes to non-linear effects. This, however, would still be a step in the right direction. A step much further in the right direction seems to be unrealistic within the PSF concept since the interaction of non-linear structural response functions with (semi)-probabilistic properties need to be included probabilistically.

5.6. Conclusion

This section systematically investigated the effects of non-linear structural response functions on the structural reliability of codified design structures. The conducted parameter studies and the two application examples reveal some of the effects. It is shown that not only the degree of non-linearity of the structural response function but also the interaction of non-linear structural response functions with (semi)-probabilistic properties has a strong effect on the structural reliability. For this reason, it is impossible to homogenize the safety level perfectly with respect to non-linear models without leaving the scope of the PSF concept. However, there is some potential to homogenize the safety level. This seems to be especially necessary in case of strongly concave structural response functions or in cases of large initial force (e.g., prestress), which both can lead to heavy overdesign. Cases of underdesign are possible if the structural response function is convex; however, the under-design appears to be acceptable in most cases.

6. Conclusion and Outlook

In this thesis, three possible adaptations of the PSF concept are analyzed (Sec. 3-5). Each section includes detailed discussions and conclusions. In this section, the most important points will be summarized and assessed in a broader context. Moreover, an outlook for each adaptation is formalized.

- The first proposed adaptation is an explicit inclusion of the effects of hidden safeties in the PSF concept (Sec. 3). Hidden safeties may be part of standard models of existing codes. These hidden safeties can remain hidden from the user, as they should already be taken into account by code-developers when calibrating the respective safety components. However, if standard models get replaced by other (potentially more advanced) models, hidden safeties need to be explicitly included via a recalibration of the respective safety components. Sec. 3 provides a framework for such a recalibration. The recalibration ensures that the average reliability of structures designed using the standard model or the replacement model is the same. The potential for higher accuracy (reduction of epistemic uncertainty) gets translated into higher material efficiency. In addition, the reliability will be more homogenous at the portfolio level.

  There is a rapid development of new models for structural design. Reasons for this include the rapid increase in computational performance, advancements in numerical methods, the development of new simulation techniques and the development of building materials or construction methods. The bureaucratic process of incorporating these new models into existing codes can often be lengthy. Therefore, the advancement of structural design codes is lagging behind the rapid development of new models. This gap could be closed by the proposed framework which gives developers/users of new models the opportunity to integrate these models themselves. This may be unpleasant for code committees, as it reduces their authority. However, strict and well-defined rules for the application of the proposed framework could hopefully dispel many of their concerns.

  Outlook: In terms of methodology, the proposed framework does not require further development. Instead, future investigations could/should be conducted on the effects of the proposed framework on both structural reliability and material consumption. This could be done either through further application examples (similar to those in section 3.3 and 3.4) or – more generally – through an analysis from a portfolio perspective. Such a portfolio analysis could estimate the total amount of material saving potential and the overall potential in homogenizing the level of safety. However, this would require not only a representative portfolio of limit states, but also a representative portfolio of model uncertainties of the respective standard and advanced models. Another possible task for the future could be the development of a

step-by-step guide for practical engineers who are not experts in this field.

- The second proposed adaptation is an extension of the PSF concept to the system level. For this purpose, a link between general structural systems and a generalized version of the Daniels system has been established. The generalization covers probabilistic load-modeling, material modeling, modeling of correlation among members and various load sharing properties. For each generalization, effective algorithms for calculating the system reliability have been developed and detailed numerical studies have been carried out. The results of these studies can be transferred to general structural systems by utilizing the link between general structural systems and the generalized Daniels system and, thus, can provide insight into system effects when designing new structures. Moreover, the generalized Daniels system is used to determine the values of an additional PSF, which increases the resistance of structures with low system reliability and decreases the resistances of structures with high system reliability. This does not only homogenize reliability at the portfolio level but also increases material efficiency.

The studies conducted on the Daniel system do provide insights that contribute to a better understanding of system effects. Moreover, the derived additional PSF reveals some potential in improving the PSF concept. However, this potential seem to be rather small in most cases. This suggests that the state of the art (structural design on element level) is mostly satisfactory and only extreme cases of system behavior require special treatment. However, the derivation of the additional PSF is based on numerous simplifications and assumptions; hence, the results should be interpreted carefully. In case of an actual implementation of the additional PSF within a code, various details would have to be improved.

Outlook: The author identifies three potential steps for further research. First of all, the generalizations of the Daniels system could be improved to include non-equal correlation between members and to include more advanced/mixed material models. These improvements go hand in hand with the second potential future step: A more accurate derivation of an additional PSF. Both, the generalization of correlation and the generalization of material models could improve the derived additional PSF. However, not only enhancements in the generalization of the Daniels system itself but also enhancements in the mirroring of general structural systems trough the generalized Daniels system are possible. It is shown that general structural systems are equivalent to a series system of generalized Daniels systems, however, this equivalence is not fully exploited due to necessary simplifications (see Sec. 4.5). The most critical of these assumptions is that actions are evenly distributed among elements and evenly redistribute in case of element failure. This simplification could be removed and non-proportional load sharing in all damage states of the structure could be taken into account (e.g., trough a modification of the Daniels system as shown in Fig. 4.19). However, this would require a representative portfolio of the load-sharing properties of structural systems, which cannot be easily formalized. A third potential future step would be the quantification of the resource saving potential and of the potential homogenization of the level of safety. This would again require a representative portfolio of the load-sharing properties of structural systems.

- The third proposed adaptation addresses the difficulties arising from non-linear structural models in the context of the PSF concept. Two design variations are examined in detail: The application of a PFS directly to the action or the application of the PSF to the action effect. The investigations are based on a newly developed measure of non-linearity, which may also be applicable within the PSF concept. The investigations show that not only the degree of non-linearity of the structural response function but also the interaction of non-linear structural response functions with (semi)-probabilistic properties has a strong effect on the structural reliability. For this reason, a homogenization of reliability at the portfolio level can only partly be reached without leaving the framework of the PSF concept. However, there is some potential for improvement within the framework of the PSF concept. This seems to be especially necessary in cases of strongly concave structural response functions or in cases of large initial forces (e.g., prestress), which both can lead to heavy over-design. Cases of under-design are possible if the structural response function is convex; however, the under-design appears to be acceptable in most cases.

  No specific proposal for an adjustment of the PSF concept has been worked out in detail when it comes to non-linear structural response functions. However, three adaptation ideas are indicated (the introduction of non-linearity thresholds, the introduction of an additional PSF and the split of the existing PSF into two PSFs applied to the action and the action effect, respectively). It appears that all three of these ideas have potential to homogenize reliability at the portfolio level and, thereby, increase material efficiency.

  Outlook: The next step would/should be the detailed elaboration of the three adaptation ideas mentioned above. However, the calibration of these adaptation ideas would require the formulation of a portfolio of limit states that is representative, especially with respect to non-linearities. The formulation of such a portfolio would require an extension of the previous methodology to multidimensional cases (so far only the one- and two-dimensional case is covered). Finally, the various adaptation ideas can be compared with each other by considering their respective effect in terms of resource savings potential and homogenization of the safety level at portfolio level.

Overall, the studies on hidden safeties, system reliability and non-linear structural response functions aim – among other goals – at an increase in material efficiency. As stated in the introduction, the efficient use of materials is one of the most challenging tasks of our generation. This task should be tackled as soon as possible (and probably should have been tackled earlier in the past). If we do find solutions soon, the reality of finite building materials will soon catch up and force us to do so [2–8]. A solution under forced circumstances will most likely be suboptimal and accompanied by many crises. The solution ideas in this thesis are a small piece of the puzzle. They are all within the scope of the PSF concept, but try to "sneak in" as much of the reliability-based approach as possible. The author hopes that in this way, more and more of the "probabilistic world" can be introduced into the old-fashioned deterministic calculus of current structural codes. In the author's opinion, it is imperative that our codes are raised to the next level of reliability-based design or, ideally, even to the level of risk-based design. The rapid development within the last decades of new calculation methods and modeling approaches and the simultaneously increasing performance of computers lead to the fact that such

a fundamental change is very well possible. We should not continue to hide behind the well-established methods out of convenience, but leave our comfort zone and dare to take the next step.

A. Portfolio of representative design situations

A portfolio is defined via the following generic LSF g, which was also used in the recent revision of the Eurocode [61].

$$
\begin{aligned}
g(\mathcal{P}_{ij}, \Theta_{R_i}, R_i, G_{S,i}, G_P, Q, a_{Q,i}, a_G) = & \, \mathcal{P}_{ij} \cdot \Theta_{R_i} \cdot R_i - \\
& - (1 - a_{Q,i}) \cdot [a_G \cdot G_{S,i} + (1 - a_G) \cdot G_P] - \\
& - a_{Q,i} \cdot Q_j
\end{aligned}
\tag{A.1}
$$

This LSF is valid for a material i and a variable action j. R_i is the material strength, Θ_{R_i} is the resistance model uncertainty, and $G_{S,i}$ is the self-weight. Q_j represents the variable action, and G_P represents the permanent action. In order to account for different design situations, the weights $a_{Q,i}$ and a_G allow representing different action compositions. Finally, $\mathcal{P}_{ij}$ is the design variable (e.g., the area of a truss or the section modulus of a beam) defined via Eqn. "6.10" of Eurocode 0 [25] as:

$$
\mathcal{P}_{ij} = \frac{\gamma_{R_i}}{\theta_{R_i,k} \cdot r_{i,k}} \cdot [(1 - a_{Q,i}) \cdot (a_G \cdot \gamma_S \cdot g_{S_i,k} + (1 - a_G) \cdot \gamma_P \cdot g_{P,k}) + a_{Q,i} \cdot \gamma_Q \cdot q_k]
\tag{A.2}
$$

Note that this form of the LSF is equivalent to the LSF derived in Eqn. 2.36; hence, it requires the same assumptions. Those assumptions that $t_R = t_{R,EC}$ is linear with respect to the material strength and through the origin and $t_S = t_{S,EC}$ is linear and through the origin.

Six different material properties R_i and three different actions Q_j are considered and weighted with $w_{R,i}$ and $w_{Q,j}$ according to their relative frequency. For each material, different load compositions are investigated via $a_{Q,i}$ and a_G (Tab. A.1 and A.2). Ten equally spaced and equally weighted values of $a_{Q,i}$ and three equally spaced and equally weighted values of a_G are considered. The distributions of each material property R_i, variable action Q_j, the associated resistance uncertainty Θ_{R_i} and Θ_{Q_j}, the self weight G_{S_i}, and the permanent load G_P are given in Tab. A.3. The values of the partial safety factors follow Eurocode 0 [25] (Tab. A.4). The characteristic values are chosen following Eurocode 1, 2, 3, 5, 6 [103, 125, 176, 179, 180] and the latest revision of the Eurocode [61] (Tab. A.5).

i	Material	$w_{R,i}\%$	$a_{Q,i}$	a_G
1	Steel yielding strength	40.0	$[0.2; 0.8]$	
2	Concrete compression strength	15.0	$[0.1; 0.7]$	
3	Re-bar yielding strength	25.0	$[0.1; 0.7]$	$[0.6; 1.0]$
4	Glulam timber bending strength	7.5	$[0.2; 0.8]$	
5	Solid timber bending strength	2.5	$[0.2; 0.8]$	
6	Masonry compression strength	10.0	$[0.1; 0.7]$	

Tab. A.1.: Material properties R_i, weights $w_{R,i}$ and ranges of $a_{Q,i}$ and a_G.

j	Action	$w_{Q,j}\%$
1	Wind	$33.\overline{33}$
2	Snow	$33.\overline{33}$
3	Imposed load	$33.\overline{33}$

Tab. A.2.: Variable actions Q_j and weights $w_{Q,j}$.

	Mean	c. o. v.
$R_1 \sim \mathcal{LN}$	1.00	0.070
$R_2 \sim \mathcal{LN}$	1.00	0.150
$R_3 \sim \mathcal{LN}$	1.00	0.070
$R_4 \sim \mathcal{LN}$	1.00	0.150
$R_5 \sim \mathcal{LN}$	1.00	0.200
$R_6 \sim \mathcal{LN}$	1.00	0.160
$\Theta_{R_1} \sim \mathcal{LN}$	1.00	0.050
$\Theta_{R_2} \sim \mathcal{LN}$	1.00	0.100
$\Theta_{R_3} \sim \mathcal{LN}$	1.00	0.100
$\Theta_{R_4} \sim \mathcal{LN}$	1.00	0.100
$\Theta_{R_5} \sim \mathcal{LN}$	1.00	0.100
$\Theta_{R_6} \sim \mathcal{LN}$	1.16	0.175
$G_{S_1} \sim \mathcal{N}$	1.00	0.040
$G_{S_2} \sim \mathcal{N}$	1.00	0.050
$G_{S_3} \sim \mathcal{N}$	1.00	0.050
$G_{S_4} \sim \mathcal{N}$	1.00	0.100
$G_{S_5} \sim \mathcal{N}$	1.00	0.100
$G_{S_6} \sim \mathcal{N}$	1.00	0.065
$G_P \sim \mathcal{N}$	1.00	0.100
$Q_1 \sim \mathcal{G}$	1.00	0.250
$Q_2 \sim \mathcal{G}$	1.00	0.400
$Q_3 \sim \mathcal{G}$	1.00	0.530
$\Theta_{Q_1} \sim \mathcal{LN}$	0.97	0.260
$\Theta_{Q_2} \sim \mathcal{LN}$	1.00	0.300
$\Theta_{Q_3} \sim \mathcal{LN}$	1.00	0.100

Tab. A.3.: Distributions used within the portfolio.

Material i	$\gamma_{R,i}$	γ_S	γ_P	γ_{Q_j}
1	1.00			
2	1.50			
3	1.15	1.35	1.35	1.5
4	1.25			
5	1.30			
6	1.50			

Tab. A.4.: Partial safety factors.

Material i	$r_{i,k}$	$\theta_{R_i,k}$	$g_{S_i,k}$
1	$\mathrm{E}[R_1] - 2 \cdot \sqrt{\mathrm{Var}[R_1]}$	$\mathrm{E}[\Theta_{R_1}]$	$F_{G_{S_1}}^{-1}(0.5)$
2	$F_{R_2}^{-1}(0.05)$	$\mathrm{E}[\Theta_{R_2}]$	$F_{G_{S_2}}^{-1}(0.5)$
3	$F_{R_3}^{-1}(0.05)$	$\mathrm{E}[\Theta_{R_3}]$	$F_{G_{S_3}}^{-1}(0.5)$
4	$F_{R_4}^{-1}(0.05)$	$\mathrm{E}[\Theta_{R_4}]$	$F_{G_{S_4}}^{-1}(0.5)$
5	$F_{R_5}^{-1}(0.05)$	$\mathrm{E}[\Theta_{R_5}]$	$F_{G_{S_5}}^{-1}(0.5)$
6	$F_{R_6}^{-1}(0.05)$	$\mathrm{E}[\Theta_{R_6}]$	$F_{G_{S_6}}^{-1}(0.5)$

Variable action j	$q_{i,k}$	$\theta_{Q_j,k}$
1	$F_{Q_1}^{-1}(0.98)$	1.1
2	$F_{Q_2}^{-1}(0.98)$	$\mathrm{E}[\Theta_{Q_2}] + \sqrt{\mathrm{Var}[\Theta_{Q_2}]}$
3	$F_{Q_3}^{-1}(0.98)$	1.0

Permanent action	$g_{P,k}$
	$F_{G_P}^{-1}(0.5)$

Tab. A.5.: Characteristic values.

7. Bibliography

[1] Nikolaus Pevsner. The term 'architect' in the middle ages. *Speculum*, 17(4):549–562, 1942.

[2] Donella H Meadows, Dennis L Meadows, Joergen Randers, and William W Behrens III. *The limits to growth*. Club of Rome, 1972.

[3] Dennis Meadows and Jorgan Randers. *The limits to growth: the 30-year update*. Routledge, 2012.

[4] Jorgen Randers. *2052: A global forecast for the next forty years*. Chelsea Green Publishing, 2012.

[5] Ivan Kitov and Oleg Kitov. Real GDP per capita since 1870. MPRA Paper 39021, University Library of Munich, Germany, May 2012.

[6] Ludewig Damian and Meyer Eike. Postwachstumsgesellschaft konkret. *Forum Ökologisch-Soziale Marktwirtschaft e.V.*, 2013.

[7] Steffen Lehndorff. Deutschland – der eingebildete Gesunde. *Atlas der Globalisierung: weniger wird mehr*, pages 102–103, 2015.

[8] Wissenschaftlicher Beirat der Bundesregierung. Hauptgutachten - Welt im Wandel Gesellschaftsvertrag für eine Große Transformation. Technical report, WBGU, 2011.

[9] Richard Schmalensee, Thomas M Stoker, and Ruth A Judson. World carbon dioxide emissions: 1950–2050. *Review of Economics and Statistics*, 80(1):15–27, 1998.

[10] Ernst Worrell, Lynn Price, Nathan Martin, Chris Hendriks, and Leticia Ozawa Meida. Carbon dioxide emissions from the global cement industry. *Annual review of energy and the environment*, 26(1):303–329, 2001.

[11] Pamela D Noyes, Matthew K McElwee, Hilary D Miller, Bryan W Clark, Lindsey A Van Tiem, Kia C Walcott, Kyle N Erwin, and Edward D Levin. The toxicology of climate change: environmental contaminants in a warming world. *Environment international*, 35(6):971–986, 2009.

[12] Blasberg Marian and Henk Malte. Wie Gold am Meer. *Die ZEIT*, 2014.

[13] Petter Næss. Unsustainable growth, unsustainable capitalism. *Journal of Critical Realism*, 5(2), 2006.

[14] Christoph Freydorf, Christian Kimmich, Thomas Koudela, Ludwig Schuster, and Ferdinand Wenzlaff. Wachstumszwänge in der Geldwirtschaft. Zwischenbericht der Wissenschaftlichen Arbeitsgruppe nachhaltiges Geld. *Wissenschaftliche Arbeitsgruppe nachhaltiges Geld*, 2012.

[15] Ferdinand Wenzlaff, Christian Kimmich, Thomas Koudela, Oliver Richters, Christoph Freydorf, and Ludwig Schuster. Wachstumszwang in der Geldwirtschaft? Theoretische Erwägungen. *Denkwerk Zukunft, Bonn*, 2012.

[16] Lise Van Susteren. The psychological impacts of the climate crisis: a call to action. *BJPsych International*, 15(2):25–26, 2018.

[17] Eric Klinenberg, Malcolm Araos, and Liz Koslov. Sociology and the climate crisis. *Annual Review of Sociology*, 46:649–669, 2020.

[18] Hartmut Rosa. *Beschleunigung: die Veränderung der Zeitstrukturen in der Moderne*. Suhrkamp Verlag, 2005.

[19] Hartmut Rosa. *Beschleunigung und Entfremdung: Entwurf einer kritischen Theorie spätmoderner Zeitlichkeit*. Suhrkamp Verlag, 2010.

[20] Hartmut Rosa. Über die Verwechslung von Kauf und Konsum: Paradoxien der spät-modernen Konsumkultur. *Die Verantwortung des Konsumenten. Über das Verhältnis von Markt, Moral und Konsum*, pages 115–132, 2011.

[21] Herczeg Márton, McKinnon David, Milios Leonidas, Bakas Ioannis, Klaassens Erik, Svatikova Katarina, and Widerberg Oscar. Resource efficiency in the building sector. Technical report, Final report Client: DG Environment, 2014.

[22] Niels Lind. The design of structural design norms. *Journal of Structural Mechanics*, 1(3):357–370, 1972.

[23] International Organization for Standardization (ISO). ISO 2394:2015 General principles on reliability for structures, 2015.

[24] JCSS. Probabilistic model code. *Joint Committee on Structural Safety*, 2001.

[25] CEN. Eurocode 0: Basis of structural design, 2002.

[26] Victor Saouma. *Lecture Notes: Structural Engineering–Analysis and Design*. Dept. of Civil Environmental and Architectural Engineering, 2016.

[27] Jacques Heyman and Heyman Jacques. *Structural analysis: A historical approach*. Cambridge University Press, 1998.

[28] David Macaulay. *Sie bauten eine Kathedrale*. dtv junior, 1985.

[29] Hans Straub. *Die Geschichte der Bauingenieurkunst*. Springer-Verlag, 2013.

[30] Karl-Eugen Kurrer. *Geschichte der Baustatik.* John Wiley & Sons, 2002.

[31] Peter Marti. *Baustatik: Grundlagen, Stabtragwerke, Flächentragwerk.* John Wiley & Sons, 2012.

[32] Beal Alasdair and Leeds Thomasons. A history of the safety factors. *The Structural Engineer*, 2011.

[33] Royal Institute of British Architects. Second report of the joint committee of reinforced concrete. 1911.

[34] British Standards Institution. Revision to BS 449. 1939.

[35] C Allin Cornell. A probability-based structural code. In *ACI Journal*, 1969.

[36] Deutsches Institut für Normung. *GruSiBau: Grundlagen zur Festlegung von Sicherheitsanforderungen für bauliche Anlagen.* Beuth Verlag, 1981.

[37] R Rackwitz. Zuverlässigkeit und Lasten im konstruktiven Ingenieurbau. *Course Notes, Technische Universität, München (1993–2004)*, 2004.

[38] Ove Ditlevsen and Henrik O Madsen. *Structural reliability methods.* Wiley New York, 1996.

[39] Daniela M Bailer-Jones. Naturwissenschaftliche modelle: Von epistemologie zu ontologie. *Argument und Analyse: Ausgewählte Sektionsvorträge des*, 4:1–11, 2002.

[40] Stephan Hartmann and Daniela Bailer-Jones. Modelle. In *Enzyklopädie Philosophie*, pages 1627–1632. Meiner Verlag, 2010.

[41] Tobias Müller. Naturwissenschaftliche perspektive und menschliches selbstverständnis. eine wissenschaftsphilosophische analyse zur unverzichtbarkeit lebensweltlicher qualitäten. *Abschied von der Lebenswelt*, pages 31–52, 2015.

[42] Immanuel Kant. *Kritik der reinen Vernunft.* 1889.

[43] Ludwig Wittgenstein. *Tractatus logico-philosophicus.* Routledge, 2013.

[44] Martin Heidegger. *Sein und Zeit.* 1927.

[45] Karl Jaspers. *Psychologie der Weltanschauungen.* 1919.

[46] Nancy Cartwright and Ernan McMullin. *How the laws of physics lie.* American Association of Physics Teachers, 1984.

[47] Nancy Cartwright. *Nature's Capacities and Their Measurement.* Oxford University Press, 1994.

[48] Nancy Cartwright. Fundamentalism vs. the patchwork of laws. *Proceedings of the Aristotelian Society*, 1994.

[49] SL Kakani and A Kakani. *Material science.* New Age International (P) Ltd., Publishers, 2004.

[50] Carl G Hempel and Paul Oppenheim. Studies in the logic of explanation. *Philosophy of science*, 15(2):135–175, 1948.

[51] Anthony Christopher Davison. *Statistical models*, volume 11. Cambridge university press, 2003.

[52] Armen Der Kiureghian and Ove Ditlevsen. Aleatory or epistemic? does it matter? *Structural Safety*, 2009.

[53] Prasanta S Bandyopadhyay and Malcolm R Forster. Philosophy of statistics: An introduction, 2011.

[54] American Society of Civil Engineers. Minimum design loads for buildings and other structures (ASCE/SEI 7-22), 2013.

[55] ACI Committee. Building code requirements for structural concrete (ACI 318-08) and commentary, 2008.

[56] American Institute of Steel Construction. Code of standard practice for steel buildings and bridges, 2000.

[57] Luc Taerwe and Stijn Matthys. *Fib model code for concrete structures 2010.* Ernst & Sohn, Wiley, 2013.

[58] Alan Gamett Davenport. The relationship of reliability to wind loading. *Journal of Wind Engineering and Industrial Aerodynamics*, 1983.

[59] Nicholas John Cook. *The Designer's Guide to Wind Loading of Building Structures: Part 1: Background, Damage Survey, Wind Data and Structural Classification.* Butterworth Publishers, 1985.

[60] Wolfgang Grasse. Lasten und Einwirkungen auf Brücken einschließlich Kombinationsregeln (DIN-Fachbericht 101). *Technical University Dresden*, 2009.

[61] Jochen Köhler, Michele Baravalle, and John Sørensen. Calibration of existing semi-probabilistic design codes. *13th International Conference on Applications of Statistics and Probability in Civil Engineering*, 2019.

[62] Nicholas Metropolis, Arianna Rosenbluth, Marshall Rosenbluth, Augusta Teller, and Edward Teller. Equation of state calculations by fast computing machines. *The journal of chemical physics*, 21(6):1087–1092, 1953.

[63] Reuven Rubinstein and Dirk Kroese. *Simulation and the Monte Carlo method*. John Wiley & Sons, 2016.

[64] Siu-Kui Au and James Beck. Estimation of small failure probabilities in high dimensions by subset simulation. *Probabilistic engineering mechanics*, 16(4):263–277, 2001.

[65] Daniel Straub and Iason Papaioannou. Bayesian updating with structural reliability methods. *Journal of Engineering Mechanics*, 141(3):04014134, 2015.

[66] Iason Papaioannou, Wolfgang Betz, Kilian Zwirglmaier, and Daniel Straub. MCMC algorithms for subset simulation. *Probabilistic Engineering Mechanics*, 41:89–103, 2015.

[67] Michael Hasofer and Nils Lind. An exact and invariant first order reliability format. *Engineering Mechanics*, 100(1):111–121, 1974.

[68] Rüdiger Rackwitz and Bernd Flessler. Structural reliability under combined random load sequences. *Computers & Structures*, 9(5):489–494, 1978.

[69] Robert E Melchers and André T Beck. *Structural reliability analysis and prediction*. John Wiley & Sons, 2018.

[70] Michael Hohenbichler and Rüdiger Rackwitz. First-order concepts in system reliability. *Structural safety*, 1(3):177–188, 1982.

[71] John Dalsgaard Sørensen. Calibration of partial safety factors in danish structural codes. In *JCSS Workshop on Reliability Based Code Calibration*, 2002.

[72] J Marková and M Holicky. Calibration of partial factors for design of concrete structures. *ICASP 2011, Zurich*, 2011.

[73] Palle Thoft-Christensen and Yoshisada Murotsu. *Application of structural systems reliability theory*. Springer Science & Business Media, 2012.

[74] Junho Song, Won-Hee Kang, Young-Joo Lee, and Junho Chun. Structural system reliability: Overview of theories and applications to optimization. *ASCE-ASME Journal of Risk and Uncertainty in Engineering Systems, Part A: Civil Engineering*, 2021.

[75] Jinxin GONG, Zhonghan YU, and Qin ZHANG. Pushover-based seismic reliability analysis of structures. *Journal of Harbin Engineering University*, 2013.

[76] Michele Baravalle. *Risk and Reliability Based Calibration of Structural Design Codes*. PhD thesis, Norwegian University of Science and Technology, 2017.

[77] Jochen Köhler and Michele Baravalle. Risk-based decision making and the calibration of structural design codes–prospects and challenges. *Civil Engineering and Environmental Systems*, 36(1):55–72, 2019.

[78] Michele Baravalle and Jochen Köhler. A risk-based approach for calibration of design codes. *Structural safety*, 78:63–75, 2019.

[79] MA Maes and GAN Thomas. Risk-based calibration of action factors in the new iso 19906 arctic offshore structures standard. *OTC Arctic Technology Conference*, 2011.

[80] Michele Baravalle and Jochen Köhler. Risk and reliability based calibration of design codes for submerged floating tunnels. *Procedia engineering*, 166:247–254, 2016.

[81] Alessio Rinaldi, Cesar De Santos-Berbel, Francesco Bella, and Maria Castro. Risk-based calibration of road sag vertical curve design guidelines on undivided highways. *Journal of transportation engineering, Part A: Systems*, 147(10):04021055, 2021.

[82] Nicolas Gayton, Alaa Mohamed, John Dalsgaard Sorensen, Maurice Pendola, and Maurice Lemaire. Calibration methods for reliability-based design codes. *Structural Safety*, 26(1):91–121, 2004.

[83] Michael Havbro Faber and John Dalsgaard Sørensen. Reliability-Based Code Calibration: The JCSS Approach. In *9th International Conference on Applications of Statistics and Probability in Civil Engineering*. Millpress, 2003.

[84] John Dalsgaard Sørensen, IB Kroon, and Michael Havbro Faber. Optimal reliability-based code calibration. *Structural Safety*, 15(3):197 – 208, 1994.

[85] ACWM Vrouwenvelder and AJM Siemes. Probabilistic calibration procedure for the derivation of partial safety factors for the netherlands building codes. *HERON, 32 (4), 1987*, 1987.

[86] Emmanuel Ardillon, Bruno Barthelet, and JD Sørensen. Probabilistic calibration of safety factors for nuclear operating installations. *ASME-PUBLICATIONS-PVP*, 376:73–82, 1998.

[87] MA Maes, S Abdelatif, and R Frederking. Recalibration of partial load factors in the Canadian offshore structures standard CAN/CSA-S471. *Canadian Journal of Civil Engineering*, 31(4):684–694, 2004.

[88] Andrzej S Nowak. Calibration of lrfd bridge code. *Journal of Structural Engineering*, 121(8):1245–1251, 1995.

[89] M.P. Byfield and D.A. Nethercot. Eurocodes - failing to standardise safety. In *Proceedings of the Institution of Civil Engineers-Civil Engineering*. Thomas Telford Ltd, 2001.

[90] M Holicky, JV Retief, and C Viljoen. Partial factors for wind actions considering hidden safety due to time-invariant components. *The 6th International Conference on Structural Engineering, Mechanics and Computation*, 2016.

[91] Andrzej S Nowak and T Tharmabala. Bridge reliability evaluation using load tests. *Journal of Structural Engineering*, 1988.

[92] Wellison José de Santana Gomes and André Beck. A conservatism index based on structural reliability and model errors. *Reliability Engineering & System Safety*, 209:107456, 2021.

[93] Henrik Stensgaard Toft, Kim Branner, John Dalsgaard Sørensen, and Peter Berring. Reliability-based calibration of partial safety factors for wind turbine blades. In *EWEA Annual Event 2011*, 2011.

[94] Maria Hänninen, Osiris Banda, and Pentti Kujala. Bayesian network model of maritime safety management. *Expert Systems with Applications*, 41(17):7837–7846, 2014.

[95] George Gazetas, Ioannis Anastasopoulos, and Evangelia Garini. Geotechnical design with apparent seismic safety factors well-bellow 1. *Soil Dynamics and Earthquake Engineering*, 57:37–45, 2014.

[96] Max Teichgräber, Jochen Köhler, and Daniel Straub. Hidden safety in structural design codes. *Engineering Structures*, 2022.

[97] Max Teichgräber, Jochen Köhler, and Daniel Straub. When advanced models can lead to lower safety: Codified design of structures against wind loads. *13th International Conference on Applications of Statistics and Probability in Civil Engineering*, 2019.

[98] Max Teichgräber, Jochen Köhler, and Daniel Straub. Über den umgang mit versteckten sicherheiten - eine fallstudie am windlastmodell des eurocode. *Baustatik - Baupraxis 14*, 2020.

[99] Max Teichgräber, Marcel Nowak, Jochen Köhler, and Daniel Straub. The effect of traffic load model assumptions on the reliability of road bridges. *6th International Symposium on Life-Cycle Civil Engineering*, 2018.

[100] Max Teichgräber, Marcel Nowak, Jochen Köhler, and Daniel Straub. A study on the effect of improved load models on structural safety. *6th International Symposium on Reliability Engineering and Risk Management*, 2018.

[101] Max Teichgräber and Daniel Straub. A study on the effects of hidden safety when assessing existing structures. *International Probabilistic Workshop*, 2022.

[102] Nico Scholten and Ton Vrouwenvelder. Eurocodes and the structural safety of existing buildings - considering the publication of the Dutch NEN 8700. *COBRA*

2009 The construction and building research conference of the Royal Institution of Chartered Surveyors, 2009.

[103] CEN. Eurocode 1: Actions on structures –part 1-4: general actions, wind actions, 2005.

[104] Alan Gamett Davenport. The application of statistical concepts to the wind loading of structures. *Proceedings of the Institution of Civil Engineers*, 1961.

[105] Hans-Juergen Niemann. The european wind loading code: Background and regulations. *Structures Congress*, 2004.

[106] Michele Baravalle and Jochen Köhler. On the probabilistic representation of the wind climate for calibration of structural design standards. *Structural safety*, 70:115–127, 2018.

[107] Alan Gamett Davenport. Proposed new international (iso) wind load standard. *Second Asia-Pacific Symposium on wind-engineering*, 1989.

[108] Ton Vrouwenvelder. The JCSS probabilistic model code. *Structural Safety*, 1997.

[109] Deutscher Wetterdienst (DWD). Wind velocity data. `ftp://ftp-cdc.dwd.de/pub/CDC/observations_germany`, 2018.

[110] Stuart Coles, Joanna Bawa, Lesley Trenner, and Pat Dorazio. *An introduction to statistical modeling of extreme values*. Springer, 2001.

[111] Svend Ole Hansen, Marie Louise Pedersen, and JD Sorensen. Probability-based calibration of pressure coefficient. In *14th international conference on wind engineering*, 2015.

[112] RL Wardlaw and GF Moss. A standard tall building model for the comparison of simulated natural winds in wind tunnels. *CAARC, CC 662m Tech*, 1970.

[113] International Organization for Standardization (ISO). Guide to the Expression of Uncertainty in Measurement, 1995.

[114] John David Anderson and J Wendt. *Computational fluid dynamics*. Springer, 1995.

[115] Niels Sørensen, Andreas Bechmann, Pierre-Elouan Réthoré, Dalibor Cavar, Mark Kelly, and I Troen. How fine is fine enough when doing CFD terrain simulations. *European Wind Energy Association*, 10, 2012.

[116] Mark Kelly and Hans Ejsing Jørgensen. Statistical characterization of roughness uncertainty and impact on wind resource estimation. *Wind Energy Science*, 2017.

[117] Yen Dora and Braeuchle Frank. Calibration and uncertainty analysis for the uc davis wind tunnel facility. *UC Davis Wind Tunnel Calibration Document*, 2000.

[118] Fei Long. *Uncertainties in pressure coefficients derived from full and model scale data.* PhD thesis, Texas Tech University, 2004.

[119] Marc L Levitan and Kishor C Mehta. Texas tech field experiments for wind loads part 1 and 2: building and pressure measuring system. *Journal of Wind Engineering and Industrial Aerodynamics*, 1992.

[120] Jill Ann Campbell. *Wind engineering research field laboratory site characterization.* PhD thesis, Texas Tech University, 1995.

[121] EN DIN. 2/na: 2012-08: Nationaler anhang–national festgelegte parameter–eurocode 1: Einwirkungen auf tragwerke–teil 2: Verkehrslasten auf brücken. *DIN Deutsches Institut für Normung eV, Berlin*, 405, 2012.

[122] Georg Merzenich and Gerhard Sedlacek. Hintergrundbericht zum eurocode 1-teil 3.2: Verkehrslasten auf straßenbrücken. *Forschung Straßenbau und Straßenverkehrstechnik*, (711), 1995.

[123] Georg Merzenich. *Entwicklung eines europäischen Verkehrslastmodells für die Bemessung von Straßenbrücken.* PhD thesis, RWTH, 1994.

[124] Marcel Nowak and Oliver Fischer. Site-specific load models for road bridges – an important tool for advanced evaluation strategies in bridge reassessment. *Beton- und Stahlbetonbau 112.*

[125] CEN. Eurocode 2: Design of concrete structures, 2004.

[126] CEN. Eurocode 0: Basis of structural design (annex c), 2002.

[127] International Energy Agency and the United Nations Environment Programme. *2018 Global Status Report: Towards a zero-emission, efficient and resilient buildings and construction sector.* UN-Environment, 2018.

[128] Max Teichgräber, Jochen Köhler, and Daniel Straub. Redundancy effects in partial safety factordesign: A link to a generalized Danielssystem. *Preprint: https://www.cee.ed.tum.de/fileadmin/w00cbe/era/Papers/2023_ Teichgraeber_Redundancy_effects_in_partial_safety_factor_design_A_ link_to_a_generalized_Daniels_system.pdf*, 2023.

[129] Henry Ellis Daniels. The statistical theory of the strength of bundles of threads. *Proceedings of the Royal Society of London. Series A. Mathematical and Physical Sciences*, 183(995):405–435, 1945.

[130] Michael Hohenbichler and Rüdiger Rackwitz. On structural reliability of parallel systems. *Reliability Engineering*, 2(1):1–6, 1981.

[131] Stephan Gollwitzer and Rüdiger Rackwitz. On the reliability of daniels systems. *Structural Safety*, 7(2-4):229–243, 1990.

[132] Stephan Gollwitzer. *Zuverlässigkeit redundanter Tragsysteme bei geometrischer und stofflicher Nichtlinearität*. PhD thesis, Technical University of Munich, 1986.

[133] Andrew Barbour. Brownian motion and a sharply curved boundary. *Advances in Applied Probability*, 13(4):736–750, 1981.

[134] Pranab Sen and Barid Bhattacharyya. Asymptotic normality of the extremum of certain sample functions. *Zeitschrift für Wahrscheinlichkeitstheorie und Verwandte Gebiete*, 34(2):113–118, 1976.

[135] Stuart Leigh Phoenix and Howard Taylor. The asymptotic strength distribution of a general fiber bundle. *Advances in Applied Probability*, 5(2):200–216, 1973.

[136] Gary Harlow and Stuart Leigh Phoenix. Probability distributions for the strength of composite materials i: two-level bounds. *International Journal of Fracture*, 17(4):347–372, 1981.

[137] Walter Rosen. Tensile failure of fibrous composites. *AIAA journal*, 2(11):1985–1991, 1964.

[138] Richard L Smith. Limit theorems and approximations for the reliability of load-sharing systems. *Advances in Applied Probability*, 15(2):304–330, 1983.

[139] Stuart Leigh Phoenix. The asymptotic distribution for the time to failure of a fiber bundle. *Advances in applied probability*, 11(1):153–187, 1979.

[140] Richard Smith and Stuart Leigh Phoenix. Asymptotic distributions for the failure of fibrous materials under series-parallel structure and equal load-sharing. 1981.

[141] Michael Hohenbichler and Rüdiger Rackwitz. Reliability of parallel systems under imposed uniform strain. *Journal of Engineering Mechanics*, 109(3):896–907, 1983.

[142] Yi-Kwei Wen and H-C Chen. On fast integration for time variant structural reliability. *Probabilistic Engineering Mechanics*, 2(3):156–162, 1987.

[143] Ronald Schneider, Sebastian Thöns, and Daniel Straub. Reliability analysis and updating of deteriorating systems with subset simulation. *Structural Safety*, 64:20–36, 2017.

[144] Iason Papaioannou, Wolfgang Betz, Kilian Zwirglmaier, and Daniel Straub. Mcmc algorithms for subset simulation. *Probabilistic Engineering Mechanics*, 2015.

[145] Stephen Raudenbush and Anthony Bryk. *Hierarchical linear models: Applications and data analysis methods*. Sage, 2008.

[146] Jesus Luque and Daniel Straub. Reliability analysis and updating of deteriorating systems with dynamic bayesian networks. *Structural Safety*, 62:34–46, 2016.

[147] Nataf A. Détermination des distribution dont les marges sont données. *Comptes rendus de l'academie des sciences*, 1962.

[148] Armen Der Kiureghian and Pei-Ling Liu. Structural reliability under incomplete probability information. *Journal of Engineering Mechanics*, 112(1):85–104, 1986.

[149] Won-Hee Kang and Junho Song. Efficient reliability analysis of general systems by sequential compounding using Dunnett-Sobel correlation model. *Proc. 10th International Conference on Structural Safety and Reliability (ICOSSAR2009), Osaka, Japan*, 2009.

[150] Henrik O Madsen, Steen Krenk, and Niels Christian Lind. *Methods of structural safety.* Courier Corporation, 2006.

[151] Vladimir Cervenka. Global Safety Format for Nonlinear Calculation of Reinforced Concrete. *Beton- und Stahlbetonbau*, 103(S1):37–42, 2008.

[152] Hendrik Schlune, Mario Plos, and Kent Gylltoft. Safety formats for non-linear analysis of concrete structures. *Magazine of Concrete Research*, 64(7):563–574, 2012.

[153] Remus Tecusan and Konrad Zilch. Sicherheitsaspekte bei nicht-linearen FEM Berechnungen [Safety aspects in non-linear FEM calculations]. *Bauingenieur*, 92(12):518–527, 2017.

[154] Paolo Castaldo, Diego Gino, and Giuseppe Mancini. Safety formats for non-linear finite element analysis of reinforced concrete structures: discussion, comparison and proposals. *Engineering Structures*, 193:136–153, 2019.

[155] Milan Holicky. Global resistance factors for reinforcedconcrete members. *ACTA POLYTECHNICA, CTU in Prague*, 2006.

[156] Sz Woliński. Global safety factor for nonlinear design of concrete. *Archives of Civil Engineering*, 57(3):331–339, 2011.

[157] A Mohamed, R Soares, and WS Venturini. Partial safety factors for homogeneous reliability of nonlinear reinforced concrete columns. *Structural Safety*, 23(2):137–156, 2001.

[158] Hendrik Schlune. *Safety evaluation of Concrete Structures with Nonlinear analysis.* PhD thesis, Chalmers Tekniska Hogskola (Sweden), 2011.

[159] Filippo Sangiorgio. *Safety format for non-linear analysis of RC structures subjected to multiple failure modes.* PhD thesis, KTH Royal Institute of Technology, 2015.

[160] Tammam Bakeer. The theory of homogeneity of nonlinear structural systems–a general basis for structural safety assessment. *arXiv preprint arXiv:2212.01423*, 2022.

[161] CEN. Eurocode 0: Basis of structural design - nationaler anhang, 2010.

[162] Max Teichgräber, Martin Fußeder, Kai-Uwe Bletzinger, and Daniel Straub. Non-linear structural models and the partial safety factor concept. *Structural Safety*, 2023.

[163] Max Teichgräber, Martin Fußeder, and Daniel Straub. Investigations on the effect of non-linear models on the reliability of partial safety factor designs. *14th International Conference on Applications of Statistics and Probability in Civil Engineering*, 2023.

[164] Martin Fußeder, Max Teichgräber, Kai-Uwe Bletzinger, Daniel Straub, and Ann-Kathrin Goldbach. Investigations on the design of membrane structures with the semi-probabilistic safety concept. *10th edition of the conference on Textile Composites and Inflatable Structures*, 2021.

[165] Martin Fußeder, Max Teichgräber, Daniel Straub, and Kai-Uwe Bletzinger. On the design of membrane structures with the partial safety factor concept – a parameter study on the infuence of structural and probabalistic properties. *Proceedings of the Tensinet Symposium*, 2023.

[166] Haig Gulvanessian, Jean-Armand Calgaro, and Milan Holicky. *Designers' Guide to Eurocode: Basis of Structural Design*. ICE Publishing, 2012.

[167] Douglas Bates and Donald Watts. Relative curvature measures of nonlinearity. *Journal of the Royal Statistical Society: Series B (Methodological)*, 42(1):1–16, 1980.

[168] Kenneth Emancipator and Martin Kroll. A quantitative measure of nonlinearity. *Clinical chemistry*, 39(5):766–772, 1993.

[169] Hugo Ramon Elizalde Siller. *Non-linear modal analysis methods for engineering structures*. PhD thesis, University of London, 2004.

[170] X Rong Li. Measure of nonlinearity for stochastic systems. pages 1073–1080, 2012.

[171] Yu Liu and X Rong Li. Measure of nonlinearity for estimation. *IEEE Transactions on Signal Processing*, 63(9):2377–2388, 2015.

[172] Jörg Uhlemann, Bernd Stimpfle, and Natalie Stranghöner. Application of the semiprobabilistic safety concept of EN 1990 in the design of prestressed membrane structures. In *Proceedings of the EUROSTEEL*, 2014.

[173] B. F. Philipp. *Methodological Treatment of Non-linear Structural Behavior in the Design, Analysis and Verification of Lightweight Structures*. Ph.D. Thesis, Technical University of Munich, Munich, 2017.

[174] N. Stranghöner, J. Uhlemann, F. Bilginoglu, K.-U. Bletzinger, H. Bögner-Balz, E. Corne, N. Gibson, P. Gosling, R. Houtman, J. Llorens, M. Malinowsky, J.-M. Marion, M. Mollaert, M. Nieger, G. Novati, F. Sahnoune, P. Siemens, B. Stimpfle,

V. Tanev, and J.-Ch. Thomas. Prospect for european guidance for the structural design of tensile membrane structures: Support to the implementation, harmonization and further developments of the eurocodes. In M. Mollaert, S. Dimova, A Pinto, and St. Denton, editors, *JRC Science and Policy Report*. European Commission, Joint Research Centre, European Union, 2016.

[175] Mike Crisfield. *Non-Linear Finite Element Analysis of Solids and Structures: Volume 2 Advanced Topics*. John Wiley & Sons, Inc., USA, 1997.

[176] CEN. Eurocode 3: Design of steel structures, 2005.

[177] Elien de Smedt, Marijke Mollaert, Lincy Pyl, Peter Gosling, Jörg Uhlemann, and Jean-Christophe Thomas. Round robin exercise 4: Reliability analysis of a simple membrane structure: a hyperbolic paraboloid, 2017.

[178] prCEN/TS, 19102:2021. *Design of tensioned membrane structures (prCEN/TS 19102:2021-04)*. CEN - European Committee for Standardization, Brussels, 2021.

[179] CEN. Eurocode 5: Design of timber structures, 2008.

[180] CEN. Eurocode 6: Design of masonry structures, 2006.